

January 2015

CHARACTERIZATION OF MITOTIC REGULATORS ACM1 AND CDC14

Michael Melesse
Purdue University

Follow this and additional works at: https://docs.lib.purdue.edu/open_access_dissertations

Recommended Citation

Melesse, Michael, "CHARACTERIZATION OF MITOTIC REGULATORS ACM1 AND CDC14" (2015). *Open Access Dissertations*. 1313.
https://docs.lib.purdue.edu/open_access_dissertations/1313

This document has been made available through Purdue e-Pubs, a service of the Purdue University Libraries. Please contact epubs@purdue.edu for additional information.

**PURDUE UNIVERSITY
GRADUATE SCHOOL
Thesis/Dissertation Acceptance**

This is to certify that the thesis/dissertation prepared

By Michael Melesse

Entitled

CHARACTERIZATION OF MITOTIC REGULATORS ACM1 AND CDC14

For the degree of Doctor of Philosophy

Is approved by the final examining committee:

Mark C. Hall

Chair

Scott Briggs

Chittaranjan Das

Joseph Kappock

To the best of my knowledge and as understood by the student in the Thesis/Dissertation Agreement, Publication Delay, and Certification Disclaimer (Graduate School Form 32), this thesis/dissertation adheres to the provisions of Purdue University's "Policy of Integrity in Research" and the use of copyright material.

Approved by Major Professor(s): Mark C. Hall

Approved by: Andy Mesecar

Head of the Departmental Graduate Program

12/8/2015

Date

CHARACTERIZATION OF MITOTIC REGULATORS ACM1 AND CDC14

A Dissertation

Submitted to the Faculty

of

Purdue University

by

Michael Melesse

In Partial Fulfillment of the

Requirements for the Degree

of

Doctor of Philosophy

December 2015

Purdue University

West Lafayette, Indiana

ACKNOWLEDGMENTS

It would have been impossible for me to complete this chapter of my academic life without the support of many. First and foremost, I would like to thank my thesis advisor, Mark Hall, for giving me the opportunity to learn from him. I truly appreciate all the encouragement, guidance and support he gave me. I would also like to thank my thesis advisory committee, Scott Briggs, Chitta Das and Joe Kappock for all the guidance and advice. I would like to thank Hana Hall and Juan Martínez for being valuable sounding boards for all things research and more. I would additionally like to thank current and former members of the Hall lab, Christie Eissler, Brendan Powers and Liang Qin and many others who have helped me with various aspects of this thesis.

I want to thank those in the Department of Biochemistry for creating an environment conducive for scientific exploration. I want to thank Jim Henderson for encouraging my teaching interests and Vikki Weake for her willingness to let me take on more responsibility in the classroom. I want to thank those in the main office, Kristi Trimble, Madia Bickett and others, who were always willing to go beyond their duties to help me with anything I needed.

The friendships I have developed over the years have sustained me throughout my time in graduate school. I would like to thank Anton Iliuk who has been a source of valuable perspectives. My friendships with Christina, Jacob, Valezzka and Wossen have been invaluable.

I also want to thank my parents, Melesse and Eyerusalem, for constantly encouraging me to pursue my academic interests and being supportive at every turn. I want to thank my sister, Hiwot, and brothers, Eyob and Aman, for making every conversation we have a highlight of my day. I would also like to thank René V., Guadalupe and René A. for all of their support.

Finally, I want to thank Verónica for the limitless support and understanding without which I would not have been able to complete this journey.

TABLE OF CONTENTS

	Page
LIST OF TABLES	viii
LIST OF FIGURES	ix
ABBREVIATIONS	xii
ABSTRACT	xiv
1 Introduction	1
1.1 Overview of cell division	1
1.2 The eukaryotic cell cycle	1
1.2.1 Stages of the cell cycle	2
1.2.2 Cyclin dependent kinase activity drives the cell cycle	3
1.3 Mitotic exit	5
1.3.1 Mitotic exit requires mitotic cyclin degradation	6
1.3.2 Reversal of Cdk mediated phosphorylation is essential for mitotic exit	6
1.4 The Ubiquitin Proteasome System (UPS)	7
1.4.1 Ubiquitination targets proteins to the proteasome	9
1.4.2 Polyubiquitin-independent proteasomal degradation	10
1.4.3 The Anaphase Promoting Complex (APC) during mitotic exit	10
1.5 Mitotic phosphatases reverse Cdk phosphorylation	17
1.5.1 PP1 and PP2A contribute to mitotic exit	17
1.5.2 Cdc14 activity counteracts Cdk1 mediated phosphorylation	18
1.5.3 Cdc14 is conserved across multiple species	20
1.5.4 <i>S. cerevisiae</i> Cdc14 is highly selective for a subset of Cdk phosphorylation sites	21
1.6 Mitotic exit as a therapeutic target	24

	Page
1.6.1	Utility of Cdc14 inhibitor development 25
1.6.2	Cdc14 inhibitors as research tools 25
2	Acm1 is degraded via an unconventional mechanism 27
2.1	Introduction 27
2.2	Results 29
2.2.1	APC ^{Cdc20} activity is not sufficient for complete Acm1 degradation 29
2.2.2	Acm1 is degraded by the 26S proteasome <i>in vivo</i> 31
2.2.3	Acm1 proteolysis requires a functional ubiquitin conjugation system 33
2.2.4	Acm1 proteolysis does not require individual E3 ligases or E2 conjugating enzymes 34
2.2.5	Acm1 proteolysis does not require assembly of ubiquitin chains 36
2.2.6	Ubiquitin conjugation sites on Acm1 are not required for its proteolysis 36
2.2.7	An N-terminal putative disordered region of Acm1 contributes to APC-independent degradation 41
2.2.8	Acm1 ^{NΔ52} is still cleared from cells at mitotic exit 42
2.2.9	Constitutive expression of stabilized Acm1 ^{NΔ52} impairs growth of <i>sic1Δ</i> cells 43
2.3	Discussion 50
2.3.1	Acm1 may be a novel ubiquitin-independent proteasome substrate 50
2.3.2	How is Acm1 recognized by the proteasome and what is the role of the Acm1 N-terminus? 51
2.3.3	Biological significance of Acm1 proteolytic mechanisms . . . 53
2.4	Conclusion 54
2.5	Materials and Methods 55
2.5.1	Strain and plasmid construction, and mutagenesis 55
2.5.2	Cell growth and cell cycle arrest 57
2.5.3	Immunoblotting 58

	Page
2.5.4 Protein stability assays	59
2.5.5 <i>In vivo</i> APC inhibition assay	60
3 Cdc14 phosphatase substrate selectivity is broadly conserved during evolution	66
3.1 Introduction	66
3.2 Results	68
3.2.1 Determination of kinetic parameters of <i>Saccharomyces cerevisiae</i> Cdc14	68
3.2.2 The <i>Fusarium graminearum</i> Cdc14 (FgCdc14) Substrate selectivity was similar to <i>S. cerevisiae</i> Cdc14	73
3.2.3 Human Cdc14A (hCDC14A) displayed substrate selectivity similar to <i>S. cerevisiae</i> Cdc14	79
3.2.4 <i>Schizosaccharomyces pombe</i> Cdc14 (Clp1) displayed substrate selectivity similar to ScCdc14	82
3.2.5 There are no major variations in Cdc14 substrate selectivity between species	83
3.3 Discussion	94
3.4 Experimental Procedure	97
3.4.1 Cdc14 purification	97
3.4.2 Phosphopeptide synthesis	99
3.4.3 Phosphopeptide Substrate Purification	100
3.4.4 <i>In vitro</i> dephosphorylation assays	100
3.4.5 An unbiased <i>in vitro</i> analysis of sequences affecting Cdc14 selectivity	101
3.4.6 Determination of steady state kinetic parameters (k_{cat}/K_m)	102
4 Cdc14 phosphatase inhibitor development	106
4.1 Introduction	106
4.1.1 Phosphatases are targets for inhibition	106
4.1.2 Cdc14 is an ideal candidate for active site binding inhibitors	107
4.1.3 Choice of Chemical library for HTS	109
4.2 Results	109

	Page
4.2.1 Cdc14 demonstrates product inhibition	109
4.2.2 Small molecule inhibitors of Cdc14 were identified	110
4.3 Discussion	123
4.4 Experimental Procedure	124
4.4.1 Purification of Cdc14	124
4.4.2 Peptide substrate preparation	125
4.4.3 Unphosphorylated peptide inhibitors	125
4.4.4 High-throughput inhibitor screen	126
4.4.5 Determination of small molecule inhibitor IC ₅₀	127
5 Summary and Future directions	129
5.1 Summary	129
5.1.1 Non-canonical mechanism for proteasomal degradation	129
5.1.2 Conservation of Cdc14 substrate selectivity	130
5.1.3 Development of Cdc14 inhibitors	131
5.2 Future Directions	131
5.2.1 Understanding Acn1 degradation	131
5.2.2 Utility of degradation resistant Acn1 in understanding APC ^{Cdh1}	132
5.2.3 Cdc14 substrate selectivity	133
5.2.4 Development of Cdc14 inhibitors	135
5.2.5 Application of Cdc14 inhibitors	136
LIST OF REFERENCES	140
Appendix: Comparison of Cdc14 catalytic efficiencies	155
Appendix: Cdc14 inhibitors	156
VITA	173

LIST OF TABLES

Table	Page
2.1 Yeast deletion strains screened for effects on Acm1 stabilization	56
2.2 Yeast strains used in this study.	61
2.3 Yeast plasmids used in this study.	62
3.1 Steady-state kinetic parameters for phosphopeptide substrates dephosphorylated by <i>S. cerevisiae</i> Cdc14.	69
3.2 Steady-state kinetic parameters for FgCdc14 catalyzed dephosphorylation of phosphopeptides.	75
3.3 Catalytic efficiency (k_{cat}/K_m) measurements of purified FgCdc14.	78
3.4 Steady-state kinetic parameters for hCDC14A catalyzed dephosphorylation of phosphopeptides.	80
3.5 Catalytic efficiency (k_{cat}/K_m) measurements of purified Clp1.	83
3.6 Comparison of catalytic efficiency of Cdc14 enzymes reveals that substrate selectivity is conserved.	95
3.7 Phosphopeptide sequences utilized in phosphatase assays for analyzing Cdc14 substrate selectivity	104
3.8 Plasmids used in this study	105
4.1 Small molecule Cdc14 inhibitors have been identified	115
4.2 Determination of k_i for Cdc14 inhibitors.	116
4.3 Unphosphorylated peptides tested as inhibitors	126
5.1 Phosphopeptide sequences for testing effects of novel substrate determinants.	134

LIST OF FIGURES

Figure	Page
1.1 The cell cycle is driven by Cdk activity.	4
1.2 The ubiquitin proteolysis system	8
1.3 APC function is essential for mitotic exit.	12
1.4 Acm1 is a pseudosubstrate inhibitor of APC ^{Cdh1}	15
1.5 Cdc14 catalytic and substrate interacting motifs are conserved	23
2.1 APC ^{Cdc20} is neither necessary nor sufficient for complete Acm1 degradation at mitotic exit.	31
2.2 Acm1 degradation requires both the 20S core particle and the 19S regulatory complex of the 26S proteasome.	33
2.3 Acm1 proteolysis requires a functional ubiquitin conjugation pathway.	34
2.4 Acm1 proteolysis does not require assembly of polyubiquitin chains.	38
2.5 Acm1 proteolysis does not require ubiquitin acceptor sites on Acm1.	40
2.6 Proteolysis of an Acm1-ProtA fusion protein in G1 requires the N-terminal 52 amino acids of Acm1.	42
2.7 Acm1 ^{NΔ52} is still cleared at mitotic exit, but constitutive expression impairs growth of <i>sic1Δ</i> cells.	44
2.8 Screening of non-essential E2 conjugases and E3 ligases for effects on 3HA-Acm15A expression level.	46
2.9 Measurements of HA-Acm15A stability in selected strains lacking nonessential E2 conjugases and E3 ligases.	47
2.10 Screening of non-essential E2 conjugases and known and putative E3 ligases for effects on Acm1 ^{5A} stability.	48
2.11 Acm1 is not degraded by purified 20S or 26S proteasomes.	49
3.1 Budding yeast Cdc14 was highly selective for phosphoserine containing phosphopeptide substrates	70
3.2 Loss of lysine three residues C-terminal to Ser(P) drastically reduced budding yeast Cdc14 activity.	71

Figure	Page
3.3 Budding yeast Cdc14 efficiently dephosphorylated phosphopeptides substrates containing a single basic residue C-terminal to phosphoSer . . .	72
3.4 FgCdc14 enzyme displays substrate selectivity similar to <i>S. cerevisiae</i> Cdc14.	74
3.5 Estimated k_{cat}/K_m values for <i>F. graminearum</i> Cdc14 obtained from initial velocity measurements	76
3.6 Estimated k_{cat}/K_m values for the catalytic domain of <i>F. graminearum</i> Cdc14 obtained from initial velocity measurements	77
3.7 hCDC14A displayed substrate selectivity similar to <i>Sc.</i> Cdc14	81
3.8 Mutations of +4 and +5 basic residues had an intermediate effect on hCDC14A activity	82
3.9 Estimated k_{cat}/K_m values of Clp1 from initial velocity measurement assays	86
3.10 λ phosphatase dephosphorylates all peptides in the phosphopeptide array.	88
3.11 k_{cat}/K_m estimates of ScCdc14 from initial velocity measurement assays.	89
3.12 k_{cat}/K_m estimates of Clp1 from initial velocity measurement assays. . .	90
3.13 k_{cat}/K_m estimates of FgCdc14 from initial velocity measurement assays.	91
3.14 k_{cat}/K_m estimates of hCDC14A from initial velocity measurement assays.	92
3.15 k_{cat}/K_m estimates of hCDC14B from initial velocity measurement assays.	93
3.16 Updated optimal substrate motif for Cdc14.	96
4.1 Acm1S3 is an effective Cdc14 inhibitor	111
4.2 Sodium tungstate inhibits Cdc14 activity with k_i of $0.82\mu\text{M}$	112
4.3 Mutations away from the ideal substrate sequence abolish ability of peptides to inhibit Cdc14 activity	113
4.4 A likely significant number of the molecules identified as Cdc14 inhibitors are pan assay interference compounds (PAINS).	114
4.5 Molecule #5224815 inhibits Cdc14 activity with a k_i of $1.3\mu\text{M}$	117
4.6 Molecule #5175170 inhibits Cdc14 activity with a k_i of $5.6\mu\text{M}$	118
4.7 Molecule #5117227 inhibits Cdc14 activity with a k_i of $5.6\mu\text{M}$	118
4.8 Molecule #5256251 inhibits Cdc14 activity with a k_i of $12.5\mu\text{M}$	119
4.9 Cdc14 inhibitors display an indeterminate inhibitory mechanism.	120

Figure	Page
4.10 Small molecule inhibitors are less potent inhibitors of <i>F. graminearum</i> Cdc14	121
4.11 Small molecule inhibitors are less potent inhibitors of hCDC14A	122
5.1 Updated model for Acn1 degradation.	130
5.2 Prediction of Acn1 disordered regions.	138
5.3 Purification of PTPs.	139
A.1 Comparison of catalytic efficiencies of Cdc14 enzymes.	155

ABBREVIATIONS

ACN	Acetonitrile
APC	The anaphase-promoting complex
ATP	Adenosine triphosphate
AZ	Antizyme
CDK	Cyclin-dependent protein kinase
DNA	Deoxyribonucleic acid
DMSO	Dimethylsulfoxide
DTT	Dithiothreitol
Fmoc	Fluorenylmethyloxycarbonyl chloride
ECL	Enhanced Chemiluminescence
EDTA	Ethyl-diamine-tetra-acetic acid
FEAR	Cdc fourteen early anaphase release
GST	Glutathione S-transferase
HECT	Homologous to E6-associated protein C-terminus
HTS	High throughput screen
IPTG	Isopropyl Beta-D-1-thiogalactopyranoside
MEN	Mitotic exit network
OD	Optical density
ODC	Ornithine decarboxylase
ORF	Open reading frame
PCR	Polymerase chain reaction
PMSF	Phenylmethylsulfonyl fluoride
PSP	Protein serine/threonine phosphatase
PTP	Protein tyrosine phosphatase

RENT	Regulator of nucleolar silencing and telophase
RING	Really interesting new gene
SAC	Spindle assembly checkpoint
SC	Synthetic complete media
SCF	Skp1/Cdc53/Cullin/F-box protein complex
SDS-PAGE	Sodium Dodecyl Sulfate-Polyacrylamide gel electrophoresis
SPB	Spindle pole body
TFA	Trifluoroacetic acid
TPR	Tetratricopeptide repeat
Ub	Ubiquitin
UPS	Ubiquitin Proteasome System
WT	Wild type
YPD	Rich media containing yeast extract, peptone, and dextrose (glucose)

ABSTRACT

Melesse, Michael Ph.D., Purdue University, December 2015. Characterization of mitotic regulators *Acm1* and *Cdc14*. Major Professor: Mark C. Hall.

Mitotic exit and cytokinesis are driven by a complex set of processes that serve to reset the eukaryotic cell cycle and allow entry into the subsequent cycle. These steps are driven by a combination of molecular events that lead to the termination of high cyclin dependent kinase (Cdk) activity and reversal of Cdk mediated phosphorylation. Proteasomal degradation of cyclins is essential for terminating Cdk activity and active dephosphorylation of Cdk mediated phosphorylation is important for the appropriate completion of the cell cycle.

The anaphase promoting complex (APC) is a ubiquitin ligase responsible for promoting events in late mitosis by polyubiquitinating, among other substrates, cyclins and targeting them for degradation. *Cdh1* is a highly conserved activator of the APC and its activity is regulated by, among other mechanisms, a pseudosubstrate inhibitor, *Acm1*. I have demonstrated that *Acm1* degradation in G1 is mediated by a non-canonical proteasomal degradation mechanism that does not require polyubiquitin conjugation. I also show that expression of an *Acm1* mutant resistant to this degradation mechanism (*Acm1*^{N Δ 52}) leads to reduced cell fitness.

The activity of mitotic phosphatases is essential for the reversal of Cdk phosphorylation at the end of the cell cycle. *Cdc14* activity is essential in budding yeast. However, it is only recently that its role in ordering late mitotic events has begun to be appreciated. By characterizing *Cdc14* substrate selectivity, using phosphopeptide substrates, it has become clear that *Cdc14* preferentially dephosphorylates a subset of Cdk phosphorylation sites. Here I show that *Cdc14* substrate selectivity is conserved across diverse species and this selectivity can be used to gain insight into

Cdc14 substrates in these organisms, where there is limited understanding of Cdc14 function.

The substrate selectivity observed for Cdc14 enzymes holds the potential for the development of selective inhibitors. I was able to show that unphosphorylated peptide containing an optimal substrate sequence is able to inhibit Cdc14 activity. This observation points to the possibility of developing inhibitors that incorporate substrate like characteristics and can take advantage of the active site architecture. I have also developed a high throughput screening strategy and utilized it to screen 50,000 small molecules for the ability to inhibit Cdc14 activity. Specific Cdc14 inhibitors hold the potential to study the effects of Cdc14 loss in organisms that have multiple paralogs of the enzyme or in which genetic manipulations are a challenge.

1. INTRODUCTION

1.1 Overview of cell division

Successful cell division requires the coordination of multiple molecular events within a cell. Precise timing of events driving cell division is an essential requirement of all dividing eukaryotic cells. In the absence of strict regulation of cell division, the potential for highly deleterious events is likely to culminate in genetic instability and cell death.

An important goal of the cell cycle is the error free transmission of genetic information from one cell to the next generation. In order to avoid errors during division, eukaryotic cells employ multiple checkpoint mechanisms that monitor proper completion of sequential steps [1]. The timing of duplication of the genome and the subsequent partition of identical copies to the new daughter cells are subject to multiple layers of regulation. Eukaryotic species share several molecular mechanisms for controlling the process of cell division. These mechanisms include regulation by protein phosphorylation and control over protein stability throughout the various stages of the cell cycle.

Understanding the mechanisms that control progress of the cell cycle is essential for understanding disease states that can occur when the regulatory mechanisms fail.

1.2 The eukaryotic cell cycle

This chapter will discuss the regulation of cell division in the budding yeast (*Saccharomyces cerevisiae*), a model organism that has historically been essential for understanding the fundamental mechanisms of cell cycle regulation [2]. For the most part, the mechanisms that regulate the yeast cell cycle apply across multiple eukary-

otes. Deviations from this will be highlighted, when appropriate, throughout this chapter.

1.2.1 Stages of the cell cycle

The cell cycle is, for the most part, a unidirectional process in which the order of events allows cells to divide and multiply while maintaining a consistent complement of genetic and cellular contents [3]. A large body of research exists characterizing the mechanisms that drive the processes of the cell cycle based on the foundational studies of the budding yeast *Saccharomyces cerevisiae* [2] and fission yeast *Schizosaccharomyces pombe* [4] cell cycles. The regulatory systems that drive the eukaryotic cell cycle are highly conserved across species [5] and the advancements in the understanding of the yeast cell cycle have been critical in elucidating control mechanisms in higher eukaryotes.

The cell cycle involves two major nuclear events, namely, chromosome replication during S phase and chromosome segregation during M phase. These stages are separated by two gap (G) phases: G1 and G2. G1 separates the end of one cycle from the start of the next, whereas G2 separates S phase and M phase. These gap phases give cells the opportunity to monitor the appropriate completion of the process in the preceding cell cycle stage and ensure conditions are appropriate to proceed to the subsequent stage [6]. In *Saccharomyces cerevisiae*, a decision point known as START during G1 allows cells to either commit to another cell cycle and initiate S phase entry when nutrient conditions are favorable or exit the cell cycle [7].

The progress from S phase to M phase is also under the regulation of surveillance processes that monitor the appropriate completion of DNA duplication [8]. Mitosis begins only after DNA synthesis has been completed. Mitosis consists of 4 phases: prophase, metaphase, anaphase, and telophase. At prophase, replicated chromosomes begin to condense and at metaphase, the sister chromatid pairs attach to spindle microtubules from both spindle poles, which align the chromosomes along the center of

the spindle apparatus. When all kinetochores are properly attached to microtubules, the cohesin complex linking sister chromatids is cleaved by separase, permitting the transition from metaphase to anaphase. During anaphase, the mitotic spindle pulls sister chromatids to opposite poles of the spindle. The final step in cell division, cytokinesis, is the physical division of the cytoplasm. A contractile ring pinches the cell into two daughter cells which inherit a complete set of chromosomes and cellular organelles.

Upon the completion of mitosis, the cell cycle is reset to the G1 state before the commencement of the subsequent cell cycle in a highly regulated manner. In fact, there are multiple checkpoints that prevent progress of the cell cycle if events do not proceed appropriately. Examples of such events include DNA damaging insults or inappropriate spindle assembly [1].

1.2.2 Cyclin dependent kinase activity drives the cell cycle

The eukaryotic cell cycle is driven by the oscillating activity of cyclin dependent kinases (Cdks) [9,10]. All Cdks require association with a cyclin subunit for enzymatic activity, hence, the regulation of this association is the major method by which their activity is controlled. In budding yeast, there is a single cyclin dependent kinase, Cdc28, and at least 11 different cyclins, which are responsible for driving the cell cycle (Figure 1.1) [11].

All Cdks are proline-directed kinases which preferentially phosphorylate the minimal consensus sequence Ser/Thr-Pro [12]. The distinct cyclin-Cdk subclasses (Figure 1.1) exhibit minor differences in their specificities outside of this minimal consensus that contribute to substrate selection [13]. The three major switch points during the cell cycle that are controlled by cyclin-Cdk activity are the START (G1/S), mitotic entry, and the metaphase-anaphase transitions [14].

Cdc28 expression varies little throughout the cell cycle [11]. Cdc28 activity and target substrates vary substantially between cell cycle stages, owing, in large part, to

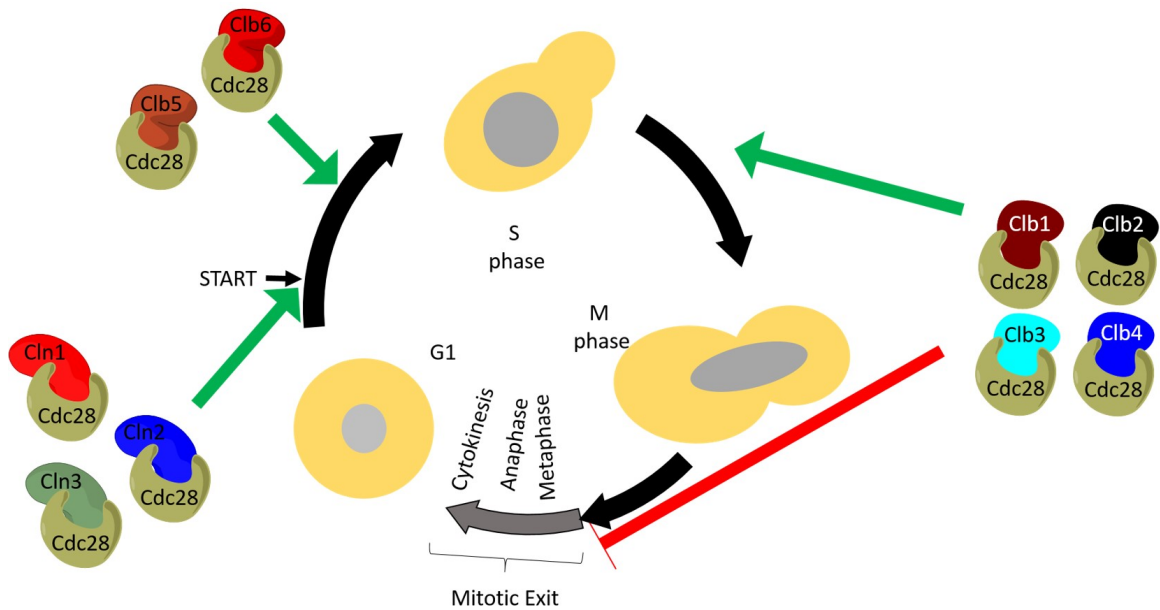


Fig. 1.1.: **The cell cycle is driven by Cdk activity.**

In budding yeast, distinct sets of cyclins activate Cdc28, a cyclin-dependent kinase (Cdk), to drive progress through the cell cycle. In G1, the cyclins Cln1, 2, and 3 promote budding and activate the S phase cyclins in preparation for S phase. In S-phase, cyclins Clb 5 and 6 promote DNA replication. The mitotic cyclins (Clb1-4) promote spindle formation and mitotic initiation and inhibit mitotic exit and cell division.

the periodic presence and/or absence of cyclins. In the cell cycle there are cyclins that prevail during G1 (Cln1, Cln2 and Cln3), S phase (Clb5 and 6) and mitosis (Clb1 and 2) [15]. Cyclin abundance at particular stages of the cell cycle is a result of the combined effects of regulated expression as well as degradation by the proteasome [16, 17]. Cdc28 activity is also regulated by post-translational modifications, namely, an inhibitory phosphorylation by the Wee1/Swe1 kinase [18], which attenuates Cdc28 activity. Cdc28 activity can also be reduced by cyclin-dependent kinase inhibitors (CKIs) such as Sic1 [15] and Far1 [19].

In budding yeast, mitotic entry is driven by the activity of B-type cyclin bound Cdc28. Mitotic Cdk activity is negatively regulated by Swe1 and activated by Mih1. Swe1 phosphorylates Cdc28, on a conserved tyrosine, to prevent premature activation until Cdc25 (Mih1 in *S. cerevisiae*) [9, 20] reverses the phosphorylation during mitotic entry. Reversal of the inhibitory Cdk phosphorylation by Mih1 and association with the B type cyclins promote maximal Cdk activation. An illustration of the effects of this regulatory system is clearly observed in fission yeast as Wee1 mutants have a shortened G2 caused by premature activation of Cdk1, whereas Cdc25 mutants never accumulate sufficient Cdk1 activity to enter mitosis [21–23].

During the metaphase-anaphase transition, Cdk1 is responsible for phosphorylating and activating the Anaphase Promoting Complex (APC), the essential E3 ubiquitin ligase required for chromosome segregation [24]. Mitotic Cdk activity also prevents mitotic exit and cytokinesis to ensure complete spindle assembly and kinetochore attachment before cells divide [17].

1.3 Mitotic exit

Mitotic exit refers to the reversal of the mitotic state to an interphase state following successful chromosomal segregation. It includes disassembly of the spindle apparatus, decondensation of chromosomes, and, in species with an open mitosis, reformation of the nuclear envelope [25]. Like all other steps of the cell cycle, mitotic

exit is under strict regulation. It is essential for cells to appropriately and equally distribute the genome duplicated during S phase to opposite poles prior to mitotic exit, since cytokinesis occurs immediately after [26]. Mitotic exit requires the elimination of all pro-mitotic signals, including Cdk activity.

As discussed above, mitotic entry is driven by increasing Cdk activity. In contrast, mitotic exit requires the reduction of Cdk activity. The requirement for Cdk inactivation prior to cytokinesis ensures that cytokinesis does not occur before completion of chromosome segregation, a process that requires Cdk activity [17]. There is increasing evidence that reduction in Cdk activity alone is not sufficient to allow mitotic exit [27]. Skoufias et al. demonstrated that in the absence of proteasomal activity, loss of Cdk1 is not sufficient for mitotic exit and that phosphatases that oppose Cdk activity are required. Failure to dephosphorylate mitotic Cdk substrates has been shown to inhibit cytokinesis in budding yeast [28]. It is becoming more evident that active reversal of Cdk phosphorylation is essential to allow cells to undergo cytokinesis and reset the cell cycle.

1.3.1 Mitotic exit requires mitotic cyclin degradation

Inactivation of Cdk activity is achieved primarily by the regulated reduction of cyclin abundance in the cell through the action of the ubiquitin proteasome system (UPS, Figure 1.2) [29]. In a variety of eukaryotes, failure to degrade mitotic cyclins leads to an arrest in mitosis [30]. The Anaphase Promoting Complex (APC) is responsible for targeting mitotic cyclins to the proteasome and is essential for mitotic exit [31].

1.3.2 Reversal of Cdk mediated phosphorylation is essential for mitotic exit

Mitotic phosphatases are required for proper progression through mitotic exit. Protein phosphatase 2A (PP2A), protein phosphatase 1 (PP1), and Cdc14 all play

roles in reversing Cdk1 mediated phosphorylation and promoting cytokinesis to varying degrees, depending on the species [32–35].

1.4 The Ubiquitin Proteasome System (UPS)

As discussed in the previous subsection, the cell cycle is driven by the activity of Cdks that phosphorylate their cognate targets [36]. Controlling the levels of cyclins controls Cdk activity which in turn determines the level of phosphorylated protein substrates. Cyclin level control is achieved both by controlling their gene transcription [37] as well as their proteolysis [29]. The majority of cyclin proteolysis is carried out by the UPS [29].

In eukaryotes, ubiquitin-mediated proteolysis is the major mechanism that eliminates proteins in a highly regulated manner, at specific times to allow progress of the cell cycle. The eukaryotic UPS is responsible for the rapid and specific degradation of cyclins, among other things, ensuring a unidirectional cell cycle. Since the characterization of the role of polyubiquitination mediated protein degradation of cyclins [29, 38], the study of the UPS has played a major role in the study of cell cycle regulation. Beyond cell cycle regulation, the UPS plays essential roles in a wide variety of biological processes including apoptosis and immune response [38].

The 26S proteasome is a multimeric, ATP-dependent protease made up of two distinct sub-complexes: one 20S and two 19S particles [39]. The 20S particle is made up of a stack of four heptameric rings containing six proteolytic active sites in the interior of the barrel [40]. The two ends of the barrel are each capped by a 19S particle, restricting access to the active sites (Figure 1.2).

The 19S particle is composed of two sub-complexes, the base and the lid. The 26S proteasome structure requires that polypeptides being degraded are unfolded and enter the barrel as extended chains. The base contains six ATPase subunits and mediates the substrate unfolding step [41]. The lid covers the base and is involved in

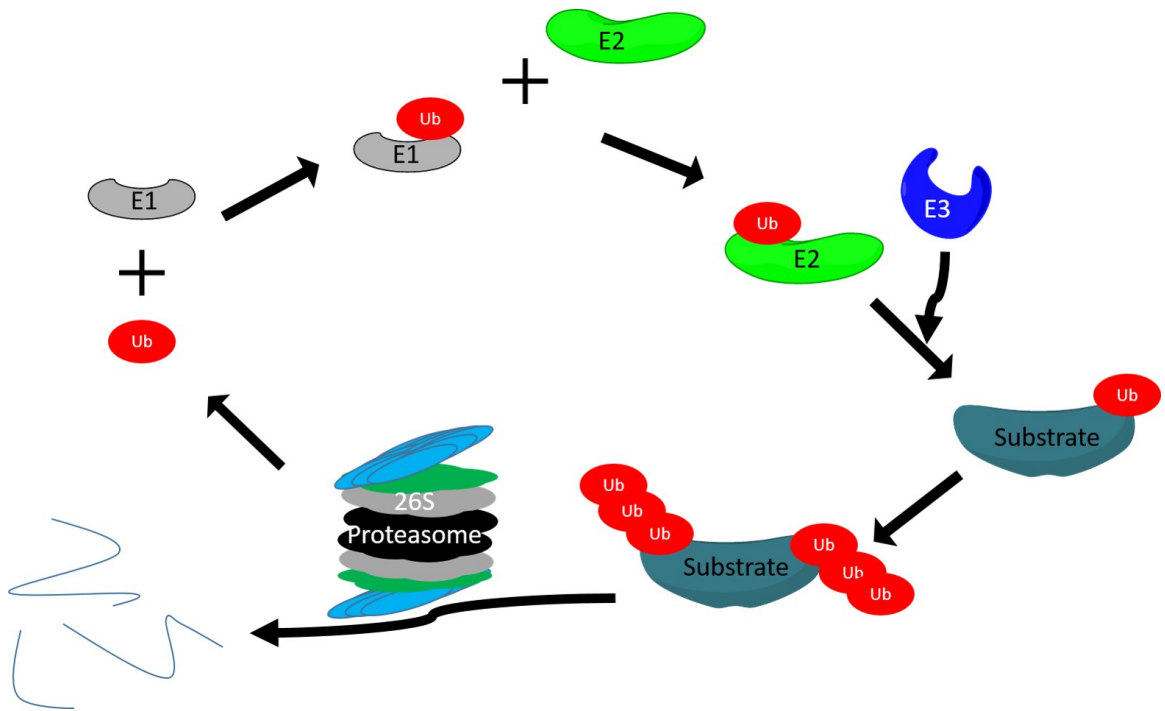


Fig. 1.2.: **The ubiquitin proteolysis system.**

Ubiquitin (Ub) is first activated in an ATP-dependent reaction to form a thioester bond with the E1 activating enzyme. Ubiquitin is then transferred to a conjugating (E2) enzyme. Substrates targeted for polyubiquitination are then modified, in conjunction with an E3 ubiquitin ligase enzyme. The E3 ligase provides selectivity and determines the identity of substrates being polyubiquitinated. Ubiquitin is covalently attached to the substrate, via an isopeptide bond, between the carboxyl group of the C-terminal Gly and the ϵ -primary amino group of a Lys residue in the substrate. Polyubiquitinated substrates are subsequently recognized by 26S proteasome and degraded. Deubiquitinating enzymes (DUBs) serve to recycle ubiquitin.

the recognition of ubiquitin chains on substrates before their translocation into the 20S core [42].

1.4.1 Ubiquitination targets proteins to the proteasome

Substrate selectivity of the proteasome is largely a product of restricted access to the proteolytic active sites [43]. A common mechanism by which substrates are targeted to the proteasome is via the attachment of polyubiquitin chains (Figure 1.2). Polyubiquitination is achieved by the covalent attachment of multiple ubiquitins to a substrate, mainly on lysine residues in a selective process. A minimum chain length of 4 ubiquitins is required for substrates to access the 26S proteasome active site [43,44]. This observation has more recently been challenged by Ying Lu, *et al.*, who have demonstrated that APC substrates with multiple ubiquitinated lysines are better proteasome substrates than those with the same number of ubiquitins conjugated, but have fewer and longer ubiquitin chains [45].

Polyubiquitinated substrate selectivity is a product of the specificity of E3 ubiquitin ligases that function downstream of E2 (ubiquitin conjugating enzymes) which are downstream of E1 (ubiquitin activating) enzymes [46] (Figure 1.2). E1 enzymes activate ubiquitin by forming a high energy thioester bond in an ATP-dependent reaction. Ubiquitin is then transferred to an E2 conjugating enzyme via a transthio-lation reaction in an E1-Ub dependent reaction to form a high-energy thioester bond between ubiquitin and the cognate E2. In *Saccharomyces cerevisiae*, there is a single E1 [47], a dozen E2s, and diverse classes of E3 ligases [46].

There are three major classes of E3 ubiquitin ligases identified thus far, the HECT (homologous to E6-associated protein C-terminus), RING (really interesting new gene) domain, and U-box (modified RING motif) E3s [48]. HECT E3 ligases contain both a substrate recognition element as well as a ubiquitin ligation active site. In contrast, RING E3s do not directly participate in the chemical transfer of ubiquitin. RING E3s are thought to function as scaffolds that bring E2 conjugating enzymes

and substrate proteins into proximity and promote the transfer of Ub directly from E2s [49].

1.4.2 Polyubiquitin-independent proteasomal degradation

Although it has been well established that ubiquitination is the major mechanism for targeting proteins to the proteasome, it is clear that alternative mechanisms exist. A well-established ubiquitin independent mechanism is the proteasomal degradation of ornithine decarboxylase (ODC) [50,51]. ODC, the first enzyme in polyamine synthesis, is targeted for degradation to the proteasome by its interaction with antizyme, a protein that becomes abundant during high cellular polyamine concentration. It has been postulated that antizyme is able to engage the 19S particle of the proteasome and deliver ODC for degradation. Outside of ODC degradation, Antizyme has been demonstrated to target Aurora-A for degradation in HeLa cells [52].

1.4.3 The Anaphase Promoting Complex (APC) during mitotic exit

In the context of the cell cycle, there are two major E3 ligases that function in cell cycle regulation, Skp1-Cullin-1-F-box protein (SCF) and the APC [53]. In budding yeast, the SCF ubiquitinates substrates to promote S phase, including the Cdk inhibitor Sic1, which allows for the activation of S phase Cdk/cyclin complexes [54,55]. The APC, on the other hand, is responsible for driving mitotic progress, namely sister chromatid segregation and mitotic exit as well as establishing and maintaining G1 [56].

The APC is responsible for ubiquitin-mediated proteolysis of numerous proteins to drive mitotic exit [57]. At the metaphase to anaphase transition the APC targets Securin (Pds1 in yeast), an inhibitor of chromosome segregation, for destruction [58]. Pds1 degradation allows for the activation of the protease separase (Esp1 in budding yeast) which is responsible for cleaving the cohesin rings that tie sister chromatids together [26,58]. The APC is also essential for the destruction of mitotic cyclins such

as Clb2 to terminate Cdk activity, allowing exit from mitosis [59]. APC also promotes destruction of components of the mitotic spindle apparatus such as Fin1, Ase1, and Cin8 in yeast to disassemble the spindle at the end of mitosis [60–62].

APC co-activators determine substrate recognition

The APC is a large, $\approx 1.5\text{MDa}$, multi-subunit E3 ubiquitin ligase complex (Figure 1.3). The human APC consists of 12 identified core subunits and the budding yeast APC has 13 [63]. The Core APC has two sub-complexes; one sub-complex contains Apc2 and Apc11 that are essential for ligase activity as well as Doc1 that is required for processive ubiquitination of substrates (Figure 1.3) [64]. The cullin domain of Apc2 interacts with the RING domain of Apc11 which is suggested to be responsible for association with both E2 ubiquitin-conjugating enzyme and a substrate [65,66]. The other sub-complex contains three TPR (tetra-trico-peptide repeat domain) proteins, Cdc27, Cdc16, and Cdc23 that mediate protein-protein interactions between subunits. Both sub-complexes are held together by the largest subunit, Apc1. Both Apc4 and Apc5 connect Apc1 to the TPR sub-complex via Cdc23.

In addition to the core subunits, APC activity requires transient association with a co-activator subunit. The core APC is present constitutively during the entire cell cycle; but association with one of its co-activators, either Cdc20 or Cdh1, in a cell cycle-dependent manner limits APC activity to mitosis and G1 [59,67–69].

The Cdc20 and Cdh1 co-activators are structurally related proteins responsible for APC's substrate selectivity [67]. These co-activators bind sequentially to the core APC as cells progress through mitosis. In budding yeast, Cdc20 is essential for anaphase onset and Pds1 degradation [70]. Most known substrates of the APC have destruction motifs (degrons) such as D-box (RxxLxxxxN) and/or KEN, which are required for their ubiquitination-dependent proteolysis [71–73]. Other sequence elements such as A-box (in Aurora A) [74], CRY box (Cdc20 in GV-stage mouse

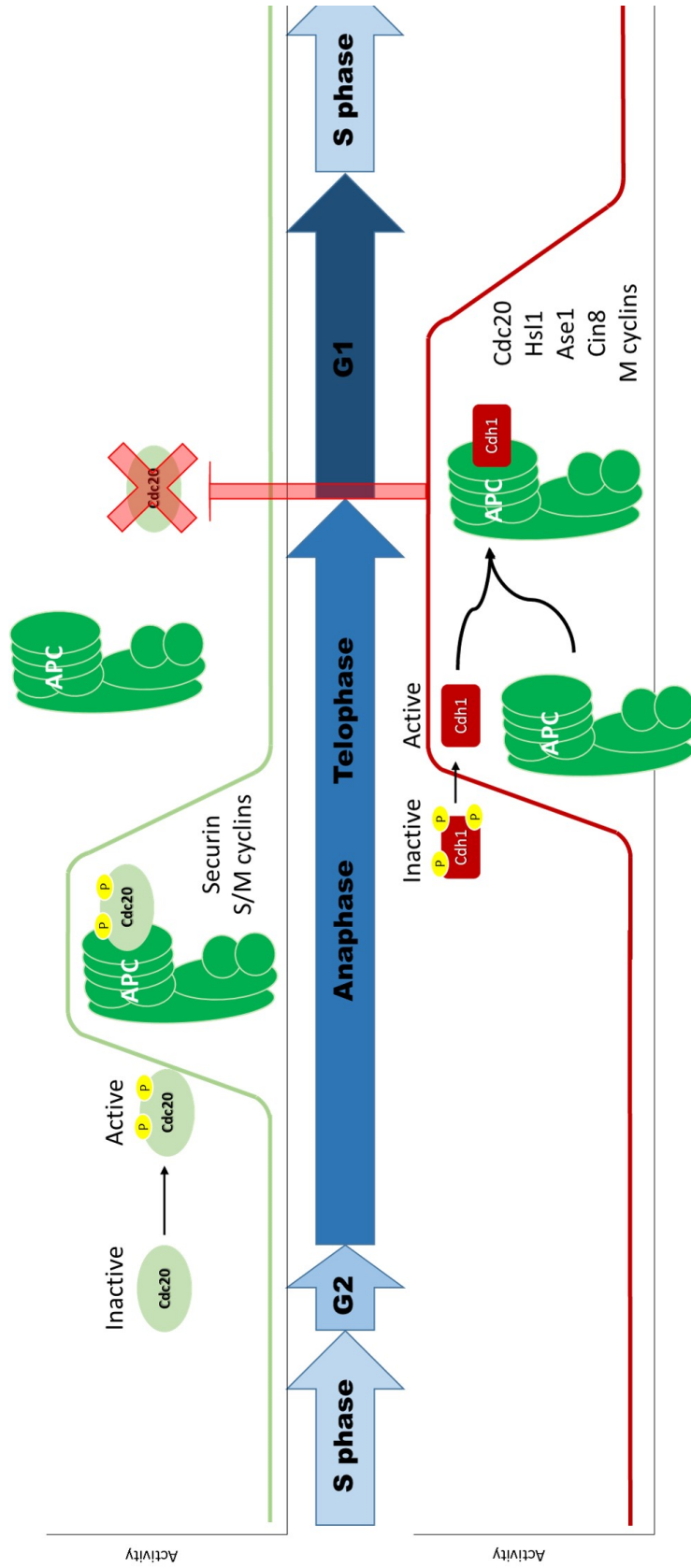


Fig. 1.3.: **APC function is essential for mitotic exit.** The APC binds to its coactivators (Cdc20 and Cdh1) sequentially during mitosis. APC^{Cdc20} activity is required for anaphase transition. In late mitosis, Cdc20 is degraded by APC^{Cdh1} following Cdh1 dephosphorylation and its association with the core APC. APC^{Cdh1} remains active during G1 and is inactivated as Cdk activity returns during S phase entry.

oocytes) [75], or O-box (degradation of ORC1 in *D. melanogaster*) [76] have also been demonstrated as recognition motifs in substrates by the APC.

Although the mechanisms by which APC and a co-activator recognize substrates and how co-activators discriminate between destruction motifs are still unclear, it is known that the co-activators are major targets for regulating APC activity. A combination of phosphorylation and protein degradation are employed to regulate APC activity. Both APC co-activators (Cdc20 and Cdh1) are highly regulated through phosphorylation by Cdk and Cdc5/Polo kinase. Cdc20 activity is largely limited to the initiation of mitotic exit, when Cdk activity is high [77] and its phosphorylation promotes Cdc20 association with the core APC resulting in the degradation of substrates like Pds1, Clb5, and Dbf4 [68, 78]. Cdc20 is also involved in the activation of Cdh1 as it degrades mitotic cyclins leading to lowered mitotic Cdk activity. The reduction in mitotic Cdk activity, in combination with Cdc14 phosphatase mediated dephosphorylation, leads to the reduction in the inhibitory phosphorylation of Cdh1 [79] and increased Cdh1 association with the core APC [34, 80].

Multiple mechanisms regulate APC^{Cdh1} activity

Cdh1 is an APC activating subunit that is homologous to Cdc20, and is able to complement Cdc20 mutants when expressed in high copy number [59]. In contrast to Cdc20, Cdh1 deletion in budding yeast is not lethal but the degradation of many proteins, like Ase1, which leads to spindle disassembly and Clb2, which, in turn, results in inactivation of mitotic cyclins, is impaired [59, 67]. APC^{Cdh1} function is also important to establish conditions necessary for DNA replication in S phase. Cdh1 and Sic1 have been demonstrated to promote efficient origin firing at origins of replication during S phase entry [81]. In mice, loss of APC^{Cdh1} has been associated with genomic instability resulting in embryonic lethality [82].

Regulation of Cdh1 is different from that of Cdc20 as Cdh1 protein abundance is fairly stable throughout the cell cycle and it is a target of multiple kinases that

regulate its activity [80,83]. Cdh1's ability to activate APC is inhibited by Cdk phosphorylation beginning in late G1 until late mitosis. Cdh1 is unable to bind the APC when phosphorylated in early mitosis and requires dephosphorylation by Cdc14 phosphatase at mitotic exit for its activation [84]. It has been shown that overexpression of an unphosphorylatable Cdh1 mutant (*cdh1-m11*) is lethal in yeast [62]. This phosphoregulation ensures that APC^{Cdc20} is activated and has degraded mitotic cyclins before APC^{Cdh1} is able to drive late mitotic events. Failure to inactivate APC^{Cdh1} also prevents accumulation of mitotic cyclins and results in G2/M phase arrest.

Acm1 is a pseudosubstrate inhibitor of APC^{Cdh1}

Several pseudosubstrate inhibitors which use degron motifs, similar to those found in APC substrates, to bind to APC and interfere with substrate binding, have been identified. Examples include Mad3, a subunit of the spindle assembly checkpoint. Mad3 is a pseudosubstrate inhibitor of the APC^{Cdc20} responsible for delaying anaphase when errors occur in chromosome attachment to the mitotic spindle by preventing the degradation of Pds1 [85]. In vertebrates, APC^{Cdh1} can be inhibited by Emi1, which is important for the stabilization of cyclin A and S phase entry [86].

In budding yeast, APC^{Cdh1} is inhibited by a pseudosubstrate called Acm1. Acm1 forms a ternary complex with Cdh1 and the 14-3-3 homologs Bmh1 and Bmh2 [88]. Acm1 inhibits APC^{Cdh1} mediated polyubiquitination of Clb2, Hsl1, and Fin1 *in vitro* [88–90]. The overexpression of Acm1 is also able to rescue the toxicity of *Cdh1-m11* overexpression [88].

Acm1 binds tightly to Cdh1 via conserved D and KEN boxes which interact with the Cdh1 WD40 domain (Figure 1.4) [88, 89, 91, 92]. The reasons why Acm1 can bind Cdh1 via its degron sequences, in the same manner as substrates, but avoid polyubiquitination and degradation are not known. There is preliminary evidence that suggests there are additional sequence elements within Acm1, proximal to its

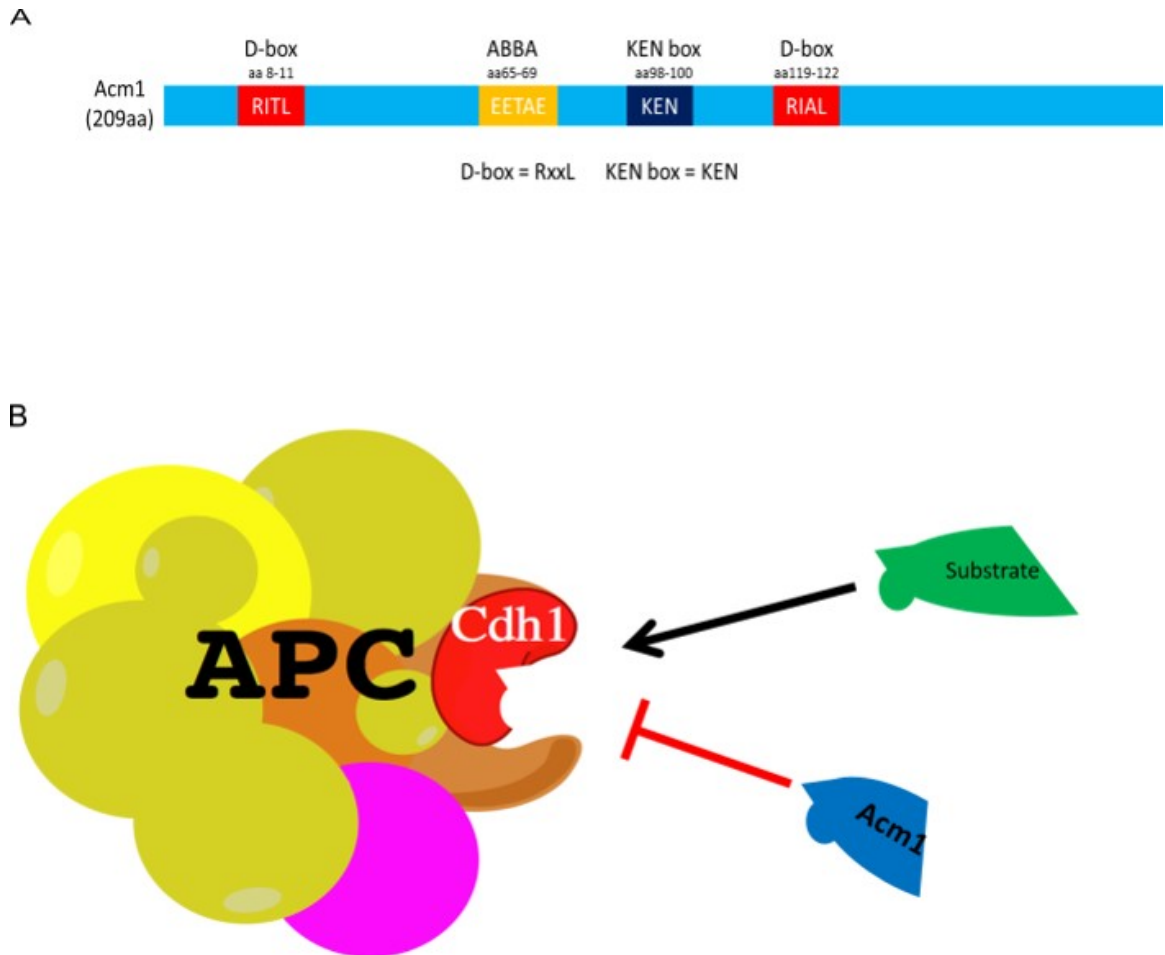


Fig. 1.4.: **Acm1 is a pseudosubstrate inhibitor of APC^{Cdh1}**

A. Acm1 contains D and KEN box sequences that are commonly found in APC^{Cdh1} substrates. These sequences are necessary for Acm1 binding to Cdh1 and its ability to inhibit substrate degradation. The ABBA motif shown is also a sequence that is known to contribute to Cdh1 binding [87].

B. Acm1 inhibits APC^{Cdh1} by competing for substrate binding sites on Cdh1.

second D box, that distinguish it from substrates, but the mechanisms are not yet clear (L. Qin, unpublished results).

Deletion of *Acm1* does not result in inappropriate activation of APC^{Cdh1} , due to the robust effect of Cdk phosphorylation. Instead, *Acm1* is important for preventing premature binding of Cdh1 to substrates, particularly the bud neck kinase Hsl1, which can impair their functions. Loss of *Acm1* leads to premature accumulation of Cdh1 at the bud neck, via interaction with Hsl1, resulting in improper positioning of the mitotic spindle along the mother-bud axis prior to nuclear division which normally ensures one set of chromosomes ends up in the bud [93].

Consistent with *Acm1*'s role as a Cdh1 inhibitor, *Acm1* protein abundance changes with the cell cycle. *Acm1* is found at higher abundance from late G1 to late mitosis [88, 89, 92] when APC^{Cdh1} is inactive. Multiple mechanisms result in *Acm1* degradation, one of which is dependent on the APC^{Cdc20} [91]. However, complete degradation of *Acm1* at the end of mitosis requires an additional APC-independent, proteasome-dependent mechanism [89, 94].

Unphosphorylatable *Acm1* mutant is constitutively degraded

Acm1 is a phosphoprotein and is a target of Cdk [92, 94]. Mass spectrometric analysis revealed that *Acm1* is phosphorylated at Cdk consensus sequences. Mutation of five Cdk sites to alanine leads to a significant reduction in *Acm1* stability in all phases of the cell cycle [94]. These data illustrate that phosphorylation of *Acm1* is necessary for its stability and dephosphorylation in late mitosis leads to its rapid degradation. Inhibition of the yeast proteasome with drug treatment causes abnormal *Acm1* protein stability [92]. The mechanism that targets *Acm1* for degradation by the proteasome is non-canonical and is discussed in Chapter 2.

1.5 Mitotic phosphatases reverse Cdk phosphorylation

Beyond the inactivation of mitotic Cdks, mitotic exit and cytokinesis require active reversal of Cdk phosphorylation by mitotic phosphatases [27]. Recent developments are beginning to shed light on the complexity of the mechanisms regulating the activity of mitotic phosphatases [35]. The protein phosphatases Cdc14, PP1 and PP2A play significant roles in reversing Cdk-dependent protein phosphorylation [32–35].

1.5.1 PP1 and PP2A contribute to mitotic exit

PP1 and PP2A are multimeric members of the serine/threonine phosphoprotein phosphatase (PSP) family of phosphatases. As is the case for many PSPs, PP1 and PP2A are regulated and their specificity defined through combinatorial interactions between a common catalytic subunit and various regulatory subunits [95]. Both have been implicated in the reversal of Cdk mediated phosphorylation, which is important for mitotic exit [35].

PP1 functions typically as a dimer consisting of a catalytic subunit (PP1c), which is encoded by *GLC7* in budding yeast [96] and is one of many regulatory subunits. The catalytic subunit is highly conserved among all eukaryotes with about 70% identity across any pairwise alignments [95]. Many of the regulatory subunits bind to PP1c through a highly conserved RVXF/W docking motif [97]. The regulatory subunits determine *in vivo* substrate specificity by either directing the holoenzyme subcellular localization and/or altering its substrate selectivity.

PP2A is a heterotrimeric complex consisting of a structural A subunit, a regulatory B subunit and a catalytic C subunit [98]. The B-regulatory subunits regulate both localization and substrate selectivity of the PP2A complex. The two B-regulatory subunits in budding yeast (Cdc55 and Rts1) bind PP2A in a mutually exclusive manner. PP2A^{Cdc55} is required for the spindle assembly checkpoint [98,99] and targets Cdc25 (Mih1) for dephosphorylation during mitosis leading to increased Cdk1 activity [100].

1.5.2 Cdc14 activity counteracts Cdk1 mediated phosphorylation

Cdc14 is a member of the dual specificity phosphatase (DSP) family, a subgroup of the larger PTP super family [101, 102]. Cdc14 phosphatases contain the active site sequence CX₅R, which is a hallmark for the protein tyrosine phosphatase (PTP) superfamily (Figure 1.5) [103]. In budding yeast, Cdc14 is the major phosphatase required for mitotic exit and remains sequestered in the nucleolus until early anaphase at which point it is able to dephosphorylate various Cdk1 substrates [34, 104].

Chromosome segregation, spindle disassembly and cytokinesis are late mitotic events requiring reversal of Cdk mediated phosphorylation. Beyond the inactivation of Cdk activity by the degradation of cyclins, Cdk substrates are need to be dephosphorylated [33]. The budding yeast phosphatase Cdc14 has, for a long time, been recognized as an essential regulator of mitotic exit. *cdc14* mutants arrest in late mitosis in a telophase like state [105]. Cdc14 triggers mitotic exit by reversal of Cdk-mediated phosphorylation [34]. Cdc14 dephosphorylates Swi5, a transcription factor for the Cdk inhibitor Sic1 [106], Sic1 itself, leading to its stabilization [34] and the APC co-activator Cdh1 [80], which targets mitotic cyclins for degradation. Dephosphorylation of Swi5 also leads to the transcriptional activation of other genes at the M/G1 transition, such as Egt2 [107], required for normal septation. Iqg1 has also recently been identified as an important Cdc14 substrate in regulating actomyosin ring contraction during cytokinesis [108]. Cdc14 function is also important for formation of the pre-replication complex (pre-RC) via dephosphorylation of the replication initiation proteins Orc2, Orc6, Cdc6, and Mcm3, to allow DNA replication in the subsequent S phase [109]. Cdc14 also regulates the localization and enzymatic activity of Yen1, a Holiday junction resolvase that plays a role in DNA damage repair [110, 111].

Cdc14 activity is tightly regulated

In accordance with its essential role in mitotic exit, Cdc14 activity is under strict regulation. Its activity is regulated both by the binding of a competitive inhibitor

as well as by its subcellular localization. For most of the cell cycle until metaphase, Cdc14 is sequestered and inhibited in the nucleolus by Net1, as part of the regulator of nucleolar silencing and telophase (RENT) complex [112–114]. Cdc14 disassociation from its inhibitor and its resulting spread, first, to the nucleoplasm in early anaphase, and then, throughout the cytoplasm in late anaphase/telophase occurs via two distinct and sequential regulatory mechanisms: the Cdc fourteen early anaphase release (FEAR) and Mitotic Exit Network (MEN) pathways, respectively. The FEAR network initiates Cdc14 release within the nucleus and its association with the spindle pole body as well as the mitotic spindle, mainly to promote proper chromosome segregation. The MEN is activated during telophase and results in the spread of Cdc14 to the cytoplasm where it drives mitotic exit and cytokinesis [35].

There is an increasing body of evidence that Cdc14's intrinsic selectivity is a driver for the order of mitotic substrate dephosphorylation. It has been shown that Cdc14 substrates are targeted in two distinct windows of time [115]. Jin et al. tested whether early Cdc14 substrates were targets of FEAR released Cdc14 and were preferentially phosphorylated by Cdk1-Clb5 and later substrates of MEN Cdc14 were Cdk1-Clb2 substrates. They observed that the release mechanism does not determine Cdc14 specificity, illustrated by the dephosphorylation of Sld2, an early anaphase substrate, by both FEAR and MEN released Cdc14, in nocodazole arrested cells. Although the decrease in Clb5 activity contributes to the steady state levels of early Cdc14 substrates and high Clb2 activity delays the loss of phosphorylation of late substrates, it does not completely account for the observed timing of substrate dephosphorylation [104]. Bouchoux et al. show that Cdh1 and Orc6, which are preferential Cdk1-Cdc5 substrates, are late Cdc14 substrates. They also show that ectopic Cdc14 expression in cells arrested in metaphase does not change the order in which Cdc14 substrates are dephosphorylated, suggesting a central role for Cdc14 as the main driver of sequential substrate dephosphorylation, independent of other mitotic events. The study also demonstrated the catalytic efficiency of Cdc14 towards Fin1, an early Cdc14 substrate

was 20 times greater than that of Orc6 [104]. The underlying reasons for this substrate preference have not yet been completely elucidated.

1.5.3 Cdc14 is conserved across multiple species

Although the Cdc14 gene is highly conserved (Figure 1.5), the reversal of mitotic phosphorylation in other eukaryotes does not strictly require Cdc14. Cdc14 homologs are found in multiple eukaryotes spanning a large evolutionary space. Studies in a variety of organisms suggest that Cdc14 is not required for Cdk inactivation or for bulk Cdk substrate dephosphorylation [116, 117]. Although these phosphatases play roles during mitotic exit, they are only essential in budding yeast. An interesting observation pointing to a functional conservation is that the two human Cdc14 paralogs (A and B) are able to rescue the *cdc14* phenotype in both budding [118, 119] and fission yeast [120]. The specific biological functions of Cdc14 in organisms other than budding yeast are still poorly characterized and the extent to which functions might be conserved across divergent eukaryotes remains unclear. A discussion of the current data is presented below.

Schizosaccharomyces pombe Cdc14 orthologue, Clp1, is kept sequestered in the nucleolus as is the case for budding yeast. However, unlike *S. cerevisiae* Cdc14, Clp1 is not essential for normal cell cycle progression and is released from the nucleolus earlier in mitosis [121]. Clp1 is mainly responsible for regulating cytokinesis and affects the timing of mitotic entry [122, 123]. Clp1 promotes mitotic exit by promoting the dephosphorylation and subsequent degradation of Cdc25. *Clp1* Δ cells display cytokinesis defects and advance prematurely into mitosis but continue to grow. Meanwhile, cells overproducing Clp1 delay Cdk1 activation but are able to progress through mitosis [122].

There are inconclusive reports regarding the function of Cdc14 in *Caenorhabditis elegans*. One group has reported that depletion of *C. elegans* Cdc14 results in embryonic lethality [124]. However, another study demonstrated that *cdc14* heterozygous

null worms are viable and fertile [125]. It was also shown that CeCdc14 localizes to the central spindle during anaphase and the midzone during telophase suggesting a role in mitotic events.

In contrast to *S. cerevisiae* Cdc14, either of the two human paralogs (hCDC14A and B) are dispensable for the cell cycle. Ectopic expression of hCDC14A results in the dephosphorylation of Wee1 and its degradation by the proteasome [126] and delays mitotic entry by counteracting Cdk1-Cyclin B1 activity [120]. Overexpression of hCDC14B has been shown to transform cells [127]. As an indicator of functional divergence between the two paralogs, this same study demonstrated that overexpression of hCDC14A did not result in transformation. hCDC14A and B also appear to localize differently during interphase; hCDC14A at the centrosome and hCDC14B at the nucleolus [128]. Specific functions and molecular targets of human Cdc14 enzymes remain poorly understood.

1.5.4 *S. cerevisiae* Cdc14 is highly selective for a subset of Cdk phosphorylation sites

The crystal structure of hCDC14B shows that it is made up of two structurally similar domains arranged in tandem [102]. The N-terminal domain (domain A, aa 44-198), thought to contribute to substrate selectivity, has no sequence similarity to other dual specificity phosphatases. The C-terminal domain (domain B, residues 213-368) contains the PTP motif. The hCDC14B active site is within the groove at the domain A and B interface.

Cdc14 phosphatases are unique, in that, despite being members of the PTP family, they have evolved to specifically dephosphorylate a subset of Cdk substrates. Cdks phosphorylate Ser/Thr-Pro sites. Cdc14 phosphatases have a strict selectivity for Cdk phosphoSer-Pro (pS-P) sites. Moreover, they strongly prefer sites followed by a basic residue at the +3 position (pS-P-X-K, where X represents any amino acid) with additional downstream basic residues enhancing activity [129, 130].

Our enzymatic studies and the crystal structure solved for hCDC14B in complex with a peptide indicate that Cdc14 substrate selectivity is primarily determined by the active site region [102]. The residues thought to contribute to catalysis and substrate binding (the acidic groove, +1 Pro binding, +3 lysine binding and pSer selectivity) highlighted in Figure 1.5 are highly conserved across multiple species. Unlike other mitotic phosphatases previously discussed, Cdc14 does not function as part of a multimeric complex. Taken together, these observations suggest that Cdc14 enzymes could display similar substrate selectivity across multiple species and may be amenable to the development of highly specific competitive inhibitors.

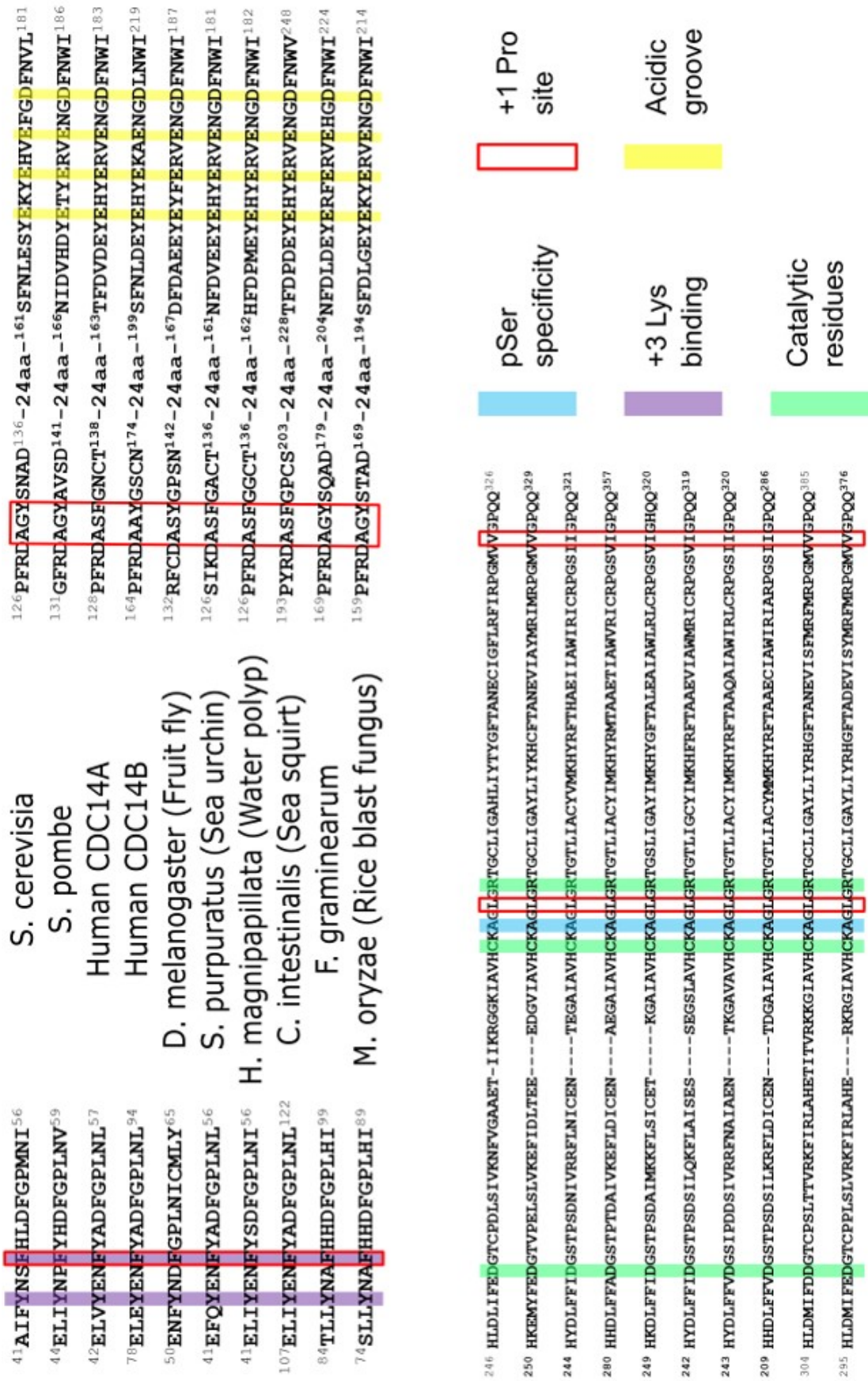


Fig. 1.5.: (Caption on next page)

Fig. 1.5.: (Previous page) **Cdc14 catalytic and substrate interacting motifs are conserved.** Alignment of Cdc14 protein sequences from an evolutionarily diverse set of organisms. The observed conservation of sequences responsible for catalysis and substrate selectivity indicates that the enzymatic behavior observed in budding yeast Cdc14 is likely to be conserved across multiple species.

1.6 Mitotic exit as a therapeutic target

One of the central characteristics of cancer cells is the loss of proliferative control [131]. This can take the form of either adaptations that allow cells to keep growth signals active or result from deactivation of growth limiting mechanisms. Inability to regulate mitotic exit and failure to achieve appropriate temporal control of mitotic exit events is a potential driving factor in the progression of cancer [132].

A chemotherapeutic strategy that has been clinically relevant in treating cancer for some time has been the chemical perturbation of mitotic spindle function by taxanes and vinca alkaloids (reviewed in [133, 134]). The strategy relies on the activation of the spindle assembly checkpoint (SAC) in the presence of a defective spindle, which inhibits APC^{Cdc20}-mediated securin and cyclin B degradation, and causes an arrest at metaphase. The sustained mitotic arrest eventually leads to programmed cell death [134]. It has been observed that cells can undergo mitotic slippage and escape from arrest by slowly degrading cyclin B1 even though the SAC is activated by these drugs [135]. Cancerous cells often develop the ability to overcome the microtubule-targeted mitotic arrest by inappropriately inducing mitotic exit, which further leads to genome instability. Thus, one of the major challenges with developing effective chemotherapies that disrupt mitotic spindle function has been avoiding slippage or other mechanisms of resistance [136].

An alternative therapeutic strategy that has been proposed is the inhibition of APC activity, because securin and cyclin B degradation by the APC is an essential step in mitotic exit [137]. The genetic ablation of Cdc20, the APC activating subunit,

in cancerous cells has been demonstrated to reduce proliferation by preventing mitotic exit [138]. Sackton et al. have also shown that a combination of two chemicals is able to block the interaction of APC with Cdc20 as well as Cdc20 with D box containing substrates, resulting in blockage of mitotic exit [139]. Another study has demonstrated that coupling microtubule disrupting drugs with the depletion of Cdc20 is capable of reducing the probability of mitotic slippage [136]. This study also found Cdc20 knockdown more effective at inducing a longer mitotic blockage, compared to spindle-perturbing drugs, which led to increased apoptosis. These studies suggest targeting mitotic exit processes is a viable and potentially more effective therapeutic strategy.

1.6.1 Utility of Cdc14 inhibitor development

As discussed above, targeting mitotic exit for chemotherapy results in improved therapeutic efficacy, especially when spindle function is simultaneously disrupted [136]. Inhibiting Cdc14 activity, which plays a role in mitotic exit, in combination with spindle disrupting drugs, might also prove to be an effective therapeutic approach. Cdc14 is also known to play a role in the G2 DNA damage response checkpoint [140]. This raises the possibility of improving the effectiveness of DNA damaging chemotherapeutic agents like doxorubicin by simultaneously inhibiting Cdc14 to prevent an effective DNA damage checkpoint response.

1.6.2 Cdc14 inhibitors as research tools

As discussed in previous sections, the role of Cdc14 in regulating the cell cycle has only been extensively studied in budding yeast, where it is essential for cell cycle progress, and in fission yeast, where it is not essential and phenotypes observed are somewhat mild. Outside of these unicellular organisms, there have not been definitive results from efforts to understand Cdc14 function. The fact that most

higher eukaryotes have multiple paralogs of the enzyme makes it more difficult to study its role, because it is not known if these paralogs are functionally redundant.

The development of a specific and high affinity inhibitor of Cdc14 has the potential to be useful in elucidating Cdc14 roles in higher eukaryotes, including humans. Such an inhibitor would allow the simultaneous inhibition of all Cdc14 activity in cells, which has, thus far, not been achieved by genetic approaches.

2. ACM1 IS DEGRADED VIA AN UNCONVENTIONAL MECHANISM

2.1 Introduction

¹Proper execution of the eukaryotic cell division cycle depends heavily on ubiquitin-mediated proteolysis, involving the conjugation of polyubiquitin chains to substrate proteins by E3 ubiquitin ligases and their subsequent recognition and degradation by the 26S proteasome [38]. Coupled with transcriptional regulation, proteolysis helps establish cell cycle-dependent protein expression profiles for many key regulators of cell division, contributing to precise control of the initiation and order of cell cycle events [53, 137]. Two large ubiquitin ligase complexes are responsible for the majority of regulated proteolysis during the cell division cycle [53, 141, 142]. One, the Skp1/cullin/F-box protein complex (SCF) is well known for promoting the degradation of G1 cyclins, cyclin-dependent kinase (Cdk) inhibitors, and numerous other substrates, and is thought to be constitutively active. However, recognition of most SCF substrates requires their cell cycle-dependent phosphorylation [143]. The second, the anaphase-promoting complex (APC), or cyclosome, targets the chromosome segregation inhibitor securin, S and M phase cyclins, and many other proteins for degradation during mitosis and G1 [144, 145]. In contrast to SCF, the activity of APC is cell cycle-regulated by several mechanisms including phosphorylation of, and inhibitor binding to, its activator proteins Cdc20 and Cdh1 [146]. Following conjugation of polyubiquitin chains to substrate lysines by SCF and APC, recognition by

1

This chapter has been reprinted from Melesse M, Choi E, Hall H, Walsh MJ, Geer MA, Hall MC (2014) Timely Activation of Budding Yeast APC^{Cdh1} Involves Degradation of Its Inhibitor, Acm1, by an Unconventional Proteolytic Mechanism. PLoS ONE 9(7): e103517. doi:10.1371/journal.pone.0103517 under the Creative Commons Attribution 4.0 International License. To view a copy of this license, visit <http://creativecommons.org/licenses/by/4.0/> or send a letter to Creative Commons, PO Box 1866, Mountain View, CA 94042, USA.

the 26S proteasome results in their irreversible degradation, and helps drive the cell cycle forward.

In this report, we describe an unconventional proteolytic mechanism, independent of SCF and APC, that helps establish the strict cell cycle expression profile of the APC inhibitor Acm1 in budding yeast. Acm1 was identified several years ago by our lab as a tight binding partner and inhibitor of the APC activator Cdh1 [88, 90]. Acm1 uses substrate-like degron sequences to competitively inhibit substrate binding to Cdh1, making it one of several pseudosubstrate inhibitors of the APC identified in diverse eukaryotes. One important function of Acm1 appears to be ensuring proper positioning of the nucleus along the mother-bud axis prior to nuclear division. Acm1 does this by limiting the premature accumulation of Cdh1 at the bud neck via interaction with its high affinity substrate Hsl1 [93], although the details of how this contributes to proper nuclear orientation remain unclear.

Acm1 expression is very tightly cell cycle-regulated. Acm1 protein is absent from G1 cells, appears around the onset of S phase, and rapidly disappears in late mitosis, after anaphase onset [88, 90, 91]. The ACM1 promoter is also cell cycle regulated as part of a large collection of genes turned on at the beginning of S phase [147]. Two distinct proteolytic mechanisms have been reported to clear cells of Acm1 at the end of mitosis. First, consistent with the cell cycle profile of Acm1 being reminiscent of APC substrates, Acm1 was shown to be a target of APC^{Cdc20} during anaphase [91].

In other studies, Acm1 was shown to be very sensitive to an APC-independent proteolytic mechanism in G1 [92, 94]. This APC-independent mechanism is inhibited by Cdk phosphorylation on Acm1 such that Acm1 is stable only during the cell cycle window of high Cdk activity. The results presented here provide confirmation of both proteolytic mechanisms but demonstrate that the APC-independent mechanism is both necessary and sufficient for complete elimination of Acm1 during mitotic exit. Interestingly, several lines of evidence suggest that this mechanism is independent of the conventional ubiquitin conjugation pathway, although it is still mediated by the 26S proteasome. This is one of the first examples of a strict cell cycle expression

pattern established by proteolytic mechanisms independent of SCF and APC. The existence of two distinct degradation pathways for Acm1 suggests it is critical for yeast cells to relieve Cdh1 inhibition in a timely manner to promote mitotic exit, cytokinesis, and establishment of the ensuing G1 and we provide evidence to support this.

2.2 Results

2.2.1 APC^{Cdc20} activity is not sufficient for complete Acm1 degradation

Acm1 was reported to be effectively eliminated via APC^{Cdc20} prior to mitotic exit [91]. However, we originally identified Acm1 as a Cdh1 binding partner at the late anaphase arrest point of a *cdc15-2* strain [88] and therefore suspected that APC^{Cdc20} might not be sufficient for complete elimination of Acm1. To test this rigorously we had a polyclonal antibody raised against recombinant Acm1 so we could monitor endogenous Acm1 protein without addition of an epitope tag. Synchronized *dbf2-2* cultures were released from α -factor-induced G1 arrest into fresh medium at 37°C so they would arrest in late anaphase, a point where APC^{Cdc20} has been activated and has targeted its substrates for degradation (Figure 2.1A and 2.1B). As expected, the levels of the well-characterized Cdc20 substrates Clb5 and Pds1 rapidly dropped as cells reached the arrest point. In contrast, the Acm1 level decreased more slowly and a substantial fraction (>30%) of Acm1 remained after a lengthy arrest.

Next, to definitively test for the presence of an APC-independent proteolytic mechanism acting on endogenous Acm1 protein in late mitosis and G1, we probed for Acm1 in extracts from synchronized cultures of a yeast strain (*apc2* Δ *apc11* Δ *cdc20* Δ *cdh1* Δ *pds1* Δ *clb5* Δ *SIC1*^{10x}) engineered to survive in the complete absence of APC activity by deletion of the essential APC substrate genes *CLB5* and *PDS1*, and 10-fold overexpression of the Cdk inhibitor Sic1 [148]. When compared with a control strain containing wild-type APC, Acm1 levels cycled normally (Figure 2.1C), being absent from G1 cells as previously reported [88]. In contrast, the APC substrate Clb2 was

strongly stabilized and present throughout the cell cycle in the absence of APC activity. These results are consistent with previous studies of overexpressed Acm1 stability in G1-arrested cells harboring a conditional APC mutant allele [92,94]. We conclude that APC^{Cdc20} is not sufficient for complete elimination of Acm1 in late mitosis and that an APC-independent mechanism is also required. In the absence of APC activity this APC-independent mechanism is sufficient for complete Acm1 elimination in late mitosis and G1. We therefore set out to characterize the APC-independent proteolytic mechanism responsible for Acm1 degradation.

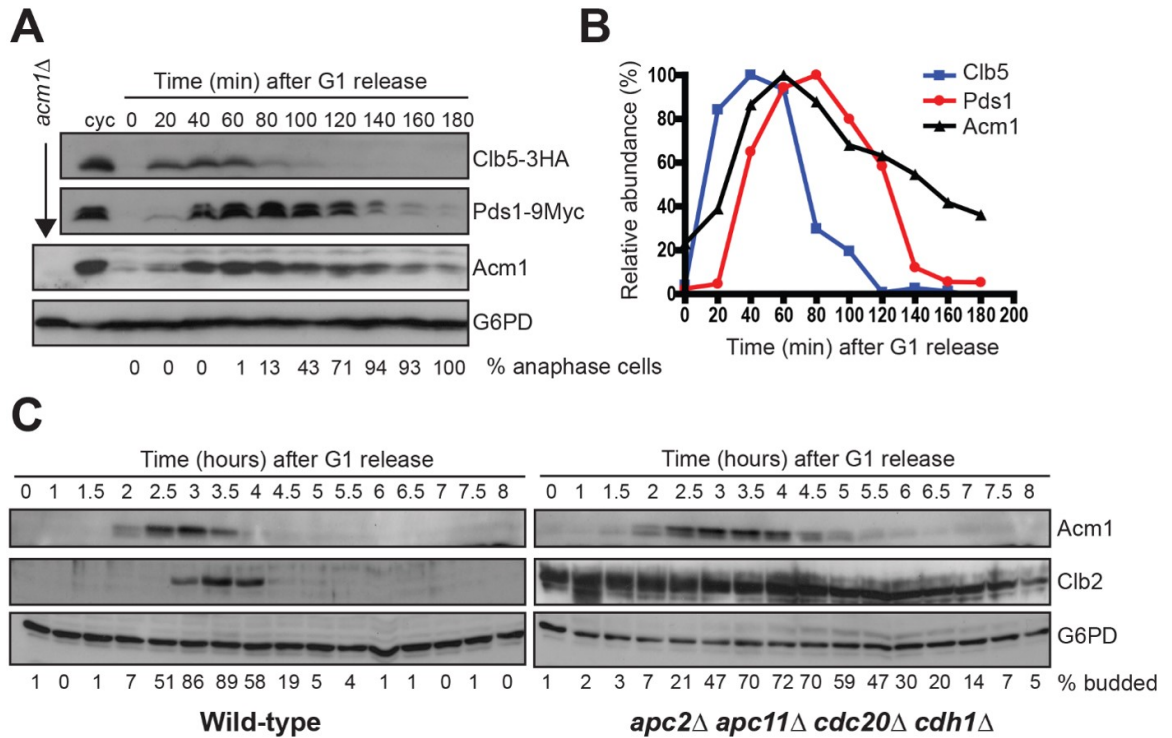


Fig. 2.1.: *APC^{Cdc20}* is neither necessary nor sufficient for complete *Acm1* degradation at mitotic exit. A) *dbf2-2* cells expressing endogenous chromosomally tagged Clb5-3HA and Pds1-9Myc were released from a G1 arrest at 37°C and the levels of Clb5, Pds1, and Acm1 monitored by immunoblotting over the indicated time period. G6PD is a loading control. Numbers under each lane were obtained by fluorescence microscopic analysis of at least 100 cells at that timepoint stained with DAPI and scored for the presence of 2 segregated DNA masses indicative of the *dbf2-2* late anaphase arrest point. cyc, asynchronous cycling cultures. B) Protein levels were quantified from the immunoblots in panel A. The abundance of each protein was plotted as a percentage of its maximal expression level. C) Extracts from synchronized cultures of yBRT135 (Wild-type) and mutant strain yBRT159 lacking several subunits of APC (*apc2Δapc11Δcdc20Δcdh1Δpds1Δclb5ΔSIC1^{10x}*) were generously provided by David Toczyski [148], and were probed for Acm1, Clb2, and the loading control G6PD by immunoblotting. The budding index under each lane, taken from [148], is used as an indicator of cell cycle progression.

2.2.2 *Acm1* is degraded by the 26S proteasome *in vivo*

Proteolysis of Acm1 in G1 can be blocked by the proteasome inhibitor MG-132 [94], suggesting that Acm1 is a substrate of the proteasome. To more rigorously characterize proteasome dependence and rule out the possibility of off-target

effects of MG-132 we compared Acm1 stability after MG-132 treatment with stability in a collection of conditional proteasome mutant strains. We used wild-type Acm1, which is unstable only in G1 cells, and an Acm1 mutant lacking Cdk phosphorylation sites (Acm1^{5A}), which is unstable throughout the cell cycle [94]. Consistent with our previous results with wild-type Acm1, 3HA-Acm1^{5A} was strongly stabilized after MG-132 treatment in a GAL1 promoter shutoff/cycloheximide chase assay (Figure 2.2A). Using the same assay, the stability of both 3HA-Acm1 and 3HA-Acm1^{5A} was measured in G1-arrested *pre1-1 pre2-2* cells harboring temperature-sensitive mutations in the $\beta 4$ and $\beta 5$ subunits of the 20S proteasome core particle [149]. Both 3HA-Acm1 and 3HA-Acm1^{5A}, as well as the control APC substrate Fin1-3HA were highly unstable in wild type G1 cells but were strongly stabilized in the *pre1-1 pre2-2* mutant strain (Figure 2.2B). These results confirm that Acm1 is degraded by the proteasome in G1. We also tested Acm1 stability in a proteasome mutant strain, *cim3-1*, with a temperature-sensitive defect in the Rpt6 ATPase subunit of the 19S regulatory particle [150], which is primarily responsible for recognition and processing of poly-ubiquitinated proteins. The *cim3-1* strain shows defective proteolysis of ubiquitinated substrates at restrictive temperature [150]. 3HA-Acm1, 3HA-Acm1^{5A}, and Fin1-3HA were all strongly stabilized in G1-arrested *cim3-1* cells (Figure 2.2C). To ensure this was not an artifact of Acm1 overexpression from the GAL1 promoter we also monitored the level of endogenous Acm1 in wild-type and conditional proteasome mutant strains at the restrictive temperature. The steady-state level of Acm1 was increased upon proteasome inactivation in both *cim3-1* and *pre1-1 pre2-2* cells (Figure 2.2D). Collectively, these results demonstrate that Acm1 proteolysis requires activity of the 26S proteasome, not just the 20S core particle, and suggested that Acm1 is likely targeted to the proteasome via polyubiquitination. We therefore set out to identify components of the ubiquitin system required for the APC-independent Acm1 proteolysis.

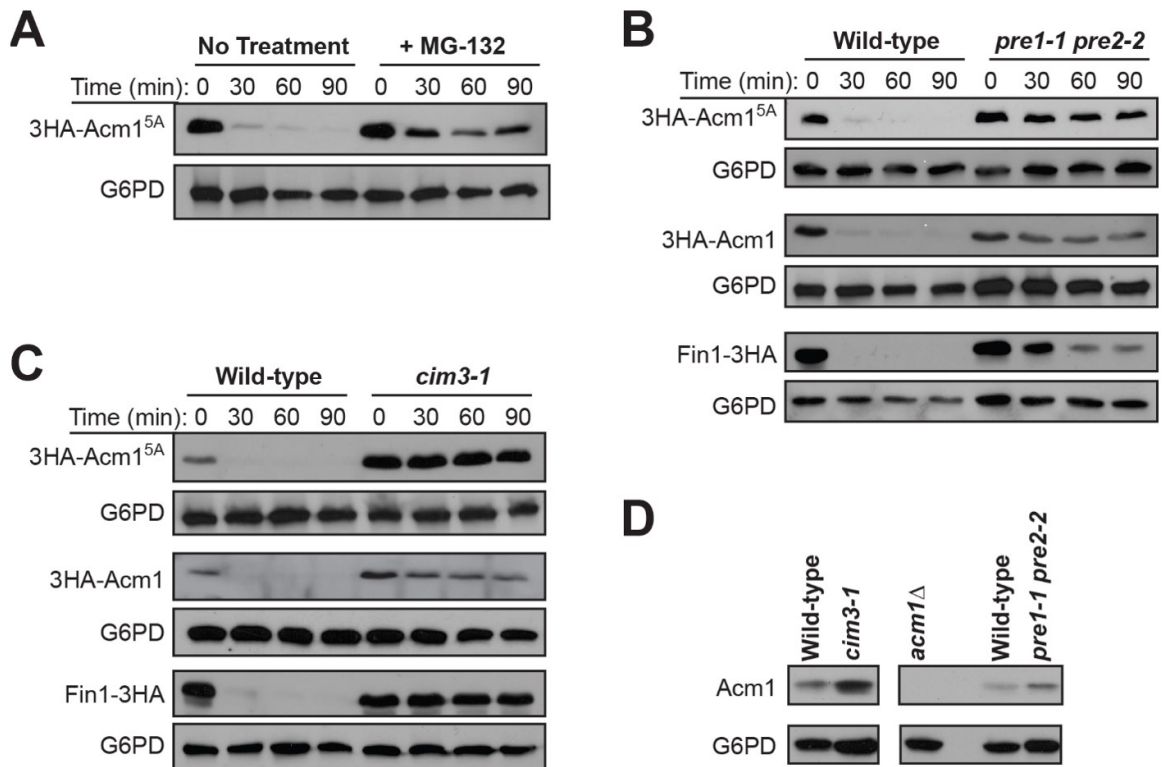


Fig. 2.2.: Acm1 degradation requires both the 20S core particle and the 19S regulatory complex of the 26S proteasome. A) Strain YKA407 carrying plasmid pHLP298 expressing 3HA-Acm1^{5A} from the GAL1 promoter was treated first with galactose to induce 3HA-Acm1^{5A} expression, second with 50 μ M MG-132 or a mock treatment, and third with glucose and cycloheximide to terminate expression (Time = 0). The level of 3HA-Acm1^{5A} was then monitored over time by immunoblotting with an HA antibody. G6PD is a loading control. B) and C) The same experiment described in panel A was performed with wild-type (YWO0607 for B, MHY753 for C) or the indicated temperature-sensitive proteasome mutant strains (YWO0612 for B, MHY754 for C) carrying plasmids expressing either 3HA-Acm1^{5A}, 3HA-Acm1, or Fin1-3HA from the GAL1 promoter. Instead of MG-132 treatment, cultures were shifted to 37 °C prior to terminating protein expression. For 3HA-Acm1, and Fin1-3HA, cells were arrested first in G1. D) The same strains from panels B and C were grown to exponential phase and shifted to the restrictive temperature to compare the steady-state level of endogenous Acm1 by immunoblotting with an anti-Acm1 antibody. G6PD was used as a loading control.

2.2.3 Acm1 proteolysis requires a functional ubiquitin conjugation system

To test if Acm1 proteolysis is generally dependent on the ubiquitin conjugation system, we measured its stability in a strain harboring a conditional mutation, *uba1-*

204, in the sole E1 ubiquitin activating enzyme in budding yeast [151]. A pulse of 3HA-Acm1 or Fin1-myc expression was induced from the GAL1 promoter in G1-arrested wild-type and *uba1-ts* cells after shift to the non-permissive temperature of 37°C (Figure 2.3). Both 3HA-Acm1 and the control protein Fin1-myc were strongly stabilized in *uba1-ts* cells compared to isogenic wild-type cells. Similar, although less dramatic, results were obtained using a second conditional E1 allele, *uba1-ts* ([152]; data not shown). We conclude that the APC-independent G1 degradation of Acm1 is dependent on a functional ubiquitin conjugation system.

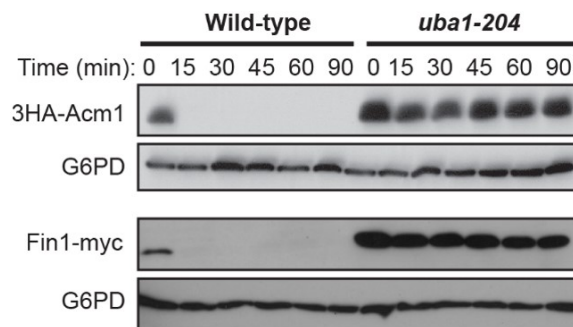


Fig. 2.3.: Acm1 proteolysis requires a functional ubiquitin conjugation pathway. Expression of 3HA-Acm1 or Fin1-myc was induced with galactose in G1-arrested wild-type (RJD3268) or *uba1-204* (RJD3269) cells at room temperature. Culture temperature was increased to 37°C prior to addition of glucose and cycloheximide. Cells were harvested at the indicated times after terminating expression and protein levels monitored by immunoblotting with anti-HA or anti-myc antibodies. G6PD is a loading control.

2.2.4 Acm1 proteolysis does not require individual E3 ligases or E2 conjugating enzymes

To identify the proteins directly responsible for Acm1 ubiquitination and proteolysis, we systematically screened a collection of yeast strains individually lacking non-essential yeast E2 ubiquitin conjugating enzymes and E3 ubiquitin ligases (Table 2-1) for effects on Acm1 stability. We used the Acm1^{5A} mutant because it is constitutively unstable and does not require cell cycle arrest in G1 to monitor effects

on stability. First, steady-state levels of 3HA-Acm1^{5A} expressed from the natural ACM1 promoter in exponentially growing E2 and E3 mutant cultures were measured by immunoblotting and compared to the level of wild-type 3HA-Acm1 in the parent strain. Surprisingly, the level of Acm1^{5A} fluctuated widely in the mutant strains, and in several cases was significantly elevated, suggesting that Acm1 stability might be increased in the absence of these ubiquitin system components (Figure 2.8). However, subsequent direct testing of stability using our inducible promoter and cycloheximide chase system failed to reveal any strong effects of these gene deletions on Acm1 half-life (Figure 2.9). We suspect that the differences in steady-state expression from the natural promoter were likely due to effects on transcription or cell cycle distribution since the ACM1 promoter is strictly cell cycle regulated [147]. Consistent with this, analysis of wild-type Acm1 and Acm1^{5A} levels in G1-arrested cultures of these deletion strains cells failed to reveal evidence of stabilization (data not shown).

To avoid problems with expression from the highly regulated ACM1 promoter we re-screened the entire collection of E2 and E3 deletion strains using the GAL1 promoter stability assay and directly monitored stability of untagged Acm1^{5A} with our Acm1 antibody. We also added strains lacking genes encoding predicted RING domains without known E3 activity and other recently verified E3 ligases (Table 2-1). Since inhibition of either the proteasome or Uba1 resulted in strongly stabilized Acm1 over the course of at least one hour in this assay, we compared the level of Acm1 at 0 and 60 minutes in each strain after addition of glucose and cycloheximide. In 47 known or putative E3 deletion strains and 10 E2 deletion strains we did not find a single case where Acm1 was stabilized comparable to MG-132 addition (Figure 2.10 and data not shown). We also found no effect of the essential E3 enzymes Rsp5 and Prp19 on Acm1 stability using strains from the tetracycline-repressible essential gene library (data not shown). The essential E3 SCF was tested previously with negative results [92] and we confirmed these results using conditional *cdc4* and *cdc53* alleles (data not shown). We conclude that Acm1 proteolysis by the APC-independent mechanism does not require any single E2-E3 modules, although we cannot rule out

the possibility that multiple redundant E3 enzymes are capable of promoting Acm1 degradation or that an unknown E3 exists that was not tested.

2.2.5 Acm1 proteolysis does not require assembly of ubiquitin chains

In parallel with the *uba1-204* experiment described above, we analyzed Acm1 stability after overexpressing a mutant ubiquitin in which all lysines have been replaced with arginine (Ub-K7R, a gift from L. Hicke, Northwestern University). This mutant blocks polyubiquitin chain extension when conjugated to a protein [153] and thereby stabilizes ubiquitin proteasome substrates. The stabilities of Acm1 and the APC substrates Fin1 and Clb2 were monitored in G1-arrested cells overexpressing either mutant or wild-type ubiquitin. As expected, Fin1 and Clb2 were highly stabilized by overexpression of Ub-K7R (Figure 2.4A). Their steady-state levels were also noticeably higher at time 0 in the presence of Ub-K7R compared to wild-type ubiquitin. In contrast, the stability of Acm1 was unaffected by the overexpressed chain-terminating Ub-K7R and the steady state level of Acm1 was similar at time 0 in both strains. Similar results were observed with 3HA-Acm1 in a *doa4* Δ strain, which has a defect in processing of ubiquitin precursors and therefore a lower level of endogenous ubiquitin for Ub-K7R to compete with (Figure 2.4B). In this case, we terminated transcription from the GAL1 promoter with glucose but did not add cycloheximide, allowing continuous synthesis and accumulation of Ub-K7R and wild-type ubiquitin. Surprisingly, these experiments reveal that Acm1 proteolysis in G1 shows no apparent dependence on assembly of poly-ubiquitin chains, a general requirement for ubiquitin-mediated proteolysis.

2.2.6 Ubiquitin conjugation sites on Acm1 are not required for its proteolysis

To independently test the dependence of Acm1 proteolysis on ubiquitination, we constructed a mutant *ACM1* allele in which all 20 lysine codons were replaced with

arginine codons. The mutant protein, 3HA-Acm1^{K0}, lacks all internal sites for ubiquitin conjugation and we added a 3HA epitope tag lacking lysines to block the native N-terminus as a potential ubiquitin conjugation site. Despite the extensive mutagenesis, 3HA-Acm1^{K0} is fully functional as a Cdh1 inhibitor *in vivo* (Figure 2.5A) because 3HA-Acm1^{K0} overexpression suppressed the toxic effect of Cdh1 overexpression like wild-type 3HA-Acm1 [88–90,92]. Thus, the mutant is biologically functional and does not suffer from global misfolding or severe structural differences compared to wild-type Acm1. We compared the stability of galactose-induced pulses of 3HA-Acm1^{K0} and 3HA-Acm1 in α -factor arrested G1 cells (Figure 2.5B). The absence of lysines had no effect on the stability of Acm1 (Figure 2.5B), suggesting that ubiquitin conjugation to Acm1 is not required for its proteolysis. Acm1 stability is dramatically increased by cyclin-dependent kinase phosphorylation [91,92,94] and as a result, Acm1 is stable in S and M phase cells. To determine if the Acm1^{K0} mutant is still regulated by phosphorylation like wild-type Acm1, we repeated the stability assay in S phase cells. Both wild-type 3HA-Acm1 and 3HA-Acm1^{K0} were comparably stable in hydroxyurea-arrested S phase cells compared to G1 (Figure 2.5C), suggesting that the mutagenesis did not perturb normal phospho-regulation of Acm1 stability.

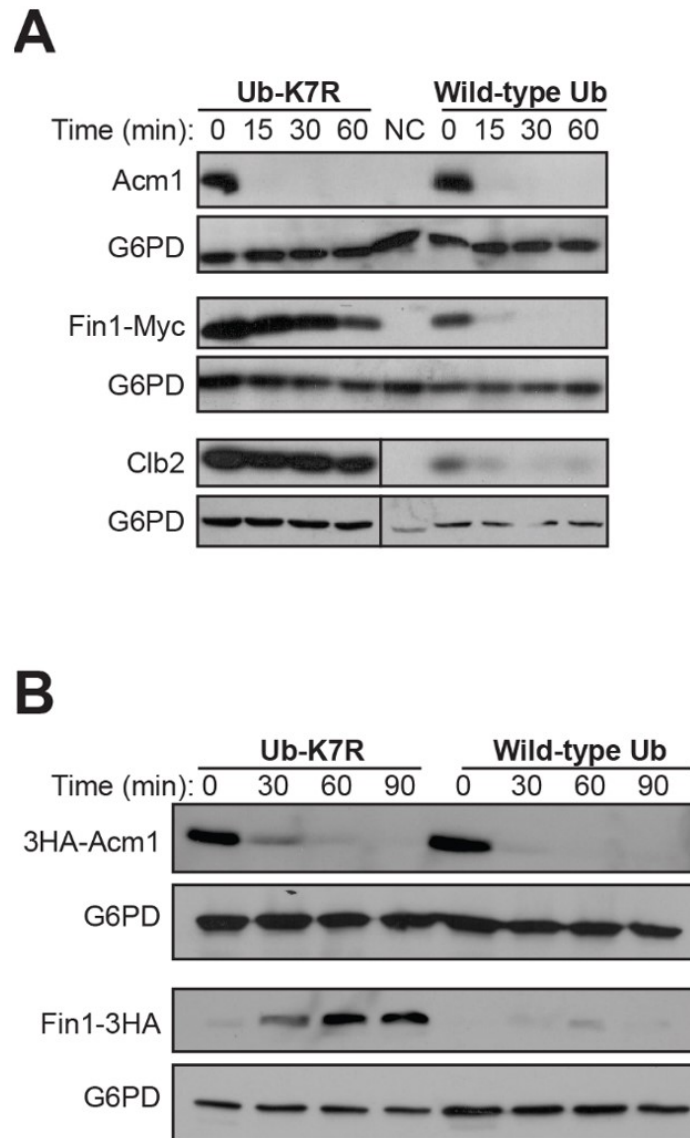


Fig. 2.4.: **Acm1 proteolysis does not require assembly of polyubiquitin chains.** A) YKA247 cells containing P_{GAL1} -driven plasmids pHLP391 (for Acm1), pESCW-Fin1-Myc, or pHLP309 (for Clb2) and P_{CUP1} -driven ubiquitin (Ub) overexpression plasmids LHP306 (for Ub-K7R mutant) or LHP308 (for wild-type Ub) were grown to early exponential phase. Cells were arrested at G1 before expression of wild-type or mutant Ub was induced with 100 mM CuSO_4 and Acm1, Fin1-myc, and Clb2 with galactose. Stability of Acm1, Fin1-Myc, and Clb2 were monitored with anti-Acm1, anti-Myc, and anti-Clb2 antibodies, respectively. G6PD is a loading control. NC, negative control without galactose induction. B) The same experiment described in panel A was performed in *doa4* Δ cells to limit the abundance of endogenous ubiquitin, and only glucose was used to terminate expression, allowing continuous synthesis of mutant or wild-type Ub. In this experiment pHLP212 was used to express 3HA-Acm1, which was detected with an anti-HA antibody and Fin1-3HA was used as a control.

Since in rare cases proteins can undergo ubiquitination at nonlysine sites, we next directly tested for ubiquitin conjugates on Acm1 in G1-arrested cells. Wild-type 3HA-Acm1 and 3HAAcm1^{K0} were compared in our stability assay with and without proteasome inhibition. Consistent with results presented above, both proteins were highly unstable in the absence of MG-132 but strongly stabilized in the presence of MG-132 (Figure 2.5D). Acm1 has been proposed to undergo weak ubiquitination and subsequent degradation mediated by APC^{Cdh1}, the enzyme it inhibits [91]. Consistent with this, we detected ubiquitin conjugates on wild-type 3HA-Acm1 in the presence of MG-132 (Figure 2.5D). Under identical conditions, ubiquitin conjugates were undetectable on 3HA-Acm1^{K0}. Since these proteins have indistinguishable half-lives in G1 cells, the ubiquitin conjugates detected on wild-type Acm1 are not likely to contribute significantly to its proteolysis under normal conditions. Importantly, these results argue that Acm1^{K0} is not targeted to the proteasome via unconventional ubiquitin linkages to non-lysine amino acids, or to the N-terminus.

Finally, we compared the levels of 3HA-Acm1 and 3HAAcm1^{K0} expressed from the natural ACM1 promoter as a function of cell cycle stage in *cdc15-2* cells (Figure 2.5E). Cells were arrested in G1 with α -factor, S with hydroxyurea, early M with nocodazole, and late M by temperature shift to 37°C and Acm1 levels compared by immunoblotting. In cycling cells and S and early M arrested cells the abundance of 3HA-Acm1 and 3HA-Acm1^{K0} was equivalent. In late M arrested cells, the abundance of 3HAAcm1^{K0} was higher than 3HA-Acm1 and was equivalent to the level in early M cells, consistent with the anaphase ubiquitin dependent proteolytic mechanism mediated by APC^{Cdc20} [91]. In support of our results from Figure 2.1, a portion of the wild-type 3HA-Acm1 was still present in these late anaphase cells, demonstrating that Acm1 is not completely eliminated by APC^{Cdc20}. Importantly, 3HA-Acm1^{K0} was undetected in G1 cells, similar to wild-type 3HA-Acm1. This strongly implies that the APC-independent proteolytic mechanism that clears Acm1 completely during mitotic exit and G1 does not involve conjugation of ubiquitin chains to Acm1.

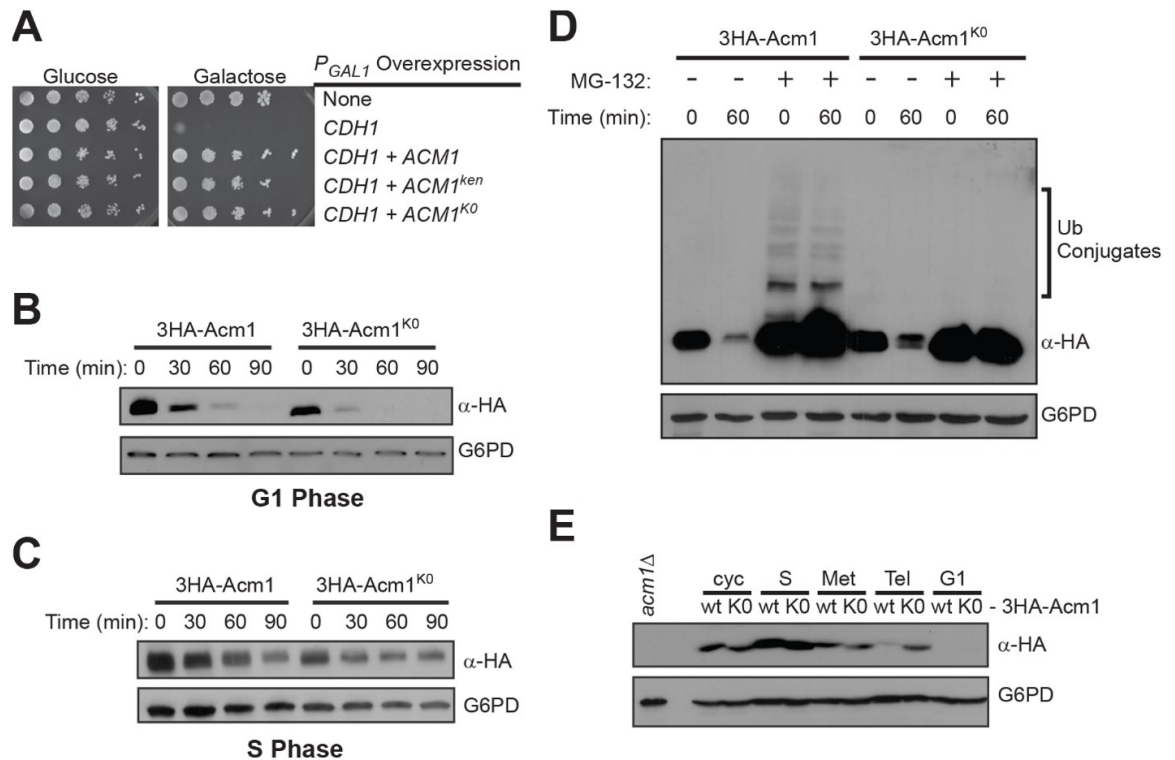


Fig. 2.5.: **Acm1 proteolysis does not require ubiquitin acceptor sites on Acm1.** A) YKA247 cells carrying P_{GAL1} expression plasmids for 3FLAG-Cdh1, 3HA-Acm1, HA-Acm1-ken, and 3HA-Acm1^{K0} in the indicated combinations were grown until mid-exponential phase. 10-fold serial dilutions were spotted on selective media containing either glucose or galactose. Plates were incubated at 30 °C for 23 days. B) and C) YKA247 cells carrying P_{GAL1} expression plasmids for 3HA-Acm1 (pHLP117) or lysine-less 3HA-Acm1^{K0} mutant (pHLP330) were grown in YP-raffinose to early exponential phase. Cells were arrested at G1 (panel B) or S phase (panel C). Stability of 3HA-Acm1 and 3HA-Acm1^{K0} was monitored over the indicated time period by immunoblotting with anti-HA antibody. G6PDH is a loading control. D) Same as panels B and C, except *pdr5Δ* cells were used and stability was monitored in the presence and absence of MG-132 as indicated. Longer immunoblot exposures were obtained for detection of ubiquitin (Ub) conjugates. E) *cdc15-2* cells carrying centromeric plasmids expressing either wild-type 3HA-Acm1 or 3HA-Acm1^{K0} from the natural ACM1 promoter were arrested at the indicated cell cycle stages as described in Materials and Methods. The level of each protein was then compared by anti-HA immunoblotting with G6PD as a loading control.

2.2.7 An N-terminal putative disordered region of Acm1 contributes to APC-independent degradation

To probe the biological significance of Acm1 degradation we needed a stable Acm1 mutant. We therefore sought truncated Acm1 variants that exhibited increased half-life in our G1 stability assay. We fused the ZZ domain of Protein A (ProtA) to the Acm1 C-terminus (for equivalent immunoblot detection of all Acm1 constructs). Full length Acm1-ProtA was highly unstable. Removal of 42 amino acids or less had little effect on the rate of Acm1-ProtA degradation (Figure 2.6A). Strikingly, removal of the 52 N-terminal amino acids strongly stabilized Acm1-ProtA in this assay and longer truncations from the N-terminus were also stable.

Although clearly required for efficient Acm1 degradation in G1, the first 52 amino acids of Acm1 were not sufficient to destabilize Protein A when fused to its N-terminus (Figure 2.6B). This suggested that other regions of Acm1 might be important as well. We found that the Acm1^{N Δ 52} protein was unstable in the absence of the C-terminal Protein A fusion (Figure 2.6C). Thus, stabilization of Acm1 in G1 required both loss of the amino terminus and modification of the C-terminus. The N-terminal region of Acm1 is predicted to be highly disordered using several secondary structure prediction algorithms (data not shown). The proteasome can directly recognize some disordered proteins and catalyze their proteolysis in the absence of ubiquitin conjugation. We purified active 20S and 26S proteasomes from yeast but found no evidence that a variety of recombinant Acm1 proteins purified from *E. coli* could be directly recognized and degraded (Figure 2.11).

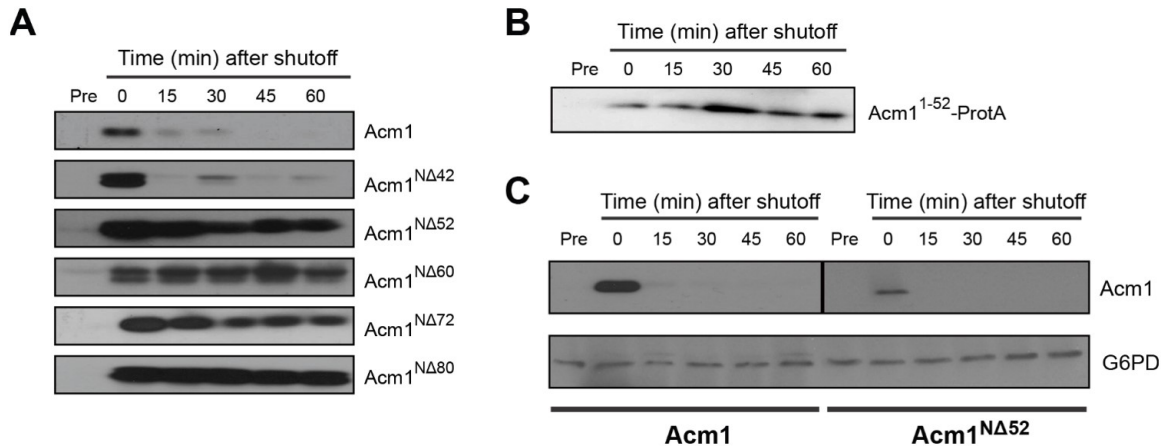


Fig. 2.6.: **Proteolysis of an Acm1-ProtA fusion protein in G1 requires the N-terminal 52 amino acids of Acm1.** A) YKA247 cells transformed with PGAL1 constructs expressing ACM1, *acm1*^{NΔ42}, *acm1*^{NΔ52}, *acm1*^{NΔ60}, *acm1*^{NΔ72} or *acm1*^{NΔ80} fused to the ZZ domain of Protein A were arrested in G1 and protein stability assayed over time by immunoblotting with anti-Protein A antibody. B) The same assay as panel A with cells expressing Acm1 amino acids 152 fused to Protein A. C) The stability of Acm1 and Acm1^{NΔ52} without the Protein A fusion were compared using the same assay as in panel A, but with anti-Acm1 antibody for immunoblot detection. G6PD is a loading control. G6PD loading controls were performed for all blots in panels A and B as well (not shown).

2.2.8 Acm1^{NΔ52} is still cleared from cells at mitotic exit

We next used the stabilized Acm1^{NΔ52} protein to study the biological significance of Acm1 proteolysis at mitotic exit. It is important to note that the N-terminus of Acm1 also contains the Cdc20-specific D-box responsible for Acm1 recognition by APC^{Cdc20} [91]. Thus, the Acm1^{NΔ52} protein should be resistant to both known proteolytic mechanisms. We predicted that failure to degrade Acm1 would prevent or delay activation of APC^{Cdh1}. To test this, strains harboring a P_{MET3}-CDC20 allele and expressing either Acm1 or Acm1^{NΔ52}-ProtA from the ACM1 promoter were blocked at metaphase by methionine addition and then released in the absence of methionine to undergo synchronous mitotic exit. The levels of Acm1 and the Cdh1 substrate Clb2 were monitored over time by immunoblotting (Figure 2.7A and 2.7B). Surprisingly, there was little difference in the decay profiles of Acm1 and Acm1^{NΔ52}-

ProtA. Moreover, we did not observe significant differences in degradation of Clb2. Similar results were observed with another Cdh1 target, Kip1 (data not shown). Thus, although Acm1^{NΔ52}-ProtA is highly stabilized in G1-arrested cells, it is still effectively cleared by cells during mitotic exit. Possible explanations for this are discussed below.

2.2.9 Constitutive expression of stabilized Acm1^{NΔ52} impairs growth of *sic1Δ* cells

Since the ACM1 promoter is cell cycle-regulated, loss of Acm1^{NΔ52} as cells exit mitosis could be in part due to termination of ACM1 transcription. To test for defects in APC^{Cdh1} function in cells expressing stabilized Acm1^{NΔ52} we expressed ACM1 and *acm1*^{NΔ52} alleles from the constitutive ADH promoter in a *sic1Δ* background. Either Sic1 or Cdh1 is sufficient for Cdk inactivation and mitotic exit in budding yeast, however loss of both is lethal. Therefore, activation of Cdh1 becomes critically important in *sic1Δ* cells. We observed a significant growth delay in *sic1Δ* cells constitutively expressing Acm1^{NΔ52} compared to wild-type Acm1, both in liquid culture and on agar plates (Figure 2.7C and 2.7D). This experiment supports the idea that clearance of Acm1 from cells is required for timely and full activation of APC^{Cdh1} at mitotic exit and in G1.

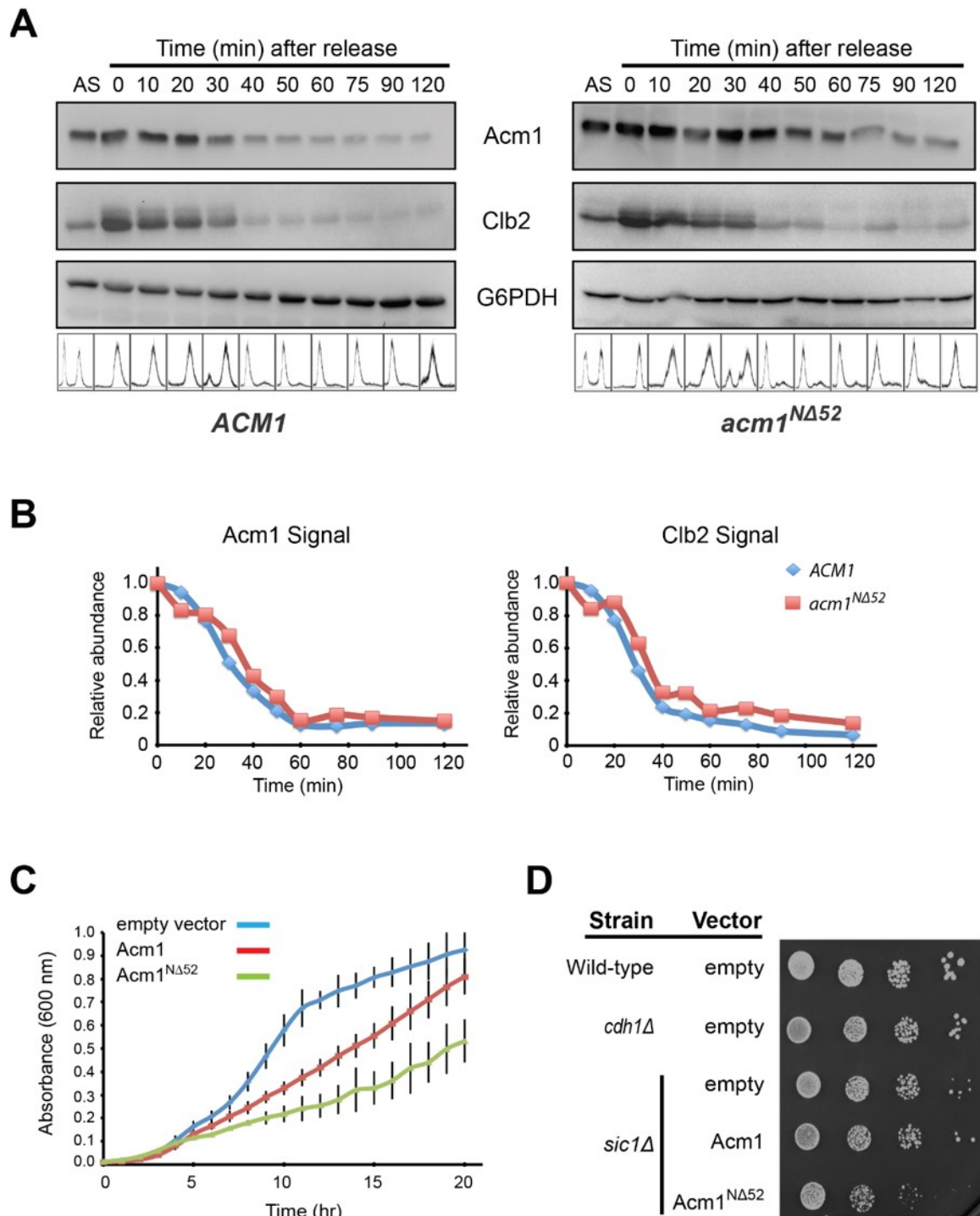


Fig. 2.7.: (Caption on next page)

Fig. 2.7.: (Previous page)

Acm1^{NΔ52} is still cleared at mitotic exit, but constitutive expression impairs growth of *sic1Δ* cells. A) YKA859 cells carrying either pHLP117 (for expression of 3HA-Acm1) or pHLP505 (for expression of Acm1^{NΔ52}-ProtA) were arrested at metaphase by methionine repression of P_{MET3}-CDC20 and then released in the absence of methionine. Cells were collected at regular intervals and analyzed by immunoblotting using antibodies against Acm1, Clb2, or G6PD (loading control). B) Quantitation of chemiluminescent immunoblots from panel A. Data are the average of 4 independent experiments. C) Growth of *sic1Δ* cells transformed with either an empty vector, pHLP361 (P_{ADH}-Acm1-ProtA) or pHLP363 (P_{ADH}-*acm1*^{NΔ52}-ProtA) were compared using a plate reader to measure absorbance at 600 nm. Data are the average of three independent experiments with standard deviation error bars. D) Serial 10-fold dilutions of the strains from panel C as well as isogenic wild-type and *cdh1Δ* strains were spotted and grown on selective agar plates.

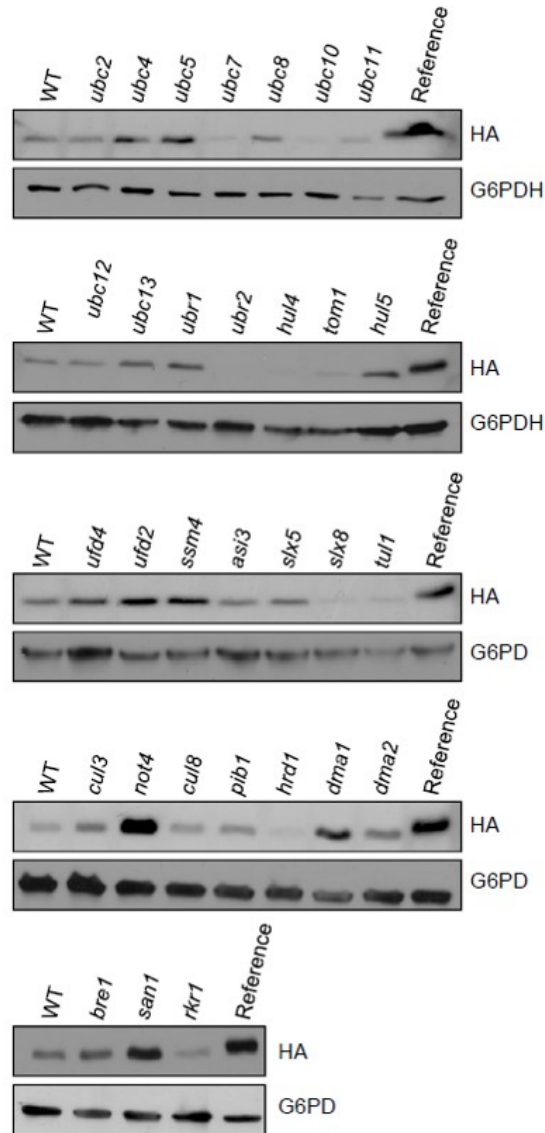


Fig. 2.8.: **Screening of non-essential E2 conjugases and E3 ligases for effects on 3HA-Acm15A expression level.** 3HA-Acm1^{5A} was expressed from the natural ACM1 promoter on a centromeric plasmid in BY4741 (WT) and deletion strains lacking the genes indicated above each lane. The steady state level of 3HA-Acm1^{5A} in asynchronous log phase cultures of each strain was compared to that of wild-type 3HA-Acm1 (labeled Reference) expressed from the same plasmid in BY4741 by immunoblotting with anti-HA antibody. G6PDH is a loading control.

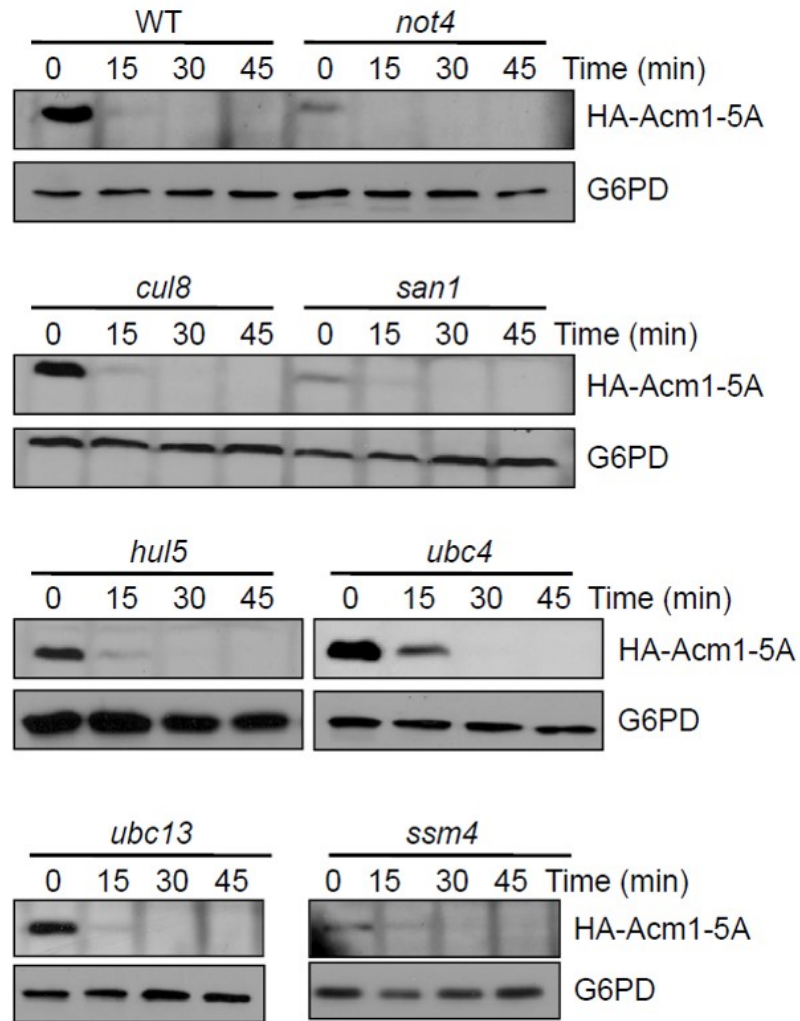


Fig. 2.9.: Measurements of HA-Acm15A stability in selected strains lacking nonessential E2 conjugases and E3 ligases. Stability of HA-Acm1^{5A} was monitored by GAL1 promoter stability assay as described in Materials and Methods in asynchronous mid-log phase cultures of the indicated gene deletion strains harboring pHLP110. Anti-HA immunoblot profiles were compared to those from MG-132 treated cells and conditional proteasome mutant strains (not shown, see Figure 2.2).

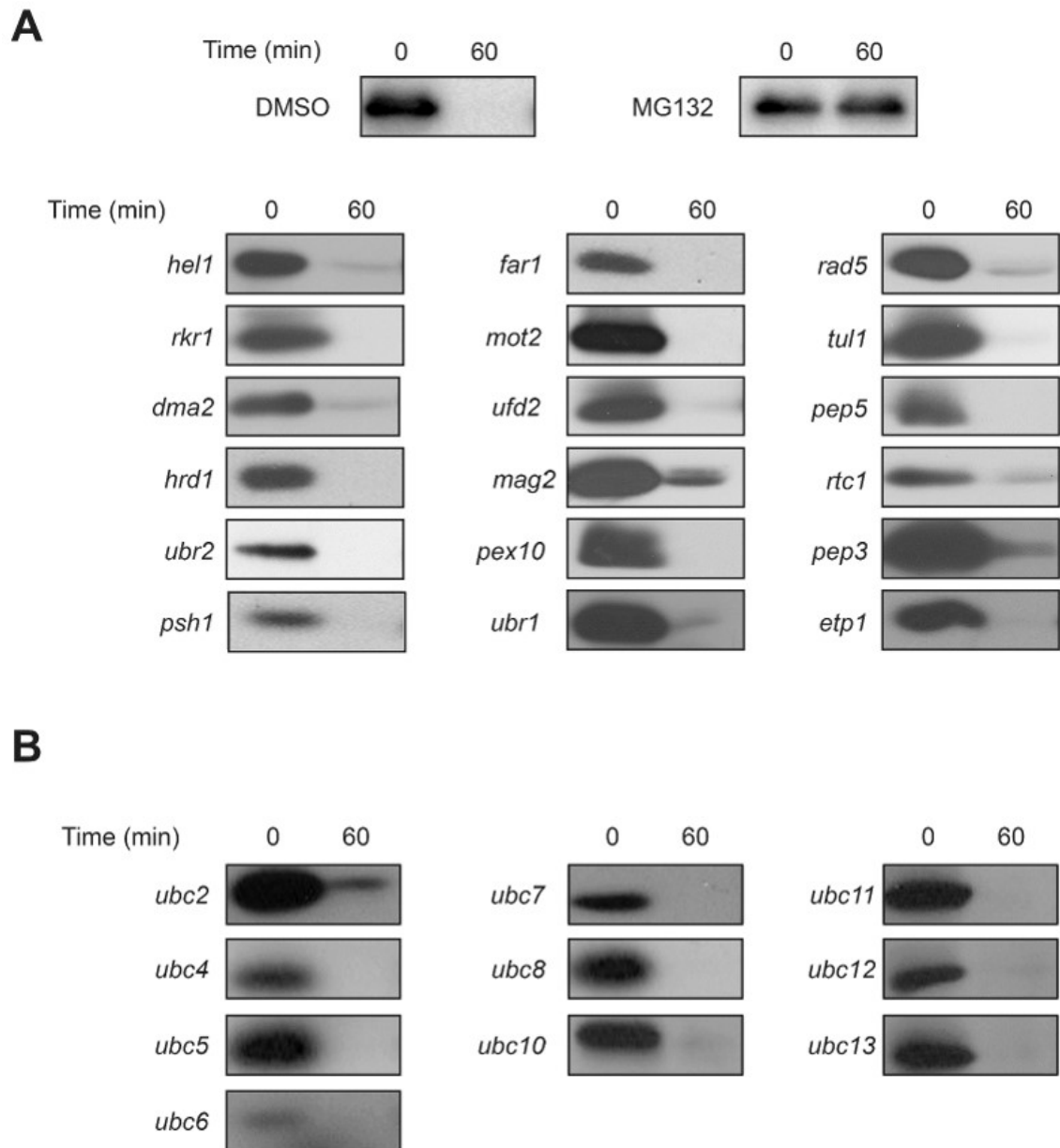


Fig. 2.10.: Screening of non-essential E2 conjugases and known and putative E3 ligases for effects on Acm1^{5A} stability. Experiments performed as in Figure 2.9 but using an untagged Acm1^{5A} variant expressed from P_{GAL1} in pHLP392 in an *acm1*Δ background. Only timepoints 0 and 60 minutes following glucose and cycloheximide addition were compared. MG-132 treatment was used as a positive control for Acm1 stabilization. Anti-Acm1 antibody was used to detect the Acm1^{5A}. Only representative E3 deletion strains are shown in panel A, but all strains listed in Table 2-1 were analyzed with similar results. Panel B shows E2 deletion strains

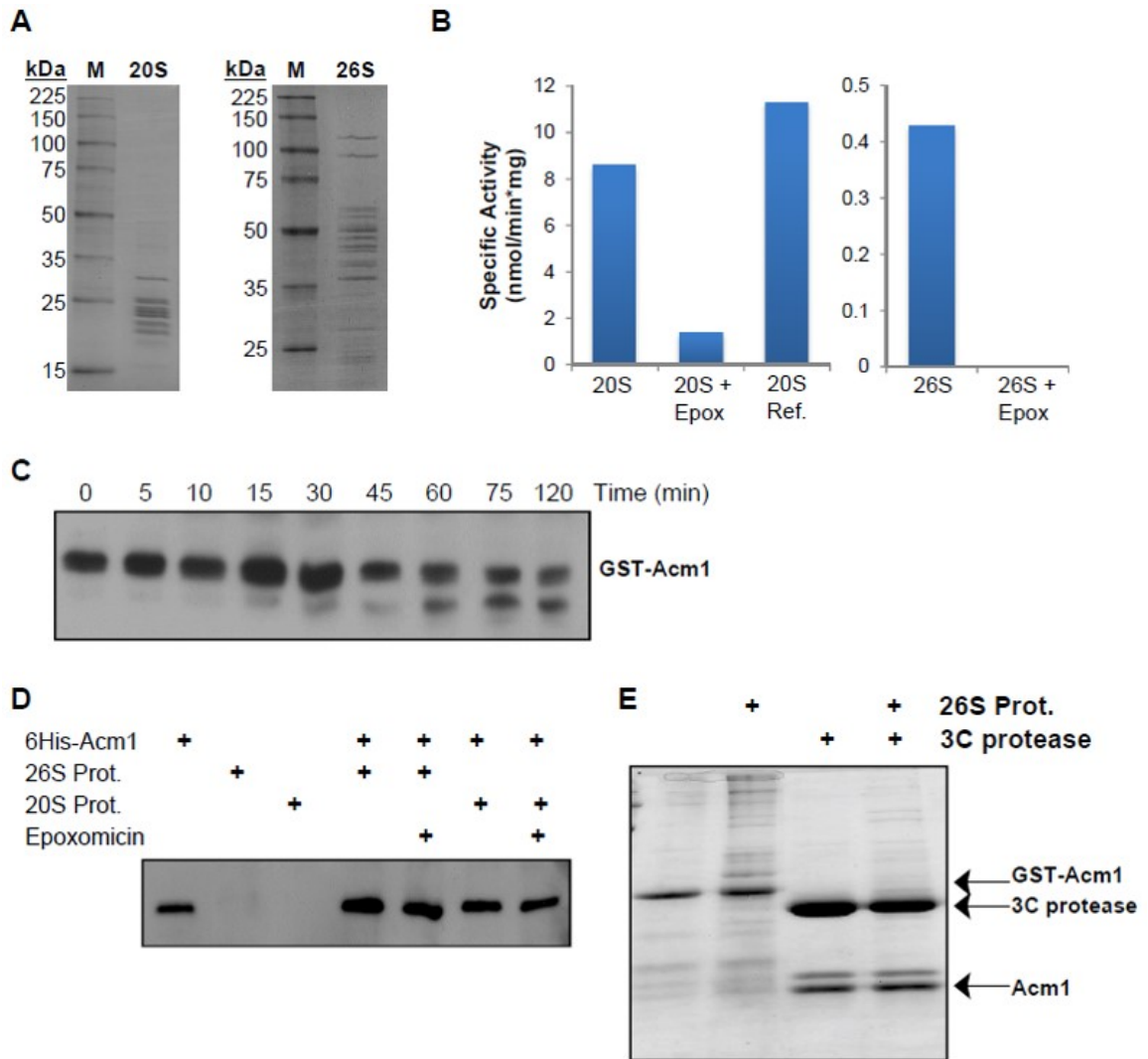


Fig. 2.11.: **Acm1 is not degraded by purified 20S or 26S proteasomes.** A) SDS-PAGE analysis of purified 20S (left) and 26S (right) proteasome preparations visualized with Coomassie blue. M, molecular weight markers. Components of the proteasomes were confirmed by mass spectrometry. B) Proteasome activities were measured using the fluorogenic substrate, Suc-LLVY-AMC. The proteasome inhibitor epoxomicin (Epox) was used to demonstrate specificity. Similar results were observed with MG-132 (not shown). A standard curve of free AMC was used to convert fluorescence signal to moles of product formed. 20S Ref is the specific activity value reported previously for budding yeast 20S proteasome in reference 55 from the main text. C) Immunoblot of recombinant purified GST-Acm1 incubated with purified 26S proteasome over time. D) Immunoblot of recombinant 6His-Acm1 alone and after incubation with purified proteasome (20S or 26S) with and without the inhibitor epoxomicin. E) GST-Acm1 and free Acm1 generated by treatment of GST-Acm1 with 3C protease were incubated with purified 26S proteasome and analyzed by SDS-PAGE and Coomassie blue staining.

2.3 Discussion

2.3.1 Acm1 may be a novel ubiquitin-independent proteasome substrate

The 26S proteasome is a large ATP-dependent protease complex consisting of a 20S core particle with a 19S regulatory particle at both ends [154, 155]. It is the primary enzymatic activity responsible for protein turnover in eukaryotic cells [156]. Although the vast majority of known proteasome substrates require ubiquitination for proteolysis, proteins can also be recognized by the proteasome without ubiquitin conjugation [157–159]. The 20S core particle alone, which is likely the predominant form of the proteasome *in vivo*, can recognize mis-folded or damaged proteins directly and catalyze their proteolysis independent of ubiquitin conjugation and ATP hydrolysis. In addition, the 26S holoenzyme can also recognize some proteins independent of ubiquitin. One recent study estimated that 20% of human proteins are subject to proteolysis by the proteasome independent of ubiquitin conjugation [160]. However, the extent to which any of this proteolysis is regulated is unclear and ubiquitin-independent proteolysis is thought to largely constitute a basal protein turnover pathway and/or a route to eliminate damaged or mis-folded proteins [158, 161].

The best-characterized ubiquitin-independent substrate of the 26S proteasome is ornithine decarboxylase (ODC), which catalyzes the rate-limiting first step in polyamine biosynthesis [162, 163]. ODC is targeted to the proteasome by a protein, termed antizyme, in response to high polyamine levels. This regulated ubiquitin-independent proteolysis serves to maintain polyamine homeostasis in cells [164]. Antizyme binding to ODC results in a conformational change that exposes a C-terminal degron in ODC recognized by the 26S proteasome [165, 166]. Antizyme itself also enhances recognition of ODC by the proteasome. The C-terminal tail of ODC may act as a structural ubiquitin mimic since it competes with ubiquitin chains for binding to the proteasome [166]. Interestingly, antizyme has also been linked to the ubiquitin independent proteasomal degradation of other proteins, including the cell cycle regulators cyclin D1 [167] and Aurora A kinase [52]. Other proteins involved in aspects of cell

cycle control with reported ubiquitin-independent proteolytic mechanisms include p53 [168], p21^{Cip1} [169–172], and Rb [173, 174]. These proteins are also destroyed by the conventional ubiquitin-proteasome pathway and it is often difficult to dissect the relative physiological contributions of ubiquitin-dependent and independent mechanisms. In addition, for all of these cases it is unclear if, and how, ubiquitin-independent proteolytic mechanisms are regulated during cell division. One possible exception to this may be human c-Fos, a proto-oncoprotein that functions as part of the AP-1 transcription factor complex involved in control of cell proliferation and other processes. c-Fos is sensitive to ubiquitin independent proteolysis and one report suggests that phosphorylation of a C-terminal degron sequence by MAP kinases specifically at the G0/G1 transition inhibits this mechanism [175]. The importance of this mechanism and its relevance in cycling cells is unclear, but it is reminiscent of what we observe with Acm1, which is also stabilized at the G1/S transition by phospho-dependent inhibition of seemingly ubiquitin-independent proteolysis.

Several features of Acm1s proteolytic mechanism reported here are reminiscent of ubiquitin-independent proteolysis. First, Acm1 degradation is insensitive to inhibition of ubiquitin chain assembly (Figure 2.4). Second, Acm1 degradation does not require acceptor lysines and does not appear to involve direct ubiquitin conjugation (Figure 2.5). Third, no individual E3 ligase or E2 conjugating enzyme is required for Acm1 proteolysis. The one notable exception is that Acm1 proteolysis does require a functional E1, suggesting that the ubiquitin conjugation system is at least indirectly required. Thus, Acm1 meets most, but not all, criteria for an ubiquitin-independent proteasome substrate [158].

2.3.2 How is Acm1 recognized by the proteasome and what is the role of the Acm1 N-terminus?

Additional work will be required to illuminate the biochemical mechanism by which Acm1 is specifically targeted to the proteasome in its dephosphorylated state.

Many ubiquitin independent proteasomal targets are thought to possess unstructured regions that mediate their direct recognition by the proteasome, much like a mis-folded protein [158, 176]. The N-terminus of Acm1 is predicted to be largely disordered (our unpublished observations) and contributes to its APC-independent proteolysis (Figure 2.6). Phosphorylation at Cdk sites in and around the Acm1 N-terminus may promote a more structured conformation that prevents degradation. Alternatively, Acm1 may interact with a proteasome targeting factor analogous to the ODC-antizyme interaction that has high affinity for dephosphorylated Acm1 but not for phosphorylated Acm1. This factor could itself be regulated by ubiquitination, thereby explaining the E1 result and general requirement for the ubiquitin system. The E1 requirement could also reflect a general role for ubiquitinated proteins in activating the 26S proteasome, a phenomenon that has some recent support [177]. Another possibility is that the Acm1 N- and/or C-terminus contain sequences that are directly recognized by a component of the proteasome. Such a sequence could act by mimicking ubiquitin as proposed for ODC, or interact with a completely distinct proteasome structure.

Despite the strong stabilization of Acm1^{N Δ 52}-ProtA in our GAL1 promoter stability assay (Figure 2.6, half-life .1 hour), it was still effectively cleared during mitotic exit when expressed from the ACM1 promoter, with kinetics similar to wild-type Acm1-ProtA. There are several possible explanations for this surprising result. Although the Cdc20-specific D-box is absent from Acm1^{N Δ 52} it is possible that removal of the N-terminal 52 amino acids makes the central D-box and/or KEN box that inhibit Cdh1 accessible to Cdc20. Cdh1 was also proposed to catalyze a slow ubiquitination and proteolysis of Acm1 [91] that, coupled with the termination of ACM1 transcription, may contribute to clearance of endogenous protein. We confirmed that the slow turnover of Acm1^{N Δ 52}-ProtA in G1 cells is Cdh1-dependent (data not shown). Finally, there may be some difference in conditions present in an α -factor arrest compared to mitotic exit that affect the turnover rate of Acm1 by the APC-independent mechanism.

2.3.3 Biological significance of Acm1 proteolytic mechanisms

Our results have confirmed the existence of two independent proteolytic mechanisms acting on Acm1. Acm1 is recognized by APC^{Cdc20} in anaphase as described previously [91] and degraded via the conventional ubiquitin pathway. However, APC^{Cdc20} is not sufficient to completely eliminate Acm1 and is not actually required for Acm1 levels to oscillate during the cell cycle (Figure 2.1). Consistent with this conclusion, mutation of the D-box in Acm1 that is recognized by Cdc20 had no noticeable effect on Acm1 stability or cell cycle expression profile [89,92]. The APC-independent mechanism, which exhibits features of ubiquitin-independent proteolysis, is sufficient to establish Acm1s cell cycle expression profile.

Why is APC^{Cdc20} insufficient for complete Acm1 degradation and why is it necessary to have two independent proteolytic mechanisms? One possibility is that two distinct cellular pools of Acm1 exist, one in the nucleus and one in the cytoplasm, and Cdc20 can only access nuclear Acm1. Although admittedly speculative, a fair amount of circumstantial evidence exists to support this possibility. Cdc20 is restricted primarily to the nucleus [178]. Cdh1, on the other hand, is restricted to the cytoplasm by Cdk phosphorylation until the end of anaphase [178]. Since Acm1 binds tightly to Cdh1 in cells arrested in late anaphase [88], it is likely that at least a portion of Acm1 remains cytoplasmic. Moreover, nuclear import of Acm1 is also negatively regulated by Cdk phosphorylation [91]. Since Acm1 levels are much higher than Cdh1 [88] a substantial pool of free Acm1 must exist that could be subject to rapid nucleocytoplasmic shuttling. When Cdc14 is first activated by the FEAR network in early anaphase, dephosphorylation of the pool of free Acm1 could trap it in the nucleus where it is recognized and targeted for degradation by APC^{Cdc20}. The Cdh1-bound pool of Acm1 would be resistant to APC^{Cdc20} by virtue of its cytoplasmic localization. This pool of Acm1 could require the second ubiquitin-independent proteolytic mechanism activated when Cdc14, released by the mitotic exit network, reaches the cytoplasm and dephosphorylates both Cdh1 and Acm1. The complexity

of Acm1 regulation in late mitosis strongly implies that timely and complete removal of Acm1 is essential for proper activation of APC^{Cdh1}, completion of mitotic cyclin degradation, and exit from mitosis. Our observation of a growth delay caused by Acm1NΔ52 expression in *sic1Δ* cells supports this.

A related question is why APC^{Cdc20} action on Acm1 is required at all, especially considering that in the absence of APC activity Acm1 levels still cycle apparently normally (Figure 2.1). The N-terminal D-box recognized by Cdc20 is highly conserved in Acm1 orthologs, suggesting that APC^{Cdc20}-mediated degradation must be important. It may be that initial depletion of the abundance of free Acm1 by APC^{Cdc20} preconditions Cdh1 for rapid activation at the appropriate time in late mitosis, maximizing the efficiency, coordination, and robustness of the mitotic exit process.

Recently, Acm1 was proposed to act as a physiological buffer for Cdh1, precisely controlling Cdh1 activity in combination with inhibitory Cdk phosphorylation to allow proper multi-step assembly of a mitotic spindle [62]. In cells expressing a Cdh1 mutant lacking inhibitory Cdk phosphorylation sites, bipolar spindle assembly was ultra-sensitive to ACM1 gene dosage. In this context, very fine control of Acm1 level by the phosphorylation sensitive and constitutively active ubiquitin-independent proteolytic mechanism could precisely control Acm1 abundance at a level representing the maximal capacity for Cdk phosphorylation. Acm1 expressed above this level would begin to exceed the capacity of Cdk to maintain it in a phosphorylated state and result in rapid proteolysis of hypophosphorylated protein. This is consistent with our unpublished observations that over-expression of Acm1 from the ADH and GAL1 promoters leads to only modest changes in steady-state level.

2.4 Conclusion

The APC-independent proteolysis of Acm1 appears to represent a unique example of highly cell cycle-regulated proteasomal degradation independent of the canonical polyubiquitin targeting system. This mechanism also reflects the existence of alter-

native ways to establish cell cycle expression profiles other than via the SCF and APC E3 ligases. Our work reinforces the cooperative interplay of transcriptional and proteolytic control in establishing strict expression windows of cell cycle regulators during cell division. Future research on this topic should reveal if the unique cell cycle proteolysis of Acm1 represents a general mechanism complementing the ubiquitin proteasome system in governing cell cycle-dependent protein levels.

2.5 Materials and Methods

2.5.1 Strain and plasmid construction, and mutagenesis

All yeast strains used in this study, except those for screening ubiquitin system mutants, are listed in Table 2. Ubiquitin system mutant strains are listed in Table 2-1. All plasmids used in this study are listed in Table S3. Strain YKA468 was constructed by recombinational insertion of a PCR product containing a 3HA epitope tag with *k^lTRP1* selectable marker at the 3' end of CLB5 and a 9MYC tag with HIS3MX6 selectable marker at the 39 end of PDS1 in the *dbf2-2* strain using plasmids pYM22 and pYM19 as templates as described [179]. Strain YKA469 was constructed by standard recombinational replacement of the ACM1 coding sequence with a PCR-generated KanMX4 selectable marker. YKA859 was constructed from FM1175 by deleting ACM1 using PCR-mediated integration of the KanMX4 marker and then inserting a 6HA:NatNT2 tag at the 39 end of KIP1 using pYM17 [179]. YKA404 was generated from Y7092 [180] by PCR-based deletion of ACM1 with the Nat1 nourseothricin resistance cassette. E3 and E2 deletion strains for screening stability of untagged Acm1^{5A} were generated by crossing YKA404 to the appropriate MATa KanMX4 gene deletion strains from Open Biosystems as described [180]. Plasmid pHLP317 expressing 3HA-Fin1 from the GAL1 promoter was constructed by subcloning the BamHI-SalI fragment from pESCW-Fin1-Myc into pESCLEu-3HA (both gifts from H. Charbonneau, Purdue University). The *acm1*^{K0} mutant allele was created in pBluescript by site-directed mutagenesis using the QuikChange Multi kit (Stratagene) and, amplified

Table 2.1: Yeast deletion strains screened for effects on *Acm1* stabilization

Non-essential E3s		Non-essential E2s	Essential E3s
ASI3	PEX12	UBC2	RSP5
ASR1	PIB1	UBC4	PRP19
BRE1	PSH1	UBC5	SCF*
CUL3	RAD5	UBC6	APC*
CUL8	RAD16	UBC7	
DMA1	RAD18	UBC8	
DMA2	RCO1	UBC10	
ETP1	RKR1	UBC11	
FAP1	RTC1	UBC12	
FAR1	SAN1	UBC13	
HEL1	SLX5		
HEL2	SLX8		
HRD1	SNT2		
HUL4	SSM4		
HUL5	TOM1		
IRC20	TUL1		
ITT1	UBR1		
MAG2	UBR2		
MOT2(NOT4)	UFD2		
NFI1	UFD4		
PEP3	ULS1		
PEP5	VPS8		
PEX2	YBR062C		
PEX10			

For all non-essential genes, deletion strains were obtained from the Open Biosystems gene deletion library and crossed to YKA404 to generate combined deletions with *acm1Δ::KanMX4*.

For essential genes RSP5 and PRP19, tetracycline-repressible strains were obtained from the Open Biosystems Tet-promoter collection.

*Effects of SCF on *Acm1* stability were tested using conditional *cdc34* and *cdc53* mutant strains (not shown and [162]). No effect was found. Lack of dependence on APC can be found in Figure 2.1 and [161].

Strains in bold were tested in both Figure 2.8 and Figure 2.10 screens. Non-essential E3 and E2 strains not in bold were only tested in the Figure 2.10 screen.

by PCR, and subcloned into the XhoI sites of pHLP117 [88] to create pHLP328 or subcloned into the SacII and XhoI sites of p415GAL1 to create pHLP329. The one lysine codon in the 3HA sequence of pHLP329 was altered to an arginine codon to create pHLP330. The *3HA-acm1^{K0}* alleles in pHLP328 and pHLP330 were confirmed by DNA sequencing. pHLP298 was constructed by sub-cloning the 3HA-ACM1^{5A} sequence from pHLP209 into p415GAL1. Plasmids for AcM1 stability experiments were constructed by first ligating the PCR-amplified ZZ domain of Protein-A into the HindIII and XhoI sites of p415GAL1 and then ligating the appropriate ACM1 PCR fragments into the PstI and HindIII sites. All plasmid constructs were confirmed by DNA sequencing.

2.5.2 Cell growth and cell cycle arrest

Standard yeast growth conditions and media were used. For G1 arrest, α -factor peptide (GenScript) was added to cultures at a final concentration of 5 mg/ml for BAR1 or 50 mg/l for *bar1* Δ strains. For S phase arrest, solid hydroxyurea (Sigma Aldrich) was added directly to cultures at 10 mg/ml. For G2/M arrest, nocodazole (Sigma Aldrich) was added at a final concentration of 15 mg/ml from a 1.5 mg/ml stock in DMSO. For telophase arrest, strains harboring temperature-sensitive MEN mutants *cdc15-2* or *dbf2-2* were grown initially at 23 °C and then shifted to 37 °C. For all temperature sensitive strains, 23 °C was used as permissive and 37 °C as restrictive temperatures. For synchronous growth from G1 to telophase, α -factor treated *cdc15-2* or *dbf2-2* cells were released from arrest by extensive washing using a vacuum filtration device and resuspension in fresh medium pre-warmed to 37 °C. Growth was continued at 37 °C and samples were removed at the indicated times for analysis. Extracts of synchronized yBR135 and yBR159 cultures for analyzing AcM1 levels in the absence of APC activity [148] were generously provided by David Toczyski (U. California San Francisco). For metaphase block and release, FM1175 and its derivatives were grown in SD-Met-Leu media (50 mL) then transferred to YPD (120

mL) supplemented with 5 mM methionine and grown for 4 hours at 30°C. Cells were then released into 120 mL of selective media (SD-Met-Leu) following vacuum filtration onto a membrane disk (0.8 mm) and washing with 100 mL of SD-Met-Leu media. Cell cycle arrests were confirmed by microscopic analysis of cell morphology and flow cytometry. Flow cytometry analysis was performed exactly as described [88] using an Accuri C6 flow cytometer (BD Biosciences). Cell cycle stage in the synchronous growth experiments was determined by 49,6-diamidino-2-phenylindole (DAPI) staining of formaldehyde-fixed cells and fluorescence microscopy to monitor nuclear division. Images were captured on an Olympus BX51 fluorescence microscope using Metamorph software (Molecular Devices, Inc.) and percentage of cells with segregated DNA masses quantified (minimum 100 cells per timepoint).

2.5.3 Immunoblotting

The following antibodies were used. Monoclonal anti-HA 12CA5 and anti-Myc 9E10 were from Roche Applied Science (catalog numbers 11666606001 and 11667149001, respectively) and were used at concentrations of 0.5 mg/ml (1:10,000 dilution) and 1 mg/ml (1:5,000 dilution), respectively. Rabbit anti-glucose-6-phosphate-dehydrogenase (G6PD) and rabbit anti-Protein A were from Sigma (catalog numbers A9521 and P3775, respectively) and were used at concentrations of 3 ng/ml (1:10,000 dilution) and 0.6 ng/ml (1:50,000 dilution), respectively. Rabbit anti-Clb2, used at 40 ng/ml (1:5,000 dilution) was from Santa Cruz Biotechnology (catalog numbers sc-9071). Horseradish peroxidase-conjugated donkey anti-rabbit and anti-mouse were from Jackson Immuno Research (catalog numbers 111-035-003 and 115-035-003, respectively) and were used at concentrations of 80 ng/ml each. Immunoblots were developed using ECL plus (GE Healthcare) or Luminata (Millipore) detection reagents.

For Acm1 polyclonal antibody production and purification, the complete ACM1 open reading frame was cloned into pGEX6P-1 (GE Healthcare) for overexpression in *E. coli* as an N-terminal GST-fusion protein. The majority of GST-Acm1 is found

in the insoluble fraction of bacterial cell extracts. Insoluble proteins were pelleted by centrifugation and resolubilized in 8 M urea, separated by SDS-PAGE and stained with Coomassie blue. The predominant band was GST-Acm1 and was excised and submitted to Pacific Immunology for polyclonal antibody production. Total Rabbit IgG was purified from serum using Protein A-agarose resin (Sigma Aldrich). Subsequently, anti-Acm1 antibodies were affinity purified using a GST-Acm1 affinity column generated by crosslinking recombinant GST-Acm1 to glutathione-agarose with disuccinimidyl suberate (Thermo Scientific). Acm1 antibody was eluted from the affinity column with 50 mM glycine pH 1.9 and immediately neutralized by addition of Tris-HCl pH 8.0 to 100 mM. Antibody specificity was tested by immunoblotting of yeast whole cell extracts using acm1D cells as a control. 1:5,000 dilutions of the affinity purified antibody were used for all immunoblots. Quantification of chemiluminescent immunoblots was performed using a Bio-Rad Laboratories ChemiDoc XRS+ digital imager and ImageLab software. Images obtained following incubation of blots with chemiluminescent reagent were analyzed using the Image Lab software. Signals were normalized to the G6PD load control signal and then to the 0 min timepoint.

2.5.4 Protein stability assays

Measurements of protein stability were performed by GAL1 promoter shutoff/cycloheximide chase assays as described [94]. Unless stated otherwise, expression was induced with 2% galactose and terminated by addition of 2% glucose and 0.5 mg/ml cycloheximide. For experiments in proteasome mutants (*cim3-1* and *pre1-1 pre2-2*), cells were first arrested with α -factor at 23 °C and then protein expression induced for 30 min prior to shift to 37 °C. For ubiquitin mutant overexpression experiments, actively growing cells were arrested with α -factor in early exponential phase ($OD_{600}=0.4$) and then $CuSO_4$ was added to 100 μ M to induce overexpression of mutant or wild-type ubiquitin from the CUP1 promoter. After 30 min 2% galactose was added to induce expression of the Acm1 or control proteins. To measure stability

of endogenous Acm1, mid-exponential phase cells were treated only with 0.5 mg/ml cycloheximide to terminate expression. For MG-132 treatment, a *pdr5* Δ strain was used to maximize efficacy [181] and cultures were treated with 50 μ M MG-132 (from 10 mM stock in DMSO) for 30 min prior to terminating expression.

For synchronized mitotic exit experiments, Acm1 or Acm1^{N52}-ProtA were expressed from the natural Acm1 promoter on CEN plasmids (pHLP117 or pHLP505, respectively) in a P_{MET3} -CDC20 background. Cultures were arrested in mitosis by Cdc20 depletion as described above and protein levels monitored over time by quantitative immunoblotting.

Screening of ubiquitin system mutant strains Yeast strains individually lacking all known non-essential E2 ubiquitin conjugating enzymes, E3 ubiquitin ligases, and proteasome components were obtained from the Open Biosystems yeast deletion library (Table 2-1). Relative levels and stability of wild type Acm1 and the Acm1^{5A} mutant [94] were measured by immunoblotting as described above. For screening of essential E3 genes, strains from the Tet-repressible essential gene library (Table 2-1) containing pHLP209 expressing 3HA-Acm1^{5A} from the ACM1 promoter were grown until mid-exponential phase and then treated with 2 μ g/ml doxycycline for 2 hrs before processing for immunoblotting.

2.5.5 *In vivo* APC inhibition assay

Inhibition of APC^{Cdh1} *in vivo* was measured exactly as described previously [88].

Spotting growth assay.

Cultures of *sic1* Δ cells transformed with either p415ADH, pHLP361 (P_{ADH} -Acm1-ProtA) or pHLP363 (P_{ADH} -acm1^{N Δ 52}-ProtA) as well as isogenic wild-type and *cdh1* Δ strains transformed with p415ADH were grown to mid-exponential phase selective

Table 2.2: Yeast strains used in this study.

Strain	Genotype	Source
BY4741	MATa <i>his3Δ1 leu2Δ0 met15Δ0 ura3Δ0</i>	Open Biosystems
W303	MATa <i>ade2-1 his3-11,15 leu2-3,112 trp1-1 ura3-1 can1-100</i>	
doa4Δ	(BY4741) MATa <i>doa4::KanMX4</i>	Open Biosystems
MHY753	MATa <i>his3-Δ200 leu2Δ1 ura3-52 lys2-801 trp1-63 ade2-101</i>	[150]
MHY754	MATa <i>his3-Δ200 leu2Δ1 ura3-52 lys2-801 trp1-63 ade2-101 cim3-1</i>	[150]
YKA247	(W303) <i>bar1::URA3 acm1::KanMX4</i>	[88]
YKA404	MAT <i>acm1::Nat1 can1::STE2pr-his5 lyp1Δ his3Δ1 leu2Δ0 ura3Δ0 met15Δ0</i>	This study
YKA407	(BY4741) MATa <i>bar1::hisG acm1::KanMX4 pdr5::URA3</i>	[94]
YWO0607	MATa <i>ura3 leu2-3,112 his3-11,15 CanS Gal+</i>	Dieter H. Wolf
YWO0612	MATa <i>ura3 leu2-3,112 his3-11,15 CanS Gal+ pre1-1 pre2-2</i>	Dieter H. Wolf
YKA468	MATa <i>ura3Δ leu2Δ ade2Δ his3Δ trp1Δ dbf2-2 CLB5-3HA:TRP1 PDS1-9MYC:HIS3</i>	This study
YKA469	(W303) MATa <i>cdc15-2 GFP-TUB1:URA3 acm1::KanMX4</i>	This study
yBR135	(W303) MATa <i>pds1::LEU2 clb5::HIS3 trp1-1::SIC1:TRP1^{10x}</i>	[148]
yBR159	(W303) MATa <i>pds1::LEU2 clb5::HIS3 trp1-1::SIC1:TRP1^{10x} apc2Δ apc11Δ cdc20Δ cdh1Δ</i>	[148]
RJD3268	(W303) MATa <i>uba1::KanMX pRS313-UBA1</i>	Ray Deshaies
RJD3269	(W303) MATa <i>uba1::KanMX pRS313-uba1-204</i>	Ray Deshaies
FM1175	(W303) MATa <i>P_{MET3}-CDC20-HA::TRP1</i>	Foong May Yeong
YKA859	(FM1175) <i>acm1::KanMX4 KIP1-6HA:NatNT2</i>	This study
<i>sic1Δ</i>	(BY4741) MATa <i>sic1::KanMX4</i>	Open Biosystems
<i>cdh1Δ</i>	(BY4741) MATa <i>cdh1::KanMX4</i>	Open Biosystems
RPN11-TAP	(BY4741) MATa <i>RPN11-TAP:HIS3MX</i>	Open Biosystems
SDL135	MATa <i>lys2-801 leu2-3,112 ura3-52 his3-Δ200 trp1-1 pre1::PRE1-TEVProA:HIS3</i>	Daniel Finley

Table 2.3: Yeast plasmids used in this study.

Name	Expressed Protein	Backbone	Marker	Origin	Promoter	Source
LHP306	Ub-K7R	YEp352	<i>URA3</i>	2 μ m	<i>CUP1</i>	[153]
LHP308	Ubiquitin	YEp352	<i>URA3</i>	2 μ m	<i>CUP1</i>	[153]
pESC ^{Trp} -Fin1	Fin1-Myc	pESC-Trp	<i>TRP1</i>	2 μ m	<i>GAL1</i>	[94]
pHLP110	HA-Acm1 ^{5A}	p415GAL1	<i>LEU2</i>	CEN/ARS	<i>GAL1</i>	[94]
pHLP117	3HA-Acm1	p415ADH	<i>LEU2</i>	CEN/ARS	<i>ACM1</i>	[88]
pHLP123	HA-Acm1 ^{ken}	p415GAL1	<i>LEU2</i>	CEN/ARS	<i>GAL1</i>	[89]
pHLP209	3HA-Acm1 ^{5A}	p415ADH	<i>LEU2</i>	CEN/ARS	<i>ACM1</i>	[94]
pHLP212	3HA-Acm1	p415GAL1	<i>LEU2</i>	CEN/ARS	<i>GAL1</i>	[94]
pHLP231	3FLAG-Cdh1	pNC219	<i>TRP1</i>	CEN/ARS	<i>GAL1</i>	[94]
pHLP298	3HA-Acm1 ^{5A}	p415GAL1	<i>LEU2</i>	CEN/ARS	<i>GAL1</i>	This study
pHLP309	Clb2	P415GALL	<i>LEU2</i>	CEN/ARS	<i>GALL</i>	This study
pHLP317	Fin1-3HA	pESC-Leu	<i>LEU2</i>	2 μ m	<i>GAL1</i>	This study
pHLP328	3HA-Acm1 ^{K0}	p415ADH	<i>LEU2</i>	CEN/ARS	<i>ACM1</i>	This study
pHLP330	3HA-Acm1 ^{K0}	p415GAL1	<i>LEU2</i>	CEN/ARS	<i>GAL1</i>	This study
pHLP391	Acm1	P415GAL1	<i>LEU2</i>	CEN/ARS	<i>GAL1</i>	This study
pHLP392	Acm1 ^{5A}	p415GAL1	<i>LEU2</i>	CEN/ARS	<i>GAL1</i>	This study
pHLP397	Acm1-ProtA	p415GAL1	<i>LEU2</i>	CEN/ARS	<i>GAL1</i>	This study
pHLP399	Acm1 ^{NΔ42} -ProtA	p415GAL1	<i>LEU2</i>	CEN/ARS	<i>GAL1</i>	This study
pHLP400	Acm1 ^{NΔ52} -ProtA	p415GAL1	<i>LEU2</i>	CEN/ARS	<i>GAL1</i>	This study
pHLP401	Acm1 ^{NΔ60} -ProtA	p415GAL1	<i>LEU2</i>	CEN/ARS	<i>GAL1</i>	This study
pHLP402	Acm1 ^{NΔ72} -ProtA	p415GAL1	<i>LEU2</i>	CEN/ARS	<i>GAL1</i>	This study
pHLP403	Acm1 ^{NΔ80} -ProtA	p415GAL1	<i>LEU2</i>	CEN/ARS	<i>GAL1</i>	This study
pHLP413	Acm1 ¹⁻¹⁸ -ProtA	p415GAL1	<i>LEU2</i>	CEN/ARS	<i>GAL1</i>	This study
pHLP414	Acm1 ¹³⁻³⁰ -ProtA	p415GAL1	<i>LEU2</i>	CEN/ARS	<i>GAL1</i>	This study
pHLP415	Acm1 ²⁵⁻⁴² -ProtA	p415GAL1	<i>LEU2</i>	CEN/ARS	<i>GAL1</i>	This study
pHLP416	Acm1 ³⁷⁻⁵⁴ -ProtA	p415GAL1	<i>LEU2</i>	CEN/ARS	<i>GAL1</i>	This study
pHLP417	Acm1 ⁴⁹⁻⁶⁶ -ProtA	p415GAL1	<i>LEU2</i>	CEN/ARS	<i>GAL1</i>	This study
pHLP503	Acm1 ¹⁻⁵² -ProtA	p415GAL1	<i>LEU2</i>	CEN/ARS	<i>GAL1</i>	This study
pHLP504	Acm1 ¹²⁻⁵² -ProtA	p415GAL1	<i>LEU2</i>	CEN/ARS	<i>GAL1</i>	This study
pHLP505	Acm1 ^{NΔ52} -ProtA	p415GAL1	<i>LEU2</i>	CEN/ARS	<i>ACM1</i>	This study
pHLP361	Acm1-ProtA	p415ADH	<i>LEU2</i>	CEN/ARS	<i>ADH1</i>	This study
pHLP363	Acm1 ^{NΔ52} -ProtA	p415ADH	<i>LEU2</i>	CEN/ARS	<i>ADH1</i>	This study

media, then washed and resuspended in sterile TE to OD₆₀₀ of 1.0. Serial 10-fold dilutions were spotted onto SD-Leu agar plates and grown at 37 °C for 2 days.

Growth rate measurements.

Growth rates were measured by diluting exponentially growing cultures to an OD₆₀₀ of 0.05 in selective media and growing in 96-well plates at 30 °C with shaking in a BioTek Synergy 2 plate reader. Absorbance measurements at 600 nm were taken every 60 minutes.

Proteasome activity assays.

Proteasomes were purified from yeast soluble whole cell extracts by IgG-agarose (Sigma-Aldrich) affinity chromatography using a protocol described previously. For 26S proteasomes, a strain expressing an RPN11-TAP fusion was used and for 20S proteasomes a strain expressing a PRE1-TEVProA fusion was used. To assay general activity of proteasome preparations, the fluorogenic substrate Suc-LLVY-AMC (Peptides International, Inc.) was used as described [55] at 100 mM in reaction buffer (50 mM Tris-HCl pH 7.4, 5 mM MgCl₂, 10% glycerol, and 1 mM ATP). Fluorescence of the hydrolyzed AMC moiety was measured at excitation and emission wavelengths of 380 and 440 nm, respectively. Specific activities of purified 26S proteasome and 20S proteasomes were measured as described [55]. Values for the 20S proteasome were comparable to that observed in other studies [55]. We did not find reports of specific activities for the budding yeast 26S proteasome on the Suc-LLVY-AMC substrate under similar conditions.

GST-Acm1 and 6His-Acm1 were purified from *E. coli* as described previously [89, 129]. The GST tag was cleaved off Acm1 with PreScission (3C) protease (GE Life Sciences). To assay degradation of purified GST-Acm1 by the 26S proteasome preparation, 200 mg of GST-Acm1 and 500 mg proteasome were mixed in 500 ml of reaction buffer with 100 mM NaCl at 30 °C and samples were collected over time and analyzed by western blot using anti-Acm1 antibody. Degradation of 6His-Acm1 by 26S and 30 °C 20S proteasomes was assayed similarly for 30 min at 30 °C. Free Acm1 was generated by pre-treatment of GST-Acm1 with 3C protease before mixing with

26S proteasome and proceeding as above. 5 mM epoxomicin (Peptides International, Inc.) was used where indicated to specifically inhibit the proteasome.

Declaration of collaborative work

The work presented in Chapter 2 has been reprinted from Melesse M, Choi E, Hall H, Walsh MJ, Geer MA, Hall MC (2014) Timely Activation of Budding Yeast APC^{Cdh1} Involves Degradation of Its Inhibitor, Acm1, by an Unconventional Proteolytic Mechanism. PLoS ONE 9(7): e103517. doi:10.1371/journal.pone.0103517 under the Creative Commons Attribution 4.0 International License. To view a copy of this license, visit <http://creativecommons.org/licenses/by/4.0/> or send a letter to Creative Commons, PO Box 1866, Mountain View, CA 94042, USA.

Contributions:

Conception and design of experiments: Melesse M., Choi E, Hall H, Hall MC.

Performed the experiments: Melesse M., Choi E, Hall H, Walsh MJ, Hall MC, Geer MA.

Data presented in Figures 2.6, 2.7, 2.10, 2.11 panels A and B were by Melesse M.

Data Analysis: Melesse M., Choi E, Hall H, Walsh MJ, Hall MC

Wrote the paper: Melesse M., Hall MC.

3. CDC14 PHOSPHATASE SUBSTRATE SELECTIVITY IS BROADLY CONSERVED DURING EVOLUTION

3.1 Introduction

Cdc14 is somewhat unique among phosphatases involved in the regulation of the cell cycle. Unlike mitotic serine/threonine phosphoprotein phosphatases (PPPs), it does not function as part of a large protein complex [95]. It is currently unclear if Cdc14 has conserved functions in evolutionarily distant species. As discussed in Chapter 1, there is little conservation of Cdc14's role in regulating the cell cycle. One method to address this current lack of knowledge is to biochemically characterize the enzyme to attempt to identify protein substrates. If one is able to define a substrate sequence preference for the enzyme *in vitro*, it would be possible to predict likely physiological substrates as has been demonstrated in budding yeast [110]. The extent to which the structural conservation of the active site results in conservation of substrates is also currently not understood.

Budding yeast Cdc14 possesses strict selectivity for phosphoserine Cdk phosphorylation sites (Ser/Thr-Pro) [110, 129]. Furthermore, substrates with multiple basic residues C-terminal to the phosphoserine are preferred. The features that determine this substrate selectivity appear to be present near the enzyme active site, in contrast to other multisubunit mitotic PSPs, whose selectivity is a product of regulatory subunit association [95]. Alanine (A285) in the active site confers selectivity for phosphoserine over phosphothreonine by steric clash with the methyl group on the phosphothreonine side chain of substrates [129]. *In silico* molecular dynamics modeling of peptide binding to hCDC14B also suggests that the preference for substrates with a +3 basic residue is a result of a cation- π interaction with solvent exposed aromatic residues proximal to the active site [110]. While several key determinants of Cdc14

specificity are well-defined, specificity has not yet been comprehensively defined. For example, possible contributions of residues N-terminal to the phosphoamino acid towards substrate recognition have not been explored. The experiments in this study aim to improve the understanding of Cdc14 substrate selectivity, mostly by defining its conservation across diverse eukaryotic species. This understanding will elucidate the extent of substrate and functional conservation across these species. Differences in substrate selectivity can also be explored in investigating divergence in function as well as in the development of inhibitors that are selective among Cdc14 enzymes.

The main goal of this project were to compare the substrate sequence selectivity of Cdc14 protein phosphatases from a diverse set of organisms and to search for additional substrate specificity determinants. The basis of this line of experiments was the discovery that budding yeast Cdc14 demonstrates preference for a subset of Cdk substrates characterized by utilizing phosphopeptide as well as whole protein substrates [129, 130, 182]. In the experiments presented below, I have expanded on the amino acid sequences that constitute optimal Cdc14 substrates. Furthermore, I have investigated the extent to which substrate selectivity observed in budding yeast Cdc14 is conserved among Cdc14 enzymes from various organisms. To this end, the substrate selectivity of Cdc14 from the fission yeast *Schizosaccharomyces pombe* (Clp1, Flp1), the plant pathogenic fungus *Fusarium graminearum* (FgCdc14) and the two paralogs of human CDC14 (hCDC14A and B) were investigated and compared to budding yeast Cdc14 using phosphopeptide substrates.

This chapter aims to investigate ScCdc14 substrate selectivity in more detail by analyzing the effects of changes in sequence on the kinetics of phosphopeptide substrate dephosphorylation. The extent to which Cdc14 selectivity is conserved across an evolutionarily diverse set of organisms is also explored. Given the Cdc14 active site conservation, I hypothesize that Cdc14 substrate selectivity is conserved among enzymes from evolutionarily distant species.

3.2 Results

3.2.1 Determination of kinetic parameters of *Saccharomyces cerevisiae* Cdc14

This study built on these previous results. Phosphopeptide variants based on the sequences of known Cdc14 substrates (Acm1pS3 and Acm1pS31 listed in Table 3.7) were used to perform steady state kinetic measurements. Unsurprisingly, the strict preference of Cdc14 for phosphoserine containing peptides was observed by the lack of catalytic activity towards phosphothreonine containing substrates in the context of both phosphopeptide sequences (Figure 3.1, Table 3.1). *Sc*Cdc14 was also highly sensitive to mutations at the +1 position C-terminal to the phosphoserine (Figure 3.1) confirming that Cdc14 was selective for proline-directed phosphorylation sites. Removal of all C-terminal basic residues (+3 to +5 positions) resulted in a drastic reduction of catalytic efficiency of *Sc*Cdc14 (Figure 3.1).

Figure 3.3, panel A and Table 3.1 demonstrated that, in the case of the Acm1pS31 phosphopeptide, Cdc14 was not sensitive to single mutations to basic residues at positions +4 and +5 C-terminal to the site of phosphorylation given that the substrate contains a lysine at +3. The requirement of a +3 basic residue was strongly demonstrated by the reduction in activity towards substrates lacking any basic residue at +3 (Figure 3.2 and Table 3.1). The data also demonstrated that the identity of the basic residue at +3 had a significant effect on Cdc14 activity, Arg being significantly less favorable to Lys. Simultaneous mutation of the +4 and +5 basic residues significantly reduced Cdc14 catalytic efficiency (Figure 3.3 panel B, Table 3.1). This reduction in activity resulted from the increase in K_m .

These observations were in agreement with Cdc14 substrate selectivity previously observed [129, 130] and provided a basis for comparing any deviations in selectivity of Cdc14 from other organisms.

Table 3.1: **Steady-state kinetic parameters for phosphopeptide substrates dephosphorylated by *S. cerevisiae* Cdc14.** Steady state kinetic parameters, k_{cat} and K_m , were determined by measuring initial velocity as a function of peptide substrate concentration and fitting the Michaelis-Menten equation to the data using nonlinear regression. The mean \pm standard deviation from three independent trials are presented. The sequence variation column shows the nomenclature for each peptide variant of the peptide provided in the sequence column (full sequences given in Table 3.7).

Sequence	Sequence variation	k_{cat} (s^{-1})	K_m (μM)	k_{cat}/K_m (M^{-1}/s^{-1})
VKGNELRpSPSKRRSQI		0.06 ± 0.015	14 ± 34	4699
	pT	0.009 ± 0.003	615 ± 535	15.3
	+3A	1.0 ± 0.05	1285 ± 133	781
	+4A	0.078 ± 0.006	16 ± 12	4951
	+5A	0.12 ± 0.02	20 ± 9.8	4512
	+3R	0.82 ± 0.03	388 ± 209	325
	+4A,+5A	0.1 ± 0.01	121 ± 48	882
	+3R,+4A,+5A	0.16 ± 0.03	600 ± 224	266
	+3A,+4A,+5A	0.018 ± 0.001	1376 ± 240	12.9
MIpSPSKKRTI		0.12 ± 0.04	193 ± 74	624
	pT	0.005 ± 0.0003	234 ± 69	23
	+1A	0.03 ± 0.002	2293 ± 355	13
	+3A	0.057 ± 0.003	1250 ± 159	45

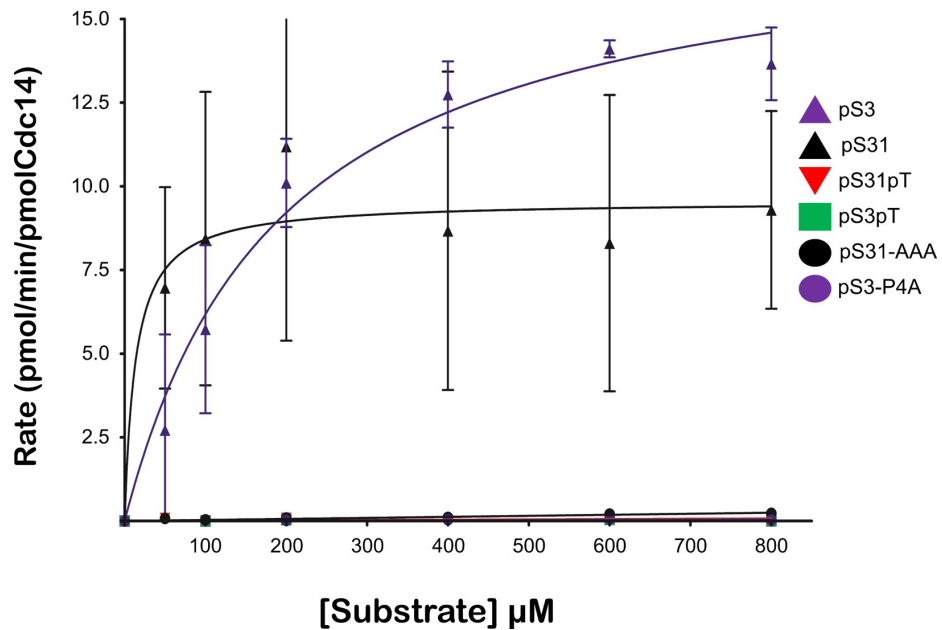


Fig. 3.1.: **Budding yeast Cdc14 was highly selective for phosphoserine containing phosphopeptide substrates** An *in vitro* dephosphorylation reaction was performed as described in the experimental procedures section. Rate of phosphopeptide dephosphorylation was plotted as a function of peptide concentration. The data were fit to the Michaelis-Menten equation using GraphPad Prism and steady-state kinetic parameters, k_{cat} and K_m , were obtained. For assays where substrate saturation was not achieved, a linear fit was generated and k_{cat}/K_m was estimated as described in the experimental procedures section. These values are reported in Table 3.1. Data represent the mean of 3 independent experiments and error bars show standard deviation of the mean. Mutations of pSer to pThr, +1 Pro and removal of all C-terminal basic residues led to a significant reduction of Cdc14 activity against phosphopeptide substrates derived from known Cdc14 substrates.

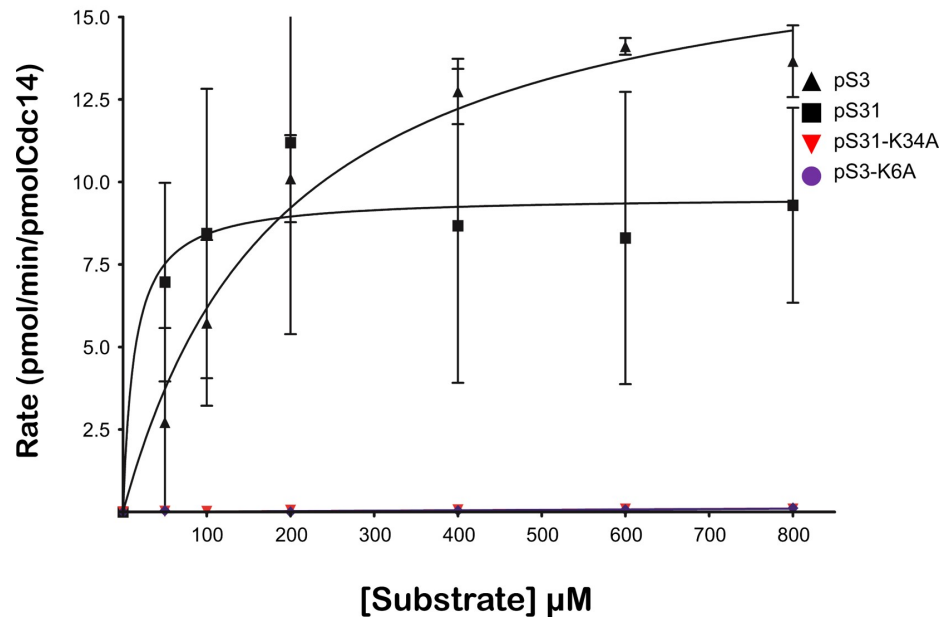


Fig. 3.2.: **Loss of lysine three residues C-terminal to Ser(P) drastically reduced budding yeast Cdc14 activity.** Mutation of the +3 lysine in two previously characterized substrates led to a significant reduction in Cdc14 activity. Rate of phosphopeptide dephosphorylation was plotted as a function of peptide concentration. The data were analyzed as described in Figure 3.1 and the kinetic parameters are reported in Table 3.1

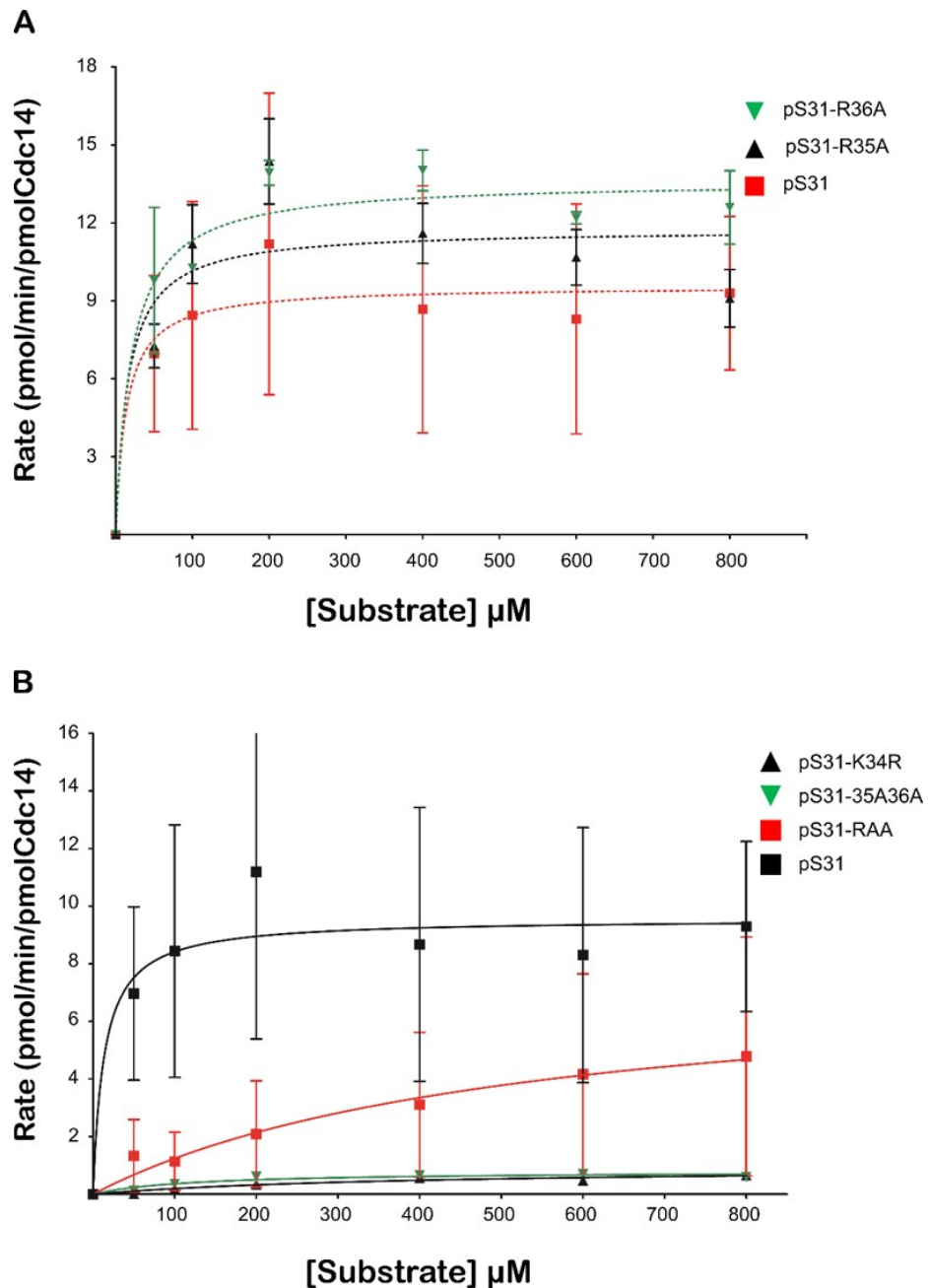


Fig. 3.3.: Budding yeast Cdc14 efficiently dephosphorylated phosphopeptides substrates containing a single basic residue C-terminal to phosphoserine. Individual mutation of basic residues at +4 and +5 residues C-terminal to the phosphoserine (**Panel A**) or changing +3 lysine to Arginine (**Panel B**) had a major effect on the activity of Cdc14. Rate of phosphopeptide dephosphorylation was plotted as a function of peptide concentration. The data were analyzed as described in Figure 3.1 and the kinetic parameters are reported in Table 3.1

3.2.2 The *Fusarium graminearum* Cdc14 (FgCdc14) Substrate selectivity was similar to *S. cerevisiae* Cdc14

F. graminearum Cdc14 (FgCdc14) shares the sequences that define the Cdc14 substrate binding site with *S. cerevisiae* Cdc14 (Figure 1.5, [102]) predicted to contribute to substrate selection based on modeling studies [110,129]. Hence, the substrate selectivity observed in budding yeast was hypothesized to be conserved for FgCdc14

As expected, FgCdc14 demonstrated a high degree of selectivity for phosphoserine containing phosphopeptides over those with either phosphothreonine or phosphotyrosine (Figures 3.4 (panels B and C) and 3.5, Tables 3.3 and 3.2). FgCdc14 was also very sensitive to the absence of a lysine at the +3 position and mutations at the +1 proline (Figures 3.4 (panel C) and 3.5). Complete lack of a C-terminal basic residue (between +3 and +5) led to a drastic reduction in catalytic efficiency. Lysine was also the preferred basic residue at +3 both in the context of the original peptide sequence and when it was the sole basic residue between positions +3 and +5. Changes to the sequence N-terminal to phosphoserine (-1 and -2 positions) have very little effect. The effects of peptide sequence mutations described above were observed with all the peptides substrates tested. The *F. graminearum* Cdc14 catalytic domain (FgCdc14^{cat}) had reduced overall enzymatic activity but the trends in substrate selectivity observed with the full length protein also apply (Figure 3.6, Table 3.3).

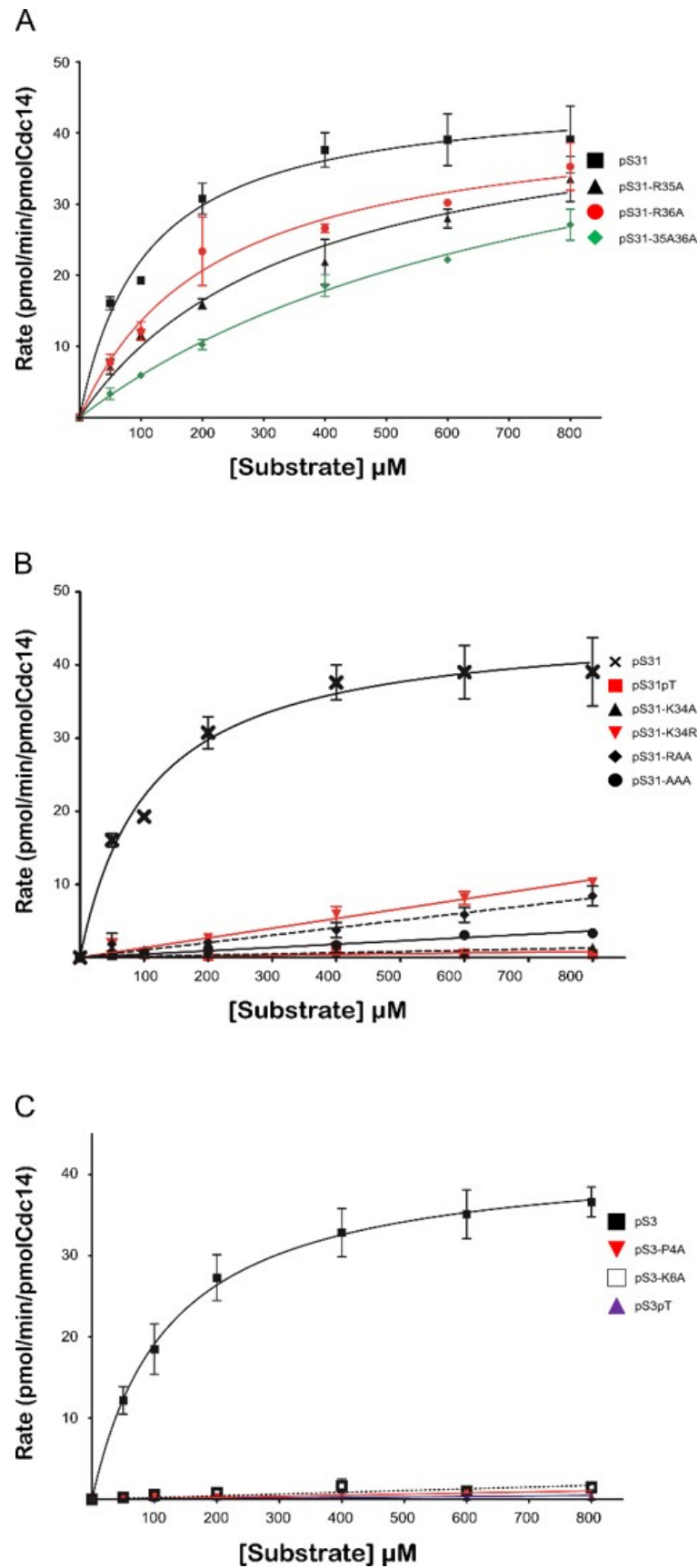


Fig. 3.4.: FgCdc14 enzyme displays substrate selectivity similar to *S. cerevisiae* Cdc14. Mutations of the +4 and +5 basic residues (**Panel A**), +3 lysine (**Panel B**), +1 proline and phosphoserine (**Panel C**) lowered FgCdc14 activity towards phosphopeptide substrates. Rate of phosphopeptide dephosphorylation was plotted as a function of peptide concentration. The data were analyzed as described in Figure 3.1 and the kinetic parameters are reported in Table 3.2

Table 3.2: **Steady-state kinetic parameters for FgCdc14 catalyzed dephosphorylation of phosphopeptides.** Steady state kinetic parameters, k_{cat} and K_m , were determined by measuring initial velocity as a function of peptide substrate concentration and fitting the Michaelis-Menten equation to the data presented in figure 3.4 using nonlinear regression. The mean \pm standard deviation from three independent trials are presented. The sequence variation column shows the nomenclature for each peptide variant of the peptide provided in the sequence column (full sequences given in Table 3.7).

Sequence	Sequence variation	k_{cat} (s^{-1})	K_m (μM)	k_{cat}/K_m (M^{-1}/s^{-1})
VKGNELRpSPSKRRSQI		0.76 ± 0.04	107 ± 23	6542
	pT	N/A	N/A	4.1^a
	+3A	N/A	N/A	56^a
	+3R	N/A	N/A	98^a
	+3R, +4A,+5A	N/A	N/A	71^a
	+4A	0.46 ± 0.05	359 ± 93	1950
	+5A	0.31 ± 0.03	219 ± 56	3196
	+4A,+5A	0.3 ± 0.04	815 ± 196	859
	+3A,+4A,+5A	N/A	N/A	19^a
MIpSPSKKRTI		0.7 ± 0.04	122 ± 25	5737
	pT	N/A	N/A	9.9^a
	+1A	N/A	N/A	21.6^a
	+3A	N/A	N/A	36.2^a

^a Steady state parameters could not be calculated for these peptides because V_{max} was not reached at the $[S]$ used. The slope of the line fit to the V vs. $[S]$ curve was applied to equation 3.4.

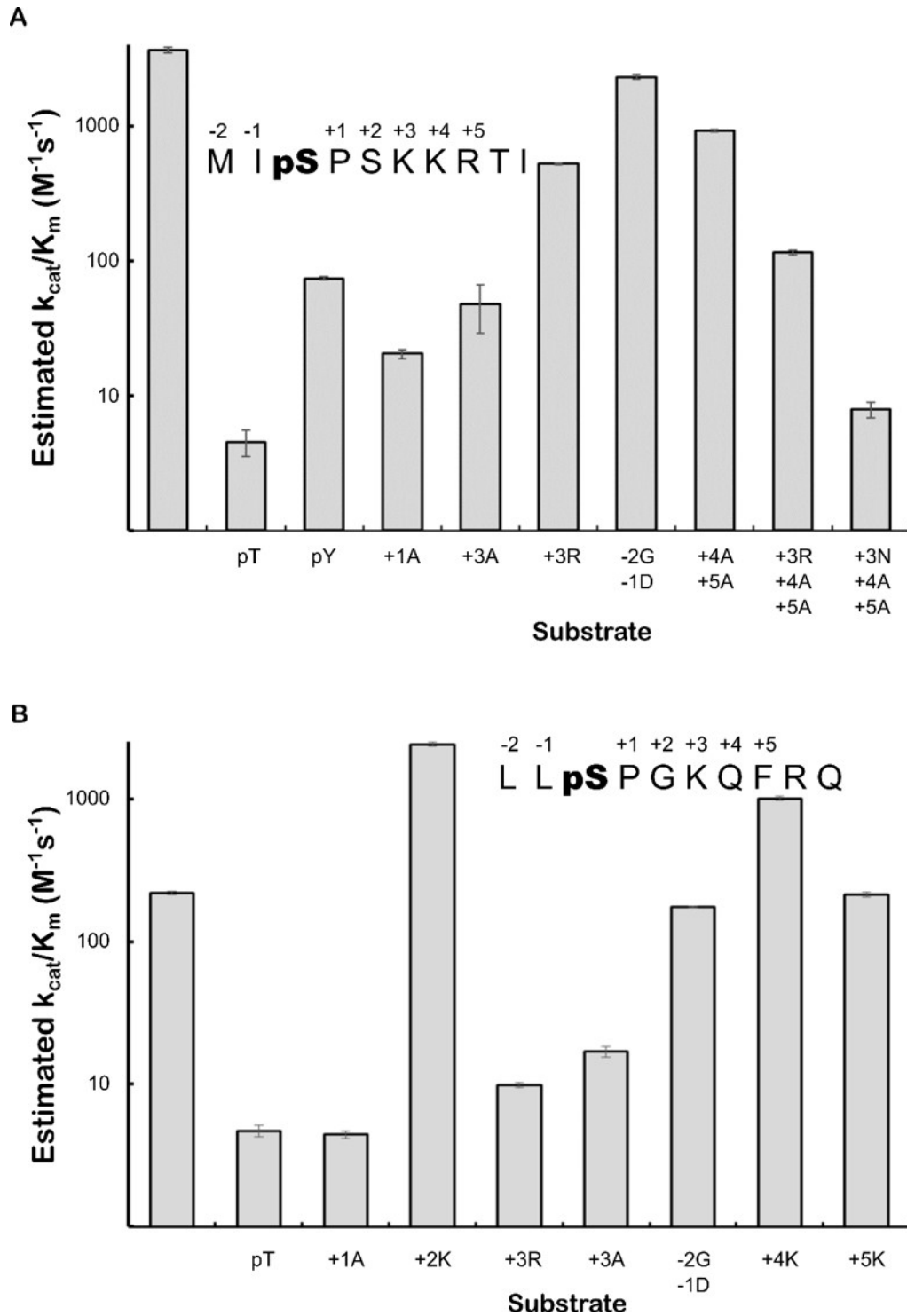


Fig. 3.5.: Estimated k_{cat}/K_m values for *F. graminearum* Cdc14 obtained from initial velocity measurements. Initial reaction velocity measurements at low concentrations (below K_m , $100\mu M$) phosphopeptides series of Acm1pS3 (**panel A**) and Cdh1pS239 (**panel B**) and $75nM$ of FgCdc14 were used to estimate apparent k_{cat}/K_m by applying equation 3.4. The first bar in each panel represents the phosphopeptide whose sequence was shown. The labels on the x axis represent the substitutions made at the positions (relative to the pSer). Data are the average of three independent experiments and error bars represent standard deviation of the mean. Apparent k_{cat}/K_m are reported in Table 3.3

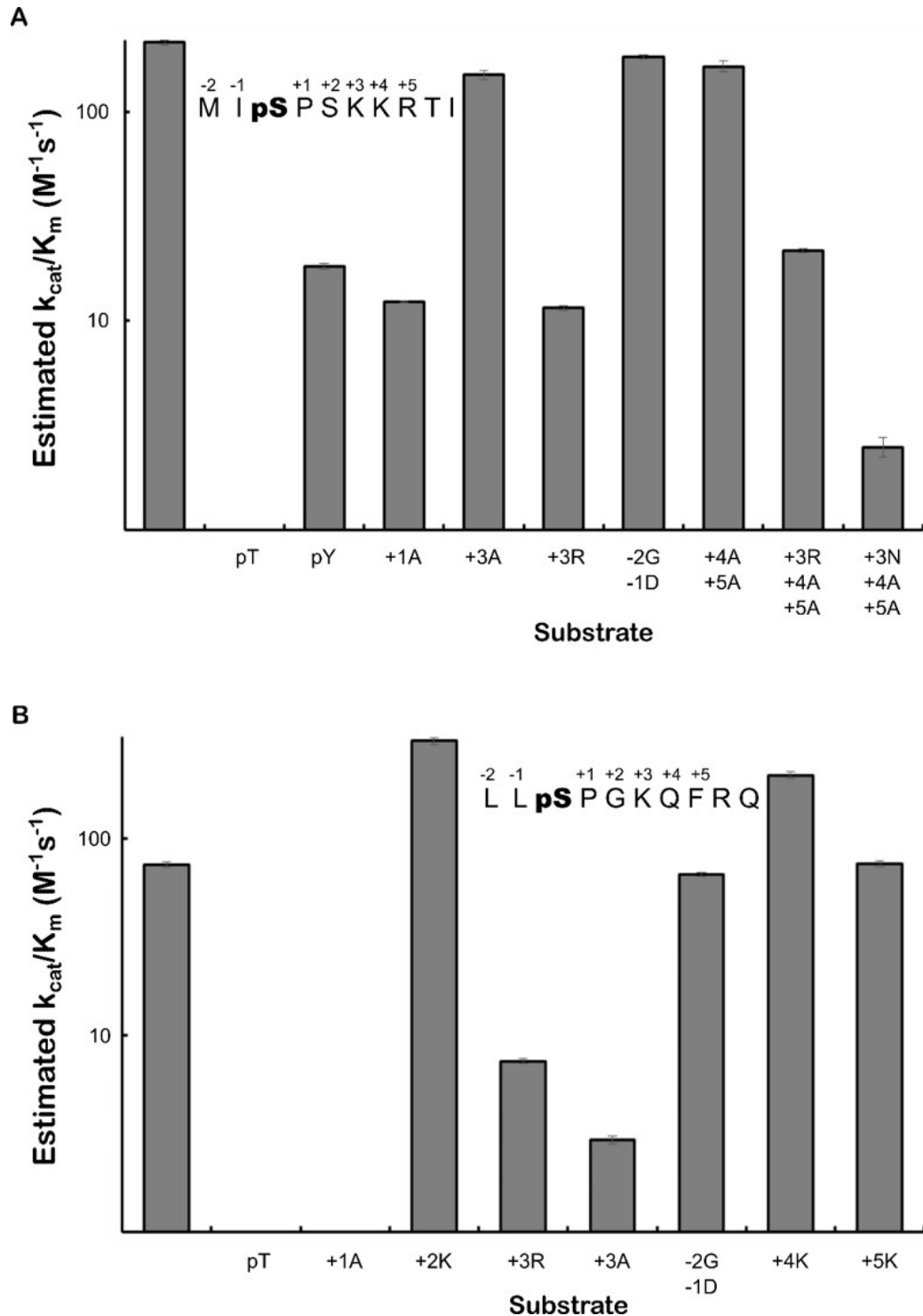


Fig. 3.6.: Estimated k_{cat}/K_m values for the catalytic domain of *F. graminearum* Cdc14 obtained from initial velocity measurements. Initial reaction velocity measurements at low concentrations (below K_m , $100\mu M$) using phosphopeptide series of AcmlpS3 (panel A) and Cdh1pS239 (panel B) and $600nM$ of FgCdc14^{cat} were used to estimate apparent k_{cat}/K_m by applying equation 3.4. The first bar in each panel represents the phosphopeptide whose sequence was shown. The labels on the x axis represent the substitutions made at the positions (relative to the pSer). Data are the average of three independent experiments and error bars represent standard deviation of the mean. Apparent k_{cat}/K_m are reported in Table 3.3

Table 3.3: **Catalytic efficiency (k_{cat}/K_m) estimates of purified FgCdc14.** Catalytic efficiency was estimated from initial velocity measurements at low substrate concentration (Figures 3.5 and 3.6) by applying equation 3.4. The mean \pm standard deviation of three independent trials are presented. The sequence variation column shows the nomenclature for each peptide variant of the peptide provided in the sequence column (full sequences given in Table 3.7).

Sequence	Sequence variation	FgCdc14 Estimated k_{cat}/K_m ($M^{-1}S^{-1}$)	FgCdc14 ^{cat} Estimated k_{cat}/K_m ($M^{-1}S^{-1}$)
		3674 ± 189	214 ± 7
MIpSPSKKRTI	pT	5 ± 1	0.29 ± 0.03
	pY	74 ± 2	18.2 ± 0.6
	+1A	21 ± 2	12.4 ± 0.2
	+3A	48 ± 19	11.5 ± 0.4
	+3R	524 ± 9	150 ± 8
	-2G,-1D	2313 ± 92	165 ± 10
	+4A,+5A	920 ± 17	183 ± 4
	+3R,+4A,+5A	115 ± 5	22 ± 1
	+3N,+4A,+5A	8 ± 1	2.5 ± 0.3
		219 ± 6	73 ± 2
LLpSPGKQFRQ	pT	4.4 ± 0.4	1.1 ± 0.1
	+1A	4.5 ± 0.3	0.97 ± 0.02
	+2K	2414 ± 75	311 ± 12
	+3A	9.9 ± 0.4	2.9 ± 0.1
	+3R	17 ± 1	7.4 ± 0.2
	-2G,-1D	174 ± 3	65 ± 1
	+4K	1007 ± 37	208 ± 8
	+5R	213 ± 8	74 ± 3

3.2.3 Human Cdc14A (hCDC14A) displayed substrate selectivity similar to *S. cerevisiae* Cdc14

The substrate selectivity observed in to ScCdc14 and FgCdc14 was similar for hCDC14A. The selectivity for phosphoserine over phosphothreonine containing phosphopeptide substrate, the necessity of a basic residue at +3 position and the requirement of a +1 proline are conserved (Figures 3.7, Table 3.4). Although Arg at +3, as the sole basic C-terminal residue was able to support Cdc14 activity, the catalytic efficiency observed was significantly attenuated (Figure 3.7).

Table 3.4: **Steady-state kinetic parameters for hCDC14A catalyzed dephosphorylation of phosphopeptides.** Steady state kinetic parameters, k_{cat} and K_m , were determined by measuring initial velocity as a function of peptide substrate concentration and fitting the Michaelis-Menten equation to the data using nonlinear regression. The mean \pm standard deviation from three independent trials are presented. The sequence variation column shows the nomenclature for each peptide variant of the peptide provided in the sequence column (full sequences given in Table 3.7).

Sequence	Sequence variation	k_{cat} (s^{-1})	K_m (μM)	k_{cat}/K_m (M^{-1}/s^{-1})
VKGNELRpSPSKRRSQI		0.08 ± 0.01	51.2 ± 5.1	1616.7
	pT	N/A	N/A	4.3^a
	+3A	0.06 ± 0.01	1500 ± 538	39.3
	+4A	0.11 ± 0.02	113 ± 10	934.8
	+5A	0.09 ± 0.03	167 ± 25.3	566.3
	+3R	0.82 ± 0.05	142 ± 30	720.5
	+3R,+4A,+5A	0.148 ± 0.007	398 ± 65	372.3
	+3A,+4A,+5A	N/A	N/A	7.3^a
MIpSPSKKRTI		0.098 ± 0.003	93.86 ± 13.73	1046
	pT	N/A	N/A	3.4^a
	+1A	N/A	N/A	11^a
	+3A	0.032 ± 0.003	353 ± 121	90.1

^a Steady state parameters could not be calculated for these peptides because V_{max} was not reached at the [s] used. The slope of the line fit to the V vs. [S] curve was applied to equation 3.4.

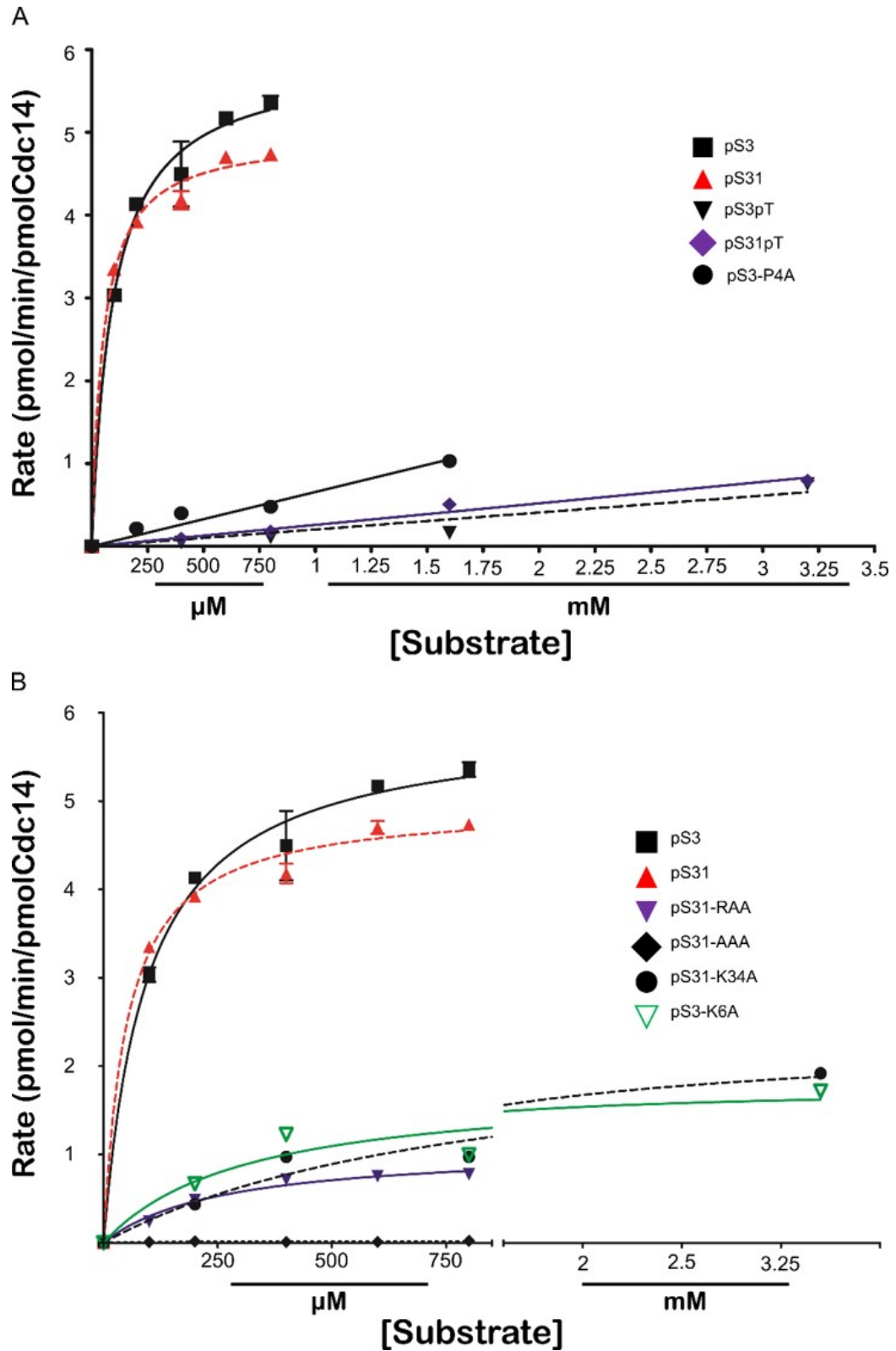


Fig. 3.7.: hCDC14A displayed substrate selectivity similar to *Sc.* Cdc14. **A.** Mutation of pSer to pThr, mutation of +1 pro, and **B.** +3 Lys led to reduction in hCDC14A activity. Rate of phosphopeptide dephosphorylation was plotted as a function of peptide concentration. The data were analyzed as described in Figure 3.1 and the kinetic parameters are reported in Table 3.4

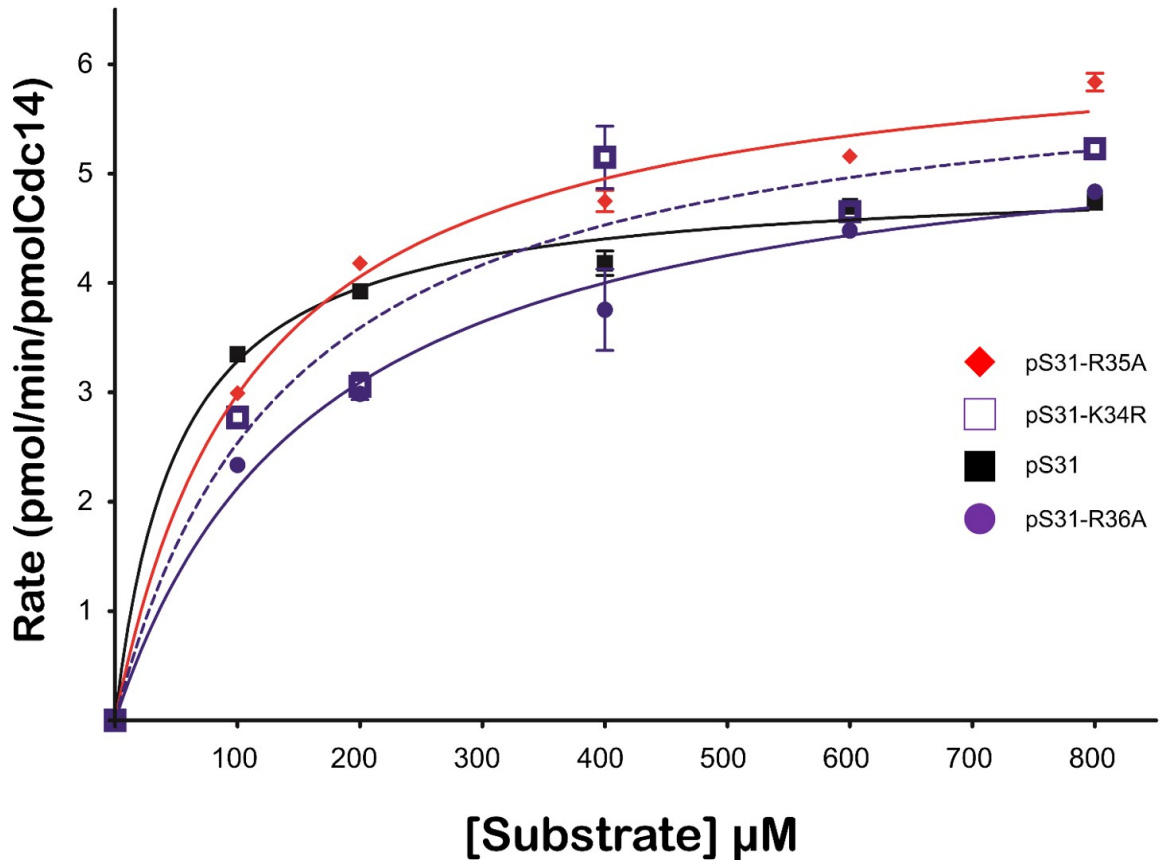


Fig. 3.8.: **Mutations of +4 and +5 basic residues had an intermediate effect on hCDC14A activity** Individual mutations of +4 and +5 basic residues and change of the +3 Lys to Arg lead to a reduction in hCDC14A activity but the effect was not as severe as complete loss of +3 basic residue. Rate of phosphopeptide dephosphorylation was plotted as a function of peptide concentration. The data were analyzed as described in Figure 3.1 and the kinetic parameters are reported in Table 3.4

3.2.4 *Schizosaccharomyces pombe* Cdc14 (Clp1) displayed substrate selectivity similar to ScCdc14

In initial velocity assays performed using Clp1, the *S. pombe* orthologue of ScCdc14, similar substrate selectivity features were observed. There was a strict preference for phosphoserine residues over phosphothreonine (Figure 3.9, Table 3.5). Loss of the +3 Lys and +1 Pro drastically reduced catalytic efficiency. Mutation of basic

residues C-terminal to the site of phosphorylation negatively impacts Clp1 activity towards both phosphopeptide substrates tested (Figure 3.9). As was the case for the other Cdc14 enzymes tested thus far, Lys was preferred at the +3 position over Arg.

Table 3.5: **Catalytic efficiency (k_{cat}/K_m) estimates of purified Clp1.** Catalytic efficiency was estimated from initial velocity measurements at low substrate concentration by applying equation 3.4. The mean \pm standard deviation of three independent trials are presented. The sequence variation column shows the nomenclature for each peptide variant of the peptide provided in the sequence column (full sequences given in Table 3.7).

Sequence	Sequence variation	Clp1 estimated k_{cat}/K_m ($M^{-1}S^{-1}$)
		374 ± 44
	pT	14.5 ± 17
	+3A	6.5 ± 14
	+4A	125 ± 43
VKGNELR p SPSKRRSQI	+5A	160 ± 24
	+3R	108 ± 18
	+4A,+5A	60 ± 10
	+3R,+4A,+5A	38 ± 26
		163 ± 24
MI p SPSKKRTI	pT	17 ± 7
	+1A	6.2 ± 5.2
	+3A	10 ± 7

3.2.5 There are no major variations in Cdc14 substrate selectivity between species

The data presented in previous sections were generated using phosphopeptides that contained a limited number of changes, based on previous observations about Cdc14 selectivity. While this revealed major determinants for specificity, it is possible that other amino acids and other positions near the phosphoamino acid could influence

substrate recognition as well. Hence, an unbiased positional scanning approach was undertaken to identify substrate positions and residues that influence dephosphorylation of the phosphopeptide substrate Cdh1pS239 (LL**p**SPGKQFR). This substrate has previously been shown to yield intermediate Cdc14 activity [129] and was ideal for observing increases as well as reductions in activity that result from changes in the peptide sequence. The quality of the phosphopeptide array was assayed by use of the Mn^{2+} -dependent λ protein phosphatase with activity towards phosphorylated serine, threonine and tyrosine residues (New England Biolabs). All peptides in the array are efficiently dephosphorylated by λ phosphatase (Figure 3.10).

The phosphopeptide array results using ScCdc14 reconfirm the observations presented in the previous section that +1 Pro was essential for high activity. Mutations of the +3 position also led to a significant drop in activity (Figure 3.11). One substantial observation was that most mutations of the +2 Gly to other amino acids led to a slight increase in activity but Pro and Val were poorly tolerated at this position. In agreement with previous results, introduction of additional Lys at +4 and +5 raised activity, a trend not observed for Arg. An interesting observation was that there were mutations in the N-terminal positions that slightly enhanced activity. Val introduction at both -1 and -2 was favorable. Tyr at position -2 led to the highest increase in activity. The reasons for the observed increases for mutations at positions -1 and -2 could be that the original amino acids at those positions are disfavored because there were multiple mutations that led to an increase in activity. This suggests that sequence immediately upstream of pSer-Pro could modulate substrate recognition to some degree. Identifying other trends in substrate selectivity was a challenge because there were no common amino acid properties, like R group charge, length, or aromaticity, that indicate a particular feature was preferred at any given position. This is an indication that there were no other major determinants of substrate selectivity that were not previously observed.

The phosphopeptide array results using Clp1 also illustrated the preference of +1 Pro and +3 Lys (Figure 3.12). However, there was activity, higher than the original

sequence, observed for changes at both +1 and +3 positions. Notably, changes to Gly and Trp at +1 and Gly at +3 led to a greater than four-fold and two-fold increase, respectively, over the starting sequence. As was observed with ScCdc14, Pro and Val at +2 were disfavored and most mutations away from the original sequence at this position led to increased activity. In agreement with previous results, introduction of additional Lys at +4 raised activity by more than three-fold as did the introduction of Gly, with Arg not being particularly favored. However, unlike ScCdc14, Arg introduction at +5 led to a greater than five-fold increase in activity whereas Lys had a relatively small effect. Changes in the N-terminal positions also enhance activity. Gly and Pro at -2 and Gln and Val at -1 resulted in a greater than five-fold increase in activity over the original sequence.

Assays with FgCdc14 also illustrated the requirement of +1 Pro and +3 Lys (Figure 3.13). Surprisingly, Gly at +1 was actually preferred over the original Pro. Pro and Val at +2 are disfavored and all mutations away from the original sequence led to more than a doubling in activity. In agreement with previous results, introduction of additional Lys at +4 raises activity, but unlike ScCdc14, Arg at this position also led to an increase. As observed with Clp1, Arg introduction at +5 also led to a greater than doubling in activity whereas Lys has a relatively small effect. Changes in the N-terminal positions also enhanced activity. Pro, Thr, and Tyr at -2 and Val and Gln at -1 resulted in a greater than four-fold increase in activity over the original sequence.

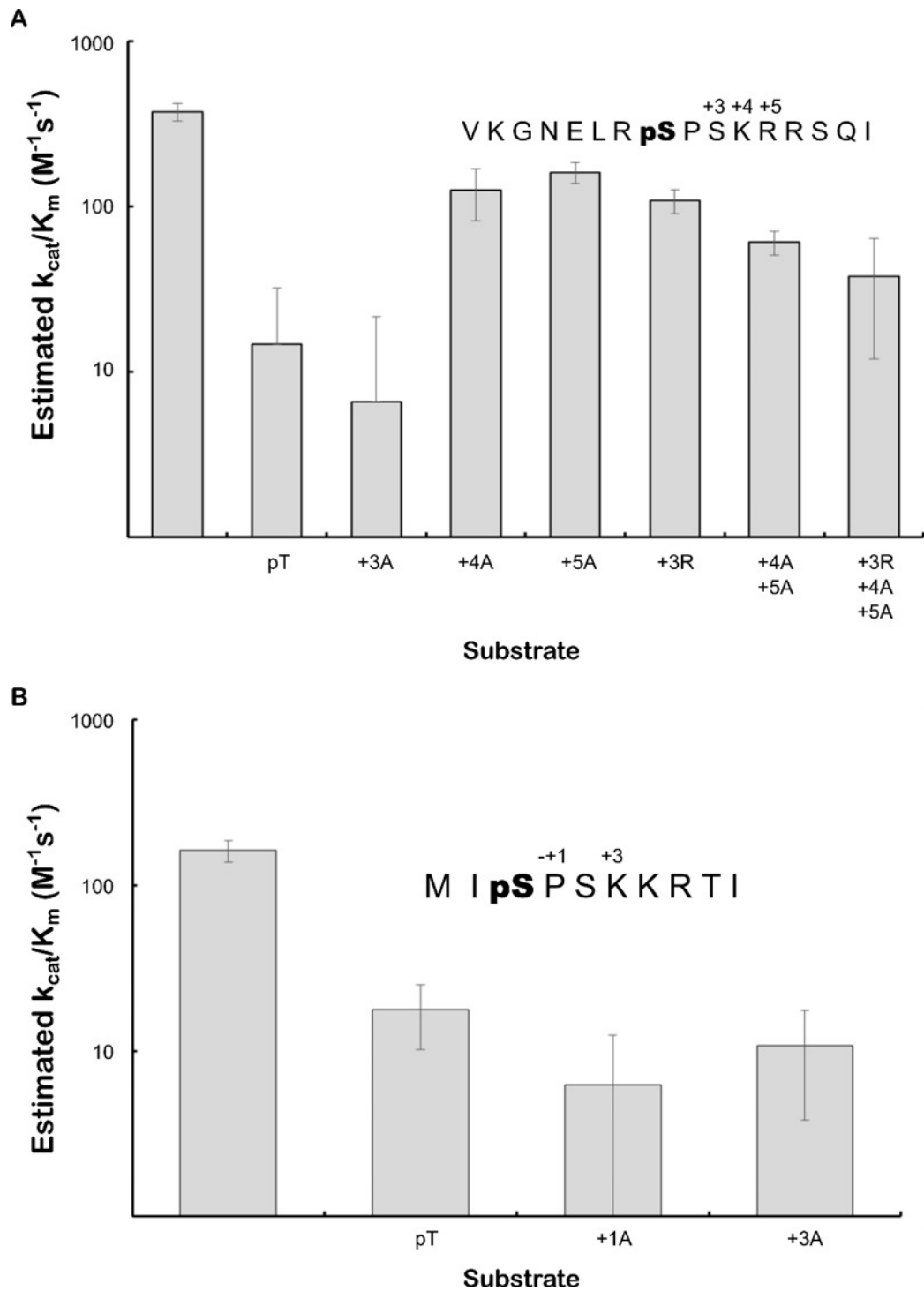


Fig. 3.9.: **Estimated k_{cat}/K_m values of Clp1 from initial velocity measurement assays** Initial reaction velocity measurements at low concentrations (below K_m) using phosphopeptide series of AcmlpS31 (**panel A**) and AcmlpS3 (**panel B**) were used to estimate apparent k_{cat}/K_m by applying equation 3.4. The first bar in each panel represents the phosphopeptide whose sequence is shown. The labels on the x axis represent the substitutions made at the positions (relative to the pSer). Data are the average of three independent experiments and error bars represent standard deviation from the mean.

There was generally low enzyme activity observed with the human Cdc14A paralog (hCDC14A) which limits the ability to make conclusions about mutations that lowered enzyme activity. Assays with hCDC14A showed that Gly and Trp at +1 position resulted in activity greater than four-fold over the original sequence, and 8 of the 18 residue changes supported as much activity as the original sequence (Figure 3.14). Lys and Ser at +2 are highly favorable, greater than four-fold, over the original sequence. In agreement with previous results, introduction of additional Lys at +4 raised activity, but unlike ScCdc14, Arg at this position also led to an increase. Introduction of Lys at +5 had little effect on hCDC14A activity. Changes in the N-terminal positions also enhanced activity; Pro and Gly at -2 and Gln at -1 resulted in a greater than four-fold increase in activity over the original sequence.

Similar to hCDC14A, enzyme activity was very low for hCDC14B. Mutation at the +1 position to Gly and Trp resulted in an increase of hCDC14B activity greater than eight-fold over the original sequence, and 8 of the 18 residue changes supported at least as much activity as the original sequence (Figure 3.15). Changes in the +3 Lys are also less detrimental, as changes to ala, Gly, Met, Pro, and Trp result in an, at least, 85% increase in activity, relative to the original sequence. This is a relatively small effect and is unlikely to be a true preference for these residues over Lys at +3. The increase in activity observed for mutation of +3 Lys to Ala is surprising because loss of the +3 Lys has been shown to drastically reduce activity of hCDC14B in an end point assay [129]. The Pro at +2 was unfavorable but all other mutations raised activity, with Asp, Glu, and Lys resulting in a greater than ten-fold increase over the original sequence. In agreement with previous results, Lys was the most favorable residue at +4. Arg at +5 also led to an increase in activity and its effect was greater than that of Lys. Pro at -2 and Gln at -1 were the most favorable residues at each position and led to an increase in activity greater than 13 and 20-fold, respectively, relative to the original sequence.

		Amino Acid																			
		A	D	E	F	G	H	I	K	L	M	N	P	Q	R	S	T	V	W	Y	
Position	-2	0.9	0.7	0.9	1.0	1.0	0.9	0.8	0.9	0.8	0.7	0.8	1.4	0.9	0.9	0.8	1.3	1.3	0.7	1.1	
	-1	0.8	0.9	0.8	0.8	0.7	0.8	0.8	0.9	N/A	0.9	0.9	0.8	1.2	1.0	0.8	0.9	1.0	0.9	0.7	
	+1	0.9	1.2	1.1	1.0	1.4	1.0	0.7	1.2	1.2	1.0	1.0	N/A	1.3	1.0	0.9	0.8	0.8	1.3	1.1	
	+2	1.0	1.0	1.4	0.7	N/A	1.1	0.8	1.0	0.8	0.8	0.8	0.9	1.0	0.7	0.9	0.8	1.0	0.9	1.1	
	+3	0.8	1.2	0.9	0.8	1.0	1.3	1.4	N/A	0.9	0.8	0.8	1.0	0.8	0.8	0.8	0.8	0.8	0.7	1.2	0.8
	+4	0.8	1.0	1.1	0.8	0.9	0.7	0.8	0.9	0.8	0.8	0.7	0.8	1.0	N/A	0.9	0.8	0.7	1.2	0.9	0.7
	+5	0.6	0.9	0.6	N/A	0.7	1.0	0.8	0.7	0.8	0.8	0.8	0.9	1.0	0.8	0.9	0.9	0.7	1.0	0.9	0.7
+6	1.3	1.3	1.3	1.0	1.0	0.5	0.8	1.0	1.0	0.8	0.9	1.0	0.9	1.3	N/A	0.8	1.0	0.9	1.1	1.1	

Fig. 3.10.: λ phosphatase dephosphorylates all peptides in the phosphopeptide array. Amount of dephosphorylated peptide (nmol) by λ phosphatase illustrates that all peptides in the phosphopeptide array are equivalently and efficiently dephosphorylated. Each cell is shaded to reflect the amount of dephosphorylated peptide (red, high; white, low) and data are an average of two trials. The original peptide sequence is highlighted by the green box. Each position is represented by a row and is numbered relative to the phosphoserine residue. Each column represents the amino acid incorporated.

Amino Acid

	A	D	E	F	G	H	I	K	L	M	N	P	Q	R	S	T	V	W	Y
-2	482.46	656.44	453.29	541.85	566.61	424.50	402.83	287.29	336.74	345.89	441.34	338.17	337.65	85.99	385.88	731.61	803.86	376.37	846.23
-1	484.21	201.76	387.95	252.28	175.04	390.66	415.95	540.82	N/A	413.51	322.40	604.00	660.31	676.10	635.50	466.52	762.95	398.26	443.95
+1	15.78	28.10	19.97	5.13	14.40	5.47	5.88	53.07	19.44	36.55	22.01	N/A	5.23	16.43	0.10	2.12	6.17	59.07	10.15
+2	622.54	598.58	862.16	271.11	N/A	686.61	652.29	761.03	601.45	546.74	597.79	19.72	962.74	432.95	555.61	580.26	38.64	616.43	642.94
+3	3.77	0.74	0.21	3.19	16.08	33.31	21.04	N/A	10.04	20.36	7.38	60.51	14.34	65.45	8.07	17.21	5.68	25.39	15.94
+4	470.51	356.93	255.36	472.31	2.12	169.43	375.20	625.61	158.04	429.60	250.47	95.99	N/A	287.69	202.08	251.84	651.40	138.92	346.57
+5	300.41	463.60	153.95	N/A	147.53	349.49	502.96	496.54	283.46	511.54	218.93	142.32	261.47	331.45	427.00	500.10	78.87	192.41	425.19
+6	396.03	158.41	70.92	320.44	205.05	163.78	83.40	164.25	159.74	85.74	424.96	228.93	378.50	N/A	160.52	345.99	236.90	643.43	359.13

Fig. 3.11.: k_{cat}/K_m estimates of ScCdc14 from initial velocity measurement assays. A summary of the estimated catalytic efficiency against a positional scanning mutant phosphopeptide library is presented. Each cell is shaded to reflect the relative activity observed (brown, high; white, low) and data are an average of two independent trials. The original peptide sequence is highlighted by the red box. Each position is represented by a row and is numbered relative to the phosphoserine residue. Each column represents the amino acid incorporated.

Amino Acid

	A	D	E	F	G	H	I	K	L	M	N	P	Q	R	S	T	V	W	Y
-2	28.81	41.17	103.34	60.59	172.95	33.55	70.35	81.13	25.28	35.69	167.28	31.78	11.15	41.36	39.68	106.97	55.30	94.70	
-1	66.91	23.14	88.94	44.33	49.53	30.20	39.78	45.91	N/A	30.11	131.04	210.87	109.94	119.51	48.05	185.40	30.39	90.15	
+1	55.48	17.38	3.25	7.25	161.61	5.11	8.09	32.15	49.63	26.21	27.04	N/A	14.68	10.69	15.98	13.01	28.16	133.17	2.32
+2	159.85	135.87	262.54	87.45	N/A	232.05	108.92	275.55	175.74	229.45	151.76	6.69	343.20	154.83	184.84	228.89	70.91	173.13	189.49
+3	39.78	25.09	30.76	6.97	63.29	36.24	7.90	N/A	9.48	24.35	10.32	27.60	2.04	3.44	1.49	2.51	2.60	39.78	3.25
+4	60.96	10.69	6.97	40.98	81.50	28.44	50.18	91.26	33.18	33.18	32.15	19.42	N/A	42.66	23.51	46.93	73.23	26.86	14.78
+5	61.34	14.22	70.35	N/A	90.98	6.97	44.98	48.79	40.89	155.94	141.72	14.78	34.94	138.94	68.21	23.05	46.56	11.90	76.02
+6	73.05	71.84	37.45	68.77	38.75	26.11	42.10	16.54	10.87	12.08	135.87	9.67	9.01	N/A	58.46	23.51	52.51	199.06	12.55

Fig. 3.12.: k_{cat}/K_m estimates of Clp1 from initial velocity measurement assays. A summary of the estimated catalytic efficiency against a positional scanning mutant phosphopeptide library is presented. Each cell is shaded to reflect the relative activity observed (brown, high; white, low) and data are an average of two independent trials. The original peptide sequence is highlighted by the red box. Each position is represented by a row and is numbered relative to the phosphoserine residue. Each column represents the amino acid incorporated.

Amino Acid

	A	D	E	F	G	H	I	K	L	M	N	P	Q	R	S	T	V	W	Y
-2	89.15	243.18	239.95	153.77	236.86	92.75	112.70	112.70	66.29	83.64	121.74	371.73	55.88	15.86	112.33	339.33	235.31	122.30	312.81
-1	119.33	58.98	148.63	73.36	51.36	74.78	103.71	80.73	N/A	94.42	97.77	182.52	290.51	138.97	204.89	96.71	418.63	77.32	181.84
+1	43.80	17.41	2.23	5.58	103.53	6.38	6.13	26.46	36.06	22.49	21.44	N/A	7.81	17.22	37.30	38.35	21.75	66.29	3.78
+2	385.30	338.96	529.41	178.06	N/A	555.93	536.60	605.80	450.73	508.28	345.28	15.61	580.77	317.21	352.96	537.59	38.23	402.28	403.14
+3	40.95	23.17	16.36	13.82	19.52	7.31	6.44	N/A	5.89	11.34	7.43	24.47	0.37	2.23	0.62	2.73	3.47	25.96	0.06
+4	110.34	38.16	32.71	125.58	1.30	84.88	82.59	259.53	19.02	104.27	50.62	26.83	N/A	113.87	39.65	47.71	208.54	38.47	37.61
+5	75.46	5.45	81.10	N/A	103.22	9.42	108.48	71.43	70.57	167.09	156.13	31.85	59.35	167.65	98.70	76.64	118.40	42.56	100.12
+6	117.03	78.19	334.81	81.91	63.26	40.15	100.74	41.08	35.38	23.61	98.45	95.60	72.98	N/A	24.10	79.12	88.53	349.93	55.51

Fig. 3.13.: k_{cat}/K_m estimates of FgCdc14 from initial velocity measurement assays. A summary of the estimated catalytic efficiency against a positional scanning mutant phosphopeptide library is presented. Each cell is shaded to reflect the relative activity observed (brown, high; white, low) and data are an average of two independent trials. The original peptide sequence is highlighted by the red box. Each position is represented by a row and is numbered relative to the phosphoserine residue. Each column represents the amino acid incorporated.

Amino Acid

	A	D	E	F	G	H	I	K	L	M	N	P	Q	R	S	T	V	W	Y
-2	34.45	42.13	65.12	45.04	103.47	16.36	52.35	46.65	19.52	45.72	18.46	103.53	14.25	15.06	29.61	20.69	56.01	24.53	18.15
-1	18.03	19.33	50.56	28.69	56.38	13.63	14.25	23.17	N/A	21.68	40.02	20.20	91.38	38.78	34.76	22.92	40.33	20.63	36.43
+1	43.74	17.78	1.80	14.68	114.06	2.85	3.97	24.29	36.31	18.59	18.28	N/A	3.72	6.01	2.54	5.58	10.78	98.32	5.58
+2	19.33	37.11	45.10	17.04	N/A	28.31	30.48	114.00	36.12	10.35	41.45	14.25	20.51	39.34	104.02	34.08	25.28	40.21	28.62
+3	11.96	5.27	7.00	6.07	21.37	13.26	6.82	N/A	5.51	21.37	6.07	29.49	7.56	9.54	1.18	3.10	4.65	22.30	5.89
+4	59.23	19.21	19.33	29.37	0.50	25.46	36.06	51.79	17.22	25.28	17.60	23.98	N/A	43.62	20.57	28.07	46.16	26.95	55.76
+5	47.95	16.98	18.40	N/A	30.30	23.54	26.08	19.64	43.62	54.83	28.75	14.81	13.32	37.11	47.58	16.98	24.29	15.98	46.34
+6	49.13	30.98	10.97	19.45	30.05	15.98	19.08	13.07	8.86	13.63	57.25	20.63	31.72	N/A	17.35	27.01	50.06	92.81	14.50

Fig. 3.14.: k_{cat}/K_m estimates of hCDC14A from initial velocity measurement assays. A summary of the estimated catalytic efficiency against a positional scanning mutant phosphopeptide library is presented. Each cell is shaded to reflect the relative activity observed (brown, high; white, low) and data are an average of two independent trials. The original peptide sequence is highlighted by the red box. Each position is represented by a row and is numbered relative to the phosphoserine residue. Each column represents the amino acid incorporated.

Amino Acid

Position	Amino Acid																			
	A	D	E	F	G	H	I	K	L	M	N	P	Q	R	S	T	V	W	Y	
-2	16.23	24.29	49.63	28.56	95.47	14.87	36.12	43.06	10.28	15.24	11.03	140.95	20.38	4.96	15.30	26.76	60.47	19.83	95.66	
-1	14.19	8.36	46.90	21.37	28.25	10.66	8.61	14.75	N/A	10.28	27.38	17.66	215.85	39.40	44.24	34.08	39.96	24.47	43.00	
+1	35.44	7.74	1.05	15.61	110.47	1.36	0.93	18.77	26.08	12.08	16.29	N/A	1.42	2.35	3.16	6.63	9.42	86.37	0.31	
+2	35.87	114.74	119.95	23.85	N/A	72.98	53.59	103.16	75.77	62.14	71.00	1.80	75.96	39.90	66.48	80.23	21.50	72.67	75.46	
+3	31.97	4.58	4.96	9.73	23.85	14.31	13.57	N/A	6.07	19.14	7.19	20.45	3.47	0.93	1.30	0.43	0.31	26.52	1.05	
+4	33.46	8.80	5.76	16.54	1.92	23.42	13.63	45.85	1.98	14.50	8.43	7.99	N/A	23.30	7.56	20.51	37.55	16.85	10.47	
+5	30.30	10.04	35.13	N/A	40.77	11.59	11.15	16.05	22.18	138.47	49.87	6.44	14.75	39.78	36.49	7.00	25.22	17.16	37.24	
+6	37.55	23.05	7.68	5.89	20.20	4.89	23.30	5.64	1.24	4.27	56.63	12.27	31.97	N/A	7.00	14.93	32.22	103.40	14.31	

Fig. 3.15.: k_{cat}/K_m estimates of hCDC14B from initial velocity measurement assays. A summary of the estimated catalytic efficiency against a positional scanning mutant phosphopeptide library is presented. Each cell is shaded to reflect the relative activity observed (brown, high; white, low) and data are an average of two independent trials. The original peptide sequence is highlighted by the red box. Each position is represented by a row and is numbered relative to the phosphoserine residue. Each column represents the amino acid incorporated.

3.3 Discussion

The main contribution of this work is the demonstration that Cdc14 substrate selectivity is conserved across multiple diverse species. The hypothesis that conservation of the active site and residues thought to contribute to substrate selectivity would result in similar substrate preference was supported by the results. The data presented in this section further expand the understanding of Cdc14's kinetic characteristics. The existence of several major determinants for substrate selectivity first observed in budding yeast Cdc14 was conserved in all the Cdc14 enzymes tested. I repeatedly observed a strong preference for phosphoserine over phosphothreonine or phosphotyrosine containing substrates. The requirement for a +1 proline as well as a +3 lysine was also observed in all enzymes. The data presented in this chapter analyzing budding yeast Cdc14 also build on the work previously performed in the Hall and Charbonneau labs characterizing substrate selectivity [129, 130]. The results strengthen the observation by demonstrating selectivity was independent of the source of the sequence chosen to design the phosphopeptide substrates. The kinetic data reveal that the substrate preference is driven both by changes in k_{cat} and K_m . Substrates that do not contain a +3 Lys show a very large increase in K_m suggesting a large role for this Lys in substrate binding.

There were some subtle differences in the effects observed for changes in the C-terminal basic residues in the dephosphorylation of Acm1pS31. Clp1 and hCDC14A were much less sensitive to mutations of the +3 Lys to Arg in contrast to FgCdc14 and ScCdc14. These differences were observed both when the mutation is made in the context of the starting sequence (Acm1pS31) or when Arg was the sole basic residue in the +3 to +5 region. ScCdc14 activity was less sensitive to mutations of the +4 and +5 Arg residues than the FgCdc14, Clp1 or hCDC14A, although this difference is not very significant (Table 3.6).

Table 3.6: **Comparison of catalytic efficiency of Cdc14 enzymes reveals that substrate selectivity is conserved.** Catalytic efficiency (k_{cat}/K_m) of Sc. Cdc14, FgCdc14 and hCDC14A towards each peptide variant of the peptide provided in the sequence column (full sequences given in Table 3.7) are compared.

Sequence	Sequence variation	Sc. Cdc14	FgCdc14	hCDC14A
		k_{cat}/K_m (M^{-1}/s^{-1})	k_{cat}/K_m (M^{-1}/s^{-1})	k_{cat}/K_m (M^{-1}/s^{-1})
VKGNELRpSPSKRRSQI		4699	6542	1616.7
	pT	15.3	4.1	4.3
	+3A	781	56	39.3
	+4A	4951	1950	934.8
	+5A	4512	3196	566.3
	+3R	325	98	720.5
	+3R,+4A,+5A	266	71	372.3
	+3A,+4A,+5A	12.9	19	7.3
MIpSPSKKRTI		624	5737	1046
	pT	23	9.9	3.4
	+1A	13	21.6	11
	+3A	45	36.2	90.1

The data obtained from the phosphopeptide positional scanning library experiment presented revealed that there are novel negative determinants of substrate selectivity. Introduction of proline and valine at +2 and glycine at +4 is not tolerated. A summary of Cdc14 enzyme selectivity features conserved across multiple species is summarized in Figure 3.16. Beyond the major determinants of selectivity, there are some residues like proline at -2, valine at -1 and tryptophan at +6 that could be minor contributors to selectivity. Arginine at -2 is disfavored for a majority of the enzymes tested. There are also some subtle differences in selectivity observed. Mutations of

the +2 position show that there are differences in Cdc14 response. For instance, Alanine at +2 is favored for most of the enzymes tested except for hCDC14A. FgCdc14 and Clp1 have a preference for His at +2 whereas the other Cdc14 enzyme do not. Thr at this position also results in enhancement of activity except for ScCdc14 and hCDC14A. Histidine preference at position +5 also varies as Clp1 and FgCdc14 don't tolerate this mutation where as other enzymes do not show an effect. The effects of these mutations need to be investigated in more detail before any firm conclusions can be made.

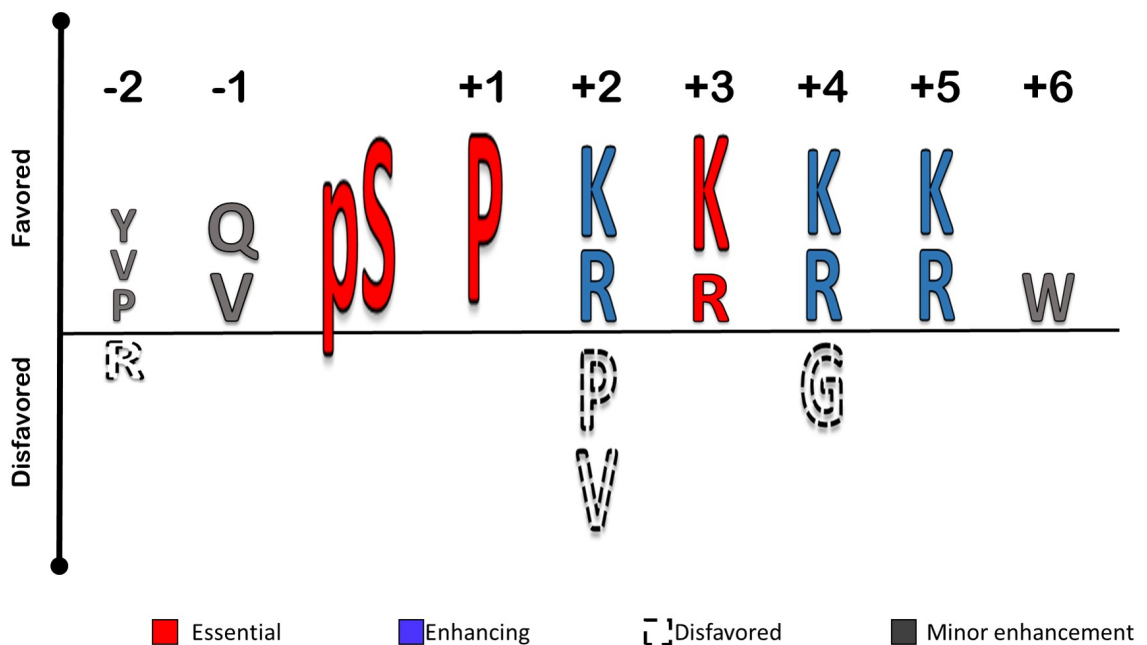


Fig. 3.16.: **Updated optimal substrate motif for Cdc14.** An improved substrate sequence motif based on the summary of Cdc14 dephosphorylation activity towards phosphopeptide substrates. Residues in Red are essential. Residues in blue enhance activity and those in black dashes are novel negative determinants of Cdc14 activity. Residues in gray have minor enhancing effects.

The data obtained from the phosphopeptide positional scanning library experiment does not allow for a complete determination of sequence preference of all the Cdc14 enzymes tested. One significant issue is that the amount of enzyme used for the assays was not normalized to yield equal activity towards the original peptide

(Cdh1pS239). This led to a low general enzyme activity against the starting phosphopeptide for all enzymes used, except ScCdc14 and FgCdc14. This error limits the ability to identify amino acids that are unfavorable. A solution is to utilize more enzyme in the assay or a more sensitive experimental approach with a larger dynamic range, like quantitative mass spectrometry, which could help alleviate the issue.

The extent to which the physiological Cdc14 substrates are conserved across the species tested is not yet clearly understood. The improved understanding of substrate selectivity presented here raises the possibility of predicting optimal substrates. This approach was applied to the *F. graminearum* Cdc14, which is important for pathogenesis, and proposed a set of potential substrates that could play a role in plant infection [183]. A similar approach can be applied to identify potential Cdc14 substrates for multiple organisms. This analysis could shed light on cellular processes in which Cdc14 might play a role.

3.4 Experimental Procedure

3.4.1 Cdc14 purification

His₆-tagged *Saccharomyces cerevisiae* Cdc14 and the catalytic domain of *Fusarium graminearum* Cdc14 (FgCdc14^{cat}, residues 1-433) were expressed in *Escherichia coli* and affinity-purified using HisPur nickel-NTA resin (Life Technologies). *Schizosaccharomyces pombe* Cdc14 (Clp1, kind gift from Dr. Kathy Gould), *Fusarium graminearum* Cdc14 (FgCdc14) and the catalytic domains of human CDC14 (hCDC14A, residues 1-379 and hCDC14B, residues 1-418) were expressed as N-terminally tagged glutathione S-transferase (GST) fusion proteins. The FgCdc14 ORF and its catalytic domain (FgCDC14^{cat}) were amplified from the first-strand cDNA by PCR, cloned into the Gateway entry vector pENTR/D-TOPO (Life Technologies), verified by DNA sequencing, and then transferred to the Gateway destination vectors (Life Technologies). pDEST15 (FgCDC14) and pDEST17 (FgCDC14^{cat}) were used to introduce an N-terminal glutathione S-transferase (GST) fusion or an N-terminal 6x histidine fusion,

respectively. GST-FgCDC14 expression was performed by transformation of BL21 (DE3) cells followed by induction with 0.4 mM isopropyl -D-thiogalactopyranoside (IPTG) for 16 hours at 25 °C. The His₆-FgCdc14^{cat} fusion was induced in BL21 AI cells (Life Technologies) with 0.2% L-arabinose. Sources of expression constructs are listed in Table 3.8 and expression of ScCdc14, Clp1 and hCDC14 A/B were as previously described [129].

Purification of all His₆-tagged proteins was performed as follows. Bacteria were lysed on ice for 30 minutes in 10 cell pellet volumes of buffer A (25 mM Tris-HCl pH 7.5, 500 mM NaCl) supplemented with 0.1% Triton X-100, 10 mM imidazole, 1 mM phenylmethylsulfonyl fluoride (PMSF), 1 μM pepstatin, 10 μM leupeptin, 1 mg/ml lysozyme, and incubated for 30 minutes. Lysate was then sonicated to reduce viscosity. For His₆FgCdc14^{cat}, in place of sonication, 25 Units/ml Universal Nuclease (Thermo Fisher) were added to the lysis mixture at the same time lysozyme was added. Lysate was then clarified as described above, and the soluble extract was incubated with 1 ml HisPur nickel-NTA resin for 1 hour at 4 °C with agitation. After batch washing sequentially with 15 ml buffer A containing 10 mM, 25 mM, and finally 40 mM imidazole, protein was eluted with 5 1 ml aliquots of buffer B containing 250 mM imidazole, collecting 1 ml fractions. Elution fractions containing high protein concentration, as determined by using a Bradford assay, were combined and dialyzed into 1L of storage buffer (25 mM Tris-HCl pH 7.5, 300 mM NaCl, 2 mM EDTA, 0.1% 2-mercaptoethanol, 40% glycerol) overnight at 4 °C. The resulting recombinant proteins were analyzed by SDS-PAGE and stored in small aliquots at -80 °C.

Purification of all GST-tagged proteins was performed as follows. Bacteria were lysed in 5 cell pellet volumes of buffer B (25 mM Tris-HCl pH 7.5, 500 mM NaCl, 2 mM EDTA, 0.1% Triton X-100, and 0.1% 2-mercaptoethanol) supplemented with 1 mM PMSF, 1 μM pepstatin, and 10 μM leupeptin. Cells were lysed for 30 minutes on ice with 1 mg/ml lysozyme and PMSF was added to lysate to 1mM. Lysate was then sonicated to reduce viscosity. Soluble extract was prepared by centrifugation at 35,000 x g for 30 minutes at 4 °C. Meanwhile, 1 ml glutathione agarose resin (EMD

Biosciences) was pre-equilibrated with buffer A. The resulting soluble extract was then incubated with glutathione resin for 1 hour at 4 °C on a rocking platform. Resin was collected by centrifugation (700 x g, 2 minutes, 4 °C) and then washed three times with 10 ml buffer A with rocking for 5 minutes at 4 °C. GST-tagged proteins were eluted by incubating the resin several times with 1 mL lysis buffer A supplemented with 10 mM reduced glutathione at 4 °C for 5 minutes followed by centrifugation. Elution fractions containing high protein concentration were pooled and dialyzed as described above. The resulting recombinant proteins were analyzed by SDS-PAGE and stored in small aliquots at -80 °C.

3.4.2 Phosphopeptide synthesis

Phosphopeptides (Table 3.7) were synthesized using CLEAR-Amide resin (Peptides International) at 50 μ mol scale by solid-phase Fluorenylmethyloxycarbonyl chloride (Fmoc) chemistry on a Prelude peptide synthesizer (Protein Technologies, Inc.). Fmoc-protected amino acids and other peptide synthesis reagents were obtained from AnaSpec Inc. (Fremont, CA, USA). Fmoc-protected amino acid monomers dissolved at 100 μ M in dimethylformamide (DMF) were added to CLEAR-Amide resin being mixed with glass beads under bubbling of N₂ gas. Each amino acid was coupled to the growing peptide for 30 minutes followed by two rounds of deprotection (2 minutes each) with a mix of 2-(6-chloro-1H-benzotriazole-1-yl)-1,1,3,3-tetramethyluronium hexafluorophosphate (95mM)/N-methylmorpholine (200mM)(HCTU/NMM). The coupling time was increased to the C-terminal Fmoc-protected amino acid monomers as described previously [184]. The only modification was that coupling times for phosphorylated amino acids was increased to 3 hours to improve incorporation. Upon completion of synthesis, peptides were cleaved from resin and resuspended in 5% acetonitrile(ACN)/0.1% Trifluoroacetic acid(TFA).

Phosphopeptide substrates (Table 3.7) were also obtained from a commercial source in crude form from Genscript Inc.

3.4.3 Phosphopeptide Substrate Purification

Crude peptides were desalted using Sep-Pak C18 cartridges (Waters Corporation) as described [185]. The concentrations of phosphopeptide stocks were measured with an ashing procedure and malachite green-ammonium molybdate dye as described previously [186].

Phosphopeptides in the peptide library were obtained from Genscript as desalted lyophilized aliquots. Each peptide was resuspended in water with a target concentration of 20mM, based on molecular weight, and phosphopeptide concentration was quantified using an alkali hydrolysis procedure adopted from [187]. A 10 μ l aliquot of a 100-fold dilution of each peptide stock was mixed with 100 μ l of 2M NaOH and heated at 100 °C for 30 minutes. The mixture was allowed to cool to room temperature then neutralized with 100 μ l of 4.7N HCl. Hydrolyzed inorganic phosphate was quantified by adding 400 μ l of the malachite green based phosphate detection reagent, BIOMOL greenTM (Enzo Life Sciences), incubating for 30 minutes at room temperature and measuring the absorbance (A_{620}). Inorganic phosphate in each well was quantified by using a standard curve prepared using sodium hydrogen phosphate (Na_2HPO_4) and processed identically as above. The standard curve was found to be linear up to 250 μ M Na_2HPO_4 .

3.4.4 *In vitro* dephosphorylation assays

Phosphopeptide dephosphorylation reactions (50 or 20 μ l) were performed in 25 mM HEPES pH7.5, 0.1% 2-mercaptoethanol, 1mM EDTA, 150mM NaCl. For most reactions Cdc14 concentrations used were 50 nM (ScCdc14), 75 nM (FgCdc14, Clp1, hCDC14A and hCDC14B), and 600nM (FgCdc14^{cat}). These concentrations were increased for poor phosphopeptide substrates. Reactions were incubated for 30 minutes at 24 °C (FgCdc14 and FgCdc14^{cat}), 30 °C (ScCdc14 and Clp1), or 37 °C (hCDC14A and hCDC14B). Reactions were stopped and dephosphorylation of substrates was measured by detecting the release of inorganic phosphate by adding 2 times reac-

tion volume of BIOMOL GreenTM reagent (ENZO Life Sciences). Absorbance at 620 nm was measured on a microplate reader and the amount of phosphate released was calculated from a standard curve generated with Na₂HPO₄ under identical solution conditions (Standard curve was linear upto 200 μ M of phosphate).

3.4.5 An unbiased *in vitro* analysis of sequences affecting Cdc14 selectivity

In order to identify phosphopeptide sequences affecting Cdc14 activity, a test of Cdc14 activity was performed on a positional scanning phosphopeptide series. The phosphopeptide series was generated based on a shortened version of a known Cdc14 substrate (Cdh1pS239, LL**p**SPGKQFR, phosphorylated residue shown in bold) by individual mutation of each position (excluding pSer) to all possible amino acids (except cysteine). This resulted in a panel of 145 phosphopeptides.

λ phosphatase (New England Biolabs) was used to test the quality of each phosphopeptide in the phosphopeptide array. 4 Units of λ phosphatase was used to dephosphorylate 1 nmol of each peptide. The reactions were performed in 20 μ l volume with buffer (25 mM HEPES pH7.2, 0.1% BME, 1 mM EDTA, 0.01% BSA, 100 mM NaCl, 1 mM MnCl₂) and incubated at 30 °C for 1 hour. Reactions were then terminated by adding 40 μ l of BIOMOL GreenTM reagent (ENZO Life Sciences). Release of inorganic phosphate was then determined by measuring absorbance at 620 nm (A₆₂₀) and utilizing a standard curve generated with sodium phosphate.

The panel of phosphopeptides was then used for *in vitro* assays to measure the activity of all available Cdc14 enzymes. The reactions were performed in 20 μ l volume with buffer (25 mM HEPES pH7.2, 0.1% BME, 1 mM EDTA, 0.01% BSA, 100 mM NaCl), 100 μ M of each phosphopeptide and Cdc14 (50 nM of *Sc*Cdc14 or Clp1 or 75 nM of hCDC14A, hCDC14B or *Fg*Cdc14). Reactions were then incubated either at 30 °C (*Sc*Cdc14, *Fg*Cdc14 and Clp1) or 37 °C (hCDC14A and hCDC14B). Reactions were then terminated by adding 40 μ l of BIOMOL GreenTM reagent (ENZO

Life Sciences). Release of inorganic phosphate was then determined by measuring absorbance at 620 nm (A_{620}) and utilizing a standard curve generated with sodium phosphate.

3.4.6 Determination of steady state kinetic parameters (k_{cat}/K_m)

To establish the assay conditions, the response of the enzyme activity to changes in reaction time was tested. The assay was found to be linear over a 1 hour period and 30 minutes was selected as an appropriate reaction time. All assays were also performed such that enzyme concentration was kept at least a 100-fold lower than that of substrate and substrate consumption was kept below 10% which allowed us to make steady-state assumptions.

Two approaches were employed to determine kinetic parameters for the assayed enzymes. The enzyme was assumed to obey Michaelis-Menten kinetics. When possible, peptide substrate was varied to establish a full substrate saturation curve. The outcome of these experiments was fit with a standard Michaelis-Menten curve (Equation 3.1, using GraphPad 3) to determine V_{max} and K_m values. k_{cat} was calculated using Equation 3.2. These results were used to calculate the catalytic efficiency (k_{cat}/K_m) of the enzyme.

Equation 3.1

$$v = V_{max} \frac{[S]}{K_m + [S]} \quad (3.1)$$

Equation 3.2

$$V_{max} = [E]_t k_{cat} \text{ i.e. } k_{cat} = \frac{V_{max}}{[E]_t} \quad (3.2)$$

where v represents the reaction velocity at a given substrate concentration ($[S]$).

For cases when a full Michaelis-Menten curve could not be generated, assays were performed such that the substrate concentration was well below the K_m . The equation below was utilized to determine the k_{cat}/K_m from the best fit line plot.

Under conditions in which $[S] \ll K_m$, equation 3.2 simplifies to

Equation 3.3

$$v \approx V_{max} \frac{[S]}{K_m} \rightarrow V_{max} \frac{1}{K_m} \approx \frac{v}{[S]} \quad (3.3)$$

Equation 3.3 can then be combined with Equation 3.2 to give Equation 3.4, which can be used to determine k_{cat}/K_m .

Equation 3.4

$$\frac{k_{cat}}{K_m} = \frac{V_{max}}{[E]_t} \frac{1}{K_m} \approx \frac{v}{[S]} \frac{1}{[E]_t} \quad (3.4)$$

Table 3.7: Phosphopeptide sequences utilized in phosphatase assays for analyzing Cdc14 substrate selectivity

Peptide Name	Sequence variation	Sequence
Acm1pS3		MI p SPSKKRTI
Acm1pS3-pS3pT	pT	MI p <u>T</u> PSKKRTI
Acm1pS3-pS3pY	pY	MI p <u>Y</u> PSKKRTI
Acm1pS3-P4A	+1A	MI p <u>S</u> ASKKRTI
Acm1pS3-K6A	+3A	MI p SP <u>S</u> AKRTI
Acm1pS3-K6R	+3R	MI p SP <u>S</u> <u>R</u> KRTI
Acm1pS3-NT	-2G,-1D	<u>GD</u> p SPSKKRTI
Acm1pS3-KAA	+4A,+5A	MI p SPSK <u>A</u> ATI
Acm1pS3-RAA	+3R,+4A,+5A	MI p SP <u>S</u> <u>R</u> ATI
Acm1pS3-NAA	+3N,+4A,+5A	MI p SP <u>S</u> <u>N</u> ATI
Acm1pS31		VKGNELR p SPSKRRSQI
Acm1pS31-pS31pT	pT	VKGNELR p <u>T</u> PSKRRSQI
Acm1pS31-K34A	+3A	VKGNELR p SP <u>S</u> <u>A</u> RRSQI
Acm1pS31-R35A	+4A	VKGNELR p SPSK <u>A</u> RSQI
Acm1pS31-R36A	+5A	VKGNELR p SPSK <u>R</u> ASQI
Acm1pS31-K34R	+3R	VKGNELR p SP <u>S</u> <u>R</u> RRSQI
Acm1pS31-35A36A	+4A,+5A	VKGNELR p SPSK <u>A</u> <u>A</u> SQI
Acm1pS31-RAA	+3R,+4A,+5A	VKGNELR p SP <u>S</u> <u>R</u> <u>A</u> SQI
Acm1pS31-AAA	+3A,+4A,+5A	VKGNELR p SP <u>S</u> <u>A</u> <u>A</u> SQI
Cdh1pS239		LL p SPGKQFRQ
Cdh1pS239-pS239pT	pT	LL p <u>T</u> PGKQFRQ
Cdh1pS239-P4A	+1A	LL p <u>S</u> AGKQFRQ
Cdh1pS239-G5K	+2A	LL p SP <u>K</u> KQFRQ
Cdh1pS239-K6A	+3A	LL p SPG <u>A</u> QFRQ
Cdh1pS239-K6R	+3R	LL p SPG <u>R</u> QFRQ
Cdh1pS239-Q7K	+4K	LL p SPG <u>K</u> KFRQ
Cdh1pS239-F8R	+5R	LL p SPGK <u>R</u> RQ
Cdh1pS239-NT	-2G,-1D	<u>GD</u> p SPGKQFRQ

Bold letters indicate a phosphorylated residue. Residues mutated from the parental sequence at the top of each group of peptides are underlined

Table 3.8: Plasmids used in this study

Name	Expressed Protein	Backbone	Marker	Promoter	Source
SB021	His ₆ -ScCdc14	pET15b	Amp	T7	[129]
pHLP486	GST-FgCdc14	pDEST15	Amp	T7	This study
pHLP524	His ₆ -FgCdc14 ^{cat}	pDEST17	Amp	T7	This study
KG2333	GST-Clp1	pGEX4T-1	Amp	tac	Gift from Dr. Kathy Gould
pGST-HCA379	GST-hCDC14A(1-379)	pET-GST	Amp	T7	[129]
pGST-HCB418	GST-hCDC14B(1-418)	pET-GST	Amp	T7	[129]

4. CDC14 PHOSPHATASE INHIBITOR DEVELOPMENT

4.1 Introduction

4.1.1 Phosphatases are targets for inhibition

Protein phosphatases are categorized based on their substrate specificity into serine/threonine phosphatases (STPs), protein histidine phosphatases (PHPs), protein tyrosine phosphatases (PTPs), and dual specific phosphatases (DSPs) [188]. These categories of phosphatases have characteristic mechanisms of catalysis and active site structures which can be exploited during the design of class specific inhibitors [189]. The major difference in the catalytic mechanism between STPs and PTP/DSPs is that STPs utilize an activated water to directly hydrolyze the substrate phospho-ester bond whereas PTPs/DSPs use a cysteine as the initial nucleophile to form a thiophosphate intermediate which is then hydrolyzed by water in a subsequent step. The active sites also differ in that PTP/DSPs have a deeper active site pocket to accommodate the large aromatic phosphotyrosine [190]. The invariable active site cysteine also has a very low pK_{α} which means it is predominantly in the thiolate ion form at neutral pH, which allows it to be an effective nucleophile but also exposes it to oxidation.

Strategies to design clinically relevant PTP/DSP phosphatase inhibitors have been much more successful than those for STPs. Most strategies use non-hydrolyzable phosphotyrosine analogs like difluorophosphono-methylphenylalanine (F_2Pmp) groups [189]. One study was able to incorporate F_2Pmp into a hexameric peptide and develop a potent inhibitor of the insulin receptor [191]. Based on the peptide sequence of optimal PTP 1B substrates, this study was able to achieve IC_{50} values of $100\mu M$ by replacing the phosphotyrosine with the non-hydrolyzable mimic F_2Pmp .

Cdc25, a potent regulator of the cell cycle, is the prototypical phosphatase target for pharmacologically relevant inhibitor design. Cdc25 is a dual specificity phosphatase (DSP) responsible for removing the inhibitory phosphorylation to activate Cdk1 [192]. Cdc25 enzymes are inactivated by the DNA damage checkpoint which leads to inactivation of Cdk1 [192]. Cdc25 phosphatases are found in all eukaryotic organisms, except in plants, and there are three paralogs of Cdc25 (A, B and C) in mammals. These paralogs are largely conserved except for their regulatory subunits. Cdc25 over-expression is also strongly associated with poor prognosis in various cancers [193]. The search for Cdc25 inhibitors has identified a wide variety of classes of molecules including quinonoids which are likely irreversible inhibitors of Cdc25 and result in cell cycle arrest [194]. Large molecules containing phosphate mimetic moieties have also been identified as potent Cdc25 inhibitors [194].

High throughput screening (HTS) strategies have been employed to identify phosphatase inhibitors. One such effort is the identification of a specific inhibitor of the STP phosphoserine phosphatase from *Mycobacterium tuberculosis* [195]; the causative pathogen of tuberculosis (TB). In an effort to combat the multi-drug resistance being observed, attempts to target essential bacterial metabolic pathways have led to identification of inhibitors required of L-serine biosynthesis [195]. A similar approach for identifying Cdc14 inhibitors could yield potent inhibitors.

4.1.2 Cdc14 is an ideal candidate for active site binding inhibitors

Ser/Thr protein phosphatases usually have highly generic active sites with little intrinsic substrate selectivity [95]. Their substrate selectivity is usually a function of regulatory subunits that define their substrate association as well as their sub-cellular localization [95]. Cdc14, a member of the dual specificity phosphatase (DSP) family of phosphatases, is unique in this respect. The determinants of substrate interaction appear to be contained within or near the active site of the enzyme [102].

Although the role of the Cdc14 phosphatase in the cell cycle has been studied extensively, it is only recently that studies into its mechanism and substrate specificity have been conducted [103, 129, 130]. *S. cerevisiae* Cdc14 has been shown to prefer multicyclic aryl phosphates when provided non-physiological small molecule substrates [103]. The catalytic efficiency difference observed among these substrates appears to be a function of differences in K_m rather than k_{cat} which indicates the active site can discriminate among substrates based on substrate affinity [103]. Cdc14 has also been shown to have a strict preference for phosphoserine containing peptide and protein substrates over those with either phosphotyrosine or phosphothreonine [129, 130]. Phosphopeptide substrates containing multiple basic residues C-terminal to the phosphoserine, particular Lys at +3 are also preferred. Taken together, Cdc14 enzymes are ideal candidates for the development of small molecule inhibitors that take advantage of the active site selectivity. And given the conservation of the enzyme structure, inhibitors developed against ScCdc14 will likely be effective against Cdc14 enzymes in multiple species.

Selective Cdc14 inhibitors have a variety of potential applications. One such application would be in the study of Cdc14 function in cells. The ability to inhibit Cdc14 function in cells would make studying Cdc14's role in organisms with multiple paralogs of the enzyme more feasible. The effort to study Cdc14 function in higher eukaryotes has been limited due to the challenges in genetically eliminating all Cdc14 function. We have also recently shown that Cdc14 function is essential for the pathogenicity of the plant pathogenic fungus *F. graminearum* [196]. Cdc14 inhibitors are potential fungistatic agents that could be used to combat crop loss.

In an attempt to identify specific Cdc14 inhibitors, a high throughput screen (HTS) was carried out.

4.1.3 Choice of Chemical library for HTS

The HTS for Cdc14 inhibitors was carried out using commercially available small molecule libraries on hand at the Drug Discovery Center at the Bindley Biosciences Facility (Purdue University, West Lafayette, IN).

The LOPAC chemical library

The LOPAC chemical library, available from Sigma Life Science, is a collection of 1,280 pharmacologically active compounds.

ChemBridge DIVERSetTM collection

This library is a collection of 20,000 molecules intended to cover a wide variety of chemical classes.

A custom Cherry-pick chemical library from Life Chemicals curated for biological activity was also used.

4.2 Results

4.2.1 Cdc14 demonstrates product inhibition

As presented in the previous chapter, Cdc14 is highly selective for substrates containing a phosphoserine, a +1 proline, and a +3 basic residue. Cdc14 steady-state kinetic profiles using an optimal peptide substrate exhibit substrate inhibition [129]. These observations raised the possibility that Cdc14 activity could be inhibited by molecules that mimic high affinity substrate features. To explore this, I first used a non-phosphorylated peptide (Acm1pS3) that contains an optimal substrate sequence and tested its ability to inhibit the dephosphorylation of the phosphorylated form of the same sequence (Acm1pS3). This peptide is able to inhibit Cdc14 activity (Figure 4.1) with an IC₅₀ of 183 (± 23) μ M and k_i of 120 μ M. This result suggests that an un-

phosphorylated peptide containing an optimal substrate sequence is able to effectively compete with substrate for Cdc14 binding. The peptide is a less effective inhibitor of Cdc14 when compared to sodium tungstate, a general inhibitor of phosphatases, which has an IC₅₀ of 1.24 (± 0.4) μM and k_i of 0.82 μM (Figure 4.2).

The observation that Cdc14 activity can be inhibited by a product peptide raised the question about which sequence elements are important for inhibition. Any changes to the unphosphorylated AcmlS3 peptide sequence away from an optimal substrate sequence eliminate its ability to inhibit Cdc14 (Figure 4.3). Peptides with mutation of the serine to threonine, +1 proline, +3 lysine or downstream basic residues are severely compromised as inhibitors compared to AcmlS3. Effective inhibition, at least in the case of AcmlS3, is only achieved when the inhibitor peptide is in excess of the substrate and contains optimal substrate sequences.

4.2.2 Small molecule inhibitors of Cdc14 were identified

The substrate selectivity of Cdc14 and the ability to inhibit its activity with peptides that contain the optimal substrate sequence raised the possibility of identifying small molecule inhibitors of Cdc14 that are competitive inhibitors. The ideal inhibitor would be able to take advantage of the same enzyme features that result in Cdc14 selectivity to specifically bind to the enzyme active site and/or the substrate interaction interface. A high throughput screen with $\sim 50,000$ small molecules, was performed via an endpoint assay, using a photometric readout, at fixed concentrations of substrate (100 μM , AcmlpS3) and inhibitor (40 μM). The screen identified a total of 116 inhibitors that were able to inhibit $>70\%$ of Cdc14 activity and some of the identified inhibitors have been characterized in more detail (Table 4.1, Figure 4.4). A detailed list of molecules identified by the HTS not yet manually confirmed are also listed in the Appendix.

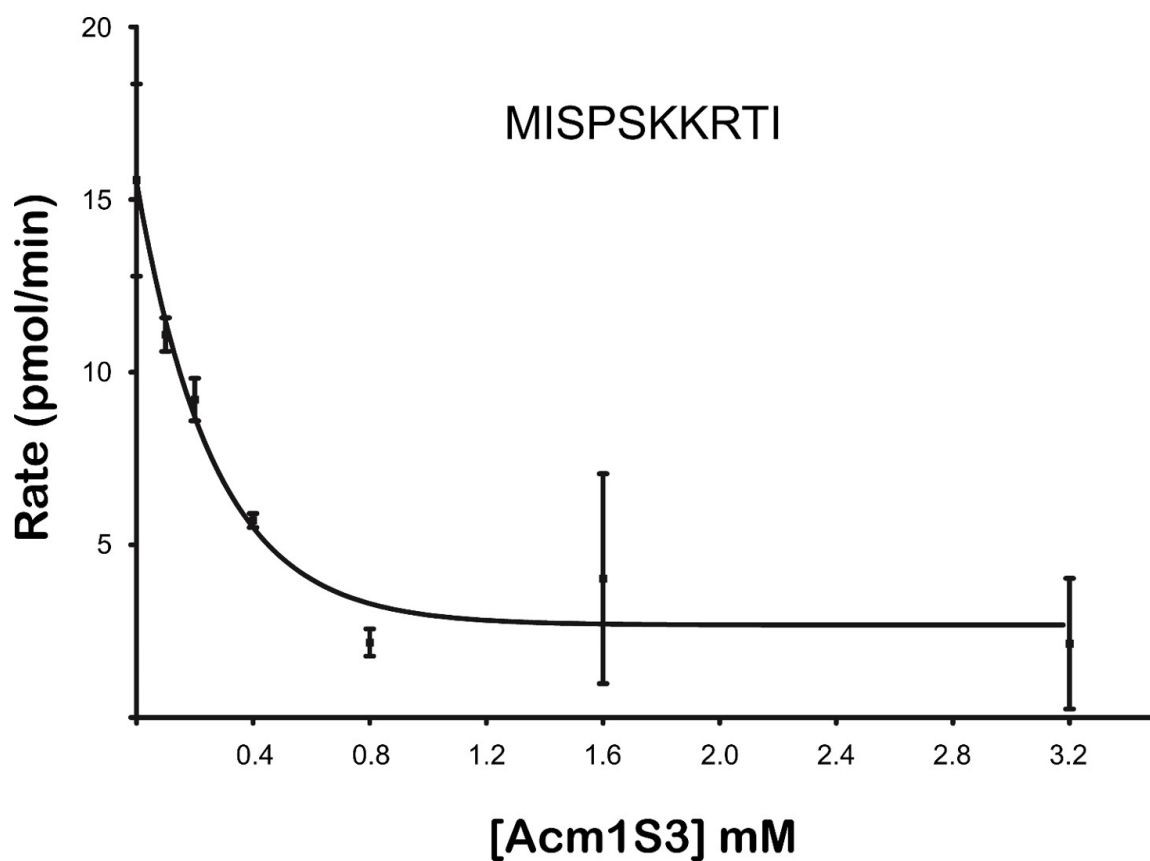


Fig. 4.1.: **Acm1S3 is an effective Cdc14 inhibitor** An unphosphorylated peptide containing an optimal substrate sequence inhibits Cdc14 activity with an IC₅₀ of 183 μ M and k_i of 120 μ M. Rate of phosphopeptide (Acm1pS3, 100 μ M) dephosphorylation is plotted as a function of inhibitor peptide concentration. Each bar represents activity observed and data are an average of three independent trials and error bars show standard deviation of the mean. Data were fit with a sigmoidal dose response curve using GraphPad Prism, as described in the methods section, to obtain IC₅₀ values.

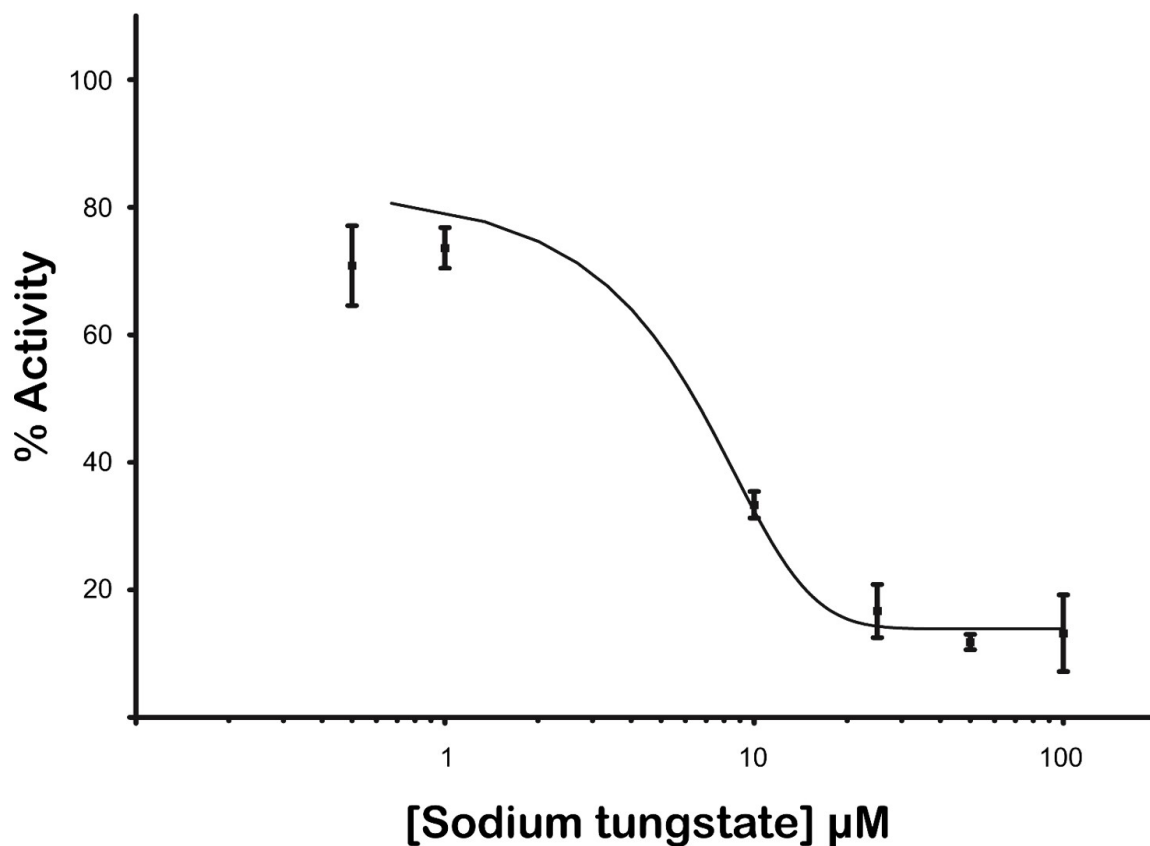


Fig. 4.2.: **Sodium tungstate inhibits Cdc14 activity with a k_i of $0.82\mu\text{M}$**
 A general phosphatase inhibitor (sodium tungstate) inhibits Cdc14 activity with an IC_{50} of $5 \pm 1.7\mu\text{M}$ and k_i of $3.3\mu\text{M}$. Rate of phosphopeptide (Acm1pS3, $100\mu\text{M}$) dephosphorylation is plotted as a function of inhibitor peptide concentration. Each point represents activity observed and data are an average of three independent trials and error bars show standard deviation of the mean. Data were fit to a sigmoidal dose response curve (Equation 4.1) using GraphPad Prism to obtain IC_{50} values. The Hill slope for this fit is -0.12 . Observing complete inhibition of Cdc14 activity is a challenge in this photometric assay.

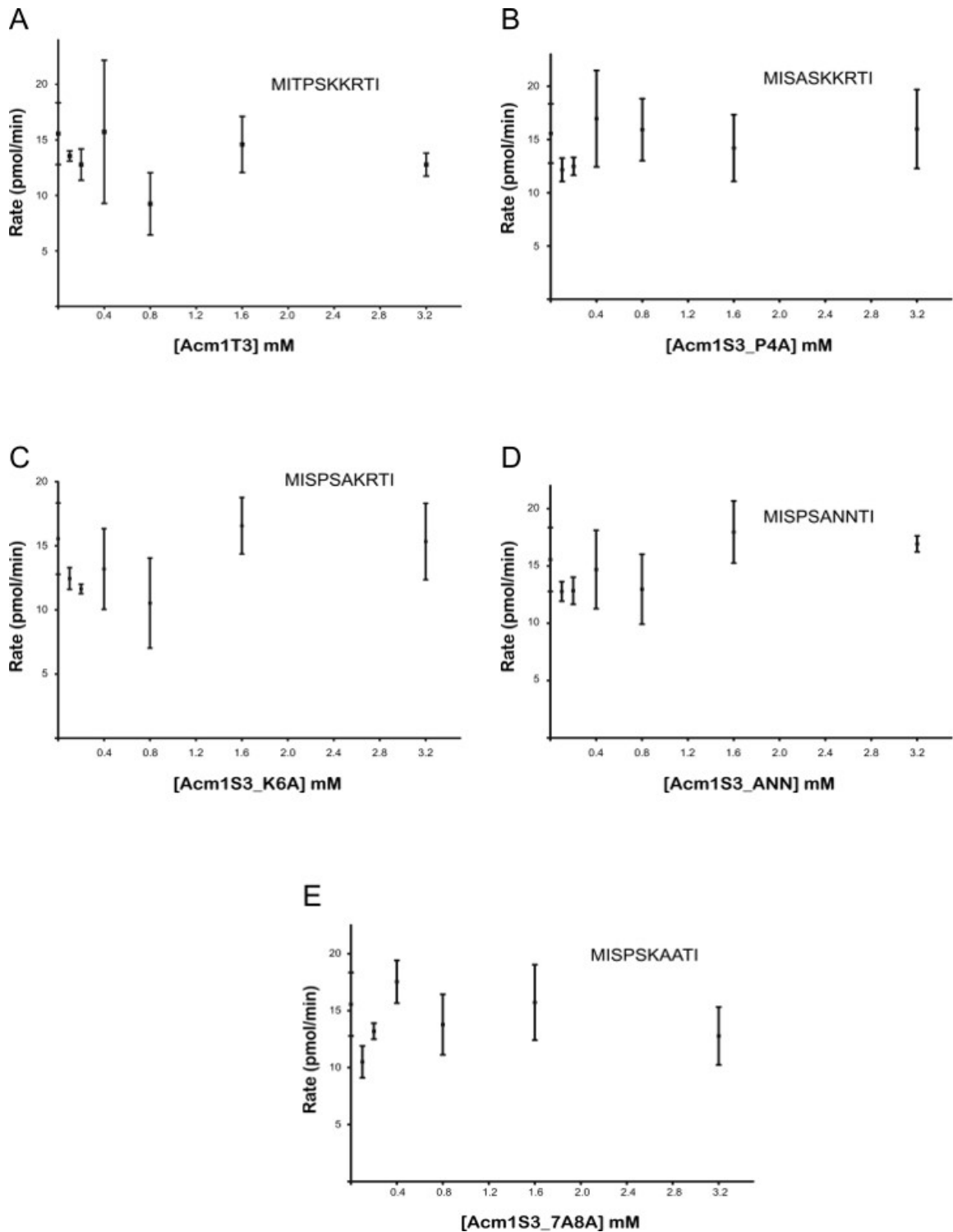


Fig. 4.3.: Mutations away from the ideal substrate sequence abolish ability of peptides to inhibit Cdc14 activity. Mutations that change serine to threonine (panel A), +1 Proline (panel B), or basic residues (+3 to 5, Panels C-E) eliminate the ability of the unphosphorylated peptide to inhibit Cdc14 activity. Each point represents activity observed and data are an average of three independent trials and error bars show standard deviation of the mean.

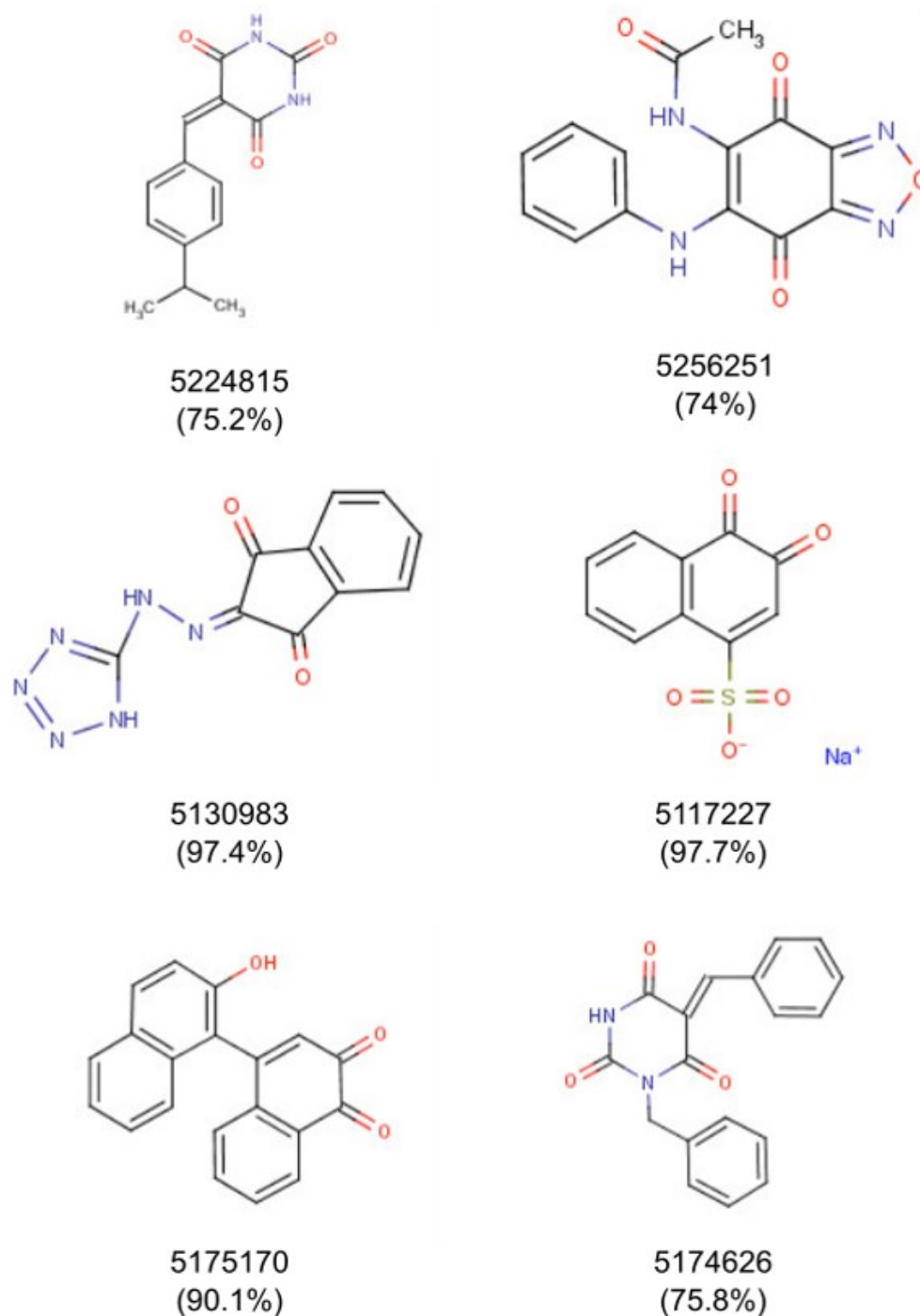


Fig. 4.4.: A likely significant number of the molecules identified as Cdc14 inhibitors are pan assay interference compounds (PAINS). The Kekulé structures of small molecule inhibitors of Cdc14 activity are presented. These molecules belong to classes of compounds like alkyldiene barbituates and quinones known to be non specific protein modifiers [197]. The number below each structure is the molecule identification number and the number in parentheses is the % inhibition of Cdc14 activity at 40 μM of inhibitor.

Table 4.1: **Small molecule Cdc14 inhibitors have been identified.** The chemical formulae, IUPAC names and % inhibition observed for inhibitors selected for further analysis are listed

Number ^a	Formula	Name	% inhibition
5117227	$C_{10}H_5O_5S.Na$	Sodium-3,4-dioxo-3,4-dihydro-1-naphthalenesulfonate	97.7
5130983	$C_{10}H_6N_6O_2$	1H-indene-1,2,3-trione 2-(1H-tetrazol-5-ylhydrazone)	97.37
5175170	$C_{20}H_{12}O_3$	2'-hydroxy-1,1'-binaphthalene-3,4-dione	90.15
5174626	$C_{18}H_{14}N_2O_3$	1-benzyl-5-benzylidene-2,4,6(1H,3H,5H)-pyrimidinetrione	75.83
5224815	$C_{14}H_{14}N_2O_3$	5-(4-isopropylbenzylidene)-2,4,6(1H,3H,5H)-pyrimidinetrione	75.2
5256251	$C_{14}H_{10}N_4O_4$	N-(6-anilino-4,7-dioxo-4,7-dihydro-2,1,3-benzoxadiazol-5-yl)acetamide	74

^a numbers represent the identification number used by the commercial source (Chem-Bridge)

Small molecule inhibitors have k_i values in the low μ M range

The subset of the small molecule inhibitors identified were analyzed to determine their IC₅₀ values. It was found that four of the small molecules significantly inhibited Cdc14 activity at low μ M concentrations. Activity of Cdc14 at a fixed [S] and varying [I] were plotted for these four inhibitors (Figures 4.5, 4.6, 4.7, and 4.8). The IC₅₀s for each of the characterized inhibitors are listed in table 4.2. These inhibitors had k_i values in the low μ M range. Two of the six potential inhibitors identified in the HTS were not effective during the confirmatory tests.

Table 4.2: **Determination of k_i for Cdc14 inhibitors.** IC50 values were determined by fitting data as described in Figures 4.5-4.9. k_i was calculated using the equation

$$k_i = \frac{IC50}{1 + \frac{[S]}{k_m}} \text{ where } [S] = 100 \mu\text{M} \text{ and } k_m = 193 \mu\text{M} \text{ (from Chapter 3).}$$

Number ^a	IC50(μM)	k_i (μM)
5224815	3 ± 1.9	1.9
5175170	6.5 ± 1.3	4.2
5117227	3.3 ± 0.8	2.1
5256251	8 ± 12	3.3

^a numbers represent the identification number used by the commercial source. Standard deviation of IC50 is indicated.

A large number of pan assay interference compounds (PAINS) were observed to inhibit Cdc14 activity

A large proportion of the inhibitors identified by the high throughput screen are molecules that have been reported as non-specific covalent protein modifiers [198]. These compounds, which include alkylidene barbiturates and quinones represented in Figure 4.4, can non-specifically react with nucleophiles found on the substrate peptide or Cdc14 to lead to the observed inhibition. It is very unlikely that these compounds can serve as the basis for developing specific Cdc14 inhibitors. In an initial attempt to investigate the mechanism of inhibition, assays were performed at a fixed inhibitor concentration and with increasing substrate concentration. ScCdc14 was first incubated with inhibitor for 5 minutes prior to substrate addition. It was expected that if the inhibitors were reversible, a higher substrate concentration would lead to higher enzyme activity. Although all four inhibitors were competed with increasing substrate concentration (Figure 4.9), it is unlikely that they are true reversible inhibitors. It is not yet possible to determine the mechanism of inhibition based on the results observed.

Small molecule inhibitors are less effective against other Cdc14s

The ability of small molecule inhibitors of ScCdc14 were tested for activity against FgCdc14. IC₅₀ values could not be determined because data could not be fit to a sigmoidal dose response curve (Figures 4.10 4.11). Given the conservation of substrate selectivity, specific Cdc14 inhibitors would be expected to be similarly effective against multiple Cdc14 enzymes. The inconsistent effect of these inhibitors against FgCdc14 and hCDC14A is a strong indication that the tested inhibitors are in fact non specific PAINS because the observed conservation of substrate selectivity would suggest a true competitive inhibitor should affect all enzymes equivalently.

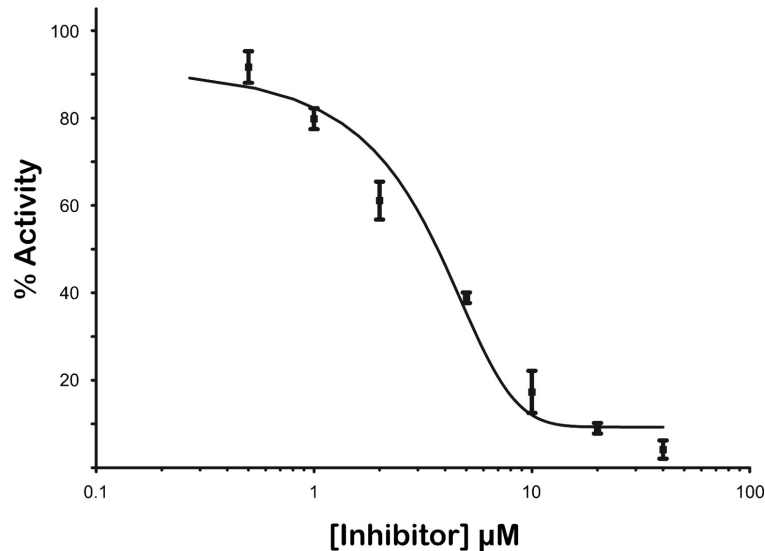


Fig. 4.5.: Molecule #5224815 inhibits Cdc14 activity with a k_i of $1.3\mu\text{M}$. Phosphopeptide dephosphorylation at a fixed substrate concentration is plotted as a function of inhibitor concentration. Activity observed without inhibitor is normalized to 100%. Data presented are an average of three independent trials and error bars shows standard deviation of the mean. Data were fit to a sigmoidal dose response curve (Equation 4.1) using GraphPad Prism to obtain IC₅₀ values. The Hill slope for this fit is -0.13.

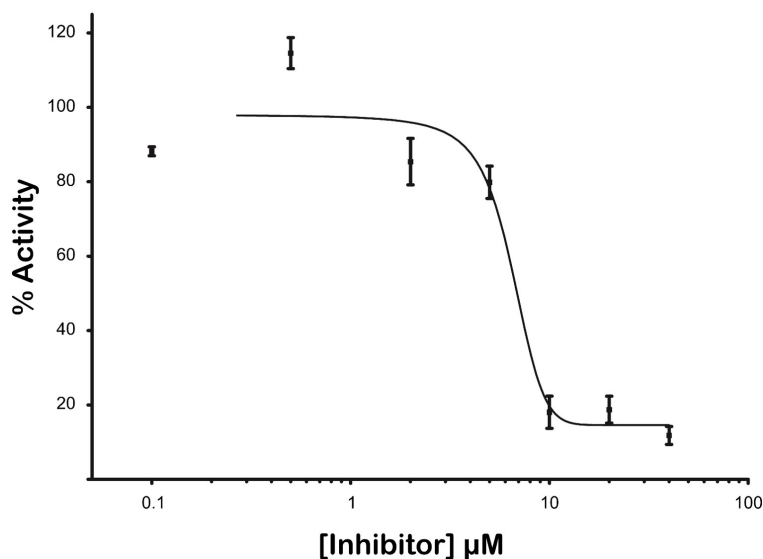


Fig. 4.6.: Molecule #5175170 inhibits Cdc14 activity with a k_i of $5.6\mu\text{M}$. Phosphopeptide dephosphorylation at a fixed substrate concentration is plotted as a function of inhibitor concentration. Activity observed without inhibitor is normalized to 100%. Data presented are an average of three independent trials and error bars shows standard deviation of the mean. Data were fit to a sigmoidal dose response curve (Equation 4.1) using GraphPad Prism to obtain IC_{50} values. The Hill slope for this fit is -0.34.

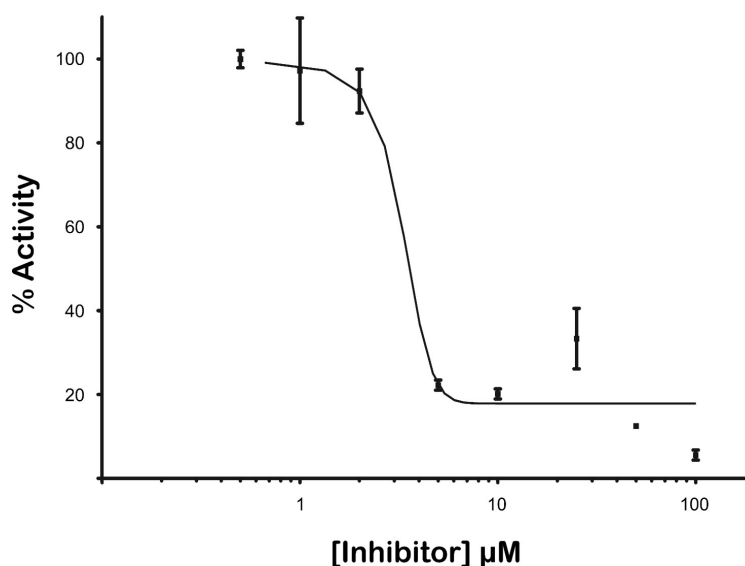


Fig. 4.7.: Molecule #5117227 inhibits Cdc14 activity with a k_i of $5.6\mu\text{M}$. Phosphopeptide dephosphorylation at a fixed substrate concentration is plotted as a function of inhibitor concentration. Activity observed without inhibitor is normalized to 100%. Data presented are an average of three independent trials and error bars shows standard deviation of the mean. Data were fit to a sigmoidal dose response curve (Equation 4.1) using GraphPad Prism to obtain IC_{50} values. The Hill slope for this fit is -0.74.

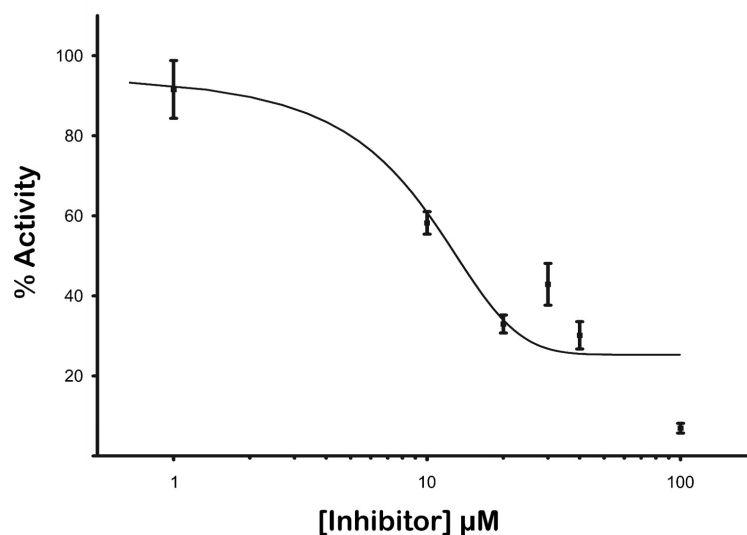


Fig. 4.8.: Molecule #5256251 inhibits Cdc14 activity with a k_i of $12.5\mu\text{M}$. Phosphopeptide dephosphorylation at a fixed substrate concentration is plotted as a function of inhibitor concentration. Activity observed without inhibitor is normalized to 100%. Data presented are an average of three independent trials and error bars shows standard deviation of the mean. Data were fit to a sigmoidal dose response curve (Equation 4.1) using GraphPad Prism to obtain IC_{50} values. The Hill slope for this fit is -0.08.

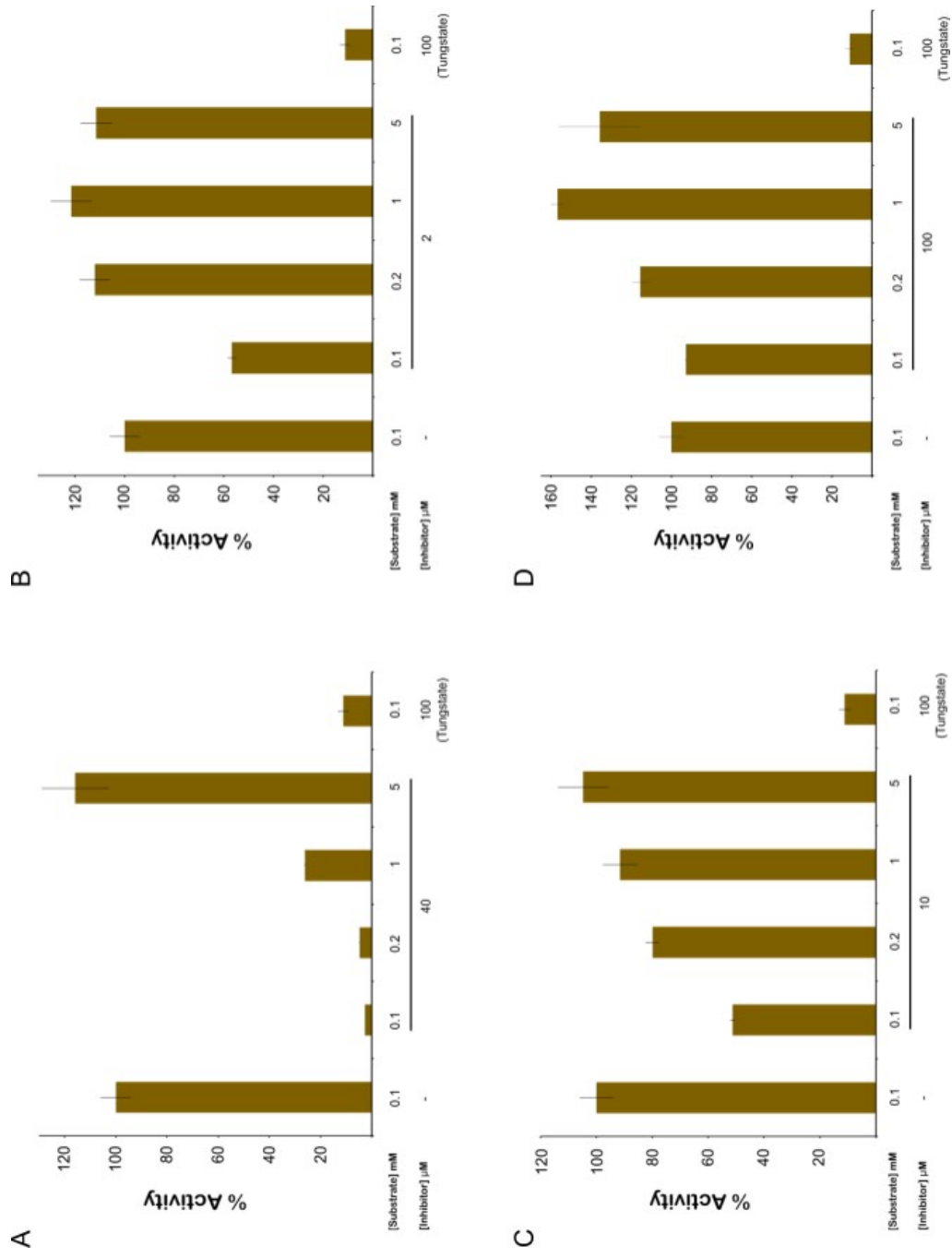


Fig. 4.9.: Cdc14 inhibitors display an indeterminate inhibitory mechanism. Cdc14 inhibitors can be competed with increasing substrate activity A.5224815 B.5117227 C.5175170 D.5256251. Phosphopeptide dephosphorylation at a fixed inhibitor concentration is plotted as a function of substrate concentration. Activity observed without inhibitor is normalized to 100%. Data presented are an average of three independent trials and error bars shows standard deviation of the mean.

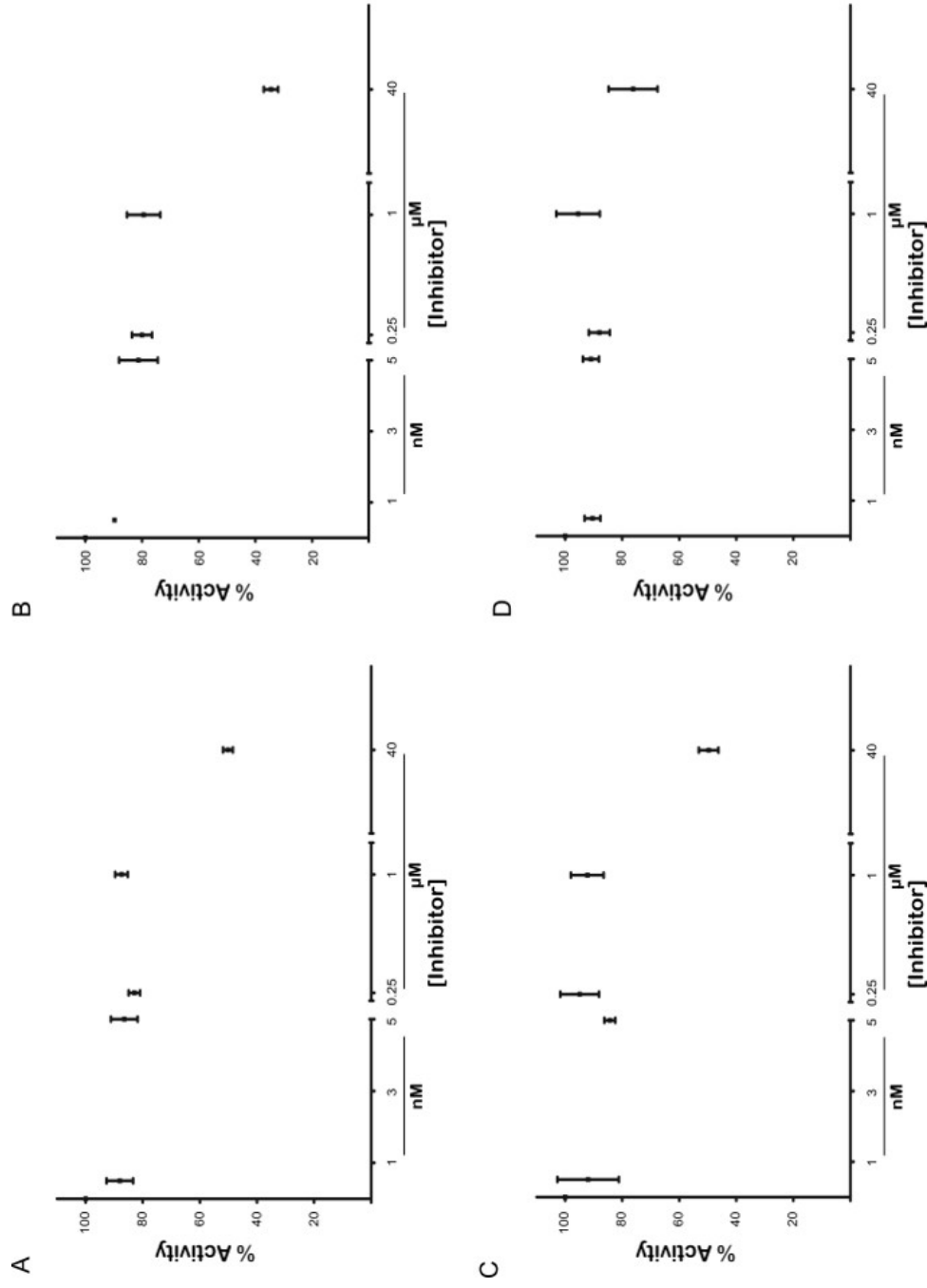


Fig. 4.10.: **Small molecule inhibitors are less potent inhibitors of *F. graminearum* Cdc14** A.5117227 B.5175170 C.5224815 D.5256251. Phosphopeptide dephosphorylation at a fixed substrate concentration is plotted as a function of inhibitor concentration. Activity observed without inhibitor is normalized to 100%. Data presented are an average of three independent trials and error bars shows standard deviation of the mean. IC50 values could not be determined because data could not be fit a sigmoidal dose response curve.

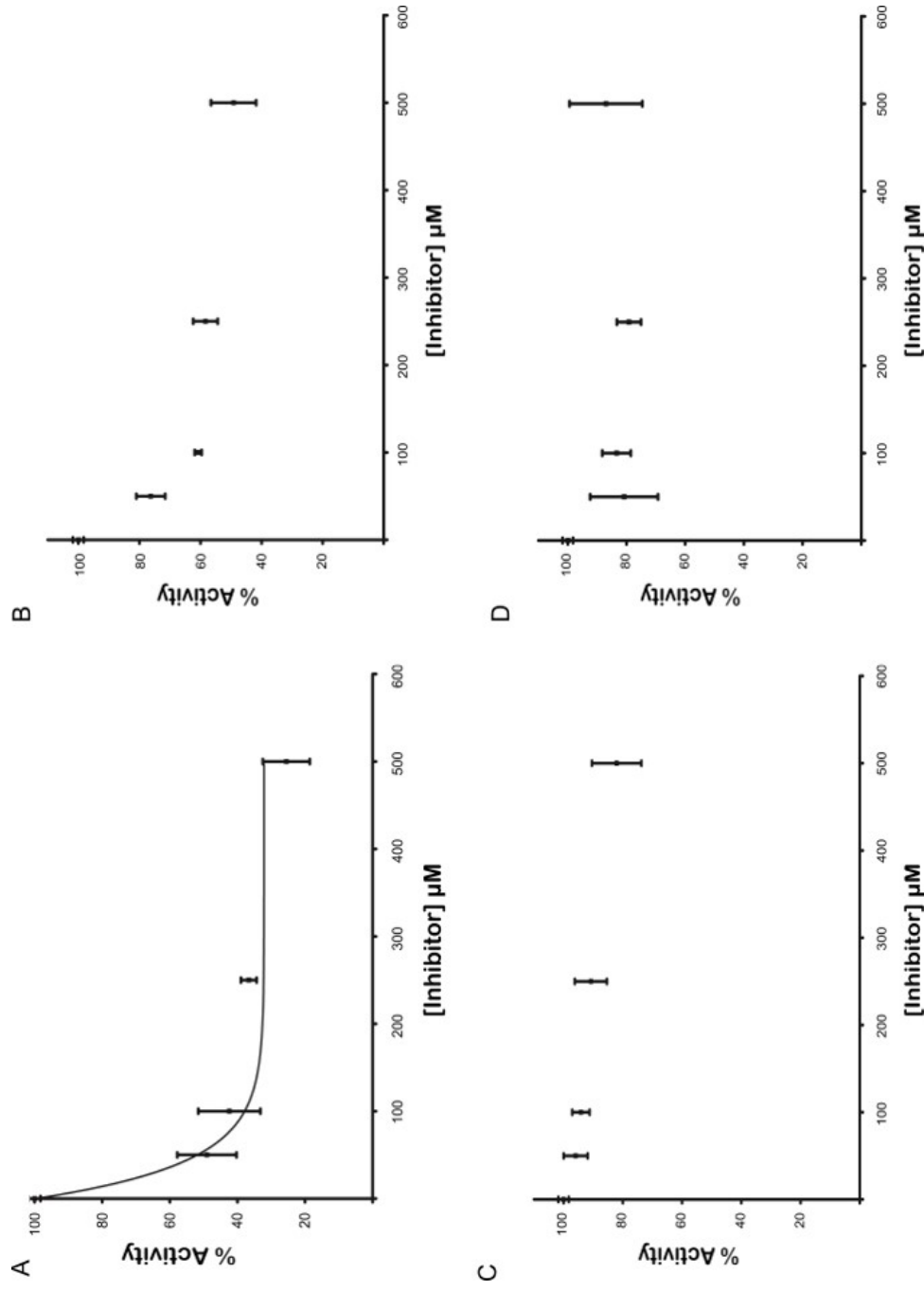


Fig. 4.11.: **Small molecule inhibitors are less potent inhibitors of hCDC14A** A.5117227 B.5175170 C.5224815 and D. 5256251. Phosphopeptide dephosphorylation at a fixed substrate concentration is plotted as a function of inhibitor concentration. Activity observed without inhibitor is normalized to 100%. Data presented are an average of three independent trials and error bars shows standard deviation of the mean. IC50 values could not be determined because data could not be fit a sigmoidal dose response curve.

4.3 Discussion

Observations that the area around the Cdc14 active site contains multiple docking sites for substrate features which provide specificity raised the possibility of identifying or developing selective small molecule inhibitors. Ideally, an initial Cdc14 inhibitor lead compound would be a competitive active site binder. This lead compound could be optimized by adding functional groups with features that interact with the adjacent substrate docking sites to create a high affinity, high specificity inhibitor. A peptide containing optimal Cdc14 substrate sequence was shown to be an effective Cdc14 inhibitor demonstrating in principal that one can use substrate docking features in the inhibitor design process. A high throughput screen using portions of two chemical libraries (50,000 compounds) was also employed to identify Cdc14 inhibitors. A small number of molecules (116) were found to inhibit >70% of Cdc14 activity. This HTS approach is yet to result in the identification of specific Cdc14 inhibitors. Many of the inhibitors are likely non-specific, belonging to classes of pan assay interference compounds (PAINS) [197].

Efforts to identify specific Cdc14 inhibitors will require removal of known PAINS from the list of inhibitors. Utilization of a virtual screening approach, in combination with a PAINS eliminating step might increase the likelihood of identifying true inhibitors. This strategy would involve only pursuing molecules that do not have chemical groups that are known to inhibit enzyme activity in a non specific manner [197]. A recent study employed such an approach to discover selective inhibitors of the histone methyltransferase SET7 [199]. If molecules that bind in the Cdc14 active site can be identified, additional functional groups could be added onto these molecules to fit either in the proline binding site or the acidic groove near the active site, thus improving affinity. This approach will most likely involve molecular combination methods that add functional groups to the lead compound in order to improve inhibitor binding to the Cdc14 substrate binding pocket.

Selective Cdc14 inhibitors have the potential to be useful in multiple applications. One major use for these molecules would be in understanding Cdc14 function in humans. The effort to study Cdc14 function in higher eukaryotes has been limited due to the challenges in genetically eliminating all Cdc14 function. The effects of inhibitors in live cells can be tested in budding yeast because elimination of Cdc14 activity has a clear observable phenotype, in which cells arrest during late mitosis in a telophase like state with large buds and segregated DNA. This phenotype can easily be assayed with microscopy techniques and would allow for efficient identification of inhibitors selective for Cdc14. The ability to inhibit Cdc14 in cultured human cells with a rapidly acting small molecule would make studies into Cdc14 function much more feasible.

Cdc14 inhibitors could have applications beyond the study of Cdc14 function. We recently showed that Cdc14 function is essential for pathogenicity of the wheat blight fungus *F. graminearum* [183]. The development of effective Cdc14 inhibitors could prove useful in the search for fungistatic agents. This possibility is made much more attractive because plants do not have Cdc14 orthologs and fungistatic agents would only be effective against the fungus. There is also a potential for using Cdc14 inhibitors in cancer therapy as supplements to DNA damaging drugs. Inhibiting Cdc14, previously demonstrated to play a role in DNA damage repair [200, 201], would impair the ability of tumor cells to recover following treatment with DNA damaging chemotherapeutics, potentially making the treatments more effective.

4.4 Experimental Procedure

4.4.1 Purification of Cdc14

Recombinant His₆-Cdc14 was purified as described in chapter 3 with modifications. An additional anion exchange purification step was added prior to dialysis into the storage buffer. Following pooling of 250 mM imidazole elution fractions, the pool was applied manually, using a syringe, to a 5 ml HiTrap desalting column (GE Life

Sciences) pre-equilibrated with desalting buffer (25 mM HEPES pH 7.4, 25 mM NaCl, 0.1% BME) and 1.7 ml fractions were collected. The column was washed with additional desalting buffer and fractions collected until protein was undetectable using a Bradford assay. Desalted fractions with highest protein concentration were then pooled and applied to a 1 ml HiTrap Q Anion exchange column (GE Life Sciences) pre-equilibrated with desalting buffer. The column was then washed with 10 ml of desalting buffer. Protein was then eluted with 10 ml stepwise increases of salt concentration to 224.5 mM, 248.25 mM, 262.5 mM, 272 mM, and 500 mM of NaCl. Elution was collected in 1.5 mL fractions and assayed for protein concentration. Fractions with highest protein content were pooled and dialyzed into storage buffer (25 mM Tris-HCl pH 7.5, 300 mM NaCl, 2 mM EDTA, 0.1% 2-mercaptoethanol, 40% glycerol) overnight at 4 °C. The resulting recombinant proteins were analyzed by SDS-PAGE and stored in small aliquots at -80 °C.

4.4.2 Peptide substrate preparation

Acm1pS3 (MIpSPSKKRTI) was synthesized by Genscript Inc. in crude form and purified using Sep-Pak C18 cartridges (Waters Corporation) as described in chapter 3 [185]. The concentrations of phosphopeptide stocks were measured with an ashing procedure and malachite green-ammonium molybdate dye as described previously [186].

4.4.3 Unphosphorylated peptide inhibitors

The ability of unphosphorylated peptides to inhibit Cdc14 activity was tested using a standard 20 μ l enzyme assay described in the Experimental Procedure section of Chapter 3. The peptides listed in Table 4.3 were added at defined concentrations before the addition of peptide substrate (Acm1pS3). In one set of experiments, the effects of increasing Acm1S3 concentration was investigated. The effects of changing

the sequence of Acm1S3 was also investigated by comparing the effects of peptides at a fixed concentration.

Table 4.3: Unphosphorylated peptides tested as inhibitors

Peptide Name	Sequence variation	Sequence
Acm1S3		MISPSKKRTI
Acm1T3	0T	MITPSKKRTI
Acm1S3_P4A	+1A	MIS <u>A</u> SKKRTI
Acm1S3_K6A	+3A	MISPS <u>A</u> KRTI
Acm1S3_K6R	+3R	MISPS <u>R</u> KRTI
Acm1S3_7A8A	+4A, +5A	MISPSK <u>AA</u> TI
Acm1S3_AAN	+3A, +4A, +5N	MISPS <u>AA</u> NTI

Mutations are underlined.

4.4.4 High-throughput inhibitor screen

The following protocol was performed by utilizing purified *ScCdc14* and Acm1pS3 in an *in vitro* reaction in which candidate inhibitors were included. The release of phosphate was quantified using a colorimetric assay. The screen was performed in two microplate formats (384 or 1536 well).

384 well format: These assays contained 75 nM *ScCdc14*, 100 μ M Acm1pS3 substrate and screened compounds at 40 μ M in a reaction volume of 50 μ l. Reactions were set up by dispensing 40 μ l of the enzyme mix in reaction buffer (25 mM HEPES pH7.5, 0.1 % BME, 1mM EDTA, 150mM NaCl) into wells of a 384 well plate. Candidate chemical inhibitors were dispensed at a volume of 200 nl/well from a stock at 10 mM in DMSO, using a pinning tool, for a final concentration of 40 μ M.

Reactions were then initiated by adding 10 μl of Acm1pS3 at 500 μM , diluted using reaction buffer, into each well and incubated for 30 minutes at room temperature. Reactions were terminated by adding 10 μl of the Malachite Green Phosphate Assay mix (BioAssay Systems) prepared as directed by the manufacturer. Following incubation for 30 minutes, the release of inorganic phosphate was calculated by using a standard curve generated with sodium phosphate under identical solution conditions.

1536 well format: These assays contained 75 nM ScCdc14, 100 μM Acm1pS3 substrate and screened compounds at 40 μM in a reaction volume of 5 μl . Reactions were set up by dispensing 4 μl of the enzyme mix in reaction buffer (25 mM HEPES pH7.2, 0.1% BME, 1mM EDTA, 100mM NaCl, 0.01% BSA) at 93.75 nM into wells of a 1536 well plate. Candidate chemical inhibitors were dispensed at a volume of 20 nl/well from a stock at 10 mM, using a pinning tool, for a final concentration of 40 μM . Reactions were then initiated by adding 1 μl of Acm1pS3 at 500 μM , diluted using reaction buffer, into each well and incubated for 1 hour at 4 °C. Reactions were terminated by adding 1 μl of the Malachite Green Phosphate Assay mix (BioAssay Systems) prepared as directed by the manufacturer. Following incubation for 30 minutes, the release of inorganic phosphate was calculated by using a standard curve generated with sodium phosphate under identical solution conditions.

4.4.5 Determination of small molecule inhibitor IC₅₀

Before a more stringent analysis of inhibitor IC₅₀ values, the ability of the molecules to inhibit Cdc14 activity was confirmed with a manual enzyme assay in which 50nM Cdc14 and 40 μM of each inhibitor were first combined and incubated for 5 minutes. Then 100 μM phosphopeptide substrate was added in a final reaction volume of 20 μl . Compounds confirmed to be inhibitors were then analyzed to determine IC₅₀ values. Cdc14 enzyme assays with 50nM Cdc14 and 100 μM Acm1pS3 substrate were set up with varying concentrations of Cdc14 inhibitors from 0.1 to 100 μM . Reactions were set up to a final volume of 20 μl and incubated at 30 °C for 30 minutes. IC₅₀ values

were estimated by comparing the observed enzymatic activity to that of an uninhibited reaction and fitting the data with a sigmoidal response curve, with a variable slope (Equation 4.1), using GraphPad Prism.

Eq.4.1

$$Y = \frac{B+(T-B)}{1+10^{((\log(IC50)-X)*h)}} \quad (4.1)$$

where X is log[inhibitor]; Y is % activity at log[inhibitor]; B is lowest % activity (initially set to 0%) ; T is highest % activity (initially set to 100%) and h is the Hill slope

5. SUMMARY AND FUTURE DIRECTIONS

5.1 Summary

The experimental results presented in this thesis address two mechanisms that regulate mitotic exit. One process is that of proteasomal degradation and the other is dephosphorylation of proteins by mitotic phosphatases. I have presented the results investigating the non-canonical mechanism by which the budding yeast protein, Acm1, is degraded by the proteasome, in a cell cycle regulated manner. I have also presented results of experiments characterizing the substrate selectivity of the mitotic phosphatase Cdc14 from an evolutionarily diverse set of organisms. In addition I have presented progress in the development of Cdc14 inhibitors. Below I will summarize the major findings and will discuss follow-up experiments.

5.1.1 Non-canonical mechanism for proteasomal degradation

When starting this project, work in the Hall lab and by others had shown that Acm1 degradation during G1 is independent of the APC and requires the proteasome [92, 94]. At the time, it was not clear how Acm1 gets targeted for proteasomal degradation and if polyubiquitination is required. My work has shown that Acm1 degradation in G1 does not require Acm1 polyubiquitination but the activity of the ubiquitin activating E1 enzyme is necessary. However, no single E2 or E3 ligase has been identified as an essential factor for Acm1 degradation. Acm1 degradation also requires the N-terminal, putative disordered region (Figure 5.2). Removal of this region leads to stabilization of Acm1 in G1. This N-terminal sequence is not a sufficient degron suggesting the requirement for additional factors. I have also shown that failure to effectively degrade Acm1 has a negative effect on cell growth. It is not

yet clear how Acm1 is targeted for degradation but the mechanism is not consistent with canonical mechanisms of proteasomal degradation. A proposed model for Acm1 degradation is given in Figure 5.1.

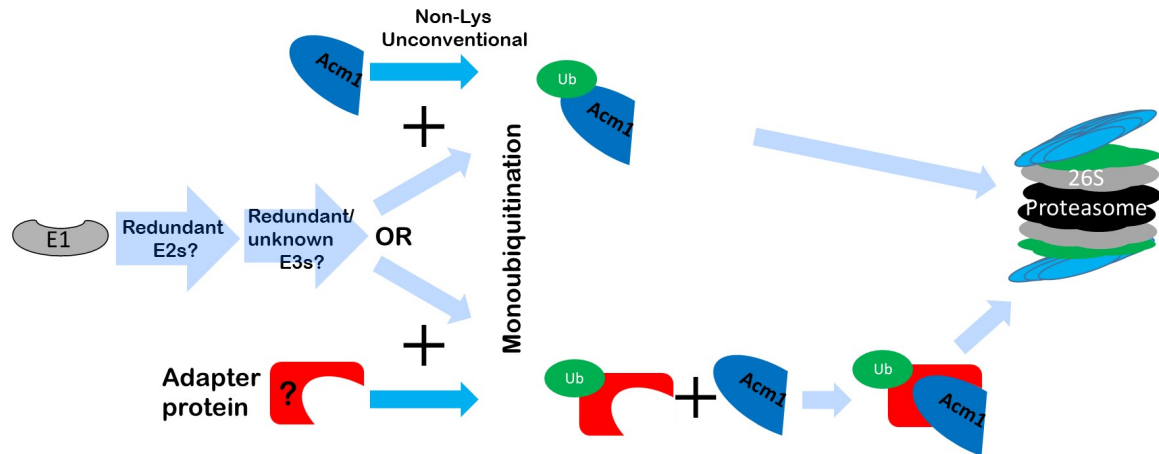


Fig. 5.1.: **Updated model for Acm1 degradation.** The model proposed for Acm1 degradation based on the current experimental evidence. This model accounts for E1 and 26S proteasome requirement for degradation. No individual E2 or E3 enzymes are required. Therefore, the model accounts for the possibility of redundant E2s or E3s that could be involved downstream of the E1 enzyme. General lysine linked ubiquitin chain attachment is not required and Acm1 lacking all ubiquitin acceptor lysines is degraded normally. This observation, however, does not rule out the unlikely possibility that Acm1 can be monoubiquitinated at unconventional residues. The herpesvirus E3 ligase, mK3, has been reported to mediate the degradation of the major histocompatibility complex I heavy chain (MCH1) by attaching ubiquitin at cysteine, serine or threonine residues [202, 203] although such an E3 is yet to be described in yeast. There is also the possibility that an adapter protein, reminiscent of Antizyme, could target Acm1 for degradation when monoubiquitinated.

5.1.2 Conservation of Cdc14 substrate selectivity

Phosphopeptide substrate-based characterization of Cdc14 substrate selectivity has been an effective tool in understanding the substrate sequence preference of Cdc14 and in predicting physiological protein substrates [129, 130]. In chapter 3, I have presented my work on investigating the extent to which the selectivity observed in *S. cerevisiae* is conserved in other species, including *S. pombe*, *F. graminearum*, and

humans. These analyses show that there is a high degree of conservation in Cdc14 substrate selectivity among this diverse set of organisms. All tested enzymes have a strict preference for phosphoserine containing substrates with +1 proline and basic residues C-terminal to the phosphorylation site. These analyses also identified novel determinants of selectivity previously not observed (Figure 3.16). Introduction of proline and valine at +2 and glycine at +3 is not tolerated.

5.1.3 Development of Cdc14 inhibitors

The substrate selectivity observed for Cdc14 enzymes raised the possibility that specific inhibitors can be identified. Chapter 4 presented the progress made towards identifying Cdc14 inhibitors. One major observation made is that a peptide containing optimal substrate sequence is able to inhibit Cdc14 activity. This observation indicated the possibility that inhibitors can be designed to take advantage of the active site features to yield selective and high affinity competitive inhibitors. A high throughput screen employed to discover such inhibitors led to the identification of inhibitors which show k_i values in the μM range. The majority of the most effective inhibitors are likely non-specific, belonging to classes of pan assay interference compounds (PAINS) [197].

5.2 Future Directions

5.2.1 Understanding Acm1 degradation

The observations made about Acm1 degradation in G1 make it an interesting case study of an unconventional proteasomal degradation mechanism. As proposed in the model for Acm1 degradation (Figure 5.1), the possibility exists that an adapter protein, analogous to antizyme, binds to Acm1 and targets it to the proteasome. Identification of this adapter protein would require stabilization of the complex by inhibiting the proteasome in G1 cells and immunopurifying the complex. A mass

spectrometric analysis of this complex could reveal any copurifying proteins. This would be followed by investigating the requirement of the adapter, by deleting the gene. The possibility of this new binding factor mediating the degradation of other proteins can also be investigated by purifying any complexes containing this protein that are enriched when the proteasome is inhibited. The effects of the gene deletion on the degradation of copurifying proteins can also elucidate if this mechanism is utilized for the degradation of other proteins. The possibility of unconventional ubiquitin attachment to Acm1 can be investigated by mutating the single Cysteine (C107), each Serine (23 in total) or Threonine (11 in total) .

The requirement of the N-terminal region of Acm1 could be due to the requirement of a disordered region to promote translocation into the proteasome active site. This possibility can be explored by replacing this region with another disordered protein sequence of similar length. The PONDR[®] algorithm also predicted the C-terminal region of Acm1 is disordered (Figure 5.2). The effects of removing this region could also be investigated to shed light on the contribution of this region to degradation, if any such effect exists.

5.2.2 Utility of degradation resistant Acm1 in understanding APC^{Cdh1}

Questions about what exactly distinguishes an APC^{Cdh1} substrate from a pseudo-substrate inhibitor remain to be answered. There is clear evidence that the sequence motifs that allow substrates to bind Cdh1 are also necessary for Acm1 binding [89]. However, there is a divergence of the fate of proteins that interact with Cdh1. One of the hypotheses put forward is that Acm1 contains additional sequence elements that result in higher binding affinity, compared to substrates, which interfere with the ability of APC^{Cdh1} to ubiquitinate Acm1. There is also a possibility that there are sequences within Acm1 that prevent ubiquitination, independent of binding affinity. In addition, the effects of mutations in *Acm1*^{N Δ 52}, the degradation resistant mutant, that destabilize the protein can be investigated in the full length protein.

The list of APC^{Cdh1} substrates is by no means exhaustive. Currently the presence of the degron sequences (D and KEN boxes) in a protein is used as an indicator that the protein is an APC substrate. This definition seems incomplete, because the likelihood of any given protein containing a D or KEN box (RXXL or KEN) sequence is fairly high and clearly not all proteins that contain these sequences are APC^{Cdh1} substrates. There are also APC^{Cdh1} substrates that contain no clearly recognizable degron. Taken together, these observations point to, as of yet, unidentified protein features characteristic of an APC substrate. Being able to identify additional APC^{Cdh1} substrates would improve the likelihood of finding new sequences that define a substrate. A degradation resistant Acm1 that is stable in G1, when APC^{Cdh1} is active, is beneficial in identifying substrates, regardless of recognition mechanism. Ability to inhibit the degradation of said protein by overexpressing *Acm1*^{N Δ 52} will be a strong indication that the protein is an APC^{Cdh1} substrate.

5.2.3 Cdc14 substrate selectivity

The results from the positional scanning peptide library assay have identified new phosphopeptide positions that influence substrate selectivity (Figure 3.16). Additional experiments are required to further investigate these effects. Determination of steady state kinetic parameters, by measuring dephosphorylation rates as a function of substrate concentration, for peptides listed in Table 5.1 would serve to more clearly characterize the influence of changes at these positions (-2,-1, and +6). Any differences in the magnitude of effects at each position could reveal variations in substrate preferences that exist among the Cdc14 enzymes tested. The effect of these mutations should also be investigated by using different phosphopeptide substrates. The effects of residues further N-terminal to the phosphoserine can also be investigated using another positional scanning library approach with a longer Cdh1pS239 peptide (DSKQLLLpSPGKQFRQ) and mutating individual residues between positions

-6 and -4. Mutations that enhance activity could then be followed up by experiments to determine the effects on kinetic parameters.

Table 5.1: **Phosphopeptide sequences for testing effects of novel substrate determinants.**

Sequence variation	Sequence
	LL p SPGKQFRQ
-2P	<u>PL</u> p SPGKQFRQ
-2G	<u>GL</u> p SPGKQFRQ
-1V	LV p SPGKQFRQ
-1Q	LQ p SPGKQFRQ
+2P	LL p SPP K QFRQ
+2V	LL p SP V KQFRQ
+4G	LL p SPGK G FRQ
+6W	LL p SPGKQ F WQ

Residues in **bold** are phosphorylated and changes in sequence are underlined.

As previous work and the data presented in Chapter 3 demonstrate, Cdc14 has a very strict selectivity. Bremmer et al. have been able to demonstrate that the Alanine 285 in the Cdc14 active site is a significant driver of phosphoserine over phosphothreonine selectivity [129]. In addition, a hypothesis has been put forward, based on the crystal structure of hCDC14B, that an acidic groove adjacent to the active site and solvent exposed aromatic amino acids are responsible for the preference for downstream basic residues and +3 lys, respectively [102, 130]. This hypothesis could be tested by mutation studies and the effects of mutating the residues that make up the acidic groove on substrate selectivity could help identify Cdc14 sequence features that drive selectivity. The effects of mutant Cdc14 with altered selectivity on cell cycle progress can also be investigated *in vivo*. This could further reveal the role for Cdc14 selectivity in defining the order of substrate dephosphorylation during

mitosis. Perturbing this order may result in the premature dephosphorylation of substrates that are normally dephosphorylated in late mitosis. An example would be Orc6 which could lead to premature origin relicensing or Iqg1 which could result in cytokinesis defects.

The improved understanding of Cdc14 substrate sequence preference from multiple organisms presents the possibility of identifying novel protein substrates for Cdc14, both in budding yeast as well as in organisms in which Cdc14 function is not well studied. The substrate selectivity can be applied to predict potential protein substrates using *in silico* searches of the organism proteome for proteins that contain matching sequences. This would make efforts to identify physiologically relevant substrates more efficient and would shed light on the role of Cdc14 in these organisms. As a demonstration of this, Yen1, a holiday junction resolvase in budding yeast was identified using a similar approach [130]. Potential substrates that could shed light on *F. graminearum* Cdc14 requirement for pathogenicity have also been compiled [183]. This same approach can be taken to elucidate hCDC14 function.

5.2.4 Development of Cdc14 inhibitors

The small molecules identified in the HTS as being Cdc14 inhibitors require careful analysis. Inhibitors that are likely non-specific, belonging to classes of pan assay interference compounds (PAINS) need to be removed from compounds selected for further development. Software tools like Pipeline Pilot (Pipeline Pilot; Accelrys Software Inc., San Diego, CA) will prove useful in streamlining this process [199]. An alternate approach would be to perform HTS with multiple Cdc14 enzymes and only pursue molecules that are effective against multiple enzymes. A structure-activity relationship analysis will help identify common molecular structures that are represented among the inhibitors. This analysis could identify a structure that can be used as a starting point for designing inhibitors that bind with higher affinity. This ap-

proach would most likely involve synthesis of derivative molecules that add functional groups that may improve inhibitor binding.

Given the challenges of using HTS with commercially available libraries that contain a large number of PAINS, an alternate approach for developing Cdc14 inhibitors might be the preferred strategy. One option is to employ a structure guided design of inhibitors that can make substrate like interactions with the enzyme active site. Peptidomimetics that contain side-chains similar to optimal substrates and altered sequences where the phosphoSer is mutated to Glu could prove useful. Main-chain substituted peptidomimetics might be better suited for use in live cells as natural peptides have issues with stability against proteolysis and poor bioavailability [204]. An alternative strategy for exploring molecules that can make multiple contacts with an enzyme active site is to start with a molecule known to bind in a phosphatase active site, like sulfonates, and explore molecule fragments that can improve binding [205].

The effects of Cdc14 inhibitors on other protein tyrosine phosphatases (PTPs) is an important indicator of inhibitor selectivity since PTPs share an oxidizable active site Cysteine, as part of the CX₅R domain. Testing inhibitor effect on PTPs like Cdc25 (Mih1) or PTP1 would help exclude inhibitors that are general oxidizers. Some human PTPs have been purified from bacteria (Figure 5.3) (expression constructs were a kind gift from Dr. Zhong-Yin Zhang).

5.2.5 Application of Cdc14 inhibitors

If any selective Cdc14 inhibitors can be identified, they might have multiple applications. One major use for these molecules would be the study of Cdc14 function in organisms that have previously been difficult to study. The challenge of accounting for multiple paralogs of the enzyme and the lack of knowledge in their functional redundancy has limited the success of efforts to study Cdc14 in higher eukaryotes. The ability to inhibit all Cdc14 activity in human cells would allow a significant progress in the understanding of Cdc14 function. The effects of inhibitors *in vivo* can

be tested in budding yeast because loss of Cdc14 leads to arrest in a telophase like state with cells having large buds which can easily be observed under a microscope. One challenge with using yeast in such an assay is the yeast cell wall, which creates a physical barrier for inhibitor entry into cells. This might require zymolyase treatment to improve inhibitor permeability. If a cell permeable Cdc14 inhibitor is identified, it would allow for a new method of arresting yeast cells in late mitosis. This would be an alternative method to the shifting of cultures to 37°C to arrest *cdc14-1* cells.

Cdc14 inhibitors could have applications beyond the study of Cdc14 function. It has recently been demonstrated that Cdc14 function is essential for pathogenicity of the wheat blight fungus *F. graminearum* [183]. Identification of Cdc14 inhibitors has the potential to lead to the development of fungistatic agents that would be selective for the fungus because plants do not have Cdc14. The ability of an identified Cdc14 inhibitor that is also effective against purified FgCdc14 can be tested for its ability to prevent plant infection by *F. graminearum*. This application may have some limitations because use of these molecules in food crops might result in unintended exposure for those consuming the crops.

There is also a therapeutic potential for using Cdc14 inhibitors in cancer treatment as supplements to DNA damaging drugs. hCDC14A and B have previously been demonstrated to play redundant roles in DNA damage repair [201]. Employing a therapeutic approach that causes DNA damage and simultaneously inhibits the recovery mechanism, would impair the ability of tumor cells to survive treatment.

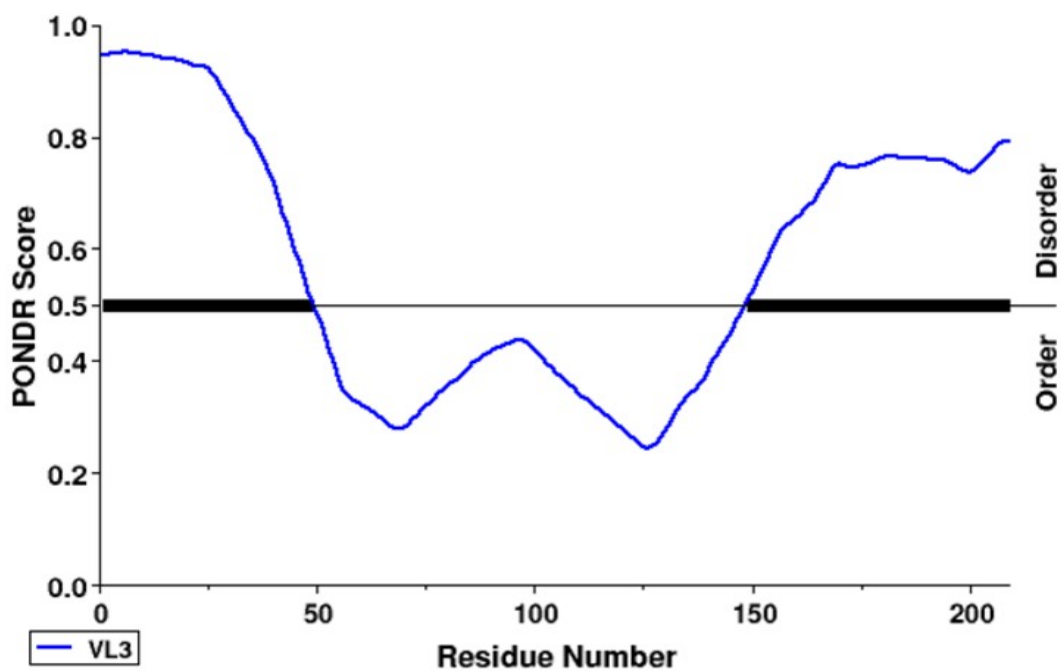


Fig. 5.2.: **Prediction of Acm1 disordered regions.** *In silico* prediction of Acm1 structural disorder using PONDNR[®]. The VL3 algorithm is used for the prediction and the application is available via the Internet at <http://pondr.com/>.

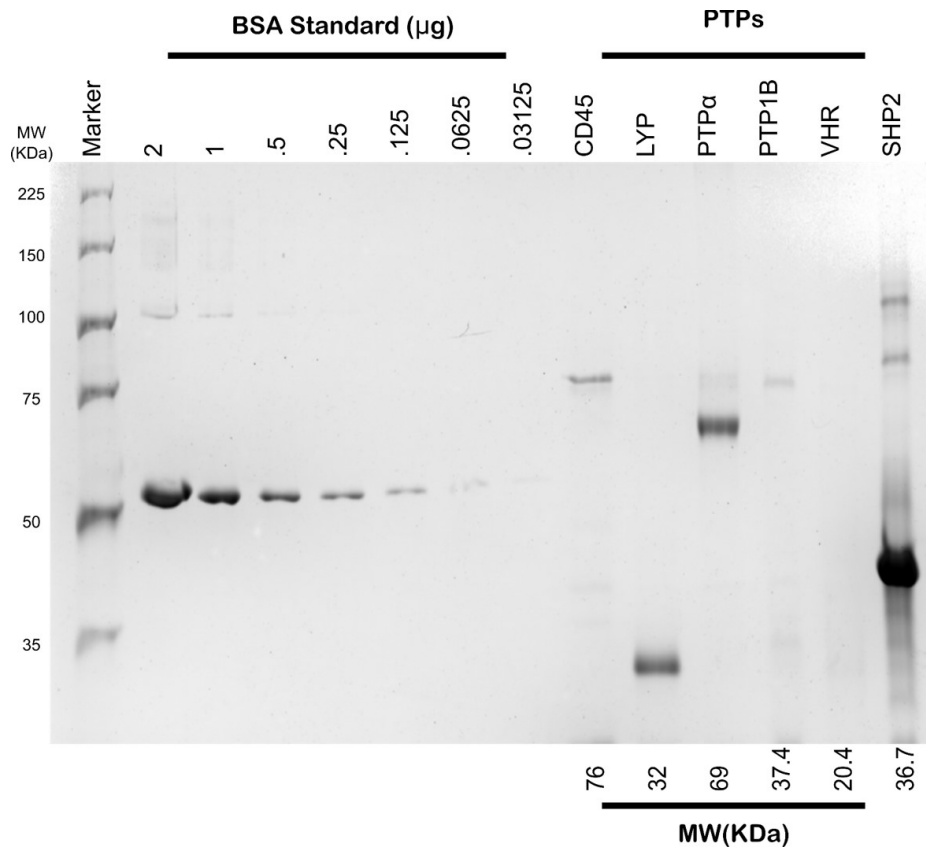


Fig. 5.3.: **Purification of PTPs.** Human protein tyrosine phosphatases were purified from bacteria and will be useful in determining selectivity of inhibitors for Cdc14.

LIST OF REFERENCES

LIST OF REFERENCES

- [1] S. J. Elledge, "Cell cycle checkpoints: preventing an identity crisis.," *Science*, vol. 274, no. 5293, pp. 1664–1672, 1996.
- [2] L. H. Hartwell, "Saccharomyces cerevisiae cell cycle.," *Bacteriol. Rev.*, vol. 38, pp. 164–198, jun 1974.
- [3] F. R. Cross, J. Roberts, and H. Weintraub, "Simple and Complex Cell Cycles," *Annual Rev. cell Biol.*, vol. 5, pp. 341–396, 1989.
- [4] P. Nurse, P. Thuriaux, and K. A. Nasmyth, "Genetic control of the cell division cycle in the fission yeast *Schizosaccharomyces pombe*," *Mol. Gen. Genet.*, vol. 146, no. 2, pp. 167–178, 1976.
- [5] H. Harashima, N. Dissmeyer, and A. Schnittger, "Cell cycle control across the eukaryotic kingdom," *Trends Cell Biol.*, vol. 23, no. 7, pp. 345–356, 2013.
- [6] J. J. Tyson and B. Novak, "Temporal organization of the cell cycle.," *Curr. Biol.*, vol. 18, pp. 759–768, sep 2008.
- [7] F. R. Cross, "Starting the cell cycle : what s the point?," *Curr. Opin. Cell Biol.*, vol. 7, pp. 790–797, 1995.
- [8] S. Asano, J.-E. Park, K. Sakchaisri, L.-R. Yu, S. Song, P. Supavilai, T. D. Veenstra, and K. S. Lee, "Concerted mechanism of Swe1/Wee1 regulation by multiple kinases in budding yeast.," *EMBO J.*, vol. 24, no. 12, pp. 2194–2204, 2005.
- [9] D. O. Morgan, "Principles of CDK regulation.," *Nature*, vol. 374, no. 6518, pp. 131–134, 1995.
- [10] J. M. Enserink and R. D. Kolodner, "An overview of Cdk1-controlled targets and processes.," *Cell Div.*, vol. 5, p. 11, jan 2010.
- [11] K. A. Nasmyth, "Control of the yeast cell cycle by the Cdc28 protein kinase.," *Curr. Opin. Cell Biol.*, vol. 5, no. 2, pp. 166–179, 1993.
- [12] M. D. Mendenhall and a. E. Hodge, "Regulation of Cdc28 cyclin-dependent protein kinase activity during the cell cycle of the yeast *Saccharomyces cerevisiae*," *Microbiol. Mol. Biol. Rev.*, vol. 62, no. 4, pp. 1191–1243, 1998.
- [13] M. Loog and D. O. Morgan, "Cyclin specificity in the phosphorylation of cyclin-dependent kinase substrates.," *Nature*, vol. 434, no. 7029, pp. 104–108, 2005.
- [14] E. L. Woodbury and D. O. Morgan, "Cdk and APC activities limit the spindle-stabilizing function of Fin1 to anaphase.," *Nat. Cell Biol.*, vol. 9, pp. 106–112, jan 2007.

- [15] M. Barberis, L. De Gioia, M. Ruzzene, S. Sarno, P. Coccetti, P. Fantucci, M. Vanoni, and L. Alberghina, “The yeast cyclin-dependent kinase inhibitor Sic1 and mammalian p27Kip1 are functional homologues with a structurally conserved inhibitory domain.,” *Biochem. J.*, vol. 387, no. Pt 3, pp. 639–647, 2005.
- [16] D. M. Koepp, J. W. Harper, and S. J. Elledge, “How the cyclin became a cyclin: regulated proteolysis in the cell cycle.,” *Cell*, vol. 97, pp. 431–4, may 1999.
- [17] J. Bloom and F. R. Cross, “Multiple levels of cyclin specificity in cell-cycle control.,” *Nat. Rev. Mol. Cell Biol.*, vol. 8, no. 2, pp. 149–160, 2007.
- [18] N. Lianga, E. C. Williams, E. K. Kennedy, C. Doré, S. Pilon, S. L. Girard, J. S. Deneault, and A. D. Rudner, “A wee1 checkpoint inhibits anaphase onset,” *J. Cell Biol.*, vol. 201, no. 6, pp. 843–862, 2013.
- [19] M. Peter and I. Herskowitz, “Direct inhibition of the yeast cyclin-dependent kinase Cdc28-Cln by Far1.,” *Science*, vol. 265, no. 5176, pp. 1228–1231, 1994.
- [20] W. G. Dunphy, “The decision to enter mitosis,” *Trends Cell Biol.*, vol. 4, no. 6, pp. 202–207, 1994.
- [21] P. Nurse, “Genetic control of cell size cell division in yeast,” *Nature*, vol. 256, pp. 547–551, 1975.
- [22] P. Russell and P. Nurse, “Schizosaccharomyces pombe and Saccharomyces cerevisiae: a look at yeasts divided.,” *Cell*, vol. 45, no. 6, pp. 781–782, 1986.
- [23] P. Russell and P. Nurse, “Negative regulation of mitosis by wee1+, a gene encoding a protein kinase homolog.,” *Cell*, vol. 49, no. 4, pp. 559–67, 1987.
- [24] C. Kraft, F. Herzog, C. Gieffers, K. Mechtler, A. Hagting, J. Pines, and J.-M. Peters, “Mitotic regulation of the human anaphase-promoting complex by phosphorylation.,” *EMBO J.*, vol. 22, pp. 6598–609, dec 2003.
- [25] A. J. Prunuske and K. S. Ullman, “The nuclear envelope: form and reformation,” *Curr. Opin. Cell Biol.*, vol. 18, no. 1, pp. 108–116, 2006.
- [26] F. Uhlmann, D. Wernic, M. a. Poupert, E. V. Koonin, and K. A. Nasmyth, “Cleavage of cohesin by the CD clan protease separin triggers anaphase in yeast.,” *Cell*, vol. 103, pp. 375–86, oct 2000.
- [27] D. a. Skoufias, R.-L. Indorato, F. Lacroix, A. Panopoulos, and R. L. Margolis, “Mitosis persists in the absence of Cdk1 activity when proteolysis or protein phosphatase activity is suppressed.,” *J. Cell Biol.*, vol. 179, pp. 671–85, nov 2007.
- [28] T. Kuilman, A. Maiolica, M. Godfrey, N. Mie Scheidel, R. Aebersold, and F. Uhlmann, “Identification of Cdk targets that control cytokinesis,” *EMBO J.*, vol. 34, no. 1, pp. 81–96, 2015.
- [29] M. Glotzer, A. A. W. Murray, and M. W. Kirschner, “Cyclin is degraded by the ubiquitin pathway,” *Nature*, vol. 349, pp. 132–138, 1991.
- [30] R. W. King, R. J. Deshaies, J. M. Peters, and M. W. Kirschner, “How proteolysis drives the cell cycle.,” *Science*, vol. 274, no. 5293, pp. 1652–1659, 1996.

- [31] C. Lindon, “Control of mitotic exit and cytokinesis by the APC/C,” *Biochem. Soc. Trans.*, vol. 36, pp. 405–10, jun 2008.
- [32] J. Q. Wu, J. Y. Guo, W. Tang, C.-S. Yang, C. D. Freel, C. Chen, A. C. Nairn, and S. Kornbluth, “PP1-mediated dephosphorylation of phosphoproteins at mitotic exit is controlled by inhibitor-1 and PP1 phosphorylation,” *Nat. Cell Biol.*, vol. 11, no. 5, pp. 644–651, 2009.
- [33] E. Queralt and F. Uhlmann, “Cdk-counteracting phosphatases unlock mitotic exit,” *Curr. Opin. Cell Biol.*, vol. 20, pp. 661–668, 2008.
- [34] R. Visintin, K. Craig, E. S. Hwang, S. Prinz, M. Tyers, and A. Amon, “The phosphatase Cdc14 triggers mitotic exit by reversal of Cdk-dependent phosphorylation,” *Mol. Cell*, vol. 2, pp. 709–18, dec 1998.
- [35] C. Wurzenberger and D. W. Gerlich, “Phosphatases: providing safe passage through mitotic exit,” *Nat. Rev. Mol. Cell Biol.*, vol. 12, pp. 469–82, jul 2011.
- [36] D. O. Morgan, “Cyclin-dependent kinases: engines, clocks, and microprocessors,” *Annu. Rev. Cell Dev. Biol.*, vol. 13, pp. 261–291, jan 1997.
- [37] J. Bähler, “Cell-cycle control of gene expression in budding and fission yeast,” *Annu. Rev. Genet.*, vol. 39, pp. 69–94, jan 2005.
- [38] A. Hershko and A. Ciechanover, “The ubiquitin system,” *Annu. Rev. Biochem.*, vol. 67, pp. 425–79, jan 1998.
- [39] D. Finley, “Recognition and processing of ubiquitin-protein conjugates by the proteasome,” *Annu. Rev. Biochem.*, vol. 78, pp. 477–513, jan 2009.
- [40] S. Murata, H. Yashiroda, and K. Tanaka, “Molecular mechanisms of proteasome assembly,” *Nat. Rev. Mol. Cell Biol.*, vol. 10, no. 2, pp. 104–15, 2009.
- [41] A. Henderson, J. Eroles, M. a. Hoyt, and P. Coffino, “Dependence of proteasome processing rate on substrate unfolding,” *J. Biol. Chem.*, vol. 286, pp. 17495–502, may 2011.
- [42] S. Elsasser and D. Finley, “Delivery of ubiquitinated substrates to protein-unfolding machines,” *Nat. Cell Biol.*, vol. 7, pp. 742–9, aug 2005.
- [43] J. S. Thrower, L. Hoffman, M. Rechsteiner, and C. M. Pickart, “Recognition of the polyubiquitin proteolytic signal,” *EMBO J.*, vol. 19, no. 1, pp. 94–102, 2000.
- [44] V. Chau, J. W. Tobias, a. Bachmair, D. Marriott, D. J. Ecker, D. K. Gonda, and a. Varshavsky, “A multiubiquitin chain is confined to specific lysine in a targeted short-lived protein,” *Science*, vol. 243, no. 4898, pp. 1576–1583, 1989.
- [45] Y. Lu, B.-h. Lee, R. W. King, D. Finley, and M. W. Kirschner, “Substrate degradation by the proteasome: A single-molecule kinetic analysis,” *Science (80-.)*, vol. 348, no. 6231, pp. 1250834–1250834, 2015.
- [46] M. Hochstrasser, “Ubiquitin-dependent protein degradation,” *Annu. Rev. Genet.*, vol. 30, pp. 405–39, jan 1996.

- [47] J. P. McGrath, S. Jentsch, and a. Varshavsky, "UBA 1: an essential yeast gene encoding ubiquitin-activating enzyme.," *EMBO J.*, vol. 10, no. 1, pp. 227–236, 1991.
- [48] H. C. Ardley and P. A. Robinson, "E3 ubiquitin ligases," *Essays Biochem.*, vol. 41, pp. 15–30, 2005.
- [49] R. J. Deshaies and C. A. P. Joazeiro, "RING domain E3 ubiquitin ligases.," *Annu. Rev. Biochem.*, vol. 78, pp. 399–434, jan 2009.
- [50] Y. Murakami, K. Tanaka, S. Matsufuji, Y. Miyazaki, and S.-i. Hayashi, "Antizyme, a protein induced by polyamines, accelerates the degradation of ornithine decarboxylase in Chinese-hamster ovary-cell extracts.," *Biochem. J.*, vol. 283, pp. 661–664, may 1992.
- [51] N. E. W. Insights, O. N. Yeast, Z. Porat, G. Landau, Z. Bercovich, D. Krutauz, M. Glickman, C. Kahana, N. E. W. Insights, O. N. Yeast, Z. Porat, G. Landau, Z. Bercovich, D. Krutauz, M. Glickman, and C. Kahana, "Yeast antizyme mediates degradation of yeast ornithine decarboxylase by yeast but not by mammalian proteasome: new insights on yeast antizyme.," *J. Biol. Chem.*, vol. 283, pp. 4528–34, feb 2008.
- [52] S. K. Lim and G. Gopalan, "Antizyme1 mediates AURKAIP1-dependent degradation of Aurora-A.," *Oncogene*, vol. 26, no. 46, pp. 6593–6603, 2007.
- [53] J. R. Skaar and M. Pagano, "Control of cell growth by the SCF and APC/C ubiquitin ligases.," *Curr. Opin. Cell Biol.*, vol. 21, pp. 816–24, dec 2009.
- [54] E. Elizabeth Patton, A. R. Willems, and M. Tyers, "Combinatorial control in ubiquitin-dependent proteolysis: Don't Skp the F-box hypothesis," *Trends Genet.*, vol. 14, no. 6, pp. 236–243, 1998.
- [55] A. R. Willems, S. Lanker, E. E. Patton, K. L. Craig, T. F. Nason, N. Mathias, R. Kobayashi, C. Wittenberg, and M. Tyers, "Cdc53 targets phosphorylated G1 cyclins for degradation by the ubiquitin proteolytic pathway," *Cell*, vol. 86, no. 3, pp. 453–463, 1996.
- [56] D. Barford, "Structural insights into anaphase-promoting complex function and mechanism.," *Philos. Trans. R. Soc. Lond. B. Biol. Sci.*, vol. 366, pp. 3605–24, dec 2011.
- [57] H. H. Lim, P. Y. Goh, and U. Surana, "Cdc20 is essential for the cyclosome-mediated proteolysis of both Pds1 and Clb2 during M phase in budding yeast.," *Curr. Biol.*, vol. 8, no. 4, pp. 231–234, 1998.
- [58] O. Cohen-Fix, J.-M. Peters, M. W. Kirschner, and D. Koshland, "Anaphase initiation in *Saccharomyces cerevisiae* is controlled by the APC-dependent degradation of the anaphase inhibitor Pds1p.," *Genes Dev*, vol. 10, pp. 3081–3093, 1996.
- [59] M. Schwab, a. S. Lutum, and W. Seufert, "Yeast Hct1 is a regulator of Clb2 cyclin proteolysis.," *Cell*, vol. 90, pp. 683–93, aug 1997.
- [60] S. Piatti, M. Venturetti, E. Chirolì, and R. Fraschini, "The spindle position checkpoint in budding yeast: the motherly care of MEN.," *Cell Div.*, vol. 1, no. 1, p. 2, 2006.

- [61] F. Gergely, “Mitosis: Cdh1 Clears the Way for Anaphase Spindle Assembly,” *Curr. Biol.*, vol. 18, no. 21, pp. R1009–R1012, 2008.
- [62] J. A. Robbins and F. R. Cross, “Requirements and Reasons for Effective Inhibition of the Anaphase Promoting Complex Activator Cdh1,” *Mol. Biol. Cell*, vol. 21, pp. 914–925, jan 2010.
- [63] J.-M. Peters, “The anaphase-promoting complex: proteolysis in mitosis and beyond,” *Mol. Cell*, vol. 9, pp. 931–43, may 2002.
- [64] B. a. Buschhorn, G. Petzold, M. Galova, P. Dube, C. Kraft, F. Herzog, H. Stark, and J.-M. Peters, “Substrate binding on the APC/C occurs between the coactivator Cdh1 and the processivity factor Doc1,” *Nat. Struct. Mol. Biol.*, vol. 18, pp. 6–13, jan 2011.
- [65] Z. Tang, B. Li, R. Bharadwaj, H. Zhu, E. Ozkan, K. Hakala, J. Deisenhofer, and H. Yu, “APC2 Cullin protein and APC11 RING protein comprise the minimal ubiquitin ligase module of the anaphase-promoting complex,” *Mol. Biol. Cell*, vol. 12, no. December, pp. 3839–3851, 2001.
- [66] B. R. Thornton, T. M. Ng, M. E. Matyskiela, C. W. Carroll, D. O. Morgan, and D. P. Toczyski, “An architectural map of the anaphase-promoting complex,” *Genes Dev.*, vol. 20, pp. 449–60, feb 2006.
- [67] R. Visintin, S. Prinz, and A. Amon, “CDC20 and CDH1: A Family of Substrate-Specific Activators of APC-Dependent Proteolysis,” *Science (80-.)*, vol. 278, pp. 460–463, oct 1997.
- [68] M. Shirayama, A. Tóth, M. Gálová, and K. A. Nasmyth, “APC(Cdc20) promotes exit from mitosis by destroying the anaphase inhibitor Pds1 and cyclin Clb5,” *Nature*, vol. 402, no. 6758, pp. 203–207, 1999.
- [69] L. a. Passmore and D. Barford, “Coactivator functions in a stoichiometric complex with anaphase-promoting complex/cyclosome to mediate substrate recognition,” *EMBO Rep.*, vol. 6, pp. 873–8, sep 2005.
- [70] M. Shirayama, W. Zachariae, R. Ciosk, and K. A. Nasmyth, “The Polo-like kinase Cdc5p and the WD-repeat protein Cdc20p/fizzy are regulators and substrates of the anaphase promoting complex in *Saccharomyces cerevisiae*,” *EMBO J.*, vol. 17, no. 5, pp. 1336–1349, 1998.
- [71] C. Pflieger and M. W. Kirschner, “The KEN box: an APC recognition signal distinct from the D box targeted by Cdh1,” *GENES Dev.*, vol. 14, pp. 655–665, 2000.
- [72] C. M. Pflieger, E. Lee, and M. W. Kirschner, “Substrate recognition by the Cdc20 and Cdh1 components of the anaphase-promoting complex,” *Genes Dev.*, vol. 15, pp. 2396–407, sep 2001.
- [73] J. L. Burton and M. J. Solomon, “D box and KEN box motifs in budding yeast Hsl1p are required for APC-mediated degradation and direct binding to Cdc20p and Cdh1p,” *Genes Dev.*, vol. 15, no. 18, pp. 2381–2395, 2001.

- [74] L. E. Littlepage and J. V. Ruderman, "Identification of a new APC/C recognition domain, the A box, which is required for the Cdh1-dependent destruction of the kinase Aurora-A during mitotic exit," *Genes Dev.*, vol. 16, no. 17, pp. 2274–2285, 2002.
- [75] A. Reis, M. Levasseur, H.-Y. Chang, D. J. Elliott, and K. T. Jones, "The CRY box: a second APCcdh1-dependent degron in mammalian cdc20," *EMBO Rep.*, vol. 7, no. 10, pp. 1040–1045, 2006.
- [76] M. Araki, H. Yu, and M. Asano, "A novel motif governs APC-dependent degradation of Drosophila ORC1 in vivo," *Genes Dev.*, vol. 19, no. 20, pp. 2458–2465, 2005.
- [77] H. Yu, "Cdc20: a WD40 activator for a cell cycle degradation machine.," *Mol. Cell*, vol. 27, pp. 3–16, jul 2007.
- [78] D. Lu, J. Y. Hsiao, N. E. Davey, V. A. Van Voorhis, S. A. Foster, C. Tang, and D. O. Morgan, "Multiple mechanisms determine the order of APC/C substrate degradation in mitosis," *J. Cell Biol.*, vol. 207, no. 1, pp. 23–39, 2014.
- [79] E. R. Kramer, N. Scheuringer, a. V. Podtelejnikov, M. Mann, and J.-M. Peters, "Mitotic regulation of the APC activator proteins CDC20 and CDH1.," *Mol. Biol. Cell*, vol. 11, no. 5, pp. 1555–1569, 2000.
- [80] S. L. Jaspersen, J. F. Charles, and D. O. Morgan, "Inhibitory phosphorylation of the APC regulator Hct1 is controlled by the kinase Cdc28 and the phosphatase Cdc14," *Curr. Biol.*, vol. 9, no. 5, pp. 227–236, 1999.
- [81] P. Ayuda-Duran, F. Devesa, F. Gomes, J. Sequeira-Mendes, C. Avila-Zarza, M. Gomez, and A. Calzada, "The CDK regulators Cdh1 and Sic1 promote efficient usage of DNA replication origins to prevent chromosomal instability at a chromosome arm," *Nucleic Acids Res.*, vol. 42, no. 11, pp. 7057–7068, 2014.
- [82] I. García-Higuera, E. Manchado, P. Dubus, M. Cañamero, J. Méndez, S. Moreno, and M. Malumbres, "Genomic stability and tumour suppression by the APC/C cofactor Cdh1.," *Nat. Cell Biol.*, vol. 10, no. 7, pp. 802–811, 2008.
- [83] M. C. Hall, E. N. E. Warren, and C. H. Borchers, "Multi-kinase phosphorylation of the APC/C activator Cdh1 revealed by mass spectrometry," *Cell Cycle*, vol. 3, no. October, pp. 1278–1284, 2004.
- [84] R. van Leuken, L. Clijsters, and R. Wolthuis, "To cell cycle, swing the APC/C," *Biochim. Biophys. Acta - Rev. Cancer*, vol. 1786, pp. 49–59, sep 2008.
- [85] J. L. Burton and M. J. Solomon, "assembly checkpoint Mad3p , a pseudosubstrate inhibitor of APC Cdc20 in the spindle assembly checkpoint," *Genes Dev.*, vol. 3, pp. 655–667, 2007.
- [86] J. Y. Hsu, J. D. R. Reimann, C. S. Sørensen, J. Lukas, and P. K. Jackson, "E2F-dependent accumulation of hEmi1 regulates S phase entry by inhibiting APC(Cdh1).," *Nat. Cell Biol.*, vol. 4, no. 5, pp. 358–366, 2002.
- [87] J. L. Burton, Y. Xiong, and M. J. Solomon, "Mechanisms of pseudosubstrate inhibition of the anaphase promoting complex by Acm1," *EMBO J.*, vol. 30, pp. 1818–1829, apr 2011.

- [88] J. S. Martinez, D.-E. Jeong, E. Choi, B. M. Billings, and M. C. Hall, "Acm1 is a negative regulator of the CDH1-dependent anaphase-promoting complex/cyclosome in budding yeast.," *Mol. Cell. Biol.*, vol. 26, no. 24, pp. 9162–76, 2006.
- [89] E. Choi, J. M. Dial, D.-E. Jeong, and M. C. Hall, "Unique D box and KEN box sequences limit ubiquitination of Acm1 and promote pseudosubstrate inhibition of the anaphase-promoting complex.," *J. Biol. Chem.*, vol. 283, pp. 23701–10, aug 2008.
- [90] J. M. Dial, E. V. E. Petrotchenko, and C. H. C. Borchers, "Inhibition of APC Cdh1 Activity by Cdh1 / Acm1 / Bmh1 Ternary Complex Formation," *J. Biol. Chem.*, vol. 282, pp. 5237–5248, feb 2007.
- [91] M. Enquist-Newman, M. Sullivan, and D. O. Morgan, "Modulation of the mitotic regulatory network by APC-dependent destruction of the Cdh1 inhibitor Acm1.," *Mol. Cell*, vol. 30, pp. 437–46, may 2008.
- [92] D. Ostapenko, J. L. Burton, R. Wang, and M. J. Solomon, "Pseudosubstrate inhibition of the anaphase-promoting complex by Acm1: regulation by proteolysis and Cdc28 phosphorylation.," *Mol. Cell. Biol.*, vol. 28, pp. 4653–64, aug 2008.
- [93] J. S. Martinez, H. Hall, M. D. Bartolowits, and M. C. Hall, "Acm1 contributes to nuclear positioning by inhibiting Cdh1-substrate interactions.," *Cell cycle*, vol. 11, pp. 384–94, jan 2012.
- [94] M. C. Hall, D.-e. Jeong, J. T. Henderson, E. Choi, S. C. Bremmer, A. B. Iliuk, and H. Charbonneau, "Cdc28 and Cdc14 control stability of the anaphase-promoting complex inhibitor Acm1.," *J. Biol. Chem.*, vol. 283, pp. 10396–407, apr 2008.
- [95] Y. Shi, "Serine/Threonine Phosphatases: Mechanism through Structure," *Cell*, vol. 139, no. 3, pp. 468–484, 2009.
- [96] P. T. W. Cohen, "Protein phosphatase 1–targeted in many directions.," *J. Cell Sci.*, vol. 115, no. Pt 2, pp. 241–256, 2002.
- [97] M. P. Egloff, D. F. Johnson, G. Moorhead, P. T. Cohen, P. Cohen, and D. Barford, "Structural basis for the recognition of regulatory subunits by the catalytic subunit of protein phosphatase 1.," *EMBO J.*, vol. 16, no. 8, pp. 1876–1887, 1997.
- [98] V. Rossio, T. Michimoto, T. Sasaki, I. Ohbayashi, Y. Kikuchi, and S. Yoshida, "Nuclear PP2A-Cdc55 prevents APC-Cdc20 activation during the spindle assembly checkpoint.," *J. Cell Sci.*, vol. 126, no. Pt 19, pp. 4396–405, 2013.
- [99] Y. Wang and D. J. Burke, "Cdc55p, the B-type regulatory subunit of protein phosphatase 2A, has multiple functions in mitosis and is required for the kinetochore/spindle checkpoint in *Saccharomyces cerevisiae*.," *Mol. Cell. Biol.*, vol. 17, no. 2, pp. 620–626, 1997.
- [100] S. Wicky, H. Tjandra, D. Schieltz, J. Yates, and D. R. Kellogg, "The Zds proteins control entry into mitosis and target protein phosphatase 2A to the Cdc25 phosphatase.," *Mol. Biol. Cell*, vol. 22, no. 1, pp. 20–32, 2011.

- [101] G. S. Taylor, "The Activity of Cdc14p, an Oligomeric Dual Specificity Protein Phosphatase from *Saccharomyces cerevisiae*, Is Required for Cell Cycle Progression," *J. Biol. Chem.*, vol. 272, pp. 24054–24063, sep 1997.
- [102] C. H. Gray, V. M. Good, N. K. Tonks, and D. Barford, "The structure of the cell cycle protein Cdc14 reveals a proline-directed protein phosphatase.," *EMBO J.*, vol. 22, pp. 3524–35, jul 2003.
- [103] W.-Q. Wang, J. N. Bembenek, K. R. Gee, H. Yu, H. Charbonneau, and Z.-Y. Zhang, "Kinetic and mechanistic studies of a cell cycle protein phosphatase Cdc14.," *J. Biol. Chem.*, vol. 279, pp. 30459–30468, jul 2004.
- [104] C. Bouchoux and F. Uhlmann, "A quantitative model for ordered Cdk substrate dephosphorylation during mitotic exit.," *Cell*, vol. 147, pp. 803–14, nov 2011.
- [105] J. Culotti and L. H. Hartwell, "Genetic control of the cell division cycle in yeast. 3. Seven genes controlling nuclear division.," *Exp. Cell Res.*, vol. 67, no. 2, pp. 389–401, 1971.
- [106] J. H. Toyn, A. L. Johnson, J. D. Donovan, W. M. Toone, and L. H. Johnston, "The Swi5 transcription factor of *Saccharomyces cerevisiae* has a role in exit from mitosis through induction of the cdk-inhibitor Sic1 in telophase.," *Genetics*, vol. 145, no. 1, pp. 85–96, 1997.
- [107] B. Kovacech, K. Nasmyth, and T. Schuster, "EGT2 gene transcription is induced predominantly by Swi5 in early G1.," *Mol. Cell. Biol.*, vol. 16, no. 7, pp. 3264–3274, 1996.
- [108] D. P. Miller, H. Hall, R. Chaparian, M. Mara, A. Mueller, M. C. Hall, and K. B. Shannon, "Dephosphorylation of Iqg1 by Cdc14 regulates cytokinesis in budding yeast," *Mol. Biol. Cell*, vol. 26, no. 16, pp. 2913–2926, 2015.
- [109] Y. Zhai, P. Y. K. Yung, L. Huo, and C. Liang, "Cdc14p resets the competency of replication licensing by dephosphorylating multiple initiation proteins during mitotic exit in budding yeast.," *J. Cell Sci.*, vol. 123, no. Pt 22, pp. 3933–43, 2010.
- [110] C. C. L. Eissler, G. Mazón, B. B. L. Powers, S. N. Savinov, L. S. Symington, and M. C. Hall, "The Cdk/Cdc14 module controls activation of the Yen1 holliday junction resolvase to promote genome stability.," *Mol. Cell*, vol. 54, pp. 80–93, apr 2014.
- [111] M. Blanco, J. Matos, and S. West, "Dual Control of Yen1 Nuclease Activity and Cellular Localization by Cdk and Cdc14 Prevents Genome Instability," *Mol. Cell*, vol. 54, no. 1, pp. 94–106, 2014.
- [112] W. Shou, J. H. Seol, A. Shevchenko, C. Baskerville, D. Moazed, Z. W. Chen, J. Jang, A. Shevchenko, H. Charbonneau, and R. J. Deshaies, "Exit from mitosis is triggered by Tem1-dependent release of the protein phosphatase Cdc14 from nucleolar RENT complex.," *Cell*, vol. 97, no. 2, pp. 233–244, 1999.
- [113] R. Visintin, E. S. Hwang, and A. Amon, "Cfi1 prevents premature exit from mitosis by anchoring Cdc14 phosphatase in the nucleolus.," *Nature*, vol. 398, no. 6730, pp. 818–823, 1999.

- [114] F. Stegmeier and A. Amon, “Closing mitosis: the functions of the Cdc14 phosphatase and its regulation,” *Annu. Rev. Genet.*, vol. 38, pp. 203–32, jan 2004.
- [115] F. Jin, H. Liu, F. Liang, R. Rizkallah, M. M. Hurt, and Y. Wang, “Temporal control of the dephosphorylation of Cdk substrates by mitotic exit pathways in budding yeast,” *Proc. Natl. Acad. Sci. U. S. A.*, vol. 105, pp. 16177–82, oct 2008.
- [116] E. Berdugo, M. V. Nachury, P. K. Jackson, and P. V. Jallepalli, “The nucleolar phosphatase Cdc14B is dispensable for chromosome segregation and mitotic exit in human cells,” *Cell Cycle*, vol. 7, no. 9, pp. 1184–1190, 2008.
- [117] A. Mocchiari and E. Schiebel, “Cdc14: a highly conserved family of phosphatases with non-conserved functions?,” *J. Cell Sci.*, vol. 123, pp. 2867–76, sep 2010.
- [118] L. Li, B. R. Ernstring, M. J. Wishart, D. L. Lohse, and J. E. Dixon, “A family of putative tumor suppressors is structurally and functionally conserved in humans and yeast,” *J. Biol. Chem.*, vol. 272, no. 47, pp. 29403–29406, 1997.
- [119] Z. Wei, S. Peddibhotla, H. Lin, X. Fang, M. Li, J. M. Rosen, P. Zhang, and C. Mice, “Early-Onset Aging and Defective DNA Damage Response in Cdc14b-Deficient Mice Early-Onset Aging and Defective DNA Damage Response in,” *Mol. Cell. Biol.*, 2011.
- [120] M. D. Vázquez-Novelle, N. Mailand, S. Ovejero, A. Bueno, and M. P. Sacristán, “Human Cdc14A phosphatase modulates the G2/M transition through Cdc25A and Cdc25B,” *J. Biol. Chem.*, vol. 285, pp. 40544–53, dec 2010.
- [121] B. a. Wolfe and K. L. Gould, “Fission yeast Clp1p phosphatase affects G2/M transition and mitotic exit through Cdc25p inactivation,” *EMBO J.*, vol. 23, pp. 919–29, feb 2004.
- [122] S. Trautmann, B. a. Wolfe, P. Jorgensen, M. Tyers, K. L. Gould, and D. McCollum, “Fission yeast Clp1p phosphatase regulates G2/M transition and coordination of cytokinesis with cell cycle progression,” *Curr. Biol.*, vol. 11, no. 12, pp. 931–940, 2001.
- [123] N. Cueille, E. Salimova, V. Esteban, M. Blanco, S. Moreno, a. Bueno, and V. Simanis, “Flp1, a fission yeast orthologue of the *s. cerevisiae* CDC14 gene, is not required for cyclin degradation or rum1p stabilisation at the end of mitosis,” *J. Cell Sci.*, vol. 114, no. Pt 14, pp. 2649–2664, 2001.
- [124] U. Gruneberg, M. Glotzer, A. Gartner, and E. a. Nigg, “The CeCDC-14 phosphatase is required for cytokinesis in the *Caenorhabditis elegans* embryo,” *J. Cell Biol.*, vol. 158, no. 5, pp. 901–914, 2002.
- [125] R. M. Saito, A. Perreault, B. Peach, J. S. Satterlee, and S. van den Heuvel, “The CDC-14 phosphatase controls developmental cell-cycle arrest in *C. elegans*,” *Nat. Cell Biol.*, vol. 6, no. 8, pp. 777–783, 2004.
- [126] S. Ovejero, P. Ayala, A. Bueno, and M. P. Sacristán, “Human Cdc14A regulates Wee1 stability by counteracting CDK-mediated phosphorylation,” *Mol. Biol. Cell*, vol. 23, pp. 4515–25, dec 2012.

- [127] M. Chiesa, M. Guillaumot, M. J. Bueno, and M. Malumbres, “The Cdc14B phosphatase displays oncogenic activity mediated by the Ras-Mek signaling pathway,” *Cell Cycle*, vol. 10, no. 10, pp. 1607–1617, 2011.
- [128] S. Trautmann and D. McCollum, “Cell cycle: new functions for Cdc14 family phosphatases,” *Curr. Biol.*, vol. 12, pp. R733–5, oct 2002.
- [129] S. C. Bremmer, H. Hall, J. S. Martinez, C. L. Eissler, T. H. Hinrichsen, S. Rossie, L. L. Parker, M. C. Hall, and H. Charbonneau, “Cdc14 phosphatases preferentially dephosphorylate a subset of cyclin-dependent kinase (Cdk) sites containing phosphoserine,” *J. Biol. Chem.*, vol. 287, pp. 1662–9, jan 2012.
- [130] C. L. Eissler, G. Mazón, B. L. Powers, S. N. Savinov, L. S. Symington, and M. C. Hall, “The Cdk/Cdc14 module controls activation of the Yen1 holliday junction resolvase to promote genome stability,” *Mol. Cell*, vol. 54, pp. 80–93, apr 2014.
- [131] M. Malumbres and M. Barbacid, “To cycle or not to cycle: a critical decision in cancer,” *Nat. Rev. Cancer*, vol. 1, no. 3, pp. 222–231, 2001.
- [132] B. A. Weaver and D. W. Cleveland, “Decoding the links between mitosis, cancer, and chemotherapy: The mitotic checkpoint, adaptation, and cell death,” *Cancer Cell*, vol. 8, no. 1, pp. 7–12, 2005.
- [133] M. A. Jordan and L. Wilson, “Microtubules and actin filaments: dynamic targets for cancer chemotherapy,” *Curr. Opin. Cell Bio.*, vol. 10, pp. 123–130, 1998.
- [134] C. L. Rieder and R. H. Medema, “No Way Out for Tumor Cells,” *Cancer Cell*, vol. 16, no. 4, pp. 274–275, 2009.
- [135] D. A. Brito and C. L. Rieder, “Mitotic Checkpoint Slippage in Humans Occurs via Cyclin B Destruction in the Presence of an Active Checkpoint,” *Curr. Biol.*, vol. 16, no. 12, pp. 1194–1200, 2006.
- [136] H. C. Huang, J. Shi, J. D. Orth, and T. J. Mitchison, “Evidence that Mitotic Exit Is a Better Cancer Therapeutic Target Than Spindle Assembly,” *Cancer Cell*, vol. 16, no. 4, pp. 347–358, 2009.
- [137] M. Sullivan and D. O. Morgan, “Finishing mitosis, one step at a time,” *Nat. Rev. Mol. Cell Biol.*, vol. 8, pp. 894–903, nov 2007.
- [138] E. Manchado, M. Guillaumot, G. de Cárcer, M. Eguren, M. Trickey, I. García-Higuera, S. Moreno, H. Yamano, M. Cañamero, and M. Malumbres, “Targeting Mitotic Exit Leads to Tumor Regression In Vivo: Modulation by Cdk1, Mast1, and the PP2A/B55 α,δ Phosphatase,” *Cancer Cell*, vol. 18, no. 6, pp. 641–654, 2010.
- [139] K. L. Sackton, N. Dimova, X. Zeng, W. Tian, M. Zhang, T. B. Sackton, J. Meaders, K. L. Pfaff, F. Sigoillot, H. Yu, X. Luo, and R. W. King, “Synergistic blockade of mitotic exit by two chemical inhibitors of the APC/C,” *Nature*, vol. 514, no. 7524, pp. 646–649, 2014.
- [140] F. Bassermann, D. Frescas, D. Guardavaccaro, L. Busino, A. Peschiaroli, and M. Pagano, “The Cdc14B-Cdh1-Plk1 axis controls the G2 DNA-damage-response checkpoint,” *Cell*, vol. 134, pp. 256–67, jul 2008.

- [141] U. Bc and J.-M. Peters, "SCF and APC: the Yin and Yang of cell cycle regulated proteolysis," *Curr. Opin. Cell Biol.*, pp. 759–768, 1998.
- [142] H. C. Vodermaier, "APC/C and SCF: Controlling each other and the cell cycle," *Curr. Biol.*, vol. 14, no. 18, pp. 787–796, 2004.
- [143] A. R. Willems, M. Schwab, and M. Tyers, "A hitchhiker's guide to the cullin ubiquitin ligases: SCF and its kin," *Biochim. Biophys. Acta - Mol. Cell Res.*, vol. 1695, no. 1-3, pp. 133–170, 2004.
- [144] J. W. Harper, J. L. Burton, and M. J. Solomon, "The anaphase-promoting complex: it's not just for mitosis any more.," *Genes Dev.*, vol. 16, pp. 2179–206, sep 2002.
- [145] J.-M. Peters, "The anaphase promoting complex/cyclosome: a machine designed to destroy," *Nat. Rev. Mol. Cell Biol.*, vol. 7, pp. 644–656, sep 2006.
- [146] J. a. Pesin and T. L. Orr-weaver, "Regulation of APC/C activators in mitosis and meiosis.," *Annu. Rev. Cell Dev. Biol.*, vol. 24, pp. 475–99, jan 2008.
- [147] P. T. Spellman, G. Sherlock, M. Q. Zhang, V. R. Iyer, K. Anders, M. B. Eisen, P. O. Brown, D. Botstein, and B. Futcher, "Comprehensive identification of cell cycle-regulated genes of the yeast *Saccharomyces cerevisiae* by microarray hybridization.," *Mol. Biol. Cell*, vol. 9, pp. 3273–97, dec 1998.
- [148] B. R. Thornton and D. P. Toczyski, "Securin and B-cyclin/CDK are the only essential targets of the APC.," *Nat. Cell Biol.*, vol. 5, no. 12, pp. 1090–1094, 2003.
- [149] W. Heinemeyer, a. Cruhler, V. Mohrle, Y. Mahe, and D. H. Wolf, "PRE2, highly homologous to the human major histocompatibility complex- linked Ring10 gene, codes for a yeast proteasome subunit necessary for chymotryptic activity and degradation of ubiquitinated proteins," *J. Biol. Chem.*, vol. 268, no. 7, pp. 5115–5120, 1993.
- [150] M. Ghislain, a. Udvardy, and C. Mann, "*S. cerevisiae* 26S protease mutants arrest cell division in G2/metaphase.," *Nature*, vol. 366, no. 6453, pp. 358–362, 1993.
- [151] N. Ghaboosi and R. J. Deshaies, "A conditional yeast E1 mutant blocks the ubiquitin-proteasome pathway and reveals a role for ubiquitin conjugates in targeting Rad23 to the proteasome," *Mol. Biol. Cell*, vol. 18, pp. 1953–1963, 2007.
- [152] R. Palanimurugan, H. Scheel, K. Hofmann, and R. J. Dohmen, "Polyamines regulate their synthesis by inducing expression and blocking degradation of ODC antizyme.," *EMBO J.*, vol. 23, no. 24, pp. 4857–4867, 2004.
- [153] J. Terrell, S. Shih, R. Dunn, and L. Hicke, "A function for monoubiquitination in the internalization of a G protein-coupled receptor.," *Mol. Cell*, vol. 1, pp. 193–202, jan 1998.
- [154] D. Voges, P. Zwickl, and W. Baumeister, "The 26S proteasome: a molecular machine designed for controlled proteolysis.," *Annu. Rev. Biochem.*, vol. 68, pp. 1015–68, jan 1999.

- [155] D. H. Wolf and W. Hilt, "The proteasome: A proteolytic nanomachine of cell regulation and waste disposal," *Biochim. Biophys. Acta - Mol. Cell Res.*, vol. 1695, no. 1-3, pp. 19–31, 2004.
- [156] K. L. Rock, C. Gramm, L. Rothstein, K. Clark, R. Stein, L. Dick, D. Hwang, and A. L. Goldberg, "Inhibitors of the proteasome block the degradation of most cell proteins and the generation of peptides presented on MHC class I molecules.," *Cell*, vol. 78, pp. 761–71, sep 1994.
- [157] M. a. Hoyt and P. Coffino, "Ubiquitin-free routes into the proteasome.," *Cell. Mol. Life Sci.*, vol. 61, pp. 1596–600, jul 2004.
- [158] I. Jariel-Encontre, G. Bossis, and M. Piechaczyk, "Ubiquitin-independent degradation of proteins by the proteasome.," *Biochim. Biophys. Acta*, vol. 1786, pp. 153–77, dec 2008.
- [159] M. Orłowski and S. Wilk, "Ubiquitin-independent proteolytic functions of the proteasome, Arch," *Biochem. Biophys.*, vol. 415, pp. 1–5, 2003.
- [160] J. M. Baugh, E. G. Viktorova, and E. V. Pilipenko, "Proteasomes can degrade a significant proportion of cellular proteins independent of ubiquitination.," *J. Mol. Biol.*, vol. 386, pp. 814–27, feb 2009.
- [161] G. Asher, N. Reuven, and Y. Shaul, "20S proteasomes and protein degradation "by default" ," *BioEssays*, vol. 28, no. 8, pp. 844–849, 2006.
- [162] S. Gandre and C. Kahana, "Degradation of ornithine decarboxylase in *Saccharomyces cerevisiae* is ubiquitin independent.," *Biochem. Biophys. Res. Commun.*, vol. 293, pp. 139–44, apr 2002.
- [163] Y. Murakami, S. Matsufuji, T. Kameji, S. Hayashi, K. Igarashi, T. Tamura, K. Tanaka, and A. Ichihara, "Ornithine decarboxylase is degraded by the 26S proteasome without ubiquitination," *Nature*, vol. 360, pp. 597–599, 1992.
- [164] P. Coffino, "Regulation of cellular polyamines by antizyme.," *Nat. Rev. Mol. Cell Biol.*, vol. 2, no. 3, pp. 188–194, 2001.
- [165] X. Li and P. Coffino, "Degradation of ornithine decarboxylase: exposure of the C-terminal target by a polyamine-inducible inhibitory protein.," *Mol. Cell. Biol.*, vol. 13, no. 4, pp. 2377–2383, 1993.
- [166] M. Zhang, C. M. Pickart, and P. Coffino, "Determinants of proteasome recognition of ornithine decarboxylase, a ubiquitin-independent substrate.," *EMBO J.*, vol. 22, pp. 1488–96, apr 2003.
- [167] R. M. Newman, A. Mobascher, U. Mangold, C. Koike, S. Diah, M. Schmidt, D. Finley, and B. R. Zetter, "Antizyme targets cyclin D1 for degradation: A novel mechanism for cell growth repression," *J. Biol. Chem.*, vol. 279, no. 40, pp. 41504–41511, 2004.
- [168] G. Asher, P. Tsvetkov, C. Kahana, and Y. Shaul, "A mechanism of ubiquitin-independent proteasomal degradation of the tumor suppressors p53 and p73," *Genes Dev.*, vol. 19, no. 3, p. 316, 2005.

- [169] X. Chen, Y. Chi, A. Bloecher, R. Aebersold, B. E. Clurman, and J. M. Roberts, "N-acetylation and ubiquitin-independent proteasomal degradation of p21 Cip1," *Mol. Cell*, vol. 16, no. 5, pp. 839–847, 2004.
- [170] X. Chen, L. F. Barton, Y. Chi, B. E. Clurman, and J. M. Roberts, "Ubiquitin-Independent Degradation of Cell-Cycle Inhibitors by the REG γ Proteasome," *Mol. Cell*, vol. 26, no. 6, pp. 843–852, 2007.
- [171] X. Li, L. Amazit, W. Long, D. M. Lonard, J. J. Monaco, and B. W. O'Malley, "Ubiquitin- and ATP-Independent Proteolytic Turnover of p21 by the REG γ -Proteasome Pathway," *Mol. Cell*, vol. 26, pp. 831–842, jun 2007.
- [172] R. J. Sheaff, J. D. Singer, J. Swanger, M. Smitherman, J. M. Roberts, and B. E. Clurman, "Proteasomal Turnover of p21 Cip1 Does Not Require p21 Cip1 Ubiquitination," *Components*, vol. 5, pp. 403–410, 2000.
- [173] R. F. Kalejta and T. Shenk, "Proteasome-dependent, ubiquitin-independent degradation of the Rb family of tumor suppressors by the human cytomegalovirus pp71 protein.," *Proc. Natl. Acad. Sci. U. S. A.*, vol. 100, no. 6, pp. 3263–3268, 2003.
- [174] P. Sdek, H. Ying, D. L. F. Chang, W. Qiu, H. Zheng, R. Touitou, M. J. Allday, and Z. X. Jim Xiao, "MDM2 promotes proteasome-dependent ubiquitin-independent degradation of retinoblastoma protein," *Mol. Cell*, vol. 20, no. 5, pp. 699–708, 2005.
- [175] P. Ferrara, E. Andermarcher, G. Bossis, C. Acquaviva, F. Brockly, I. Jariel-Encontre, and M. Piechaczyk, "The structural determinants responsible for c-Fos protein proteasomal degradation differ according to the conditions of expression.," *Oncogene*, vol. 22, no. 10, pp. 1461–1474, 2003.
- [176] A. Forster and C. P. Hill, "Proteasome degradation: enter the substrate," *Trends Cell Biol.*, vol. 13, pp. 550–553, nov 2003.
- [177] A. Peth, N. Kukushkin, M. Bossé, and A. L. Goldberg, "Ubiquitinated proteins activate the proteasomal ATPases by binding to Usp14 or Uch37 homologs," *J. Biol. Chem.*, vol. 288, no. 11, pp. 7781–7790, 2013.
- [178] M. Jaquenoud, F. van Drogen, and M. Peter, "Cell cycle-dependent nuclear export of Cdh1p may contribute to the inactivation of APC/C(Cdh1).," *EMBO J.*, vol. 21, pp. 6515–26, dec 2002.
- [179] C. Janke, M. M. Magiera, N. Rathfelder, C. Taxis, S. Reber, H. Maekawa, A. Moreno-Borchart, G. Doenges, E. Schwob, E. Schiebel, and M. Knop, "A versatile toolbox for PCR-based tagging of yeast genes: new fluorescent proteins, more markers and promoter substitution cassettes.," *Yeast*, vol. 21, pp. 947–62, aug 2004.
- [180] A. H. Y. Tong and C. Boone, "Synthetic genetic array analysis in *Saccharomyces cerevisiae*," *Methods Mol. Biol.*, 2006.
- [181] C. Liu, J. Apodaca, L. E. Davis, and H. Rao, "Proteasome inhibition in wild-type yeast *Saccharomyces cerevisiae* cells," *Biotechniques*, vol. 42, no. 2, pp. 158–162, 2007.

- [182] C. L. Eissler, S. C. Bremmer, J. S. Martinez, L. L. Parker, H. Charbonneau, and M. C. Hall, "A general strategy for studying multisite protein phosphorylation using label-free selected reaction monitoring mass spectrometry.," *Anal. Biochem.*, vol. 418, pp. 267–275, jul 2011.
- [183] C. Li, M. Melesse, S. Zhang, C. Hao, C. Wang, H. Zhang, M. C. Hall, and J.-R. Xu, "FgCDC 14 regulates cytokinesis, morphogenesis, and pathogenesis in *Fusarium graminearum*," *Mol. Microbiol.*, pp. n/a–n/a, oct 2015.
- [184] E. a. Placzek, M. P. Plebanek, A. M. Lipchik, S. R. Kidd, and L. L. Parker, "A peptide biosensor for detecting intracellular Abl kinase activity using matrix-assisted laser desorption/ionization time-of-flight mass spectrometry," *Anal. Biochem.*, vol. 397, no. 1, pp. 73–78, 2010.
- [185] B. L. Powers, M. Melesse, C. L. Eissler, H. Charbonneau, and M. C. Hall, "Measuring Activity and Specificity of Protein Phosphatases," *Methods Mol. Biol.*, vol. 1342, pp. 221–235, 2016.
- [186] J. E. Buss and J. T. Stull, "Measurement of chemical phosphate in proteins.," *Methods Enzymol.*, vol. 99, no. 1974, pp. 7–14, 1983.
- [187] P. Ekman and O. Jäger, "Quantification of subnanomolar amounts of phosphate bound to seryl and threonyl residues in phosphoproteins using alkaline hydrolysis and malachite green.," 1993.
- [188] X. Li, M. Wilmanns, J. Thornton, and M. Köhn, "Elucidating human phosphatase-substrate networks.," *Sci. Signal.*, vol. 6, p. rs10, may 2013.
- [189] V. V. Vintonyak, A. P. Antonchick, D. Rauh, and H. Waldmann, "The therapeutic potential of phosphatase inhibitors," *Curr. Opin. Chem. Biol.*, vol. 13, no. 3, pp. 272–283, 2009.
- [190] N. K. Tonks, "Protein tyrosine phosphatases: from genes, to function, to disease.," *Nat. Rev. Mol. Cell Biol.*, vol. 7, no. 11, pp. 833–846, 2006.
- [191] T. R. Burke, H. K. Kole, and P. P. Roller, "Potent inhibition of insulin receptor dephosphorylation by a hexamer peptide containing the phosphotyrosyl mimetic F2Pmp.," 1994.
- [192] J. a. Perry and S. Kornbluth, "Cdc25 and Wee1: analogous opposites?," *Cell Div.*, vol. 2, p. 12, 2007.
- [193] R. Boutros, V. Lobjois, and B. Ducommun, "CDC25 phosphatases in cancer cells: key players? Good targets?," *Nat. Rev. Cancer*, vol. 7, no. 7, pp. 495–507, 2007.
- [194] M. O. Contour-Galcerá, A. Sidhu, G. Prévost, D. Bigg, and B. Ducommun, "What's new on CDC25 phosphatase inhibitors," *Pharmacol. Ther.*, vol. 115, no. 1, pp. 1–12, 2007.
- [195] G. Arora, P. Tiwari, R. S. Mandal, A. Gupta, D. Sharma, S. Saha, and R. Singh, "High Throughput Screen Identifies Small Molecule Inhibitors Specific for Mycobacterium tuberculosis Phosphoserine Phosphatase.," *J. Biol. Chem.*, vol. 289, no. 36, pp. 0–31, 2014.

- [196] C. Li, M. Melesse, S. Zhang, C. Hao, C. Wang, H. Zhang, M. C. Hall, and J.-R. Xu, “FgCDC₁₄ regulates cytokinesis, morphogenesis, and pathogenesis in *Fusarium graminearum*,” *Mol. Microbiol.*, vol. 98, no. 4, pp. 770–786, 2015.
- [197] J. B. Baell, L. Ferrins, H. Falk, and G. Nikolakopoulos, “PAINS: Relevance to tool compound discovery and fragment-based screening,” *Aust. J. Chem.*, vol. 66, no. 12, pp. 1483–1494, 2013.
- [198] J. B. Baell and G. a. Holloway, “New substructure filters for removal of pan assay interference compounds (PAINS) from screening libraries and for their exclusion in bioassays,” *J. Med. Chem.*, vol. 53, no. 7, pp. 2719–2740, 2010.
- [199] F. Meng, S. Cheng, H. Ding, S. Liu, Y. Liu, K. Zhu, S. Chen, J. Lu, Y. Xie, L. Li, R. Liu, Z. Shi, Y. Zhou, Y.-C. Liu, M. Zheng, H. Jiang, W. Lu, H. Liu, and C. Luo, “Discovery and Optimization of Novel, Selective Histone Methyltransferase SET7 Inhibitors by Pharmacophore- and Docking-Based Virtual Screening,” *J. Med. Chem.*, p. 150930084435009, 2015.
- [200] H. Lin, K. Ha, G. Lu, X. Fang, R. Cheng, Q. Zuo, and P. Zhang, “Cdc14A and Cdc14B Redundantly Regulate DNA Double-Strand Break Repair,” *Mol. Cell. Biol.*, vol. 35, no. 21, pp. 3657–3668, 2015.
- [201] A. Mocciaro, E. Berdough, K. Zeng, E. Black, P. Vagnarelli, W. Earnshaw, D. Gillespie, P. Jallepalli, and E. Schiebel, “Vertebrate cells genetically deficient for Cdc14A or Cdc14B retain DNA damage checkpoint proficiency but are impaired in DNA repair,” *J. Cell Biol.*, vol. 189, pp. 631–9, may 2010.
- [202] K. Cadwell and L. Coscoy, “Ubiquitination on nonlysine residues by a viral E3 ubiquitin ligase,” *Science*, vol. 309, pp. 127–30, jul 2005.
- [203] X. Wang, R. a. Herr, W.-J. Chua, L. Lybarger, E. J. H. J. Wiertz, and T. H. Hansen, “Ubiquitination of serine, threonine, or lysine residues on the cytoplasmic tail can induce ERAD of MHC-I by viral E3 ligase mK3,” *J. Cell Biol.*, vol. 177, pp. 613–24, may 2007.
- [204] J. Vagner, H. Qu, and V. J. Hruby, “Peptidomimetics, a synthetic tool of drug discovery,” *Curr. Opin. Chem. Biol.*, vol. 12, pp. 292–296, jun 2008.
- [205] S. Liu, B. Zhou, H. Yang, Y. He, Z. X. Jiang, S. Kumar, L. Wu, and Z. Y. Zhang, “Aryl vinyl sulfonates and sulfones as active site-directed and mechanism-based probes for protein tyrosine phosphatases,” *J. Am. Chem. Soc.*, vol. 130, no. 26, pp. 8251–8260, 2008.

APPENDIX

Appendix: Comparison of Cdc14 catalytic efficiencies

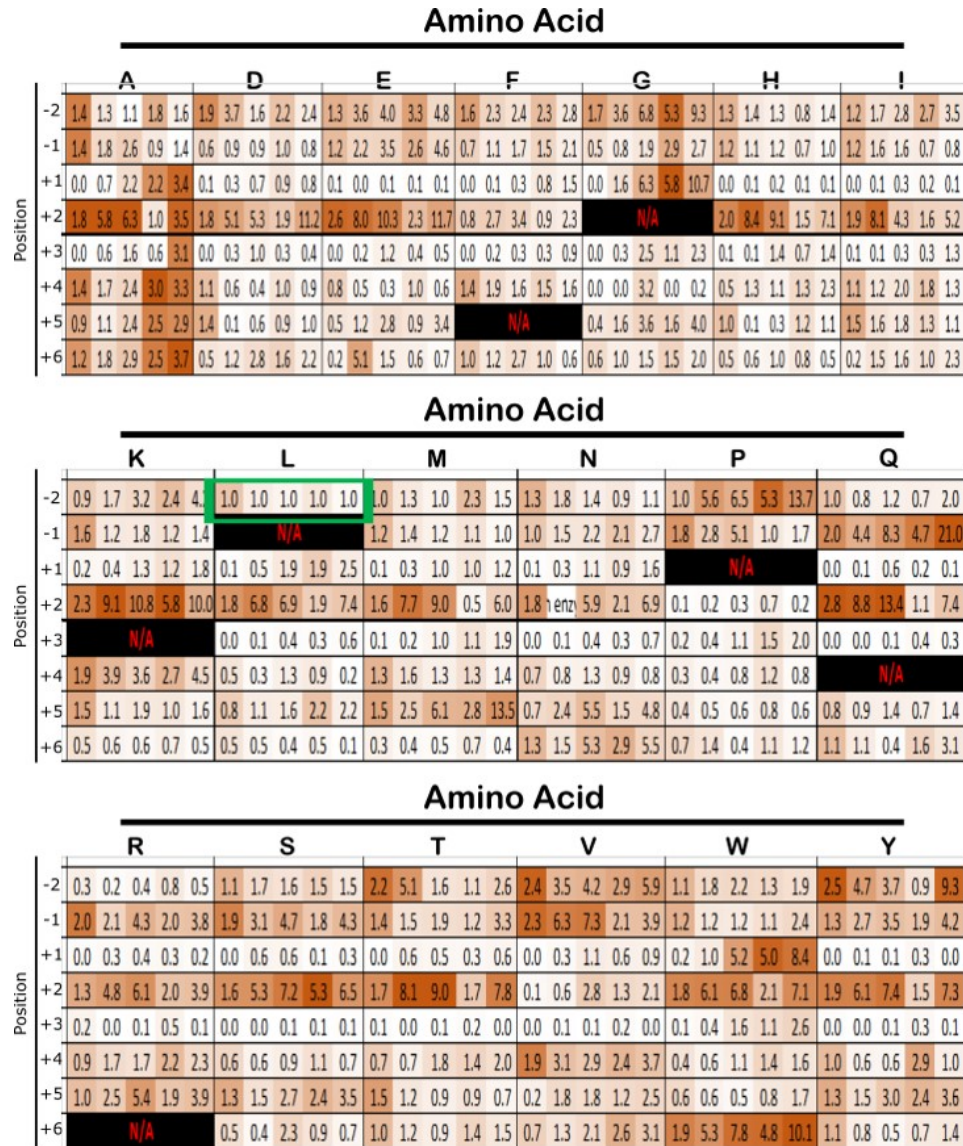
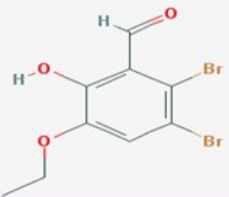
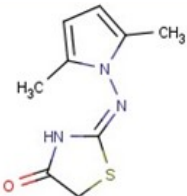
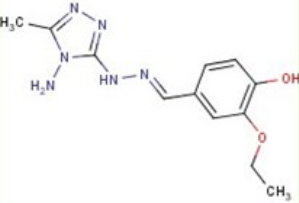


Fig. A.1.: **Comparison of catalytic efficiencies of Cdc14 enzymes.** Catalytic efficiencies of Cdc14 enzymes are normalized to that observed for the starting sequence (Green box) for each enzyme. Each box contains the activity observed (in order from left to right) for Sc.Cdc14, FgCdc14, Clp1, hCDC14A and hCDC14B and each value is shaded to reflect activity (dark,high-white,low).

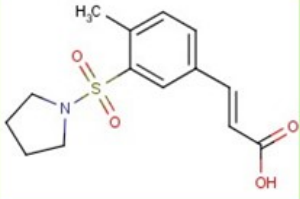
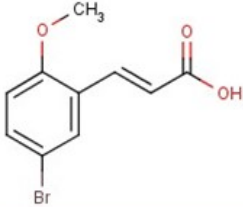
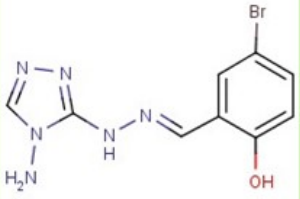
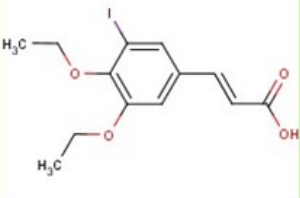
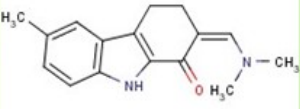
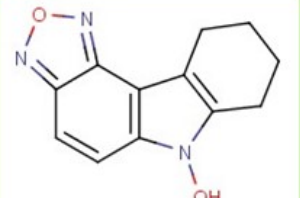
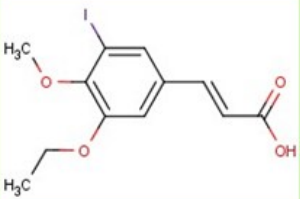
Appendix: Cdc14 inhibitors

A list of Cdc14 inhibitors identified by a high throughput screen is provided below. There are two sets of inhibitors organized by the chemical library in which they are found. The inhibitors are also ranked based on the observed % inhibition of Cdc14 activity. Molecules selected for manual confirmation and detailed characterization are indicated by green shading.

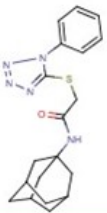
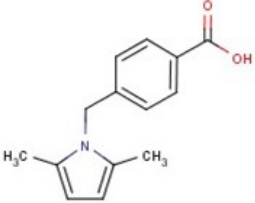
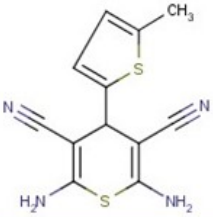
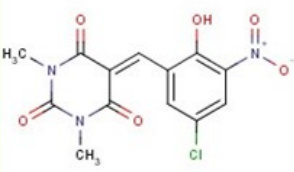
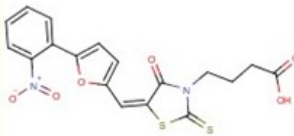
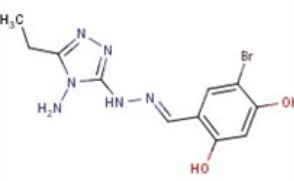
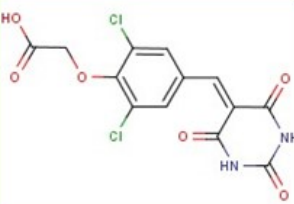
The first set of molecules are from the DIVERSet commercial chemical library available from ChemBridge.

Mol Name	Structure	% inhibition	ID
2,3-dibromo-5-ethoxy-6-hydroxybenzaldehyde		104.63	5249940
2-[(2,5-dimethyl-1H-pyrrol-1-yl)imino]-1,3-thiazolidin-4-one		104.42	6075635
3-ethoxy-4-hydroxybenzaldehyde (4-amino-5-methyl-4H-1,2,4-triazol-3-yl)hydrazone		103.92	5380140

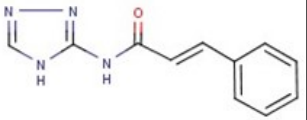
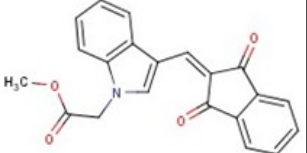
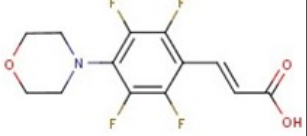
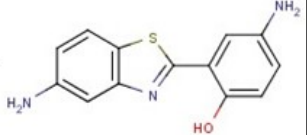
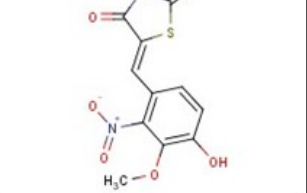
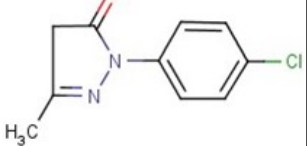
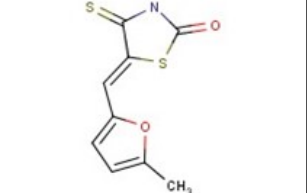
Mol Name	Structure	% inhibition	ID
3-bromo-5-chloro-2-hydroxybenzaldehyde (4-amino-4H-1,2,4-triazol-3-yl)hydrazone		102.53	5380833
3-(5-bromo-2,4-dimethoxyphenyl)acrylic acid		102.36	5959689
3-(3-bromo-4-ethoxy-5-methoxyphenyl)acrylic acid		101.45	5957528
3-[3-(4-methoxy-1-naphthyl)acryloyl]-4,6-dimethyl-2(1H)-pyridinone		101.00	5259576
5,5-dimethyl-5,6-dihydropyrazolo[3,4-a][3]benzazepin-3(2H)-one		99.76	6034891
3-[4-methoxy-3-(1-pyrrolidinylsulfonyl)phenyl]acrylic acid		99.48	5932946
1-(3-ethoxyphenyl)-5-(2-furylmethylene)-2-thioxodihydro-4,6(1H,5H)-pyrimidinedione		99.03	5994703

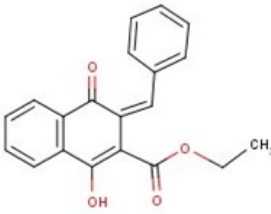
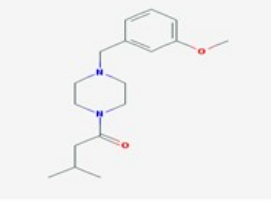
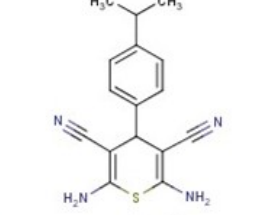
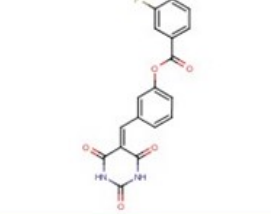
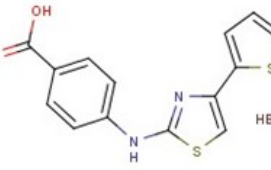
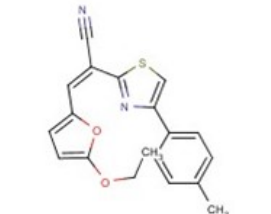
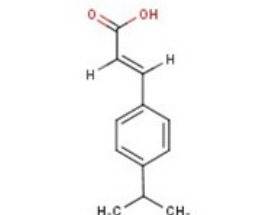
Mol Name	Structure	% inhibition	ID
3-[4-methyl-3-(1-pyrrolidinylsulfonyl)phenyl]acrylic acid		98.62	6630407
3-(5-bromo-2-methoxyphenyl)acrylic acid		98.60	6632609
5-bromo-2-hydroxybenzaldehyde (4-amino-4H-1,2,4-triazol-3-yl)hydrazone		97.86	5313868
3-(3,4-diethoxy-5-iodophenyl)acrylic acid		97.83	5977518
2-[(dimethylamino)methylene]-6-methyl-2,3,4,9-tetrahydro-1H-carbazol-1-one		96.53	5870649
7,8,9,10-tetrahydro-6H-[1,2,5]oxadiazolo[3,4-c]carbazol-6-ol		96.26	5256350
3-(3-ethoxy-5-iodo-4-methoxyphenyl)acrylic acid		95.25	5959502

Mol Name	Structure	% inhibition	ID
1-methyl-5-(4-methylbenzylidene)-2,4,6(1H,3H,5H)-pyrimidinetrione		94.64	5986268
2-amino-4-(2,3-dichlorophenyl)-7-hydroxy-4H-chromene-3-carbonitrile		93.92	5281200
4,6-dimethyl-3-[3-(1-naphthyl)acryloyl]-2(1H)-pyridinone		93.74	5255691
2-[4-[acetyl(phenyl)amino]-1,3-butadien-1-yl]-3-ethyl-1,3-benzothiazol-3-ium iodide		93.71	5107928
3-[5-(2-bromophenyl)-2-furyl]acrylic acid		91.99	6048056
6-[5-(4-nitrobenzylidene)-4-oxo-2-thioxo-1,3-thiazolidin-3-yl]hexanoic acid		91.96	5258413
4-[(3,4-dimethoxybenzylidene)amino]phenol		91.53	5105269

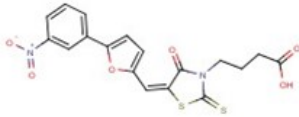
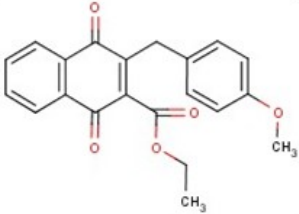
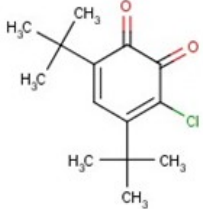
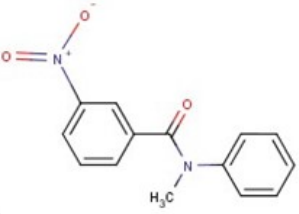
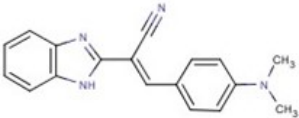
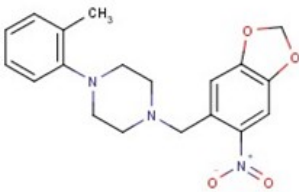
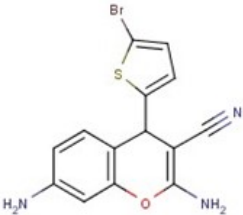
Mol Name	Structure	% inhibition	ID
N-1-adamantyl-2-[(1-phenyl-1H-tetrazol-5-yl)thio]acetamide		91.37	5946882
4-[(2,5-dimethyl-1H-pyrrol-1-yl)methyl]benzoic acid		91.37	5957378
2,6-diamino-4-(5-methyl-2-thienyl)-4H-thiopyran-3,5-dicarbonitrile		91.26	5303694
5-(5-chloro-2-hydroxy-3-nitrobenzylidene)-1,3-dimethyl-2,4,6(1H,3H,5H)-pyrimidinetrione		91.05	6634468
4-(5-[[5-(2-nitrophenyl)-2-furyl]methylene]-4-oxo-2-thioxo-1,3-thiazolidin-3-yl)butanoic acid		91.02	5881305
5-bromo-2,4-dihydroxybenzaldehyde (4-amino-5-ethyl-4H-1,2,4-triazol-3-yl)hydrazone		90.86	5379969
{2,6-dichloro-4-[(2,4,6-trioxotetrahydro-5(2H)-pyrimidinylidene)methyl]phenoxy}acetic acid		90.71	5977418

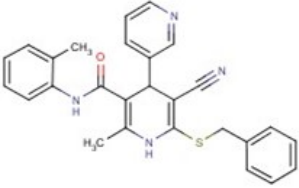
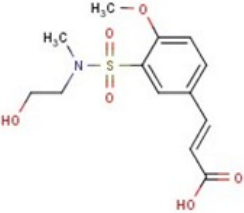
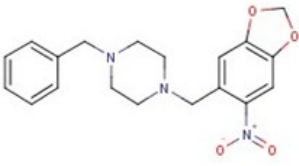
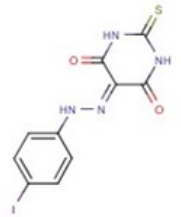
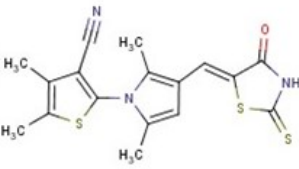
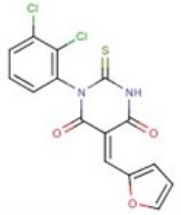
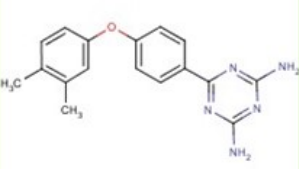
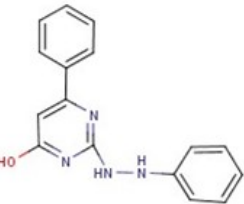
Mol Name	Structure	% inhibition	ID
1-(9H-xanthen-9-ylcarbonyl)azepane		90.40	5875313
5-(4-chlorophenyl)-2,4-pentadienoic acid		89.99	6056530
2-amino-4-(5-bromo-2-methoxyphenyl)-7-hydroxy-4H-chromene-3-carbonitrile		89.76	5280295
2,6-diamino-4-(5-butyl-2-thienyl)-4H-thiopyran-3,5-dicarbonitrile		89.62	5347207
2,6-dimethyl-4-[(4-methylphenyl)amino]phenol		89.29	5944406
6,7-dimethoxy-2-(1-naphthylmethyl)-1,2,3,4-tetrahydroisoquinoline		88.18	5261307
potassium 4-{2-[4-(dipropylamino)benzylidene]hydrazino}benzenesulfonate		87.78	5310589

Mol Name	Structure	% inhibition	ID
3-phenyl-N-4H-1,2,4-triazol-3-ylacrylamide		85.62	5325873
methyl {3-[(1,3-dioxo-1,3-dihydro-2H-inden-2-ylidene)methyl]-1H-indol-1-yl}acetate		85.59	6192997
3-[2,3,5,6-tetrafluoro-4-(4-morpholinyl)phenyl]acrylic acid		85.57	6574560
4-amino-2-(5-amino-1,3-benzothiazol-2-yl)phenol		85.33	5312639
5-(4-hydroxy-3-methoxy-2-nitrobenzylidene)-2-thioxo-1,3-thiazolidin-4-one		84.94	6382163
2-(4-chlorophenyl)-5-methyl-2,4-dihydro-3H-pyrazol-3-one		84.57	5303531
5-[(5-methyl-2-furyl)methylene]-4-thioxo-1,3-thiazolidin-2-one		84.37	6119414

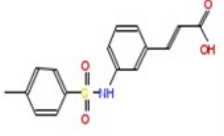
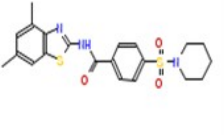
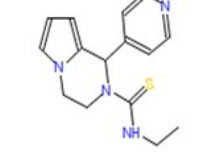
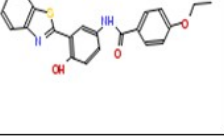
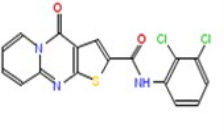
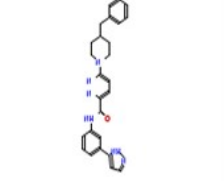
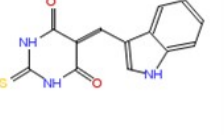
Mol Name	Structure	% inhibition	ID
ethyl 3-benzylidene-1-hydroxy-4-oxo-3,4-dihydro-2-naphthalenecarboxylate		84.25	5882380
1-(3-methoxybenzyl)-4-(3-methylbutanoyl)piperazine		84.03	5934789
2,6-diamino-4-(4-isopropylphenyl)-4H-thiopyran-3,5-dicarbonitrile		83.92	5301168
3-[(2,4,6-trioxotetrahydro-5(2H)-pyrimidinylidene)methyl]phenyl 3-fluorobenzoate		83.53	6404329
4-[[4-(2-thienyl)-1,3-thiazol-2-yl]amino]benzoic acid hydrobromide		83.09	5931887
3-(5-ethoxy-2-furyl)-2-[4-(4-methylphenyl)-1,3-thiazol-2-yl]acrylonitrile		82.83	5252596
3-(4-isopropylphenyl)acrylic acid		82.59	5135290

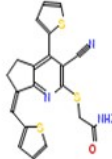
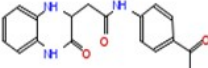
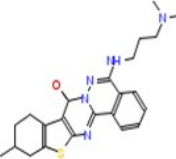
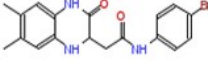
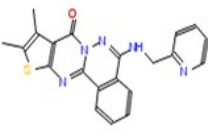
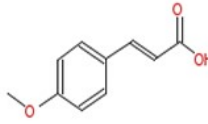
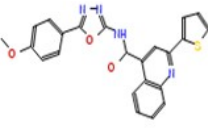
Mol Name	Structure	% inhibition	ID
2-[5-(4-bromobenzylidene)-4-oxo-2-thioxo-1,3-thiazolidin-3-yl]-3-methylbutanoic acid		82.59	5275805
3,3'-(1,3-phenylene)bisacrylic acid		82.43	5310510
2-amino-4-(2-chlorophenyl)-7-hydroxy-4H-chromene-3-carbonitrile		82.39	5275706
5-[3-bromo-4-(2-propyn-1-yloxy)benzylidene]-2,4,6-(1H,3H,5H)-pyrimidinetrione		81.33	5948296
1-(2,5-dihydroxyphenyl)tetrahydro-2H-thiopyranium chloride hydrate		81.07	5251606
3-(5-methoxy-2-furyl)-2-[4-(4-methoxyphenyl)-1,3-thiazol-2-yl]acrylonitrile		80.59	5252582
3-[(2,4,6-trioxotetrahydro-5(2H)-pyrimidinylidene)methyl]phenyl 4-methylbenzenesulfonate		80.10	6082917

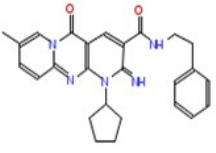
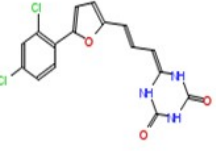
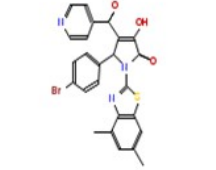
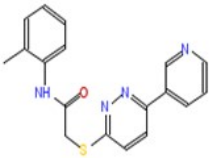
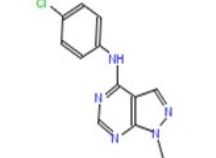
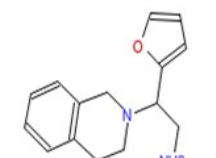
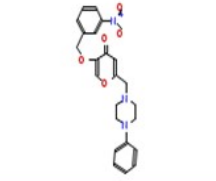
Mol Name	Structure	% inhibition	ID
4-(5-[[5-(3-nitrophenyl)-2-furyl]methylene]-4-oxo-2-thioxo-1,3-thiazolidin-3-yl)butanoic acid		79.73	5872119
ethyl 3-(4-methoxybenzyl)-1,4-dioxo-1,4-dihydro-2-naphthalenecarboxylate		79.33	5325842
4,6-di-tert-butyl-3-chlorobenzo-1,2-quinone		78.93	5317249
N-methyl-3-nitro-N-phenylbenzamide		78.84	5351078
2-(1H-benzimidazol-2-yl)-3-[4-(dimethylamino)phenyl]acrylonitrile		78.55	5376445
1-(2-methylphenyl)-4-[(6-nitro-1,3-benzodioxol-5-yl)methyl]piperazine		78.41	5265847
2,7-diamino-4-(5-bromo-2-thienyl)-4H-chromene-3-carbonitrile		77.96	5284211

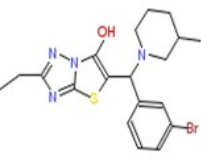
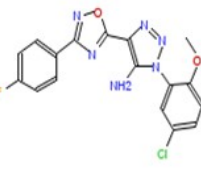
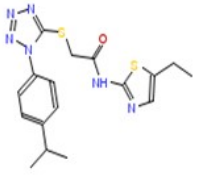
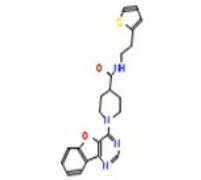
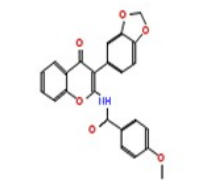
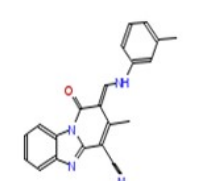
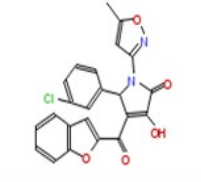
Mol Name	Structure	% inhibition	ID
6'-(benzylthio)-5'-cyano-2'-methyl-N-(2-methylphenyl)-1',4'-dihydro-3,4'-bipyridine-3'-carboxamide		77.73	5312383
3-(3-[(2-hydroxyethyl)(methylamino)sulfonyl]-4-methoxyphenyl)acrylic acid		77.65	6630522
1-benzyl-4-[(6-nitro-1,3-benzodioxol-5-yl)methyl]piperazine		77.04	5263139
2-thioxodihydro-4,5,6(1H)-pyrimidinetrione 5-[(4-iodophenyl)hydrazone]		76.99	5268606
2-{2,5-dimethyl-3-[(4-oxo-2-thioxo-1,3-thiazolidin-5-ylidene)methyl]-1H-pyrrol-1-yl}-4,5-dimethyl-3-thiophenecarbonitrile		76.77	6092310
1-(2,3-dichlorophenyl)-5-(2-furylmethylene)-2-thioxodihydro-4,6(1H,5H)-pyrimidinedione		76.57	6320032
6-[4-(3,4-dimethylphenoxy)phenyl]-1,3,5-triazine-2,4-diamine		75.66	5253542
6-phenyl-2-(2-phenylhydrazino)-4-pyrimidinol		74.83	5340620

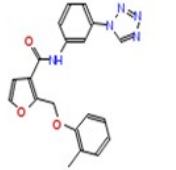
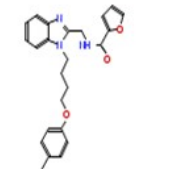
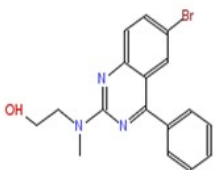
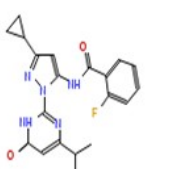
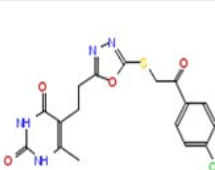
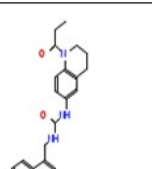
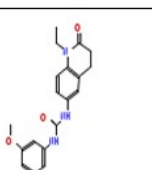
The molecules below are from a custom library of small molecules.

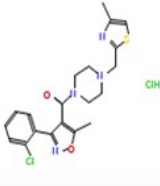
Mol Name	Structure	PubChem CID	% Inhibition
3-(3-[[[4-methylphenyl)sulfonyl]amino]phenyl]acrylic acid		737087	108.63
N-(4,6-dimethyl-1,3-benzothiazol-2-yl)-4-(1-piperidyl)sulfonylbenzamide		1185419	108.42
N-Ethyl-1-(4-pyridinyl)-3,4-dihydropyrrolo[1,2-a]pyrazine-2(1H)-carbothioamide		5075831	108.01
N-[3-(1,3-Benzothiazol-2-yl)-4-hydroxyphenyl]-4-ethoxybenzamide		3087565	107.80
N-(2,3-Dichlorophenyl)-4-oxo-4H-pyrido[1,2-a]thieno[2,3-d]pyrimidine-2-carboxamide		2158379	106.87
N-(3-(1H-pyrazol-5-yl)phenyl)-6-(4-benzylpiperidin-1-yl)pyridazine-3-carboxamide		71778653	106.73
5-(1H-indol-3-ylmethylidene)-2-sulfanylidene-1,3-diazinane-4,6-dione		5380241	106.64

Mol Name	Structure	PubChem CID	% Inhibition
2-[4-oxo-3-(2-phenylethyl)-5-thiophen-2-ylthieno[2,3-d]pyrimidin-2-yl]sulfanylacetonitrile		2570225	105.31
N-(4-acetylphenyl)-2-(3-oxo-2,4-dihydro-1H-quinoxalin-2-yl)acetamide		2938755	104.81
5-[[3-(Dimethylamino)propyl]amino]-11-methyl-9,10,11,12-tetrahydro-8H-[1]benzothieno[2',3':4,5]pyrimido[2,1-a]phthalazin-8-one		3427243	101.88
N-(4-bromophenyl)-2-(6,7-dimethyl-3-oxo-1,2,3,4-tetrahydroquinoxalin-2-yl)acetamide		5100913	96.96
9,10-dimethyl-5-((pyridin-2-ylmethyl)amino)-8H-thieno[2',3':4,5]pyrimido[2,1-a]phthalazin-8-one		1186194	96.83
4-Methoxycinnamic acid		699414	94.62
N-[5-(4-methoxyphenyl)-1,3,4-oxadiazol-2-yl]-2-thiophen-2-ylquinoline-4-carboxamide		5111944	94.60

Mol Name	Structure	PubChem CID	% Inhibition
1-cyclopentyl-2-imino-8-methyl-5-oxo-N-(2-phenylethyl)dipyrido[1,2-d:3',4'-f]pyrimidine-3-carboxamide		4131216	93.37
6-[(E)-3-[5-(2,4-dichlorophenyl)furan-2-yl]prop-2-enylidene]-1,3,5-triazinane-2,4-dione		1528071	89.23
(4E)-5-(4-bromophenyl)-1-(4,6-dimethyl-1,3-benzothiazol-2-yl)-4-[hydroxy(pyridin-4-yl)methylidene]pyrrolidine-2,3-dione		5810743	88.40
N-(2-methylphenyl)-2-(6-pyridin-3-ylpyridazin-3-yl)sulfanylacetamide		7222429	87.25
n-(4-chlorophenyl)-1-methyl-1h-pyrazolo[3,4-d]pyrimidin-4-amine		219777	84.29
2-(3,4-dihydro-1H-isoquinolin-2-yl)-2-(furan-2-yl)ethanamine		16786675	84.00
5-[(3-nitrophenyl)methoxy]-2-[(4-phenylpiperazin-1-yl)methyl]pyran-4-one		7178469	83.82

Mol Name	Structure	PubChem CID	% Inhibition
5-[(3-bromophenyl)-(3-methylpiperidin-1-yl)methyl]-2-ethyl-[1,3]thiazolo[3,2-b][1,2,4]triazol-6-ol		18575985	81.34
3-(5-chloro-2-methoxyphenyl)-5-[3-(4-fluorophenyl)-1,2,4-oxadiazol-5-yl]triazol-4-amine		18591827	80.95
N-(5-ethyl-1,3-thiazol-2-yl)-2-[1-(4-propan-2-ylphenyl)tetrazol-5-yl]sulfanylacetamide		7463917	79.49
1-([1]benzofuro[3,2-d]pyrimidin-4-yl)-N-(2-thiophen-2-ylethyl)piperidine-4-carboxamide		46393058	75.36
N-[3-(1,3-benzodioxol-5-yl)-4-oxochromen-2-yl]-4-methoxybenzamide		4906192	74.44
(2E)-3-Methyl-2-[[[(3-methylphenyl)amino]methylene]-1-oxo-1,2-dihydropyrido[1,2-a]benzimidazole-4-carbonitrile		6521527	74.35
3-(1-benzofuran-2-carbonyl)-2-(3-chlorophenyl)-4-hydroxy-1-(5-methyl-1,2-oxazol-3-yl)-2H-pyrrol-5-one		3694202	73.51

Mol Name	Structure	PubChem CID	% Inhibition
2-[(2-methylphenoxy)methyl]-N-[3-(tetrazol-1-yl)phenyl]furan-3-carboxamide		8073829	73.30
N-[[1-[4-(4-methylphenoxy)butyl]benzimidazol-2-yl]methyl]furan-2-carboxamide		16619332	72.45
2-[(6-bromo-4-phenylquinazolin-2-yl)-methylamino]ethanol		6461946	71.86
N-[5-cyclopropyl-2-(4-oxo-6-propan-2-yl-1H-pyrimidin-2-yl)pyrazol-3-yl]-2-fluorobenzamide		42419668	71.52
5-[2-[5-[2-(4-chlorophenyl)-2-oxoethyl]sulfanyl-1,3,4-oxadiazol-2-yl]ethyl]-6-methyl-1H-pyrimidine-2,4-dione		44072011	71.00
1-(naphthalen-1-ylmethyl)-3-(1-propanoyl-3,4-dihydro-2H-quinolin-6-yl)urea		30373933	71.00
1-(3,5-dimethoxyphenyl)-3-(1-ethyl-2-oxo-3,4-dihydroquinolin-6-yl)urea		30376265	70.88

Mol Name	Structure	PubChem CID	% Inhibition
[3-(2-chlorophenyl)-5-methyl-1,2-oxazol-4-yl]-[4-[(4-methyl-1,3-thiazol-2-yl)methyl]piperazin-1-yl]methanone		29697836	70.39

VITA

VITA

MICHAEL MELESSE

Personal Data

EMAIL: mmelesse@purdue.edu
 CELLPHONE: (503) 750-1838
 LINKEDIN: www.linkedin.com/in/mmelesse/
 ADDRESS: Department of Biochemistry, Purdue University
 1203 West State St., West Lafayette, IN 47907

Education

DECEMBER 2015 Ph.D. in BIOCHEMISTRY, **Purdue University**
 West Lafayette, IN
 Advisor: Dr. Mark C. HALL
 MAY 2008 B.A. in BIOCHEMISTRY AND MOLECULAR BIOLOGY,
Reed College, Portland, OR
 Advisor: Dr. Ronald W. MCCLARD

PUBLICATIONS

Melesse M., Choi E., Hall H., Walsh M.J., and Hall M.C., Timely activation of budding yeast APC^{Cdh1} involves degradation of its inhibitor, Acm1, by an unconventional proteolytic mechanism, *PLoS One*, 9(7): e103517. doi:10.1371/journal.pone.0103517

Powers B.L., **Melesse M.**, Eissler C.E., Charbonneau H., and Hall M.C., Measuring activity and specificity of protein phosphatases, *Methods in Molecular Biology.*, 2016; Vol. 1342:221-35. doi:10.1007/978-1-4939-2957-3

Li C., **Melesse M.**, Zhang H, Hao C., Wang C., Zhang H., Hall M.C., Xu J.R., FgCDC14 regulates cytokinesis, morphogenesis, and pathogenesis in *Fusarium graminearum*, *Molecular Microbiology*, 2015 Aug. doi: 10.1111/mmi.13157.

In Preparation

Qin L., **Melesse M.**, Guimaraes D., Hall M.C., Reevaluation of APC^{Cdh1} degron sequences

Iliuk A., Li L., **Melesse M.**, Hall M.C. and Tao W.A., Multiplexed imaging of protein phosphorylation on membrane based on Ti(IV) functionalized nanopolymer, *Angewandte Chemie*

RESEARCH EXPERIENCE

Current	<p>Ph.D. Candidate Department of Biochemistry, Purdue University, West Lafayette, IN</p> <ul style="list-style-type: none"> • Topic: Cell cycle regulation, protein degradation. Identification of the degradation mechanism of the <i>Saccharomyces cerevisiae</i> protein Acml. PI: Dr. Mark C. Hall. • Topic: Cell cycle regulation, protein phosphorylation. Determination of the substrate selectivity of a cell cycle regulated phosphatase, Cdc14. PI: Dr. Mark C. Hall
FALL 2008 - SUMMER 2009	<p>Research Assistant Oregon Health and Sciences University, Portland, OR</p> <ul style="list-style-type: none"> • Research assistant for project entitled “ Identification of ligands of Anaplastic lymphoma kinase in <i>Mus musculus</i>”. Biochemical characterization of protein substrates. PI: Dr. Joseph Weiss
FALL 2007 TO SUMMER 2008	<p>Undergraduate Research Assistant Chemistry Department, Reed College, Portland, OR</p> <ul style="list-style-type: none"> • Undergraduate year long thesis project entitled “Site-directed mutation of the <i>Saccharomyces cerevisiae</i> OPRTase flexible loop: potential application to structural studies”. PI: Dr. Ronald W. McClard.
SUMMER 2007	<p>Undergraduate Summer Research Assistant Chemistry Department, Reed College, Portland, OR</p> <ul style="list-style-type: none"> • Worked on a summer research project towards the organic synthesis of a pH switch for selective delivery of radioactive iodine into cancerous cells. PI: Dr. Patrick G. McDougal.

HONORS AND AWARDS

- AUG. 2015 **Bird Stair Fellowship award**, Department of Biochemistry, Purdue University
- APRIL 2015 **Outstanding Teaching Assistant Award**, Department of Biochemistry, Purdue University
- FEB. 2015 **Bird Stair Fellowship award**, Department of Biochemistry, Purdue University
- APRIL 2014 **Henry Weiner Travel Award**, Department of Biochemistry, Purdue University
- SEPT. 2009 **Ross Fellowship**, Purdue Graduate School, Purdue University
- IN PROGRESS **Graduate Teacher Certificate**, Center for Instructional Excellence, Purdue University
- AUG. 2004 **National Honors Society**, International Community School of Addis Ababa
- AUG. 2004 **International Baccalaureate diploma** International Community School of Addis Ababa

TEACHING EXPERIENCE

- | | | |
|-------------|----------------------------------------------|-------------------------|
| FALL 2015 | BCHM221 Small Molecule Biochemistry | Dr. Steven S. Broyles |
| SUMMER 2015 | BCHM309 Biochemistry Lab | Dr. Orla Hart |
| SPRING 2015 | BCHM100 Introduction to Biochemistry | Dr. Vikki Weake |
| FALL 2014 | BCHM100 Introduction to Biochemistry | Dr. Clint C. Chapple |
| SPRING 2014 | BCHM100 Introduction to Biochemistry | Dr. Vikki Weake |
| FALL 2013 | BCHM309 Biochemistry Lab (2 sections) | Independent |
| SPRING 2013 | BCHM695 Macromolecules | Dr. Ann L. Kirchmaier |
| SPRING 2012 | BCHM307 Biochemistry | Dr. James C. Clemens |
| SPRING 2011 | BCHM309 Biochemistry Lab (2 sections) | Dr. James T. Henderson. |

MENTORING

- SUMMER 2014 Denise Ward, NSF Research Experience for Undergraduate (REU) program
- SPRING 2014 Ryan Chaparian, Biochemistry undergraduate student
- SUMMER 2013 Perla Cruz, Summer Undergraduate Research Foundation (SURF) program
- SUMMER 2012 Mercedes Leland, Biochemistry undergraduate student
- to SPRING 2013
- SPRING 2012 Michael Walsh, Biochemistry undergraduate student
- to FALL 2013
- SUMMER 2011 George Habib, Summer Undergraduate Research Foundation (SURF) program
- SPRING and Matt Berret, Biochemistry undergraduate student
- FALL 2011

PROFESSIONAL ACTIVITIES

- Chair
 - Graduate student invited lecture committee, Biochemistry department, Purdue University (Fall 2013)
- Poster judge
 - REU (Research Experience for Undergraduates) / SURF (Summer Undergraduate Research Fellowships) Program, Purdue University (July 25, 2013)
 - Biochemistry department research retreat, Turkey Run State Park, (September 24, 2011)
 - SURF Program, Purdue University (August 3, 2011)
- Member
 - Graduate student advisory board, College of Agriculture, Purdue University (Spring 2012 - Present)
 - Grades appeal committee, College of Agriculture, Purdue University (Fall 2012, Fall 2013-Spring 2014)
 - Graduate student invited lecture committee, Biochemistry department, Purdue University (Spring 2012)
 - Awards committee, College of Agriculture, Purdue University (Fall 2012)
 - Graduate student invited lecture committee, Biochemistry department, Purdue (Fall 2010)

SEMINARS AND POSTER PRESENTATIONS

- AUG. 21, 2015 Cdc14 phosphatase substrate selectivity is conserved
Biochemistry Department Annual Retreat, Poster
- NOV. 12, 2014 Identification of Cdc14 phosphatase inhibitors and applications to cancer
Purdue Cancer Center Research Retreat, Poster
- OCT. 17, 2014 Understanding and exploiting Cdc14 substrate selectivity
Biochemistry Departmental Graduate student and Postdoc seminar series, Purdue University, Seminar
- JULY 13-18, 2014 Towards the design of Cdc14 phosphatase inhibitors
FASEB Yeast Chromosome Structure, Replication and Segregation, Poster
- NOV. 15, 2013 Characterization of the mechanism and biological function of Acml degradation
Biochemistry Departmental Graduate student and Postdoc seminar series, Purdue University, Seminar
- SEPT. 28-29, 2013 Determining the function of Acml degradation
Midwestern Yeast Meeting, Northwestern University, Poster
- April 19, 2013 A cell cycle regulated proteolytic mechanism independent of ubiquitin conjugation to the substrate
Ubiquitination Processes and Their Role in Cancer, Mini-Symposium and Poster Session, Purdue University, Poster

SEMINARS AND POSTER PRESENTATIONS (cont.)

- AUG. 17, 2012 Determining the mechanism for Acm1 (APC^{Cdh1} modulator 1) degradation
Biochemistry Department Annual Retreat, Turkey Run state park, Poster
- MARCH 9, 2012 Characterization of Acm1 degradation
Biochemistry Departmental Graduate student and Postdoc seminar series, Purdue University, Seminar
- DEC. 11, 2011 Polyubiquitination independent degradation of Acm1
Cell cycle regulation group meeting, Purdue University, Seminar
- SEP. 24, 2011 Identification of proteins required for degradation of the APC inhibitor Acm1
Biochemistry Department Annual Retreat, Turkey Run state park, Poster
- NOV. 12, 2010 Characterization of the proteasome mediated degradation of Acm1
Biochemistry Departmental Graduate student and Postdoc seminar series, Purdue University, Seminar
- OCT. 2, 2010 Identification of proteins required for degradation of the APC inhibitor Acm1
Biochemistry Department Annual Retreat, Turkey Run state park, Poster

TECHNICAL SKILLS

- Biochemistry* Protein purification, (co-)immunopurification, pulse-chase analysis, high-throughput chemical screening, enzymatic assays (experimental and data analysis).
- Analytical* Flow cytometry, MS (MALDI-TOF), chromatography (thin layer, ion exchange, SEC, HPLC, RPC), quantitative western blot, titrations, photo-spectrophotometry, Agarose and PAGE electrophoresis.
- Molecular biology* Cloning: primer design, restriction digest analysis, ligations, transformation, RNA extraction, reverse transcription, PCR, DNA purification, DNA quantification and extraction, TOPO® and Gateway® cloning, genetic modification of yeast (gene deletion, genomic tagging).
- Cellular biology* liquid and solid culture of yeast and bacteria, cell cycle synchronization; microscopy: fluorescence and light.

OTHER ACTIVITIES

Safety committee	Member, lab safety committee Bindley Biosciences Center (BBC) , West Lafayette, IN (July 2014 - Present).
Peer mentor	Peer mentor program, Reed College , Portland, OR (August 2005 - May 2008).
Co-founder and president	International Students Union, Reed College , Portland, OR (Aug. 2005 - May 2008).
Intern	Multicultural Resources Center, Reed College , Portland, OR (Jan. 2005 - May 2006).